Technische Universität München

Fachgebiet Molekulare Katalyse

Development of new methods for the production of highly reactive polyisobutenes

Silvana Rach

Vollständiger Abdruck der von der Fakultät für Chemie der Technischen Universität München zur Erlangung des akademischen Grades eines

Doktors der Naturwissenschaften

genehmigten Dissertation.

Für meine Familie und Timo

Die vorliegende Arbeit entstand in der Zeit von Oktober 2007 bis Oktober 2010 am Anorganisch-Chemischen Institut der Technischen Universität München.

Mein besonderer Dank gilt meinem verehrten Lehrer

Herrn Professor Dr. Fritz E. Kühn

für die Aufnahme in seinen Arbeitskreis, für das Vertrauen, und die große Freiheit, die mir während meiner Arbeit erteilt wurde.

Acknowledgments

The most exciting phrase to hear in science, the one that heralds new discoveries, is not

"Eureka!" but "That's funny..."

Isaac Asimov (1920-1992), Russian biochemist and author

Index

X. Appendix   151

Abbreviations

Ac	acetate
Anal. calcd.	analysis calculated
ATRP	Atom Transfer Radical Polymerization
AZBN	azobis(isobutyronitrile)
bp	boiling point
bpy	2,2'-bipyridine
br	broad
Bu	butyl
cod	1,5-cyclooctadiene
Cp*	1,2,3,4,5-pentamethylcyclopentadienyl-
d	doublet
δ	chemical shift
dppe	1,2-bis(diphenylphosphino)ethane
DTBP	2,6-di-tert-butylpyridine
EPR	electron paramagnetic resonance
eq.	equivalents
Et	ethyl
HR-PIBs	highly reactive poyisobutenes
Hz	Hertz
J	coupling constant
m	multiplet (NMR)
m	middle (IR, Raman)
MALDI	matri assisted laser desorption/ionization
MCM	mobile crystalline material
Me	methyl
MHz	Megahertz

NOESY	nuclear overhauser enhancement spectroscopy
NMR	nuclear magnetic resonance
OAc	acetate rest
OEt$_2$	diethyl ether
OLED	organic light emitting diode
PDI	polydispersity index
Ph	phenyl
PIB	polyisobutene
ppm	parts per million
rt	room temperature
s	singlet (NMR)
s	strong (IR, Raman)
t	triplet (NMR), tertiary
techn.	technical
TGA	thermogravimetric analysis
THF	tetrahydrofurane
TOF	time-of-flight
tr.	traces
V	volume
virt.	virtual
vs	very strong
ν	wave number
WCA	weakly coordinating anion

I. Introduction

Polyisobutenes are important for numerous industrial applications such as the manufacture of insulations, tubes and tyre-inliners, as well as oil additives and sealants.[1] For this reason, several 100,000 tonnes are produced, each year.[2]

The history of poly(2-methyl-propene)s ("polyisobutenes") began in 1873, when *Buttlerow* and *Gorjainow* reported the first synthesis of triisobutene *via* the reaction of isobutene with "weak" sulphuric acid.[3] More than fifty years later, it was observed that heated silicates can initiate the polymerization of isobutene, yielding mixtures of low molecular weight oligomers.[4] The breakthrough for commercialization came only a few years later with the process of *Otto* and *Müller-Conradi* which still operates in an almost unchanged manner since it was first established in 1938 by IG Farben in Ludwigshafen, Germany (see Figure1.1.1).[1a, 5] The obtained high molecular weight polyisobutenes are still on market under the name Oppanol® B.
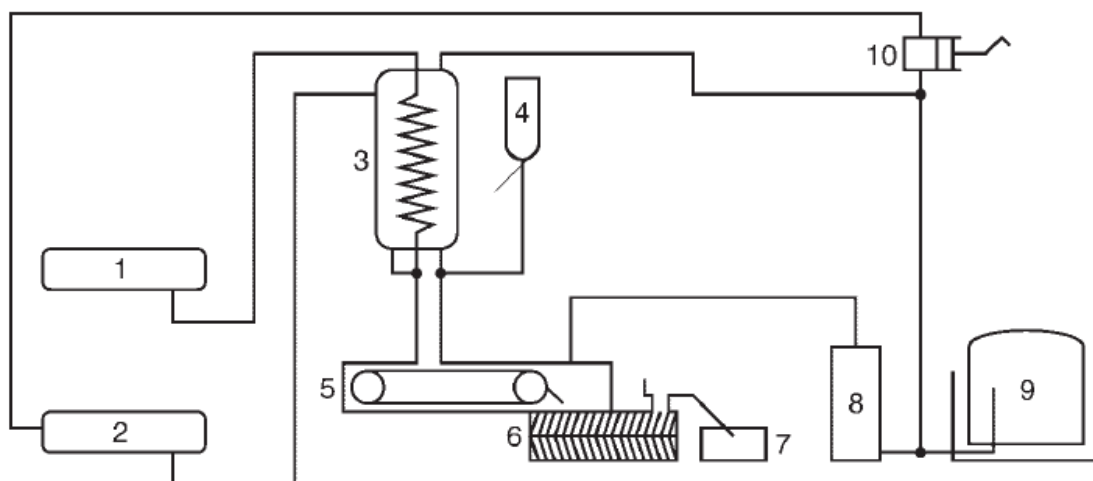
Figure 1.1.1 Process for the manufacture of Oppanol® B. 1: liquid isobutene, 2: liquid ethylene as cooling medium, 3: cooler-mixer, 4: BF_3-ethylene reservoir, 5: continuous belt, 6: compacting rolls, 7: product, 8: CaO to purify ethylene recycle, 9: gasometer, 10: compressor.[1a]

The produced unmodified polyisobutenes consist of unbranched, perfectly saturated carbon chains forming helices with eight monomer units per turn. This material, regardless of molecular weight, shows outstanding properties like low glass transition temperature, thermal

conductivity, permittivity and dielectric loss as well as high disruptive strength and resistivity. It is resistant to ageing and rotting, extraordinarily chemically robust and non-toxic. Additionally, it is one of the best known carbon-based barriers for gases. Further improvement of the desired properties can be obtained by blending with other polymers (*e.g.* polyethylene), fillers (*e.g.* graphite) and asphalt compounds. For example, the addition of polypropylene can enhance the impact strength. Alternatively, modification of polyisobutene can be achieved by copolymerization *e.g.* with halogenated derivatives, isoprene, styrene or divinylbenzene.[1a, 1c, 6]

1. Polymerization of isobutene

Isobutene is one of the few olefins that can be easily polymerized to virtually any molecular weight. Thus, commercially available homo-polyisobutenes (PIBs) are classified according to their molecular weights and resulting characteristic properties. Generally, they can be divided into the three groups: high-, medium- and low-molecular weight PIBs.

Rubber-like high-molecular weight PIBs (M_n > 300 kg·mol^{-1}) are used as chewing gum base as well as in non-crosslinked rubber goods and vulcanizable butyl rubber products (*e.g.* inner liners in the manufacture of tyres). Medium-molecular weight PIBs with molecular weights between 40 and 120 kg·mol^{-1} are highly viscous liquids, mainly applied as raw material for glues and sealants, as well as viscosity index conditioner in mineral oil industry. Colorless, honey-like low-molecular weight PIBs have molecular weights between 0.3 and 3 kg·mol^{-1}. This latter category is, with a 750,000 t/a production worldwide, by far the most important industrial class of isobutene polymers. It comprises the so-called conventional low-molecular weight PIBs that usually contain less than 10 % exo-terminal C=C bonds and the highly reactive PIBs which contain more than 60 % exo-terminal C=C functionalities (see Scheme 1.1.1). [1a, 1c, 7]
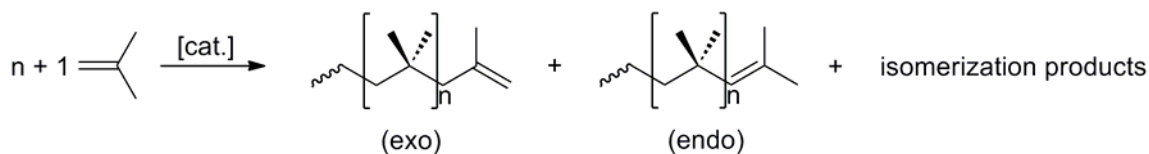
Scheme 1.1.1. General scheme for the polymerization of isobutene leading to polymers with different ratios of exo and endo terminal olefinic groups dependant on the catalyst.

The term highly reactive PIB (HRPIB) originates from the facile Functionalization of the exo-terminal olefin moiety. Numerous functionalized PIB´s with reactive end groups are commercially available (Glissopal® or Keropur® from BASF SE and Ultravis).
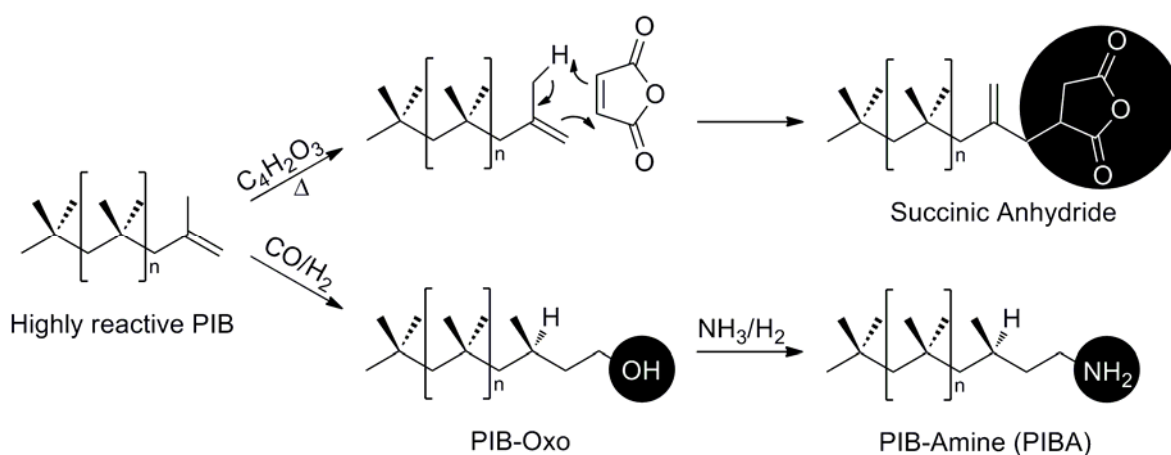
Scheme 1.1.2. Functionalization of highly reactive polyisobutene with reactive end-groups.[8]

Upon reaction of HRPIB with maleic anhydride or hydroformylation with successive hydroamination the polymers are functionalized with succinic anhydride or amino end groups, respectively. These polymers can be, either directly or as intermediate, used as detergents in fuel formulations. Through attachment of their polar functionalized end groups to metal surfaces, surface active detergents can form protective films. As a result the formation of cokelike residues or ice crystals on inlet system surfaces (see Figure 1.1.2) is prevented or at higher detergent concentration even reversed. Additionally, this effect facilitates dispergation of particles and in consequence hinders deposition. Thus, utilization of these dispersants in engine oils (up to 10 weight percent) helps to avoid agglomerations, coagulations and precipitations of insoluble substances as well as corrosion. When

fuctionalized HRPIB´s are applied in gasoline and diesel additives the injection system is protected and cleaned.
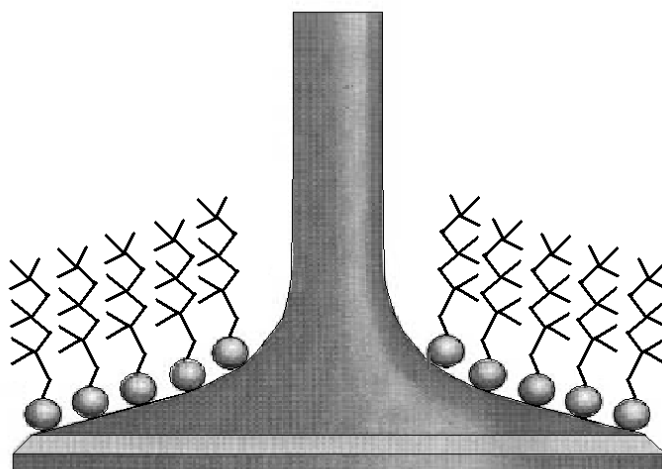
Figure 1.1.2. Schematic picture of the protecting detergent effect of functionalized highly reactive polyisotutenes on a fuel intake valve.[8a]

Besides polyisobutene derivatives can be directly used as lubricants or as components of lubricant formulations. Therein, they act as thickening or lubricating agents, control deposits and improve the quality of exhaust emissions and enhance anti-scuffing protection.

Application of these additives increases oil change intervals for motor engines, reduces oil consumption and increases fuel-efficiency (200 ppm of additives reduce fuel consumption by 4 %). As the need for the reduction of exhaust gases and fine dust particles rises, the requirements as well as the demand for environmentally benign additives grow rapidly. Polyisobutene based fuel additives are especially interesting due to their extraordinary resistance against chemicals and low toxicity combined with excellent detergent and lubrication properties. Beside the explained application as oil or fuel additives HRPIB´s can be used as tackifiers and softeners in insulating oils, sealing compounds or adhesives.[2, 6, 8a, 9]

Because HRPIB´s and their derivatives are usually regarded as being the most appropriate substances for these applications, their production has increased alongside the demand for improved production processes and new high-quality products. Due to the importance of the functionalization, generation of a high content of easily accessible exo-terminal olefin

functional groups during polymerization is a fundamental task. Furthermore, development of new eco-friendly and cost-effective industrial processes increases the necessity of fundamental research in this area.

1.1 Industrial production of highly reactive polyisobutenes

The importance of HRPIBs can be inferred from the rising production capacities for this class of polymers. An example for this observation is BASF SE, with the start up of a new production plant in Ludwigshafen, Germany in June 2010. In this way, the German annual production capacity is increased from 25,000 metric tonnes to 40,000 metric tonnes. This is accompanied by a significant capacity increase of the BASF SE production plant in Antwerp, Belgium (2009) from 25,000 metric tons to 100,000 metric tons (annual).

To date industrial production of PIBs is carried out either by initiation with protic or Lewis acids (*e.g.* $AlCl_3$, BCl_3 and BF_3). The latter case requires addition of a proton source as co-initiator in traces, contaminations such as water, hydrochlorides or hydrofluorides.[1c, 10] As the reaction is exothermic and the polymerization degree is strongly dependant on the reaction temperature (see Equation 1.1.1) a controlled process requires careful temperature regulation.

$$\ln M_n \sim 1/T \qquad\qquad \textbf{Equation 1.1.1}$$

Therefore low temperatures (-10 °C to -103.7 °C) have to be applied in present industrial processes. Cooling can be provided by the evaporation of low boiling solvents, such as methylene chloride, methyl chloride or liquid ethylene (boiling points 39,7; -23,8; -103.7 °C respectively). In consequence the energy consumption of these processes is immense for the regeneration of the cooling medium (compression).[1, 6, 10b, 11]

Generally, low molecular weight polyisobutenes can be produced by two different ways: either by direct polymerization or by degradation of high molecular polymers. In direct polymerization a relatively high reaction temperature is required due to the inverse dependence of the average degree of polymerization from the reaction temperature. Therefore the majority of all industrially produced low-molecular weight PIBs are manufactured by direct cationic polymerization in chlorinated solvents, *via* initiation with a proton source in the presence of Lewis acids. The proton source can be an excess of the respective Lewis acids (*e.g.* BF_3) which reacts with traces of water (see Scheme 1.1.3) or hydrogen halide impurities. The generated protons add to the olefin, yielding a carbenium ion, which is assumed to start chain growth by addition of further monomer. The tendency of transfer reactions increases with increasing temperature. Thus low temperatures are needed for undisturbed chain growing and the formation of higher molecular weights. Termination occurs either by reaction of impurities or by addition of agents such as water or methanol.[1c, 6]
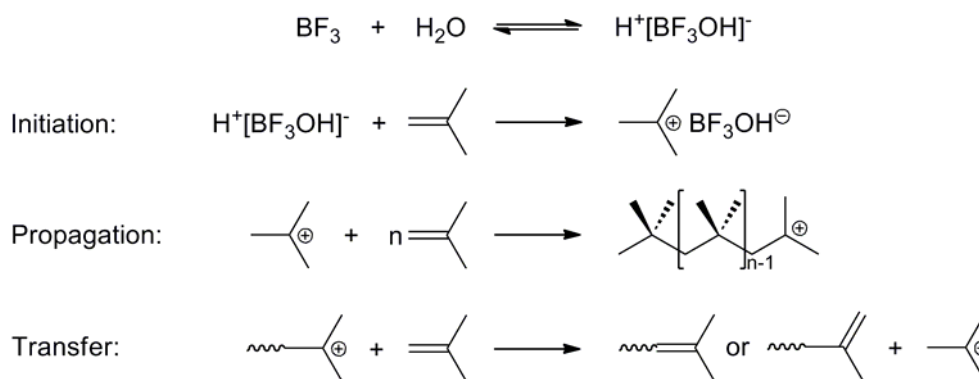
Scheme 1.1.3. Basic steps of the polymerization of isobutene; anion omitted in propagation and transfer steps.[1c, 6]

Besides considerable energy consumption for cooling, the use of chlorinated solvents (and halogenated Lewis acids) leads to large quantities of halogen containing solid waste, in addition to thousands of tons of chlorine-containing waste water.[9d] An additional drawback of this method is that catalysis with halogen-containing Lewis acids results in the addition of halogens to the polymer (this is mainly a problem of HRPIBs, with their extremely active exo-

terminal double bonds) resulting in the formation of halogen-containing by-products which can only be removed with difficulty, often persisting as contaminations (see Scheme 1.1.4).
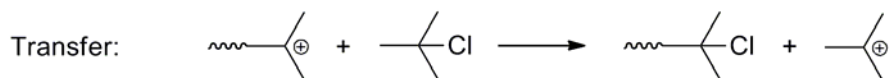
Scheme 1.1.4. Reaction of the reactive chain end with chlorinated impurities.[1c]

These halogenated by-products decompose upon exposure to air, releasing hydrogen halides that lead to corrosion of tanks and devices. Besides this, the exo C=C bond content decreases during storage. That is assumed to be due to the released hydrogen halides or acidic contaminants which cause an isomerization of the terminal double bonds.[9b] Additionally, termination of the growing polymer chains with methanol often results in OH-terminated polymers and a further loss of unsaturated end groups.[12] These drawbacks can only be completely eliminated by development of new industrial processes.

1.2 Progresses in the production of highly reactive polyisobutenes

Many attempts were made to find better methods for the manufacture of highly reactive polyisobutenes.[13] *Baird et al.*, for example, as well as *Shaffer* and *Ashbaugh* were the first who tested initiation with (pentafluorophenyl)borate (a weakly coordinating anion, WCA) based activators in combination with cyclopentadienyl complexes to form metallocene-like complexes, *e.g.* $Cp^*TiMe_3/B(C_6F_5)_3$ ([Cp^*TiMe_2]$^+$[$MeB(C_6F_5)_3$]$^-$) and traditional metallocenes (used as insertion polymerization catalysts for olefins) to form initiator systems such as $Cp_2^*ZrMe_2/Ph_3C[B(C_6F_5)_4]$. Additionally, tetrakis(pentafluorophenyl)borates were directly used as $Ph_3C[B(C_6F_5)_4]$ and $R_3CCl/Li[B(C_6F_5)_4]$ (R_3CCl = 1,3-bis(1-chloro-1-methylethyl)-5-*tert*-butylbenzene).[13a, 14] Some of these compounds were successfully applied for polymerization of isobutene in non-chlorinated solvents such as toluene. Depending on the reaction conditions, low molecular weight polyisobutenes were generated, as well. However all of procedures required temperatures of -20 °C or lower and the obtained degree of exo C=C bonds is not detailed in the respective literature. Interestingly, only recently *Bochmann*

et al. found a way to synthesize medium molecular weight polyisobutenes with a high content of terminal double bonds in temperature ranges between -90 and +35 °C, by means of alkyl zinc chloride-based initiator systems such as EtZnCl/*t*BuCl in CH_2Cl_2 (see Scheme 1.1.5).[15]
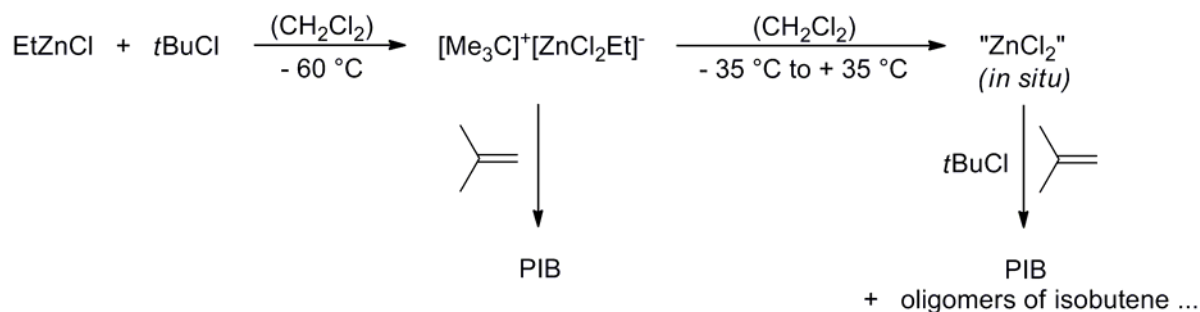
Scheme 1.1.5 Polymerization of isobutene by means of EtZnCl with *t*BuCl.[15]

1.3 Nitrile-stabilized transition metal complexes with weakly coordinating, polyfluorinated borate anions as new mediators for the polymerization of isobutene

In 2003 *Kühn et al.* achieved the production of highly reactive low molecular weight polyisobutenes at room temperature, using complexes of the general formula $[Mn(CH_3CN)_6][A]$ (A = $B(C_6F_5)_4^-$, $B(C_6H_3(CF_3)_2)_4^-$, $(C_6F_5)_3B-C_3H_3N_2-B(C_6F_5)_3^-$) as mediator.[16] In the following years, other acetonitrile ligated divalent transition metal cations with polyfluorinated borate anions were effectively tested as mediators for the polymerization of isobutene (see Figure 1.1.3).[16-17] In contrast to complexes containing less weakly coordinating anions such as BF_4^-, which were shown to be inactive,[16] these compounds were able to polymerize isobutene at room temperature. HRPIBs were produced with adjustable molecular weights between 0.5 and 1.4 kg·mol^{-1} and a content of terminal C=C bonds of more than 80 %. Most interestingly the reaction was also possible in non-chlorinated solvents like toluene. Concerning convenient reaction conditions (*i.e.*, use of non-chlorinated solvents, room temperature as reaction temperature) which are associated with an excellent content of exo-positioned terminal double bonds, the best results were achieved with $[Cu(CH_3CN)_6][B(C_6F_5)_4]_2$ and $[Cu(CH_3CN)_6][B(C_6H_3(CF_3)_2)_4]_2$ in toluene as solvent (obtained isobutene conversions: 72 to 92%; exo amount of the terminal double bonds: 76 to 85% at a reaction temperature of 30 °C).[17b]
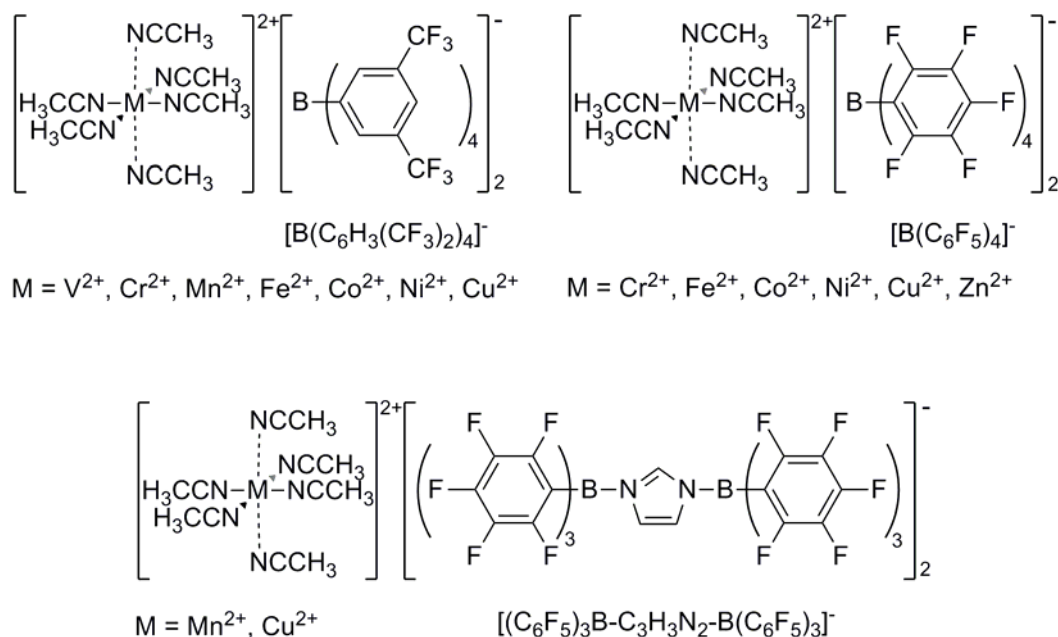
Figure 1.1.3. General structure of acetonitrile ligated divalent transition metal complexes with polyfluorinated borate anions.[2]

The solubility of the complexes in non-polar, chlorine-free solvents could even be increased by exchanging the acetonitrile ligands with benzonitrile. $[Cu(C_6H_5CN)_6][B(C_6F_5)_4]_2$, which is the most active complex known to date, reduced the reaction time to 15 min ($\approx$ 76% exo double bonds; 73% conversion in toluene and 30 °C; $c_{complex}$ = 0.5·10^{-4} mol/L, $c_{isobutene}$ = 1.78 mol/L).[9d] A small number of chlorinated, acetonitrile ligated molybdenum(III) complexes was recently found to be comparably active and soluble in non-polar solvents (see Figure 1.1.4).[10b] Application of nitrile-ligated transition metal complexes with weakly coordinating anions in large-scale processes would decrease energy consumption compared to the currently running production plants and the formation of high amounts of chlorine-containing waste could be avoided. An additional benefit is that until now, no chloride or hydroxyl (from methanol used for termination) end groups have been observed, using the new complexes. For this reason, in contrast to polymers obtained by conventional initiatation, each polyisobutene chain contains functionalizable unsaturated (end) groups.[12, 18]
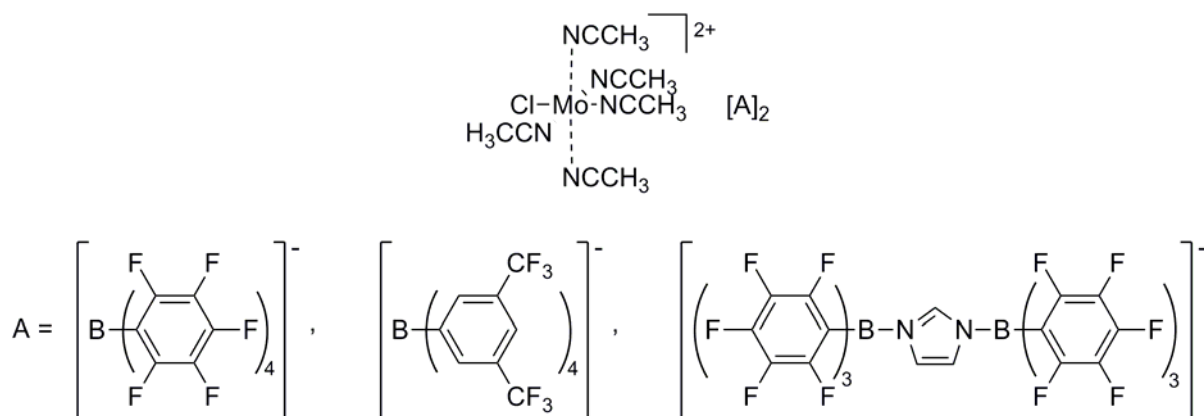
Figure 1.1.4. General structure of acetonitrile stabilized molybdenum(III) complexes with weakly coordinating anions that were tested for the polymerization of isobutene.

However, amongst all benefits, the most important advantage of these nitrile ligated transition metal complexes with their weakly coordinating counter anions is the possibility of controlling the reactivity and selectivity of the polymerization reaction under comparatively mild operating conditions. Thus, the use of these complexes is not only more efficient but also more environmentally compliant. Consequently, in the last few years they have attracted the interest of industry.[2, 19]

2. Nitrile ligated transition metal complexes with weakly coordinating anions

2.1 Weakly coordinating anions

Weakly (or non-) coordinating anions (WCAs) can be characterized by low overall charge and high degree of charge delocalization. Their advantageous properties as counter anions in metal complexes support the creation of vacant coordination sites in addition to a generation of "naked" metal ions. Thus, WCAs are able to enhance the reactivity of their cationic counterparts by increased accessibility and coordination strength. This has led to significant interest in both synthesis and catalysis.[20]

The expression "non-coordinating anion" was originally created to describe anions like $[ClO_4]^-$, $[SO_3CF_3]^-$, $[SO_3F]^-$, $[BF_4]^-$, $[PF_6]^-$, $[AsF_6]^-$, and $[SbF_6]^-$, which were shown to be non-coordinating in aqueous solutions.[20a] However, X-ray crystallography revealed that very

often, these anions can easily coordinate to cationic centers.[21] Besides, the factual

existence of an anion that has no capability at all for coordination in the condensed phase is

today believed to be "as unlikely as that of a free proton".[22] This was accounted for by

adopting the term "weakly coordinating anion" (WCA). Nevertheless, it is possible to find

conditions where the chemical environment of the ions can be neglected in first

approximation.[23] An anion will preferentially coordinate with the most electrophilic and

sterically accessible moiety in its environment. Thus, for the generation of more weakly

coordinating anions, the negative charge has to be delocalized over a large area of non-

nucleophilic and chemically robust building blocks.[20b] Following this underlying principle, a

large number of anions has been synthesized during the last decades.[20b, 24] The exchange

of fluorine atoms in BF_4^- ions for phenyl groups, for example, leads to bulky $[BAr^F_4]^-$ ions

$(Ar^F = -C_6F_5,$[24c] $-C_6H_3$-3,5-$(CF_3)_2,$[25] etc.). Other examples for relatively weakly coordinating

anions are BPh_4^-, $CB_{11}H_{12}^-$, and related carborane anions, closo borates (closo-$[B_{21}H_{18}]^-$,[26]

closo-$[B_{12}F_{12}]^{2-}$,[27] etc.), $[OTeF_5]^-$ and its derivatives, polyoxoanions such as $[PW_{12}O_{40}]^{3-}$,

$[HC(SO_2CF_3)_2]^-$, $[C_{60}]^-$, $[B(o-C_6H_4O_2)_2]^-$, anionic methylalumoxanes (MAO), and the hydride

sponge $[H(1,8-C_{10}H_6(BMe_2)_2)]^-$ (see Figure 1.2.1).[20a]
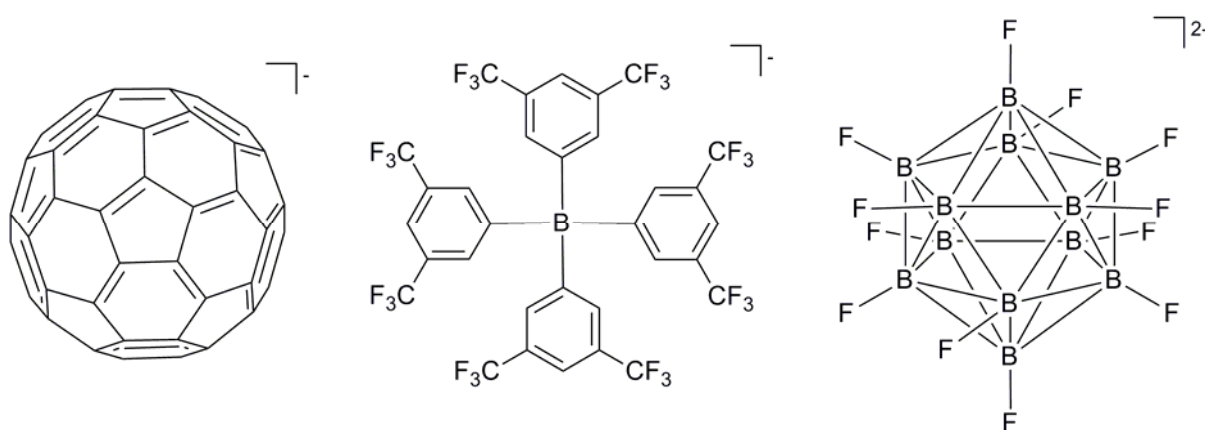
Figure 1.2.1. Schematic structures of the exemplary WCAs $[C_{60}]^-$,[28] $[B(C_6H_3$-3,5-$(CF_3)_2)_4]^-$[29] and closo-$[B_{12}F_{12}]^{2-}$.[27]

A number of strategies exist for introducing a designated WCA into a system in exchange for

a more coordinating substituent or ligand. For instance, abstraction of a methyl group from

$[Cp_2M(CH_3)_x]$ (M = Ti, Zr, Hf, Ta; x = 2, 3) by strong organometallic Lewis acids, e.g. $B(C_6F_5)_3$

leads to the formation of $[Cp_2MMe^+][MeB(C_6F_5)_3^-]$.[30] However, WCAs can also be attached *via* hydride and alkyl abstraction, with the reaction of the $[Ph_3C]^+$ salt of the WCA with $[Cp_2M(CH_3)_x]$ (M = Ti, Zr, Hf, Ta; x = 2, 3) yielding $[Cp_2M(CH_3)_{x-1}][A]$ (A = WCA) as a prototype.[20b, 30] Moreover, weakly coordinating anions can be introduced into a system through metathesis reactions of $M^+[A]^-$ ([A]- = WCA, M = univalent metal, such as Li, Na, K, Ag, Tl) with either labile or covalently bound halide ligands.[24b, 31]
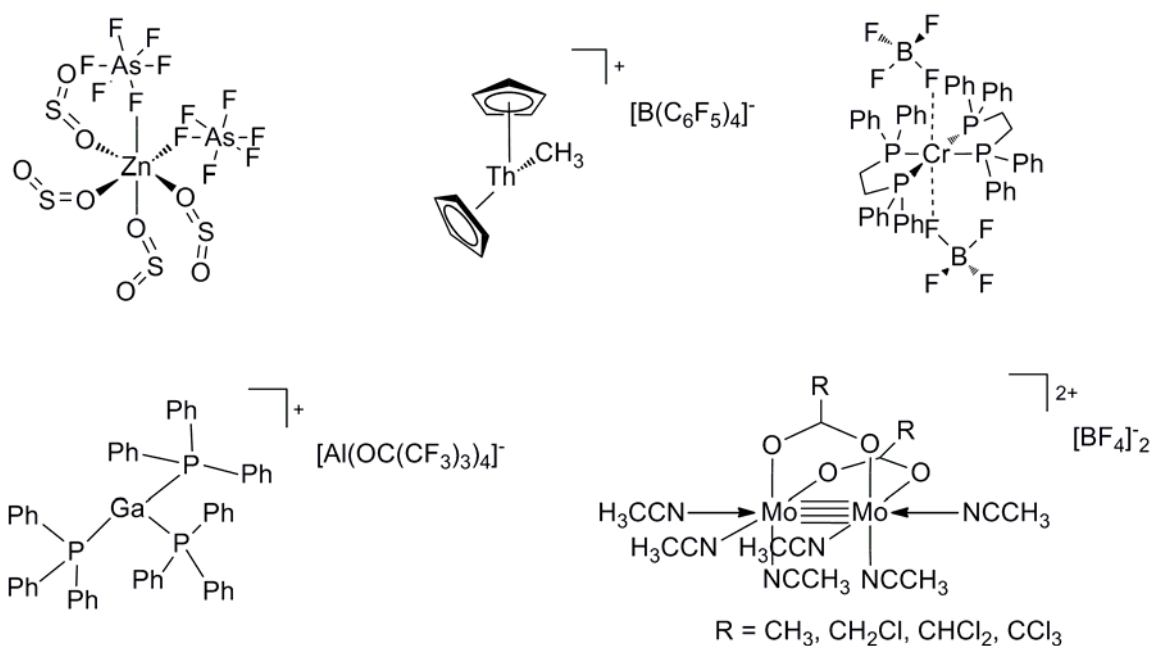
Figure 1.2.2. Schematic structures of the complexes $[Zn(SO_2)_4(AsF_6)_2]$,[32] $[Cp'_2ThCH_3][B(C_6F_5)_4]$,[33] $[Cr(dppe)_2][BF_4]_2$,[34] *cis*-$[Mo_2(m\text{-}O_2CR)_2(CH_3CN)_6][BF_4]_2$ (R = Me, CH_2Cl, $CHCl_2$, CCl_3)[35] and $[Ga(PPh_3)_3][Al(OC(CF_3)_3)_4]$.[36]

To account for the importance of weakly coordinating anions, several reviews have been written by *Krossing* and *Raabe*,[20b] *Macchioni*[37] and *Strauss*,[20a] over the past few years, regarding the robustness of different WCAs and their influence on chemical reactions. Besides, *Chen* and *Marks* highlight the versatile and important role as co-catalysts for olefin polymerization due to their role in the formation of highly active catalyst species.[30]

2.2 Synthesis of nitrile ligated complexes

Numerous complexes, with main group[38] transition metal[39] and lanthanide element[40] cations, which are stabilized by neutral, non-aqueous ligands have been applied in various chemical processes.[41] For applications both in synthesis and catalysis, complexes ligated with easily dissociable (in general donor) solvent molecules have proven to be exceptionally effective. These ligands can be easily replaced by more strongly coordinating donors, other metal cores or by substrates.[42] Thus the resulting complexes are perfectly suitable starting materials for the synthesis of other complexes,[34, 43] inorganic materials[44] and catalysts.[45] Amongst the complexes with easily exchangeable ligands the nitrile coordinated ones are not only the longest known[46] and best studied,[47] but also have found industrial applications.[30] The synthesis of complexes of the general formulae $[M(RCN)_{2,4,5,6}][A]_{1,2}$ and $[MX(RCN)_5][A]_2$ (M = transition metal ion; A = counterion; R = organic fragment; X = halide) can be carried out using several methods, among them oxidation of metals with nitrosonium salts of the intended counteranion,[48] or dehydration of aqueous salts.[49] Many other options exist,[36, 50] but the most commonly used method to introduce weakly coordinating anions to organonitrile complexes is the aforementioned usage of metathesis reagents such as potassium, amine and silver salts in nitrile solvents (see Scheme 1.2.1).[24b]

$$Cu \ + \ 2\,NOClO_4 \ \xrightarrow[\text{rt}]{(CH_3CN)} \ [Cu(CH_3CN)_4][ClO_4]_2 \ + \ 2\,NO$$

$$[M(H_2O)_x][BF_4]_2 \ \xrightarrow[\Delta,\ \text{sieves}]{(CH_3CN)} \ [M(CH_3CN)_x][BF_4]_2 \ + \ x\,H_2O \quad (M = Mn,\ Fe,\ Co,\ Ni,\ Cu)$$

$$CuCl_2 \ + \ 2\,Ag[B(C_6F_5)_4] \ \xrightarrow[\text{rt}]{(C_6H_5CN)} \ [Cu(C_6H_5CN)_6][B(C_6F_5)_4]_2 \ + \ 2\,AgCl$$
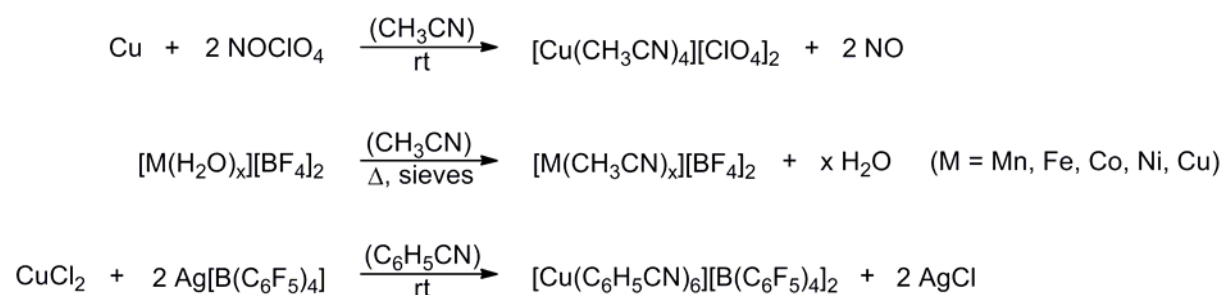
Scheme 1.2.1 Possible pathways for the preparation of nitrile-ligated transition metal complexes with weakly coordinating anions.[9d, 48-49]

Since these compounds exhibit a versatile applicability, the interest in the exploration of their properties is enormous and a multitude of promising compounds has been synthesized and characterized during the last decades.[16, 30, 35, 51] Meanwhile, nitrile ligated monomeric

complexes with weakly coordinating counter anions of nearly every first row and a number of second and third row transition metals have been reported.[17b, 31a, 32, 34, 39c, 52]

2.3 Immobilization of nitrile ligated transition metal complexes – state of the art

In light of a shortage of fossil fuels approaching at an alarming rate, the requirement of more efficient chemical processes is increasing rapidly. In order to lower energy consumption, making use of catalysis is of high importance in chemical manufacturing. Today, 80 to 90 % of all industrial chemical processes depend on catalysis.[53] However, typically about 80 % of the energy consumption and expense of a process arises from the separation of products and catalyst from the reaction mixture.[54] With regard to the fact that catalysts are often the most expensive component in the reaction mixture the optimal combination of high catalyst efficiency and good catalyst recyclability from the reaction mixture is of critical importance.

The main advantages of homogeneous transition metal catalysts are the accessibility of all active sites, their uniform structure and the possibility to control speed and selectivity by catalyst design under comparatively mild operating conditions. But a short lifetime and problematic separation from the products make the reuse of homogeneous catalysts difficult and their application often uneconomical in large scale application. Thus, heterogeneous catalysts are in general regarded as being more desirable for use in industrial processes. However, heterogeneous catalysts often have severe drawbacks, such as low selectivity, low activity (and low concentration of accessible active sites), or harsh (energy intensive) reaction conditions. One method of overcoming these drawbacks and combining the positive aspects of both homogeneous and heterogeneous catalysis is the formation of so called "hybrid catalysts" to which heterogenized homogeneous catalysts are classified (see Figure 1.2.1).[55] Heterogenization can be realized by attaching homogeneous catalysts either to organic polymers[56] or to inorganic supports[57] in a manner that the ligand sphere is preserved around the metal and the complex remains accessible.
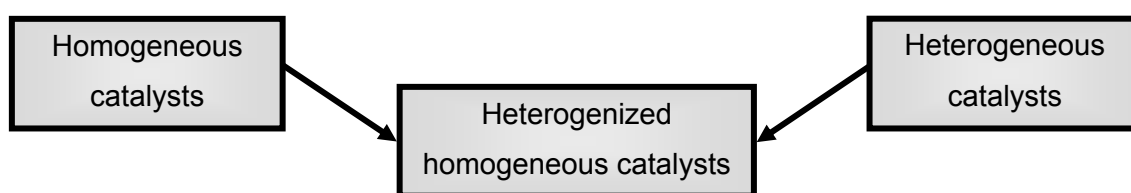
Figure 1.2.1 Schematic combination of homogeneous and heterogeneous catalysts towards heterogenized homogenous catalysts.

Much effort has been made to convert homogeneous into heterogeneous catalysts *via* anchoring on insoluble support materials. Surface organometallic chemistry describes in this respect the immobilization of isolated ions, atoms, molecular complexes, or clusters on support surfaces or in their pores. Additional work has been made in terms of grafting of organometallic complexes to support materials by long and flexible linkers. Whereby mainly inert materials, typically composed of amorphous silica, are used as supports.[53a]

Covalent binding is by far the most frequently used and also most sophisticated strategy, as this binding may be strong enough to withstand even extremely harsh reaction conditions. Covalent immobilization can be carried out either by copolymerization of functionalized ligands with a suitable comonomer, or by grafting functionalized ligands as well as metal complexes with reactive groups onto a preformed support. Most important is that the heterogenization is carried out in a way that does not hamper the catalytic activity. Problems can occur, when bonds between metals and ligands are broken and reformed during catalytic reactions. In this case, the catalyst may break away from the support and become dissolved. This leaching process leads to loss of catalyst activity.

An alternative but less commonly used approach involves ionic binding and adsorption. A range of support materials with ion-exchange capabilities can be used, including organic or inorganic ion exchange resins, mesoporous silicates and zeolites. The advantage of heterogenization by ionic binding and adsorption is the relative ease of preparation of the immobilisation of metal cations and complexes by simple procedures, mostly even without the necessity of previously functionalizing ligands. For encapsulation or entrapment no interaction between catalyst and support material are required and therefore reaction

conditions are close to homogeneously catalyzed processes. Only obligation is that the catalyst must be larger than the pores of the support material to prevent loss of the catalyst during the course of the reaction and the target molecules need to be smaller than these pores.

The described techniques have their advantages and disadvantages; which of them will finally be chosen depends above all on the reaction conditions and the nature of the catalysts.[55, 58] In the case of nitrile ligated transition metal complexes with weakly coordinating anions, each of these methods seems to be feasible and indeed, several approaches have been undertaken in these directions, either by anchoring the cations or the anions.

2.3.1 Anchoring *via* the cation

Inorganic support

Silica materials which are frequently used for immobilization are MCM-41, MCM-48 (MCM = Mobile Crystalline Material) and the mesoporous molecular sieve SBA-15 (SBA = Silica-Block poly(Alkylene oxide). MCM-41 consists of hexagonally packed one-dimensional channels which are embedded in a matrix of amorphous silica, have pore diameters which are tuneable in a range between 20 and 100 Å and have notably high surface areas (> 1000 m^2g^{-1}), high pore volumes (> 1 cm^3g^{-1}) and very narrow pore size distributions.[59] MCM-48 consists of two independent, intricately interwoven networks of mesoporous channels, which makes the pore system accessible in three dimensions. It has a surface area exceeding 1500 m^2g^{-1}, pore volumes > 1 cm^3g^{-1} and a very narrow pore size distribution, as well.[60] Among the examined mesoporous materials, SBA-15 has by far the largest pore size. It has highly ordered hexagonally arranged meso channels, with thick walls, adjustable pore sizes from 3 to 30 nm, a high chemical and thermal stability and again exhibits a narrow pore size distribution.[61]

Several methods were tested for the anchoring of nitrile-ligated transition metal complexes to these mesoporous silica surfaces. Direct grafting by substitution of a metal-bonded nitrile

group by a surface-bound hydroxyl group leads to the loss of a weakly coordinating anion. The Lewis acidity of the metal is reduced by the formation of an oxygen-metal bond. In consequence metal charge is reduced resulting in a complete loss of activity for isobutene polymerization.[62] In contrast, immobilization on silica material that had been derivatized with pyrazolpyridine ligands (see Scheme 1.2.2) seemed to be more convenient, as the charge of the metal core was maintained.[63]
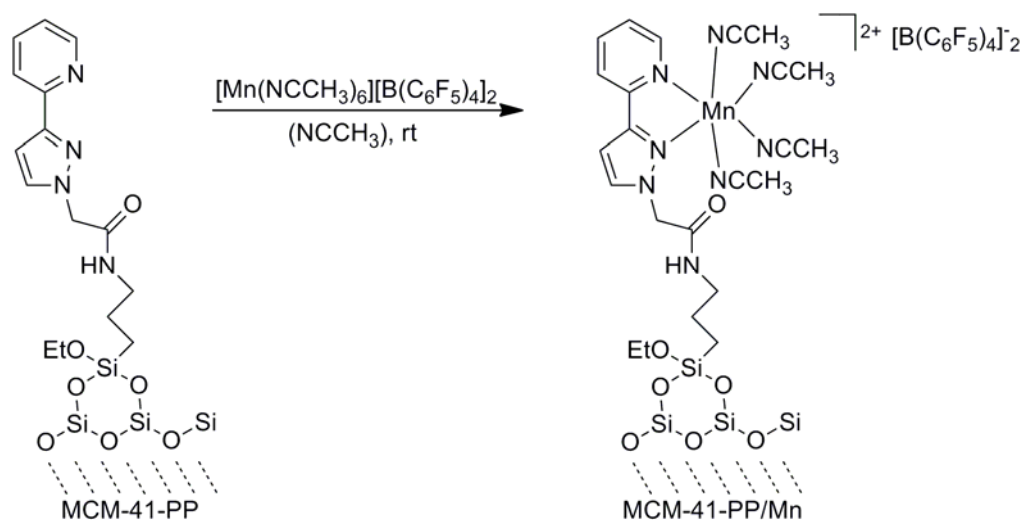
Scheme 1.2.2 Anchoring of $[Mn(CH_3CN)_6][B(C_6F_5)_4]_2$ on modified MCM-41.[63]

The additional electron density provided by the neutral bidentate Lewis base ligand is known to significantly reduce the catalytic activity of the cation. It was shown again that the immobilized catalyst exhibits no activity in isobutene polymerization, whereas reduced activity was reported in another reaction.[62] Accompanied by the fact that only one third of the pyrazolpyridine ligands are coordinated to the manganese centers, residual N-donor groups remain uncoordinated and thus have the possibility to interfere with intermediates which are formed during the polymerization reaction.

A different procedure which was expected to avoid the drawbacks of the above-mentioned methods was grafting *via* the partial ion exchange of H^+ or Na^+ cations present in the surface of the mesoporous materials H-AlMCM-41, Na-AlMCM-41, H-AlMCM-48, or Na-AlMCM-48 by nitrile ligated transition metal cations. By means of this method, the cation and one of the noncoordinating anions remain basically unchanged. This approach was used for the synthesis of different systems: $[Mn(CH_3CN)_6][B(C_6F_5)_4]_2$ grafted on H-AlMCM-41/48 or Na-

AlMCM-41/48 (see Scheme 1.2.3)[62] and $[Cu(CH_3CN)_6][B(C_6F_5)_4]_2$, heterogenized on Na-AlMCM-41 or Na-AlMCM-48.[64]
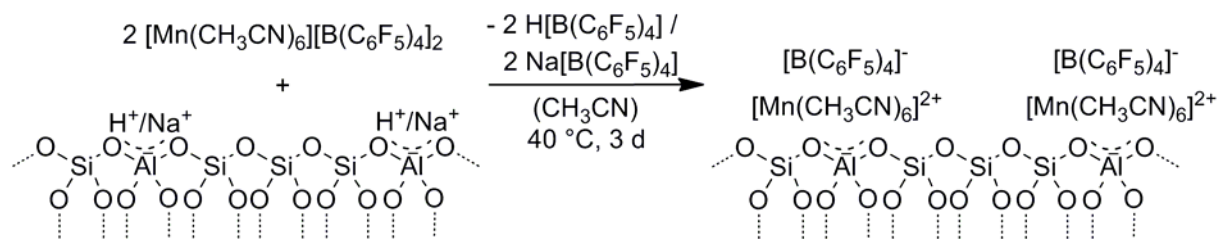
Scheme 1.2.3 Immoblilization of $[Mn(CH_3CN)_6][B(C_6F_5)_4]_2$ on a mesoporous silica surface.[62]

When tested as catalyst for olefin aziridination, the immobilized copper complexes generate product yields in the same order of magnitude as those of the homogeneous systems or even higher.[64] However to date, the grafted manganese system is the only heterogenized complex which shows a degree of activity in isobutene polymerization, albeit only with product yields of 3 to 8 %. The low activity is most likely due to the presence of remaining H^+/Na^+ ions on the surface (the support material itself is inactive), influencing the polymerization process negatively.[62]

To take advantage of the larger pore size of SBA-15 and to test a further anchoring technique, $[Cu(CH_3CN)_6][B\{C_6H_3(m\text{-}CF_3)_2\}_4]_2$ was grafted on the surface of aminosilane-modified SBA-15 (see Figure 1.2.2).[65]
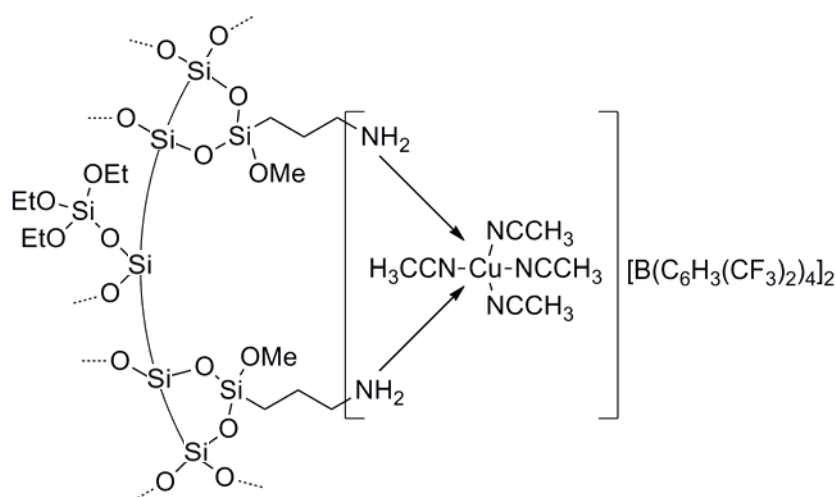
Figure 1.2.2. Schematic description for the immobilization product of $[Cu(CH_3CN)_6][B(C_6H_3(CF_3)_2)_4]_2$ on SBA-15.[65]

The heterogeneous complex showed in several cases even better performance than its homogeneous counterpart *e.g.* as catalyst in aldehyde olefination,[65] but failed in the polymerization of isobutene, most likely due to the basicity of the nitrile groups.

Organic support

As support of nitrile ligated complexes on inorganic materials failed, focus was moved towards organic support materials. Classic example is the coordination of metal organic compounds on polymers which have easily accessible coordinating functionalities. This should allow both stability and uniformity of the obtained materials. Hence, the two copper complexes $[Cu(CH_3CN)_6][B\{C_6H_3(m\text{-}CF_3)_2\}_4]_2$ and $[Cu(CH_3CN)_6][B(C_6F_5)_4]_2$ were immobilized on poly(4-vinylpyridine) (P4vP) *via* the pendant pyridine N-donor groups (see Scheme 1.2.4).
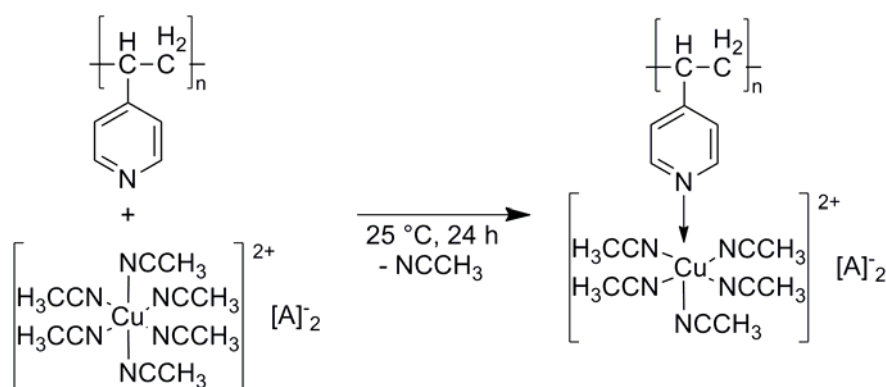
Scheme 1.2.4 Anchoring of $[Cu(CH_3CN)_6][A]_2$ $(A = B(C_6F_5)_4^-, B(C_6H_3(CF_3)_2)_4^-)$ on poly(4-vinylpyridine).[66]

This material was shown to be highly reactive in olefin cyclopropanation and in the case of cyclooctene, the activity of the immobilized catalysts was even higher than that of the unsupported complexes.[66] But again they did not show any activity in isobutene polymerization. This is presumably due to an excessively strong donor effect of the pyridine nitrogen that affects the Lewis acidity of the metal core as well as to unreacted pyridine groups that may, as already mentioned above, hamper the polymerization reaction.

2.3.2 Anchoring *via* the anion

Another approach was the fixation of the anion to MCM-41 (see Scheme 1.2.5). In this way, the Lewis acidity and coordination accessibility of the metal center was not expected to be affected negatively. Thus, the activity of the complex was proposed to remain unchanged or even improved.
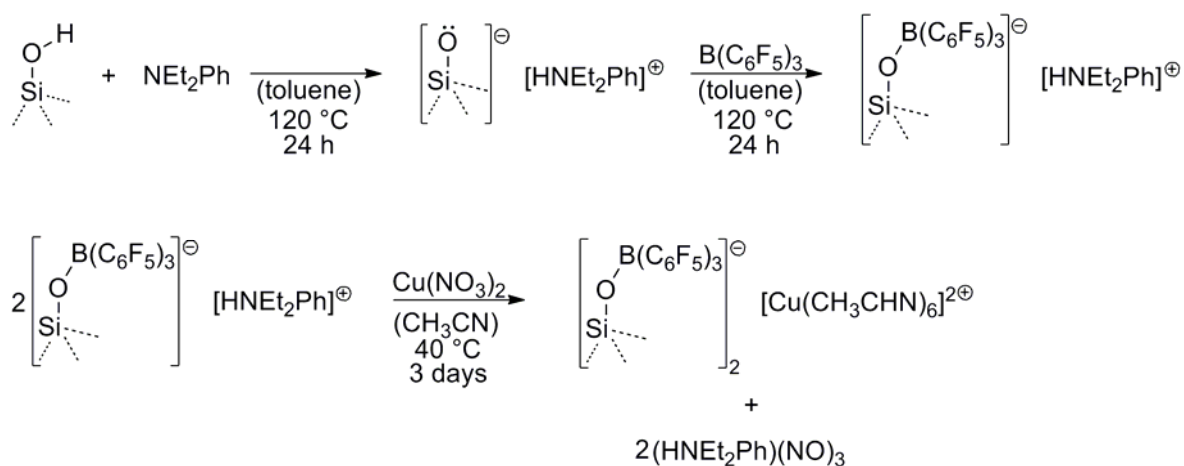
Scheme 1.2.5 Anchoring of $[Cu(CH_3CN)_6][B(C_6F_5)_4]_2$ on modified MCM-41.

Again, this composite showed good performance in a different reaction, the styrene cyclopropanation,[67] but was intriguingly not active at all in the polymerization of isobutene. Up to now no active heterogenized organonitrile ligated metal-based mediators for this polymerization reaction are reported.

II. Objectives of this work

Nitrile stabilized transition metal complexes with weakly coordinating counter anions (WCAs) are more efficient and environmentally benign starting materials for the polymerization of isobutene, yielding highly reactive polyisobutene, than the cationic initiators which are currently applied in industry. However, for commercial use, the methods by which these complexes are synthesized have to be improved concerning reproducibility and efficiency.

Therefore, one focus of this work is set on the development of more efficient methods for the production of these mediators for isobutene polymerization reported by *Kühn et al.*. The new route for synthetic access to these complexes has to circumvent the expensive silver salts of WCAs usually employed as metathesis reagents. Additionally a successful heterogenization of these compounds could lead to significant improvements in the applicability of this system. To date no method has been found to generate active heterogenized nitrile ligated complexes for isobutene polymerization. Thus, low molecular weight WCA based model compounds are designed which, after subsequent reaction with metal precursors, could be used as test systems for heterogenization of these mediators.

However, since the detailed polymerization mechanism with the aforementioned complexes is still unknown, the creation of more effective mediators is problematic. To gain additional insight test experiments are designed and conducted based on available literature data combined with new considerations. These experiments include screening of potential mediators for isobutene polymerization activity and model systems for detailed investigation of possible initiation reactions.

References

[1]   a) J. P. Kennedy, E. Maréchal, in *Carbocationic Polymerization*, John Wiley & Sons, New York, **1982**, pp. 475; b) P. H. Plesch, in *The Chemistry of Cationic Polymerization* (Ed.: P. H. Plesch), Pergamon Press, Oxford, **1963**, pp. 142; c) O. Nuyken, M. Vierle, F. E. Kühn, Y. Zhang, *Macromol. Symp.* **2006**, *236*, 69.

[2]   S. F. Rach, F. E. Kühn, *Sustainability* **2009**, *1*, 35.

[3]   A. Buttlerow, V. Gorjainow, *Ber. dtsch. chem. Ges.* **1873**, *6*, 561.

[4]   a) S. W. Lebedew, E. P. Filonenko, *Ber. dtsch. chem. Ges.* **1925**, *58*, 163; b) S. W. Lebedew, G. G. Kablianski, *Ber. dtsch. chem. Ges.* **1930**, *63*, 103.

[5]   a) M. Otto, M. M. Cunradi, in *Chemical Abstracts* (Ed.: I. F. AG), Germany, **1937**; b) J. P. Kennedy, John Wiley & Sons, New York, **1975**, pp. 10.

[6]   a) W. Immel, in *Ullmanns Encyclopädie der technischen Chemie, Vol. 19*, 4 ed. (Ed.: F. Ullmann), Verlag Chemie Weinheim, **1980**, pp. 216; b) E. N. Kresge, R. H. Schatz, H.-C. Wang, in *Encyclopedia of polymer science and engineering, Vol. 8*, 2 ed. (Eds.: H. F. Mark, N. Bikales, C. G. Overberger, G. Menges), Wiley USA, **1987**, pp. 423.

[7]   H. Güterbock, *Polyisobutylen und Mischpolymerisate*, Springer, Berlin, **1959**.

[8]   a) S. Nikezić, Nedeljković, *Tribology in industry* **2002**, *24*, 39; b) J. D. Burrington, J. R. Johnson, J. K. Pudelski, *Top. Catal.* **2003**, *23*, 175.

[9]   a) H. P. Rath, H. Mach, H. Schwahn, P. Schreyer, E. K. Fehr, BASF AG (DE), **1994**, *EP19940108434*; b) H. P. Rath, T. Perner, E. Schauß, BASF AG (DE), **2005**, *DE10361633A1*; c) H. Auer, D. Borchers, T. Wettling, BASF AG (DE), **2008**, *EP20020782447*; d) Y. Li, L. T. Voon, H. Y. Yeong, A. K. Hijazi, N. Radhakrishnan, K. Köhler, B. Voit, O. Nuyken, F. E. Kühn, *Chem. Eur. J.* **2008**, *14*, 7997; e) B. Wilson, *Industrial Lubrication and Tribology* **1995**, *47*, 4; f) D. Franz, R. Kummer, H. Mach, H. P. Rath, BASF AG (DE)., **1989**, *4859210*.

[10]   a) K. E. Russel, L. G. M. C. Vail, in *Fourth International Symposium on Cationic Polymerization, Vol. 56* (Ed.: J. P. Kennedy), John Wiley & Sons, University of Akron,

Ohio, **1976**, pp. 183; b) A. K. Hijazi, N. Radhakrishnan, K. R. Jain, E. Herdtweck, O. Nuyken, H.-M. Walter, P. Hanefeld, B. Voit, F. E. Kühn, *Angew. Chem. Int. Ed.* **2007**, *46*, 7290.

[11]   a) J. Si, J. P. Kennedy, *J. Polym. Sci. A: Polym. Chem.* **1994**, *32*, 2011; b) K. E. Russel, in *Cationic Polymerisation and Related Complexes* (Ed.: P. H. Plesch), H. Heffer & Sons Ltd. , University College of North Staffordshire, **1952**, pp. 114.

[12]   O. Nuyken, M. Vierle, *Des. Monomers Polym.* **2005**, *8*, 91.

[13]   a) T. D. Shaffer, J. R. Ashbaugh, *J. Polym. Sci. A: Polym. Chem.* **1997**, *35*, 329; b) H. P. Rath, BASF AG., **1995**, *US005408018A*; c) H. Auer, U. Kanne, A. De Vos, Keil & Weinkauf, **2004**, *US2040039141A1*.

[14]   a) F. Barsan, M. C. Baird, *J. Chem. Soc., Chem. Commun.* **1995**, 1065; b)F. Barsan, A. R. Karam, M. A. Parent, M. C. Baird, *Macromolecules* **1998**, *31*, 8439.

[15]   a) A. Guerrero, K. Kulbaba, M. Bochmann, *Macromolecules* **2007**, *40*, 4124; b) A. Guerrero, K. Kulbaba, M. Bochmann, *Macromol. Chem. Phys.* **2008**, *209*, 1714.

[16]   M. Vierle, Y. Zhang, E. Herdtweck, M. Bohnenpoll, O. Nuyken, F. E. Kühn, *Angew. Chem. Int. Ed.* **2003**, *42*, 1307.

[17]   a) A. K. Hijazi, A. Al Hmaideen, S. Syukri, N. Radhakrishnan, E. Herdtweck, B. Voit, F. E. Kühn, *Eur. J. Inorg. Chem.* **2008**, *2008*, 2892; b) A. K. Hijazi, H. Y. Yeong, Y. Zhang, E. Herdtweck, O. Nuyken, F. E. Kühn, *Macromol. Rapid Commun.* **2007**, *28*, 670; c) M. Vierle, Y. Zhang, A. M. Santos, K. Köhler, C. Haeßner, E. Herdtweck, M. Bohnenpoll, O. Nuyken, F. E. Kühn, *Chem. Eur. J.* **2004**, *10*, 6323; d) N. Radhakrishnan, A. K. Hijazi, H. Komber, B. Voit, S. Zschoche, F. E. Kühn, O. Nuyken, M. Walter, P. Hanefeld, *J. Polym. Sci., Part A: Polym. Chem.* **2007**, *45*, 5636.

[18]   M. S. C. Fleet, P. H. Plesch, in *Cationic Polymerisation and Related Complexes* (Ed.: P. H. Plesch), W. Heffer & Sons Ltd., University College of North Staffordshire, **1952**, pp. 119.

[19]   a) P. Hanefeld, V. Böhm, M. Sigl, N. Challand, M. Röper, H.-M. Walter, B. Voigt, F. E. Kühn, A. K. Hijazi, R. K. Narayanan, Germany, BASF AG (DE), **2007**, *DE200510055817A1*; b) H. P. Rath, H.-M. Walter, O. Nuyken, F. E. Kühn, Y. Zhang, H. Y. Yeong, BASF AG (DE), **2007**, *WO2007020246A1*; c) H.-M. Walter, P. Hanefeld, F. E. Kühn, S. Ayyamperumal, A. Hijazi, B. Voit, R. K. Narayanan, BASF AG (DE), **2007**, *DE102005038284A1*; d) H.-M. Walter, M. Herrlich-Loos, F. E. Kühn, Y. Zhang, B. Voit, R. K. Narayanan, BASF AG (DE), **2007**, *WO207020247A2*.

[20]   a) S. H. Strauss, *Chem. Rev.* **1993**, *93*, 927; b) I. Krossing, I. Raabe, *Angew. Chem. Int. Ed.* **2004**, *43*, 2066; c) S. F. Rach, F. E. Kühn, *Chem. Rev.* **2009**, *109*, 2061; d) R. Sheldon, *Chem. Commun.* **2001**, 2399.

[21]   a) M. R. Rosenthal, *J. Chem. Educ.* **1973**, *50*, 331; b) W. Beck, K. Sünkel, *Chem. Rev.* **1988**, *88*, 1405.

[22]   a) K. Seppelt, *Angew. Chem.* **1993**, *105*, 1074; b) K. Seppelt, *Angew. Chem. Int. Ed.* **1993**, *32*, 1025.

[23]   a) M. Bochmann, *Angew. Chem.* **1992**, *104*, 1206; b) M. Bochmann, *Angew. Chem. Int. Ed.* **1992**, *31*, 1181.

[24]   a) F. Barrière, W. E. Geiger, *J. Am. Chem. Soc.* **2006**, *128*, 3980; b) W. E. Buschmann, J. S. Miller, *Inorg. Synth.* **2002**, *33*, 83; c) A. G. Massey, A. J. Park, *J. Organomet. Chem.* **1964**, *2*, 245.

[25]   J. H. Golden, P. F. Mutolo, E. B. Lobkovsky, F. J. DiSalvo, *Inorg. Chem.* **1994**, *33*, 5374.

[26]   E. Bernhardt, D. J. Brauer, M. Finze, H. Willner, *Angew. Chem. Int. Ed.* **2007**, *46*, 2927.

[27]   S. V. Ivanov, S. M. Miller, O. P. Anderson, K. A. Solntsev, S. H. Strauss, *J. Am. Chem. Soc.* **2003**, *125*, 4694.

[28]   A. Pénicaud, J. Hsu, C. A. Reed, A. Koch, K. C. Khemani, P. M. Allemand, F. Wudl, *J. Am. Chem. Soc.* **1991**, *113*, 6698.

[29]   M. Brookhart, B. Grant, A. F. Volpe, *Organometallics* **1992**, *11*, 3920.

[30] E. Y. X. Chen, T. J. Marks, *Chem. Rev.* **2000**, *100*, 1391.

[31] a) W. E. Buschmann, J. S. Miller, *Chem. Eur. J.* **1998**, *4*, 1731; b) G. Bodizs, I. Raabe, R. Scopelliti, I. Krossing, L. Helm, *Dalton. Trans.* **2009**, 5137.

[32] Ö. N. Akkus, A. Decken, C. Knapp, J. Passmore, *J. Chem. Cryst.* **2006**, *36*, 321.

[33] X. Yang, C. Stern, T. J. Marks, *Organometallics* **1991**, *10*, 840.

[34] R. T. Henriques, E. Herdtweck, F. E. Kühn, A. D. Lopes, J. Mink, C. C. Romão, *J. Chem. Soc., Dalton Trans.* **1998**, 1293.

[35] F. E. Kühn, J. R. Ismeier, D. Schön, W.-M. Xue, G. Zhang, O. Nuyken, *Macromol. Rapid. Commun.* **1999**, *20*, 555.

[36] J. M. Slattery, A. Higelin, T. Bayer, I. Krossing, *Angew. Chem. Int. Ed.* **2010**, *49*, 3228.

[37] A. Macchioni, *Chem. Rev.* **2005**, *105*, 2039.

[38] a) C. D. Schmulbach, *J. Inorg. Nucl. Chem.* **1964**, *26*, 745; b) E. T. Hitchcock, P. J. Elving, *Anal. Chim. Acta* **1963**, *28*, 417; c) P. Sobota, T. Pluzinski, T. Lis, *Polyhedron* **1984**, *3*, 45.

[39] a) F. A. Cotton, R. Francis, *J. Am. Chem. Soc.* **1960**, *82*, 2986; b) R. S. Drago, D. W. Meek, M. D. Joesten, L. LaRoche, *Inorg. Chem.* **1963**, *2*, 124; c) J. J. Habeeb, F. F. Said, D. G. Tuck, *J. Chem. Soc., Dalton Trans.* **1981**, 118; d) D. W. Meek, R. S. Drago, T. S. Piper, *Inorg. Chem.* **1962**, *1*, 285; e) H. Meerwein, V. Hederich, K. Wunderlich, *Arch. Pharm.* **1958**, *291*, 541; f) S. F. Pavkovic, D. W. Meek, *Inorg. Chem.* **1965**, *4*, 1091.

[40] a) G. B. Deacon, B. Görtler, P. C. Junk, E. Lork, R. Mews, J. Petersen, B. Zemva, *J. Am. Chem. Soc., Dalton Trans.* **1998**, 3887; b) W. J. Evans, M. A. Johnston, M. A. Greci, T. S. Gummersheimer, J. W. Ziller, *Polyhedron* **2003**, *22*, 119; c) G. Heckmann, M. Niemeyer, *J. Am. Chem. Soc.* **2000**, *122*, 4227.

[41] a) E. Albizzati, E. Giannetti, U. Giannini, *Makromol. Chem., Rapid Commun.* **1984**, *5*, 673; b R. G. Salomon, J. K. Kochi, *J. Am. Chem. Soc.* **1973**, *95*, 3300; c) M. McCann,

in *Catalysis by Di-and Polynuclear Metal Cluster Complexes* (Eds.: R. D. Adams, F. A. Cotton), Wiley-VCH, New York, **1998**, pp. 145.

[42] a) F. A. Cotton, F. E. Kühn, *Inorg. Chim. Acta* **1996**, *252*, 257; b) F. A. Cotton, L. M. Daniels, S. C. Haefner, F. E. Kühn, *Inorg. Chim. Acta* **1999**, *287*, 159.

[43] B. N. Storhoff, H. C. Lewis Jr, *Coord. Chem. Rev.* **1977**, *23*, 1.

[44] a) H. Zhao, R. A. Heintz, K. R. Dunbar, R. D. Rogers, *J. Am. Chem. Soc.* **1996**, *118*, 12844; b) G. M. Finniss, E. Canadell, C. Campana, K. R. Dunbar, *Angew. Chem. Int. Ed. Engl.* **1996**, *35*, 2771.

[45] A. Sen, *Acc. Chem. Res.* **1988**, *21*, 421.

[46] W. Henke, *Liebigs Ann. Chem.* **1858**, *106*, 280.

[47] M. Kubota, D. L. Johnston, *J. Inorg. Nucl. Chem.* **1967**, *29*, 769.

[48] B. J. Hathaway, A. E. Underhill, *J. Chem. Soc.* **1960**, 3705.

[49] R. A. Heintz, J. A. Smith, P. S. Szalay, A. Weisgerber, K. R. Dunbar, *Inorg. Synth.* **2002**, *33*, 75.

[50] a) G. J. Kubas, *Inorg. Synth.* **1979**, *19*, 90; b) M. Huber, A. Kurek, I. Krossing, R. Mülhaupt, H. Schnöckel, *Z. anorg. allg. Chem.* **2009**, *635*, 1787.

[51] a) A. Sen, T.-W. Lai, *J. Am. Chem. Soc.* **1981**, *103*, 4627; b) A. Sen, T. W. Lai, *Inorg. Chem.* **1984**, *23*, 3257.

[52] a) F. E. Kühn, D. Schön, G. Zhang, O. Nuyken, *J. Macromol. Sci, Pure Appl. Chem. A* **2000**, *37*, 971; b) E. B. Vickers, I. D. Giles, J. S. Miller, *Chem. Mater.* **2005**, *17*, 1667; c) B. J. Hathaway, D. G. Holah, A. E. Underhill, *J. Chem. Soc.* **1962**, 2444; d) M. J. Sisley, Y. Yano, T. W. Swaddle, *Inorg. Chem.* **1982**, *21*, 1141; e) F. K. Meyer, K. E. Newman, A. E. Merbach, *Inorg. Chem.* **1979**, *18*, 2142; f) C. M. Duff, G. A. Heath, *J. Chem. Soc., Dalton Trans.* **1991**, 2401; g) M. E. Prater, L. E. Pence, R. Clérac, G. M. Finniss, C. Campana, P. Auban-Senzier, D. Jérome, E. Canadell, K. R. Dunbar, *J. Am. Chem. Soc.* **1999**, *121*, 8005; h) B. v. Ahsen, B. Bley, S. Proemmel, R. Wartchow, H. Willner, *Z. anorg. allg. Chem.* **1998**, *624*, 1125; i) V. W.-W. Yam, K.-L. Yu, E. C.-C. Cheng, P. K.-Y. Yeung, K.-K. Cheung, N. Zhu, *Chem. Eur. J.* **2002**, *8*,

4121; j) O. F. Wendt, N.-F. K. Kaiser, L. I. Elding, *J. Chem. Soc., Dalton Trans.* **1997**, 4733; k) R. Kissner, P. Latal, G. Geier, *J. Chem. Soc., Chem. Commun.* **1993**, 136.

[53] a) A. Thomas, M. Driess, *Angew. Chem. Int. Ed.* **2009**, *48*, 1890; b) C. Copéret, M. Chabanas, R. P. Saint-Arroman, J.-M. Basset, *Angew. Chem. Int. Ed.* **2003**, *42*, 156.

[54] Sir J. M. Thomas, *Chem. Cat. Chem.* **2010**, *2*, 127.

[55] a) D. J. Cole-Hamilton, *Science* **2003**, *299*, 1702; b) N. End, K.-U. Schöning, *Top. Curr. Chem.* **2004**, *242*, 241.

[56] a) H. Friedrich, N. Singh, *Catal. Lett.* **2006**, *110*, 61; b) N. E. Leadbeater, M. Marco, *Chem. Rev.* **2002**, *102*, 3217; c) C. A. McNamara, M. J. Dixon, M. Bradley, *Chem. Rev.* **2002**, *102*, 3275; d) A. K. Kakkar, *Chem. Rev.* **2002**, *102*, 3579.

[57] a) Q. Zhuang, A. Fukuoka, T. Fujimoto, K. Tanaka, M. Ichikawa, *J. Chem. Soc., Chem. Commun.* **1991**, 745; b) D. E. De Vos, M. Dams, B. F. Sels, P. A. Jacobs, *Chem. Rev.* **2002**, *102*, 3615.

[58] a) A. Corma, H. Garcia, *Adv. Synth. Catal.* **2006**, *348*, 1391; b) G. G. Hlatky, *Chem. Rev.* **2000**, *100*, 1347; c) P. McMorn, G. J. Hutchings, *Chem. Soc. Rev.* **2004**, *33*, 108.

[59] a) J. S. Beck, J. C. Vartuli, W. J. Roth, M. E. Leonowicz, C. T. Kresge, K. D. Schmitt, C.-T. W. Chu, D. H. Olson, E. W. Sheppard, S. B. McCullen, J. B. Higgins, J. L. Schlenker, *J. Am. Chem. Soc.* **1992**, *114*, 10834; b) P. Ferreira, F. E. Kühn, *Trends in Inorganic Chemistry* **2001**, *7*, 89.

[60] a) C. Pettito, A. Galarneau, M.-F. Driole, B. Chiche, B. Alonso, F. Di Renzo, F. Fajula, *Chem. Mater.* **2005**, *17*, 2120; b) B. Boote, H. Subramanian, K. T. Ranjit, *Chem. Commun.* **2007**, 4543.

[61] a) B. L. Newalkar, S. Komarneni, H. Katsuki, *Chem. Commun.* **2000**, 2389; b) A. Sayari, Y. Yang, *Chem. Mater.* **2005**, *17*, 6108; c) M. Can, B. Akça, A. Yilmaz, D. Üner, *Turk. J. Phys.* **2005**, *29*, 287; d) D. Zhao, J. Feng, Q. Huo, N. Melosh, G. H. Fredrickson, B. F. Chmelka, G. D. Stucky, *Science* **1998**, *279*, 548.

[62]   A. Sakthivel, A. K. Hijazi, H. Y. Yeong, K. Köhler, O. Nuyken, F. E. Kühn, *J. Mater. Chem.* **2005**, *15*, 4441.

[63]   S. Gago, Y. Zhang, A. M. Santos, K. Köhler, F. E. Kühn, J. A. Fernandes, M. Pillinger, A. A. Valente, T. M. Santos, P. J. A. Ribeiro-Claro, I. S. Gonçalves, *Micropor. Mesopor. Mater.* **2004**, *76*, 131.

[64]   A. Sakthivel, A. K. Hijazi, M. Hanzlik, A. S. T. Chiang, F. E. Kühn, *Appl. Catal., A* **2005**, *294*, 161.

[65]   A. Sakthivel, A. K. Hijazi, A. I. A. Hmaideen, F. E. Kühn, *Micropor. Mesopor. Mater.* **2006**, *96*, 293.

[66]   S. Syukri, A. K. Hijazi, A. Sakthivel, A. I. Al-Hmaideen, F. E. Kühn, *Inorg. Chim. Acta* **2007**, *360*, 197.

[67]   S. Syukri, C. E. Fischer, A. Al Hmaideen, Y. Li, Y. Zheng, F. E. Kühn, *Micropor. Mesopor. Mater.* **2008**, *113*, 171.

III. Mechanistic investigations on the role of nitrile ligated transition metal complexes with weakly coordinating counter anions in the polymerization of isobutene

1. Prior Knowledge

1.1 Background

The production of highly reactive polyisobutenes by more efficient and environmental benign methods is of huge commercial interest. Hence, various scientific groups work on this field and have developed improved processes.[1] Several years ago, *Kühn et al.* designed a technique for the polymerization of isobutene, leading to low molecular weight polymers with a high content of terminal exo C=C bonds at room temperature.[2] Only a few years later it was discovered that the employed transition metal complexes of the general formula $[M(CH_3CN)_6][A]$ (M = first row transition metal, A = $B(C_6F_5)_4^-$, $B(C_6H_3(CF_3)_2)_4^-$, $(C_6F_5)_3B$-$C_3H_3N_2$-$B(C_6F_5)_3^-$) perform even better in non-chlorinated solvents like toluene, if the acetonitrile ligands are exchanged by benzonitrile.[3] Additionally, various attempts have been made to improve these complexes[4] or to heterogenize the existing ones on insoluble substrates whilst retaining of their activity.[5] However, because of a lack of progress in both approaches, knowledge of the detailed mechanism of the polymerization of isobutene is of utmost importance for the design of improved mediators.

Therefore different mechanism concepts as well as improved synthesis and characterization of active mediators in the isobutene polymerization are detailed in this chapter. This includes a summary of already reported data in the context of newly obtained results from a model system. These insights and theories are also discussed for a transfer to the parent polymerization system.

1.2 Proposed mechanisms

Several mechanisms seem possible for the cationic polymerization of isobutene using organonitrile ligated transition metal complexes with weakly coordinating counter anions (WCA) as mediators.[6] This work focuses on the initiation (see Scheme 3.1.1). The reason for the extremely high content of terminal C=C bonds of up to 92 % in the obtainable polymers is disregarded at this point due to the complexity of the system.[3]
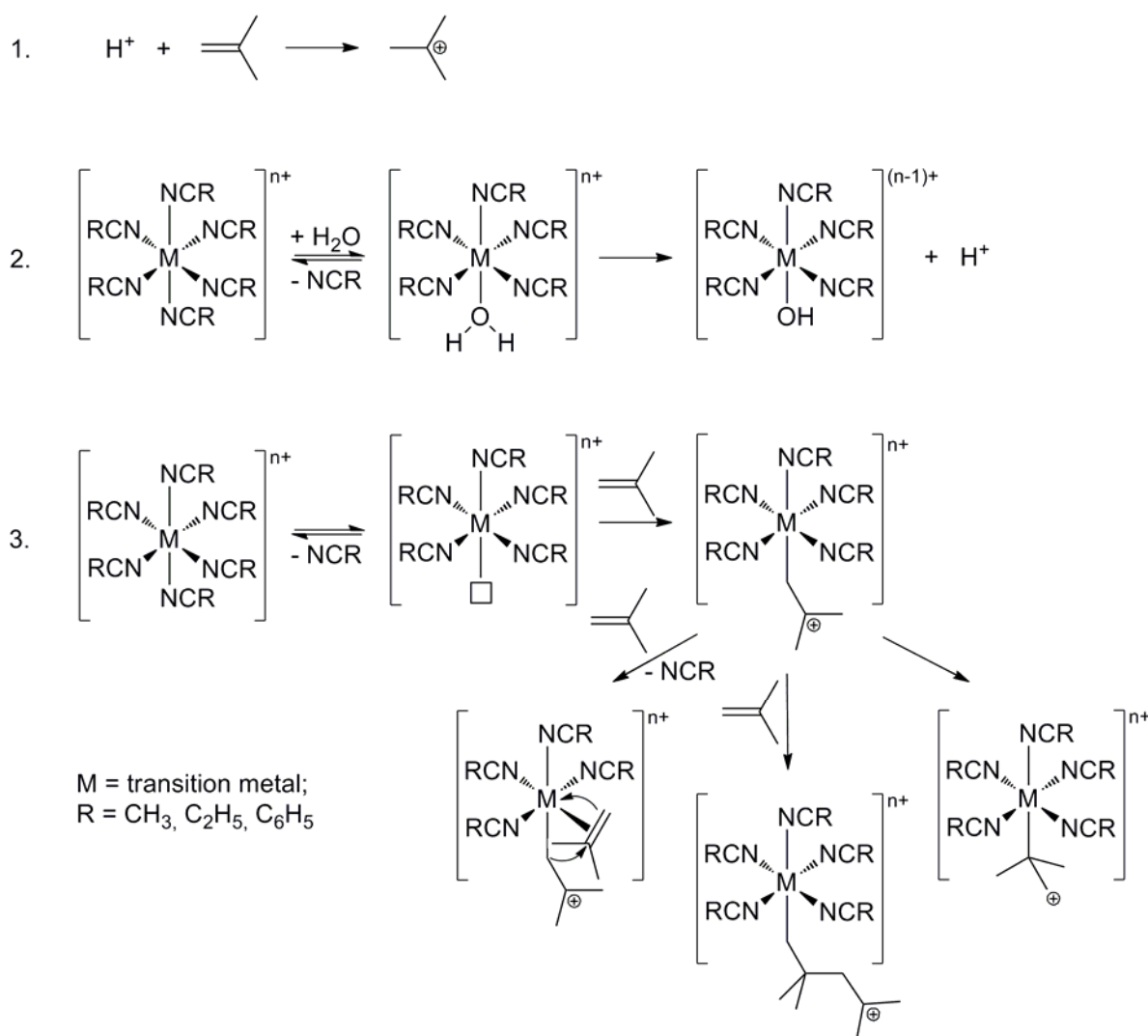
Scheme 3.1.1. Three potential initiation mechanisms for cationic polymerization of isobutene.[6]

One possibility for the development of a cationic species would be the initiation by protons which are formed in the reaction of water traces with impurities (see Scheme 3.1.1, pathway 1). Another idea is that weakly coordinating nitrile ligands could be replaced by water traces and release protons which react with isobutene (see Scheme 3.1.1, pathway 2). These two

pathways would depend on the presence of impurities in the reaction mechanism. If these can be excluded, initiation by replacement of a ligand with a monomer and generation of a cationic metal-alkyl species could be possible. This mechanism seemed to be more likely but critical information *e.g.* on the formation of the alkyl-cation species were not available (see Scheme 3.1.1, pathway 3).[6] However, according to recently published theoretical calculations none of these three mechanisms have been found to be feasible.[7]

1.3 Observations and examinations: State of the art

Since the first polymerization of isobutene with acetonitrile ligated manganese complexes with weakly coordinating borate anions in 2003[2a] many attempts have been made to identify the mechanism of this reaction. Even though the exact mechanism has not been identified, so far, important hints have been obtained, which are summarized in the following paragraphs:

1.3.1 Influence of reaction conditions and mediators on the polymerization of isobutene

- **Reaction Temperature**

Organonitrile ligated transition metal complexes with weakly coordinating counter anions are able to polymerize isobutene slightly above room temperature. However, it has to be mentioned that reaction is very slow below rt and no conversion can be observed at temperatures significantly below 0 °C. This stands in contrast to initiation with protonic and Lewis acids, applied in commercial scale which requires temperatures far below 0 °C (up to ~ -100 °C).[2]

- **Dependence of molecular weight on conversion**

Additionally, unlike in the classic living cationic polymerization with common initiators, the average degree of polymerization decreases with increasing conversion, as well as with decreasing complex concentration.[2b, 3, 8] This contradicts the generally accepted behavior for an ionic polymerization (Chapter III. 4.1).

- **Sequential monomer feed experiments**

Moreover, polymerization continues after complete conversion and subsequent re-addition of monomer. After continuation no increased molecular masses are obtained. Creation of new chains leads to formation of new polymer with the same attributes.[6]

- **Chain Transfer**

Due to chain transfer reactions the content of exo C=C bonds decreases and the PDI increases with prolonged reaction time.[3, 8b]

- **Active Mediators**

Apart from varying activities and slightly different product properties nearly all divalent transition metal complexes of the general formula $[M(RCN)_6][A]$ (M = Cr^{2+}, Mn^{2+}, Fe^{2+}, Co^{2+}, Ni^{2+}, Cu^{2+}, Zn^{2+}, $MoCl^{2+}$; R = CH_3, C_2H_5, C_6H_5; A = $B(C_6F_5)_4^-$, $B(C_6H_3(CF_3)_2)_4^-$, $(C_6F_5)_3B$-$C_3H_3N_2$-$B(C_6F_5)_3^-$) show similar behavior in isobutene polymerization.[2a, 3-4, 8b, 9]

- **Polydispersity**

Depending on reaction conditions and applied metal mediator the PDIs in the isobutene polymerization range from 1.3[3] to 3.5[8a]. In copolymerization reactions with styrene the PDI can reach as high as 8.8[8a]. A concentration dependant behaviour of the PDI could not be recognized, but the Mn(II) mediated system shows clear increase of the PDI with the reaction time.[3, 8a]

- **Dependence on oxidation state of the metal**

Upon comparison of $[Ag(I)(CH_3CN)_6][A]$ complexes with the respective divalent compounds (see above) it was shown to be inactive.[2b]

In summary of the above mentioned observations, mainly collected from data reported for the Mn(II) systems, several key properties of the present polymerization mechanism can be deducted. This is only viable if one general polymerization mechanism is supposed for all active divalent nitrile ligated transition metal mediators, a reasonable assumption due to their similar behaviour in this reaction.

The reaction mechanism clearly shows non-living behaviour with chain transfer. Nevertheless, a stable species able to be reactivated after monomer consumption and indications of polymerization control leading to relatively low PDIs in certain systems under specific conditions can be postulated.

- **Influence of water on the isobutene polymerization**

As traces of water play a decisive role in at least two of three potential mechanisms (see above), the effect of water on the conversion of isobutene to poly(isobutene) was investigated.

On the one hand, experiments with manganese- ($[Mn(CH_3CN)_6][B(C_6F_5)_4]_2$) as well as with copper complexes show that an excess of up to a tenfold of water compared to complex concentration has only limited effect on the isobutene conversion (see Figure 3.1.1, similar figure for the copper compound in literature).[2b, 3]
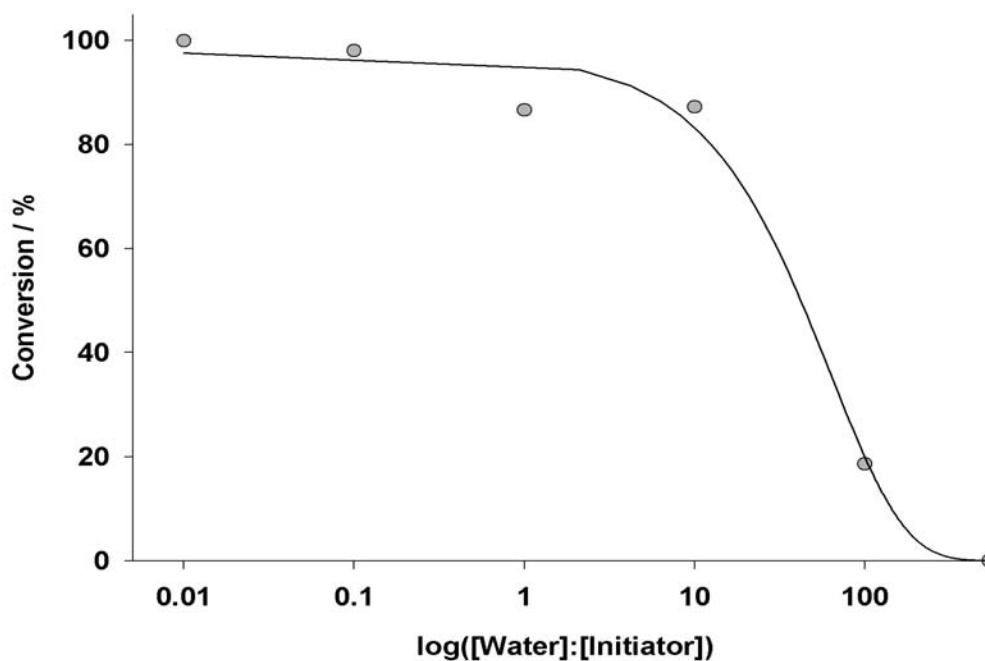
Figure 3.1.1. Polymerization of isobutene with $[Mn(CH_3CN)_6][B(C_6F_5)_4]_2$, conversion as a function of log([water]:[initiator]) ($c_{initiator} = 2.5 \cdot 10^{-4}$ mol/L, $c_{isobutene} = 1.38$ mol/L, $V_{CH2Cl2} = 20$ mL, T = 30 °C, t = 16 h).[2b]

Hence, these acetonitrile coordinated complexes seem to be rather tolerant towards water, instead of water sensitive. The high concentration of water necessary for a significant drop in activity can only ambiguously seen in context of the proposed mechanisms.

On the other hand, the water content has a drastic effect on the molar mass of the polymeric product (see Figure 3.1.2).[2b] Therefore, present water has to be regarded as a chain transfer agent in this context.
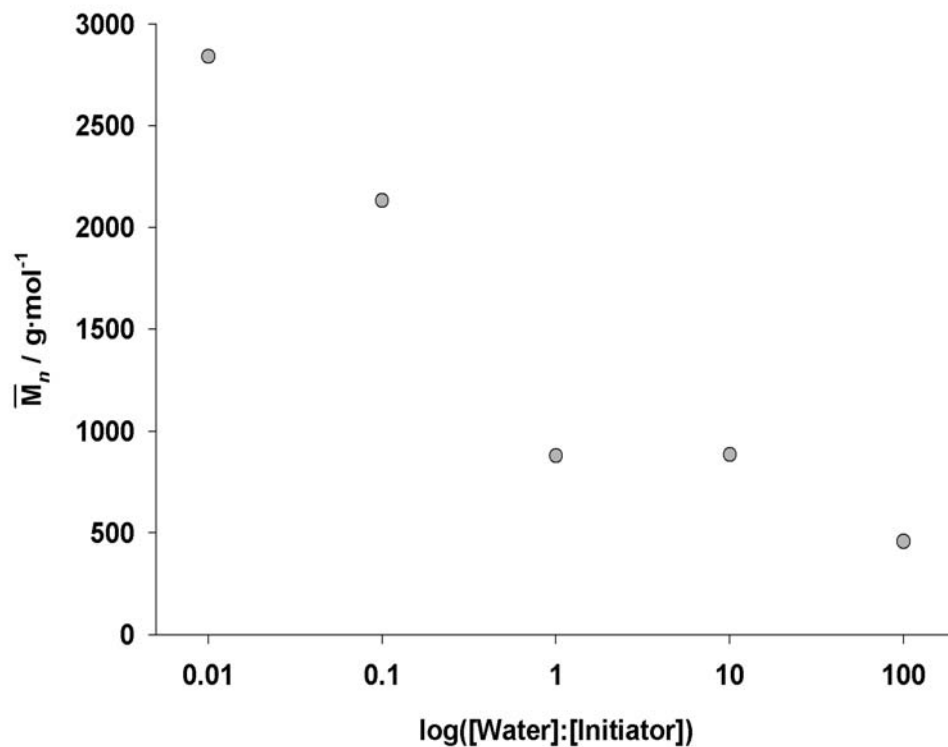
Figure 3.1.2. Polymerization of isobutene with $[Mn(CH_3CN)_6][B(C_6F_5)_4]_2$; molecular weight as a function of log([water]:[initiator]) ($c_{initiator} = 2.5 \cdot 10^{-4}$ mol/L, $c_{isobutene} = 1.38$ mol/L, $V_{CH2Cl2} = 20$ mL, T = 30 °C, t = 16 h).[2b]

2. Mechanistic studies in the poylmerization of isobutene: influence of oxidation state and coordination environment

2.1 Introduction

The inactivity of a nitrile coordinated sliver/WCA salt (see above) prompted us to detailed investigations into the polymerization mechanism.[2b] To verify the assumption that neither compounds with metal atoms in the oxidation state +1 nor those with less weakly coordinating counter anions are active mediators for the polymerization of isobutene, several exemplary systems have been synthesized and tested for their performance.

Since the nitrile (aceto- or benzonitrile) ligated Cu(II) complexes with polyfluorinated phenyl borate anions and $[Zn(CH_3CN)_6][B(C_6F_5)_4]_2$ are in dichloromethane as solvent the most active mediators of this class in isobutene polymerization so far, copper and zinc based complexes were selected for the investigation. This is accompanied by the stability of Cu(II) and Zn(II) complexes to enable comparison of experiments.[3, 8b] Additionally the activity of all alkali metal containing precursors, which were used for the synthesis of the aforementioned complexes was examined to exclude possible effects.

2.2 Results and Discussion

2.2.1 Synthesis of the alkali precursors

The alkali metal M(I) salts $Li[B(C_6F_5)_4]$ and $K[B(C_6F_5)_4]$ were prepared by literature procedures (see Scheme 3.2.1).[3, 9]

1. a) $3 \, C_6F_5Br \xrightarrow[\substack{-78\ °C,\ (pentane) \\ -\ 4\ n\text{-}BuBr}]{n\text{-}BuLi} 3 \, C_6F_5Li \xrightarrow[\substack{-78\ °C,\ (pentane) \\ -\ 3\ LiBr}]{BBr_3} B(C_6F_5)_3$

b) $C_6F_5I \xrightarrow[\substack{-78\ °C,\ (Et_2O) \\ -\ n\text{-}BuI}]{n\text{-}BuLi} LiC_6F_5 \xrightarrow[\substack{-40\ °C,\ (pentane)}]{B(C_6F_5)_3} Li[B(C_6F_5)_4]$

2. $4 \, C_6F_5Br \xrightarrow[\substack{-78\ °C,\ (Et_2O) \\ -\ 4\ n\text{-}BuBr}]{n\text{-}BuLi} 4 \, C_6F_5Li \xrightarrow[\substack{-78\ °C,\ (Et_2O) \\ -\ 3\ LiCl}]{BCl_3} Li[B(C_6F_5)_4] \xrightarrow[\substack{rt,\ (H_2O) \\ -\ LiCl}]{KCl} K[B(C_6F_5)_4]$
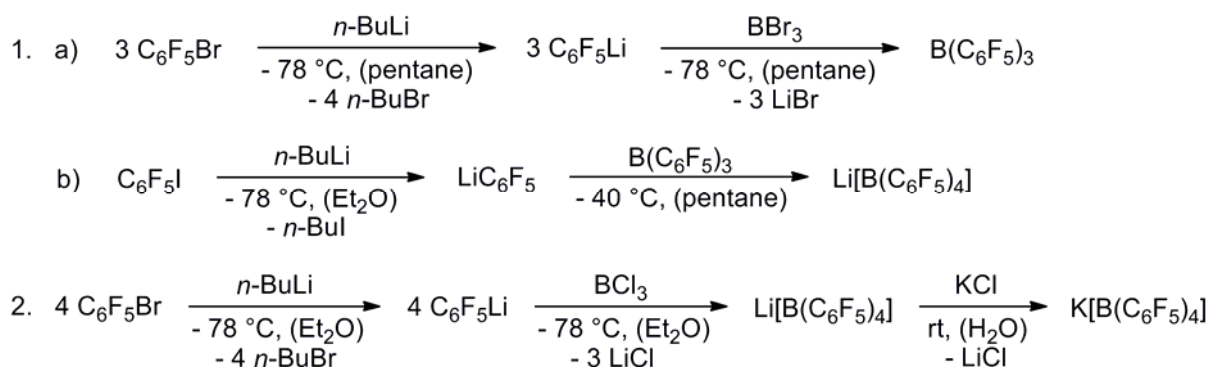
Scheme 3.2.1. Synthesis of $Li[B(C_6F_5)_4]$ (1) and $K[B(C_6F_5)_4]$ (2).

2.2.2 Synthesis of Cu-complexes

Copper is one of the few transition metals which, in oxidation state +1, forms stable solutions in acetonitrile with weakly coordinating anions.[10] This circumstance is critical for the suitability of this metal in test experiments to determine the importance of the metal oxidation state in isobutene polymerization. The designated complexes, $[Cu(I)(CH_3CN)_4][BF_4]$ and $[Cu(I)(CH_3CN)_4][B(C_6F_5)_4]$, were synthesized by reported procedures (see Scheme 3.2.2), except that the reaction mixture for the formation of $[Cu(I)(CH_3CN)_4][BF_4]$ is only heated to 45 °C, due to decomposition in solution above 50 °C.[11]

1. $Cu + NOBF_4 \xrightarrow[\substack{45\ °C \\ -\ NO}]{(CH_3CN)} [Cu(CH_3CN)_4][BF_4]$

2. $[Cu(CH_3CN)_4][PF_6] + Li[B(C_6F_5)_4] \xrightarrow[\substack{(1.\ CH_3CN) \\ (2.\ H_2O) \\ -\ Li[PF_6]}]{} [Cu(CH_3CN)_4][B(C_6F_5)_4]$
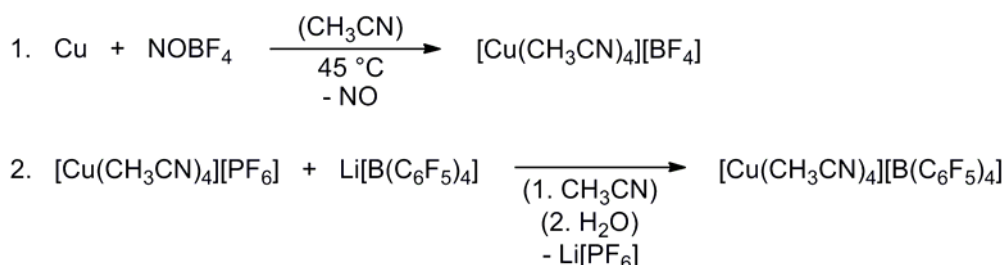
Scheme 3.2.2. Preparation of $[Cu(I)(CH_3CN)_4][BF_4]$ (1) and $[Cu(I)(CH_3CN)_4][B(C_6F_5)_4]$ (2).

2.2.3 Synthesis of $[Cu(II)(CH_3CN)_4][BF_4]_2$ and $[Zn(II)(CH_3CN)_6][BF_4]_2$

To investigate the influence of the anion nature on isobutene polymerization, tetrafluorophenylborate, a weakly coordinating anion which is known to be stronger bonded to the respective cations compared to tetrakis(terafluorophenyl)borate, was chosen. Although complexes with this counter anion were described as inactive earlier,[2a] these compounds moved back into focus due to the observation that in $[Zn(II)(CH_3CN)_6][BF_4]_2$ the tetrafluoroborate anion is not coordinated to the metal center (see Figure 3.2.1). Thus, it was

expected that the zinc complex was more active than the respective complex $[Cu(CH_3CN)_4][BF_4]_2$ in which the anions are coordinated to the metal core (see Figure 3.2.2). The crystal structure of these complexes could be determined in this work giving detailed information on the anion behavior.
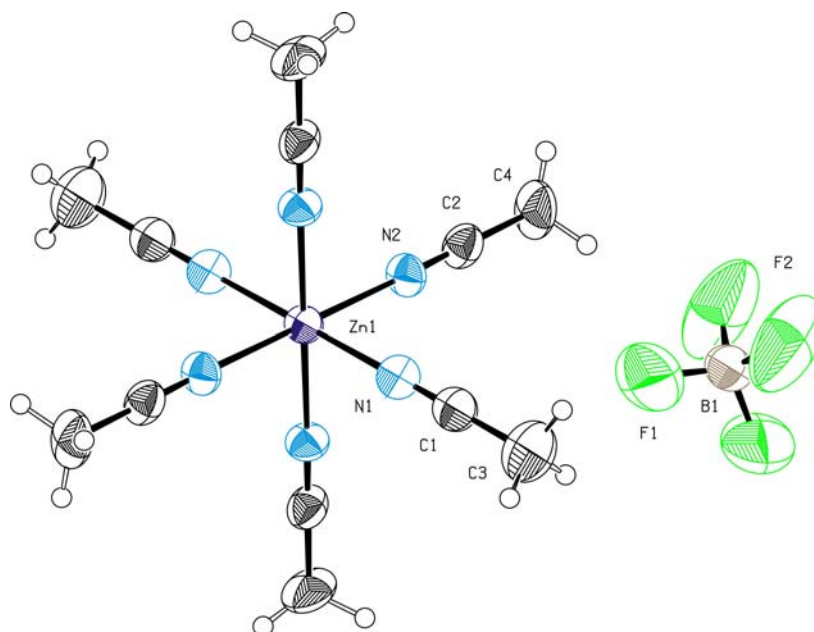
Figure 3.2.1. ORTEP drawing of the fragment $[Zn(CH_3CN)_6]^{2+}[BF_4]^-$ at 173 K with thermal ellipsoids set at the 50 % probability level. The second anion is omitted for clarity.
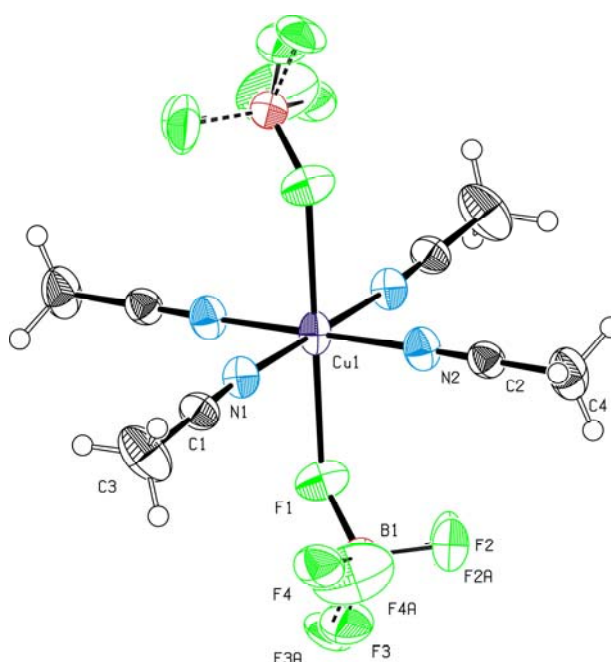
Figure 3.2.2. ORTEP drawing of the preliminary X-ray structure of $[Cu(CH_3CN)_4][BF_4]_2$ at 173 K with thermal ellipsoids set at the 50 % probability level. BF_4^- ions are disordered because of possible rotation.

38

[Zn(II)(CH$_3$CN)$_6$][BF$_4$]$_2$ can easily be synthesized by the reaction of metal powder with nitrosonium tetrafluoroborate in acetonitrile, as published by Hathaway *et al.* (see Scheme 3.2.2 1 b).[12] The synthetic attempts to produce Cu(II) complexes led to the formation of mixtures composed of mainly Cu(II) and, to a lesser extent, Cu(I) species. Copper in oxidation state +1 can be more favored dependant on the solvent. This behavior is observed upon reaction of elemental copper with NOBF$_4$ in acetonitrile (see above). Mainly the thermodynamically more stable [Cu(CH$_3$CN)$_4$][BF$_4$] is obtained at room temperature, and the pure Cu(I) species at elevated temperatures. This is in contrast to Fe, Co, Ni and Zn which only form [M(CH$_3$CN)$_{4/6}$][BF$_4$]$_2$ (M = transition metal).[11b, 12-13] Additionally, light,[14] can also induce reduction of Cu(II). Recent reports suggest the use of ethyl acetate as solvent instead of a nitrile (supposedly ethyl acetate stabilizes Cu(II) but not Cu(I) in solution) and exchange ethyl acetate by nitrile ligands afterwards.[12-13] However, a different observation was made, as not only the desired product, but also its Cu(I) congener was formed.

Nevertheless, both the Cu(II) and the Zn(II) complex can be prepared according to a method which was published by *De Souza et al.* for nickel with HBF$_4$ (see Scheme 3.2.3 1 a and 2).[15] In contrast to the herein used nickel acetate, zinc(II)- as well as copper(II)- acetate are neither soluble in dichloromethane, nor in acetonitrile allowing facile monitoring of the reaction process. However, [Cu(CH$_3$CN)$_4$][BF$_4$]$_2$ can not be produced in acetonitrile directly, as again not only the copper(II) species of the desired product, but a mixture with the [Cu(CH$_3$CN)$_4$][BF$_4$] is formed. Thus, this reaction was performed in dichloromethane and acetonitrile was added to the solution afterwards. The desired complexes can be isolated from concentrated acetonitrile solutions by overlaying with pentane/hexane and diethyl ether (5:1:10).

1. a) $Zn(CH_3COO)_2$ + $2\ HBF_4{\cdot}Et_2O$ $\xrightarrow[\substack{-\ 2\ CH_3COOH \\ -\ 2\ Et_2O}]{(CH_3CN)}$ $[Zn(CH_3CN)_6][BF_4]_2$

   b) Zn + $2\ NOBF_4$ $\xrightarrow[-\ 2\ NO]{(CH_3CN)}$ $[Zn(CH_3CN)_6][BF_4]_2$

2. $1/2\ \{Cu(CH_3COO)_2\}_2$ + $2\ HBF_4{\cdot}Et_2O$ $\xrightarrow[\substack{-\ 2\ CH_3COOH \\ -\ 2\ Et_2O}]{\substack{(CH_3CN) \\ (CH_2Cl_2)}}$ $[Cu(CH_3CN)_4][BF_4]_2$
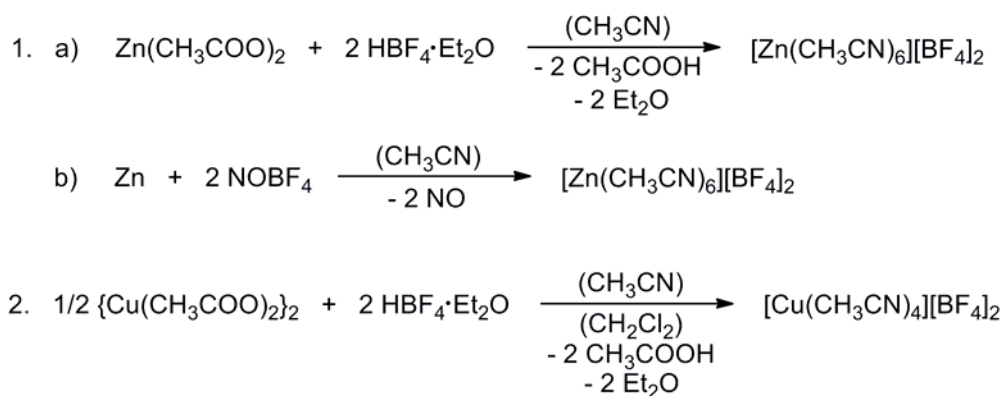
Scheme 3.2.3. Synthesis of $[Zn(II)(CH_3CN)_6][BF_4]_2$ (1) and $[Cu(II)(CH_3CN)_4][BF_4]_2$ (2).

2.2.4 Results of the polymerization investigations

Table 3.2.1 gives an overview on the test experiments conducted for this investigation.

When $Li[B(C_6F_5)_4]$ and $K[B(C_6F_5)_4]$ were tested for isobutene polymerization under the typical reaction conditions (solvent = dichloromethane, T = 30 °C) both compounds did not yield any observable product (see Table 3.2.1). Hence, it can be excluded that traces of remaining precursors contribute to complex activity.

As expected, both complexes $[Cu(I)(CH_3CN)_4][BF_4]$ and $[Cu(I)(CH_3CN)_4][B(C_6F_5)_4$ were inactive in isobutene polymerization as well as the analogous silver complexes (see Table 3.2.1). Hence, the formation of transition states with metals in the oxidation state +1 as active species during the reaction can be excluded.

$[Cu(II)(CH_3CN)_4][BF_4]_2$ and $[Zn(II)(CH_3CN)_6][BF_4]_2$ were expected to behave differently in isobutene polymerization due to the different anion coordination. Unfortunately both complexes showed low activity. Nevertheless, the copper complex produced oligomers and the respective zinc complex yielded polymeric isobutene.

The different results (oligomer vs. polymer) could originate from the stronger coordination in the Cu(II)-tetrafluoroborate salt. However, also the metal center has a clear influence on the obtained polymer, which can be deduced from the reported values for tetrakis(pentafluorophenyl)borate coordinated Zn(II) and Cu(II) complexes in isobutene polymerization.[3, 8b]

Table 3.2.1. Résumé of the polymerization results of the test-complexes.

complex	$c_{complex}$	$c_{isobutene}$	t	yield (qualitative)
	$[10^{-4}$ mol/L]	[mol/L]	[h]	
K[B(C$_6$F$_5$)$_4$]	2.5	1.38	1	-
Li[B(C$_6$F$_5$)$_4$]	2.5	1.38	1	-
[Cu(CH$_3$CN)$_6$][B(C$_6$F$_5$)$_4$]$_2$[3]	1	1.76	0.5	polymer
[Zn(CH$_3$CN)$_6$][B(C$_6$F$_5$)$_4$]$_2$[8b]	0.5	1.78	1	polymer
[Cu(CH$_3$CN)$_4$][B(C$_6$F$_5$)$_4$]	2.5	1.38	1	-
[Cu(CH$_3$CN)$_4$][BF$_4$]	2.5	1.38	1	-
[Cu(CH$_3$CN)$_4$][BF$_4$]$_2$	2.5	1.38	1	traces of oligomer
[Zn(CH$_3$CN)$_6$][BF$_4$]$_2$	2.5	1.38	1	traces of polymer

Solvent = dichloromethane, T = 30 °C. The polymerization experiments were conducted at the Leibniz-Institut für Polymerforschung Dresden by *Ms.C. H. Y. Yeong*.

2.3 Conclusions

As predicted, the tested K(I)- and Li(I)-salts with [B(C$_6$F$_5$)$_4$]$^-$ as counter anion, as well as acetonitrile ligated Cu(I)-complexes with [B(C$_6$F$_5$)$_4$]$^-$ and [BF$_4$]$^-$ anions were not active in isobutene polymerization. Polymerizations with [Cu(II)(CH$_3$CN)$_4$][BF$_4$]$_2$ and [Zn(II)(CH$_3$CN)$_6$][BF$_4$]$_2$ as mediators did only lead to the formation of traces of product. However, it is interesting to note that only oligomer was obtained in the case where [BF$_4$]$^-$ is coordinated to the metal center. But polymer was obtained when [BF$_4$]$^-$ in first approximation is not coordinated.

Thus a) the oxidation state b) the nature of the metal ion and c) the coordination ability of the anion can be assumed to influence the degree of polymerization and, when compared with literature known results for nitrile ligated Cu(II) and Zn(II) complexes with the [B(C$_6$F$_5$)$_4$]$^-$ counter anion, also the yield.

3. Interference abilities of a potential proton trap with nitrile ligated transition metal complexes

3.1 Background

Proton traps are often applied in cationic polymerizations of alkenes to avoid polymerization by protic impurities. Since 2,6-di-*tert*-butylpyridine (DTBP) is known to be unable to stabilize carbocations or to form complexes with Lewis acids, carrying out polymerizations of isobutene in its presence is common.[16]

Thus, DTBP was also applied in isobutene polymerization with nitrile-ligated transition metal complexes possessing polyfluorinated phenylborates counter anions as mediators.[17] However, expected well-defined homopolymers of isobutene were not obtained. Addition of stoichiometric amounts of DTBP related to the amount of mediator completely inhibited the polymerization reaction. This allows two interpretations. Either the mechanism is of cationic origin, involving protons formed from the reaction of residual water with the complex. Or DTBP can act as a "catalyst" poison which can interact with the reaction system.

To provide evidence for the latter case several tests have been conducted. These were performed with $[Zn(CH_3CN)_{4/6}][B(C_6F_5)_4]_2$, one of the best diamagnetic nitrile ligated mediators for isobutene polymerization.[8b] Thus, not only X-ray crystallography experiments were possible but these could also be combined with mechanistic investigations *via* NMR-spectroscopy. The employed complex was synthesized in a new facile two-step procedure involving the so called "Jutzi-acid" $[H(Et_2O)_2][B(C_6F_5)_4]$[18] which was produced *via* an optimized reaction.

3.2 Synthesis of $[Zn(CH_3CN)_{4/6}][B(C_6F_5)_4]_2$

Complexes containing WCAs can be prepared *via* several strategies (see Chapter I. 2.2).[13, 15, 19] However, in the class of complexes dealt with herein, WCAs are mainly introduced by metathesis reactions of their respective silver salts and halides of the desired transition metal.[8b, 20] The silver based reactants are cost intensive and residual impurities difficult to

separate from the product. Therefore, silver-containing starting materials were avoided in the development of a new reaction pathway.

In this chapter an improved method for the synthesis, using $[H(Et_2O)_2][B(C_6F_5)_4]$ and full characterization of $[Zn(CH_3CN)_{4/6}][B(C_6F_5)_4]_2$ is presented.

3.2.1 Synthesis of the precursor

The synthesis of $[H(Et_2O)_2][B(C_6F_5)_4]$ was improved over the years. Nevertheless, it requires three steps (see Scheme 3.3.1) and at least three days, with an overall yield of 26 % (see Table 3.3.1).

1. $3\ C_6F_5Br \xrightarrow[\substack{-78\ °C,\ (light\ petroleum)\\ -\ 4\ n\text{-BuBr}}]{n\text{-BuLi}} 3\ C_6F_5Li \xrightarrow[\substack{-78\ °C,\ (light\ petroleum)\\ -\ 3\ LiBr}]{BBr_3} B(C_6F_5)_3$

2. $C_6F_5I \xrightarrow[\substack{-78\ °C,\ (Et_2O)\\ -\ n\text{-BuI}}]{n\text{-BuLi}} LiC_6F_5 \xrightarrow[\substack{-40\ °C,\ (pentane)}]{B(C_6F_5)_3} Li[B(C_6F_5)_4]$

3. $Li[B(C_6F_5)_4] \xrightarrow[\substack{-30\ °C,\ (Et_2O)\\ -\ LiCl}]{HCl_{(g)}} [H(OEt_2)_2][B(C_6F_5)_4]$
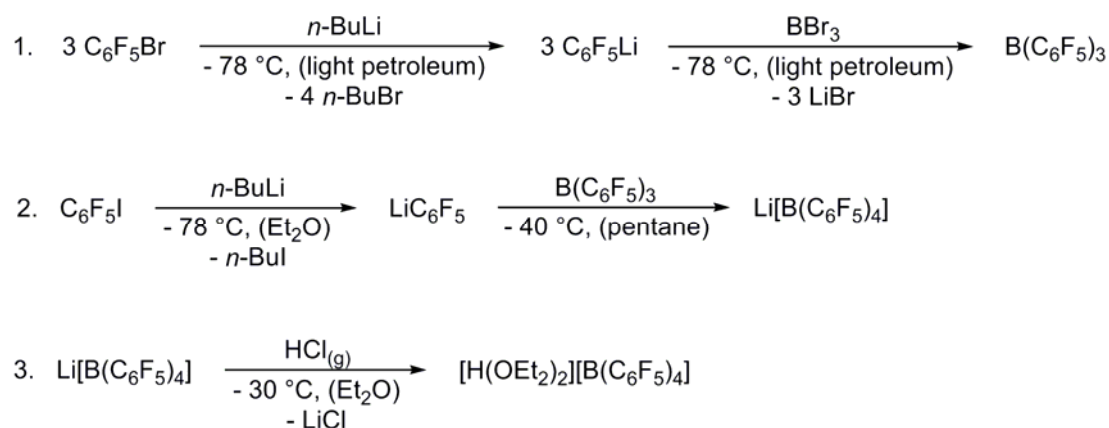
Scheme 3.3.1. Original procedure to synthesize $[H(Et_2O)_2][B(C_6F_5)_4]$.[9, 18, 21]

Table 3.3.1. Comparison of the two procedures for the synthesis of $[H(Et_2O)_2][B(C_6F_5)_4]$.

Procedure	Steps	Yield per step (%)	Overall Yield (%)
[9, 18, 21]	3	1: 48	
		2: 83	
		3: 65	26
This work	1	38	38

This synthesis was optimized to a one step reaction. The first part of the *in situ* reaction is the formation of lithium tetrakis(pentafluorophenyl)borate (see Chapter III. 2.2.1) as an intermediate. As no interferences with side products were expected, HCl in diethyl ether was

directly added to the reaction mixture. This approach resulted in a yield of 38 % oxonium acid after repeated purification with pentane.

$$4\ C_6F_5I \xrightarrow[\substack{-78\ °C,\ (Et_2O) \\ -\ 4\ n\text{-BuI}}]{n\text{-BuLi}} 4\ C_6F_5Li \xrightarrow[\substack{-78\ °C,\ (Et_2O) \\ -\ 3\ LiCl}]{BCl_3} Li[B(C_6F_5)_4] \xrightarrow[\substack{0\ °C,\ (Et_2O) \\ -\ LiCl}]{HCl} [H(OEt_2)_2][B(C_6F_5)_4]$$
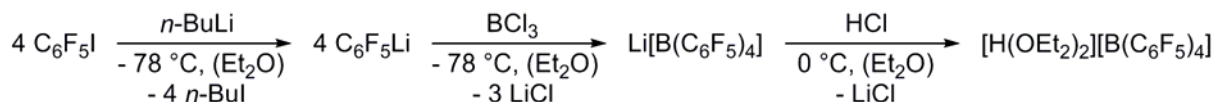
Scheme 3.3.2. Improved synthesis of $[H(Et_2O)_2][B(C_6F_5)_4]$.

3.2.2 Synthesis of $[Zn(CH_3CN)_{4/6}][B(C_6F_5)_4]_2$

The original synthesis of $[Zn(CH_3CN)_6][B(C_6F_5)_4]_2$ is carried out in acetonitrile, starting from $ZnCl_2$ and the silver salt of $[B(C_6F_5)_4]^-$ (see Scheme 3.3.3). This synthesis only results in a yield of 65.5 % (see Table 3.3.2).[8b]

$$ZnCl_2 \xrightarrow[-\ 2\ AgCl]{2\ [Ag(CH_3CN)_4][B(C_6F_5)_4]} [Zn(CH_3CN)_6][B(C_6F_5)_4]_2$$
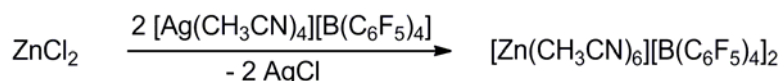
Scheme 3.3.3. Original procedure for the synthesis of $[Zn(CH_3CN)_6][B(C_6F_5)_4]_2$ (solvent: acetonitrile).

Table 3.3.2. Comparison of the two procedures for the synthesis of $[Zn(CH_3CN)_x][B(C_6F_5)_4]_2$ (x = 4, 6).

Procedure	Silver agent	Steps	Yield (%)
[8b]	Yes	1	65.5
This work	No	1	81

The synthesis of $[Zn(CH_3CN)_{4/6}][B(C_6F_5)_4]_2$ can be carried out in two steps similar to the one of $[EtZn(OEt_2)_3][B(C_6F_5)_4]$,[22] which can be prepared by reaction of diethyl zinc with $[H(Et_2O)_2][B(C_6F_5)_4]$ in almost 80 % yield.[23] The reported reaction was carried out stoichiometrically, opening the possibility to conduct the reaction in a ratio of 1:2 to abstract the second alkyl group. Driving force is the evolution of gaseous ethane.

Direct reaction of the starting materials in acetonitrile as solvent resulted in the formation of the desired compound and by-products, reducing the effectivity. As analogous side reactions with solvents such as toluene were already described in the literature,[23] it was decided to conduct the reaction in diethyl ether. Subsequent exchange of the solvent ligands against

acetonitrile (see Scheme 3.3.4) yielded the desired product in good yield (81 %) (see Table 3.3.2).

$$Zn(C_2H_5)_2 \xrightarrow[\substack{- 4\ OEt_2 \\ - 2\ C_2H_6}]{2\ [H(OEt_2)_2][B(C_6F_5)_4]} [Zn(CH_3CN)_{4/6}][B(C_6F_5)_4]_2$$
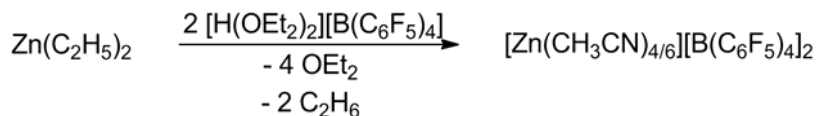
Scheme 3.3.4. Synthesis of $[Zn(CH_3CN)_{4/6}][B(C_6F_5)_4]_2$ (solvent: diethyl ether, acetonitrile).

3.3 Characterization

The complex $[Zn(CH_3CN)_6][B(C_6F_5)_4]_2$ is described to be coordinated with six acetonitrile ligands.[8b] However, elementary analysis indicated the presence of only five nitrile ligands with the improved synthesis method for preparation of the complex. Furthermore, the obtained crystal structures show that the question regarding the correct number of ligands can not be answered this easily. Indeed, a mixture of four (see Figure 3.3.1) and six (not displayed because of disorder of the metal center) coordinated complexes could be identified. This is in accordance with the IR spectra (Nujol) which show three ν_{CN} absorptions (ν_{CN} = 2324, 2297, 2285 cm^{-1}), instead of one or two for the defined complexes. The literature also describes this compound as "creamy" instead of crystalline, residual solvent-free.[8b]

This implies that either the data corresponded to the values of a complex plus additional free ligand or that it was not possible to obtain adequate data for the dry compound as it would persistently loose its ligands before and during the measurements. The problems in obtaining reliable data using elementary analysis, due to solvent loss, was already described by *Buschmann* and *Miller* for similar acetonitrile ligated transition metal complexes with weakly coordinating polyfluorinated borates.[20]

This is supported by theoretical calculations of *Wasada et al.*[24] about exchange reactions on hexa acetonitrile solvated transition metal cations in the formal oxidation state +2. Here it could be demonstrated how close binding energies for five, six and seven ligated complexes are, and how little energy is needed for transition between these states. This explains how unlikely it is to receive consistent data for a compound that actually is, according to thermogravimetric analysis (TGA), the least stable amongst the first row transition metals.
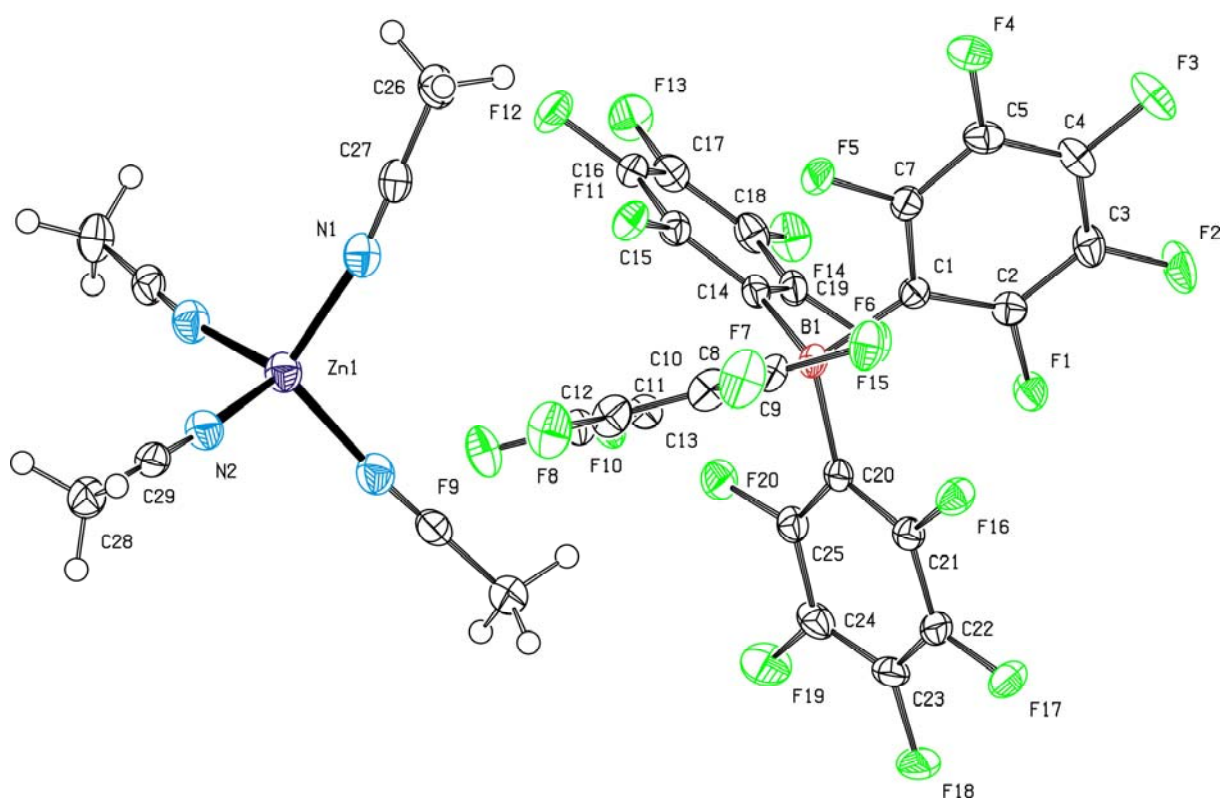
Figure 3.3.1. ORTEP style depiction of a fragment of $[Zn(CH_3CN)_4][B(C_6F_5)_4]_2$ in the solid state. Thermal ellipsoids are drawn at the 50 % probability level. One of the anions is omitted for clarity.

3.4 Reaction of 2,6-di-*tert*-butylpyridine (DTBP) with $[Zn(CH_3CN)_{4/6}][B(C_6F_5)_4]_2$

As mentioned above the known proton trap DTBP was applied in isobutene polymerization with mediators, similar to the presented Zn(II) complex.[17] The stoichiometric presence of this amine in respect to the metal completely prevented polymerization. To test possible reaction between DTBP and the complex a series of experiments was conducted. Interference of DTBP with the metal could stem from coordination, although this amine is often successfully used as a proton trap. The steric hindrance of the *tert*-butyl groups is known to prevent coordination to larger cations.[16] However, as explained above the proposed reaction mechanisms involving formation of protons as active species are based on traces of water as impurity. The required DTBP/metal ratio of 1/1 for a complete deactivation indicates a contradiction with the proposed mechanism and favors a direct reaction with the mediator.

3.4.1 ^{1}H-NMR and NOESY measurements

One possible cause for the observed deactivation by addition of stoichiometric amounts of DTBP could be a strong coordination of the (donor) pyridine-nitrogen to the metal core of the complex despite the steric bulk of the *tert*-butyl groups (see Figure 3.3.2). Such an interaction should be observable by NOESY spectroscopy. In this case a clear interaction of the *tert*-butyl groups with the equatorially coordinated acetonitrile ligands is expected.

The ideal test system involves the $[Zn(CH_3CN)_6][B(C_6F_5)_4]_2$ complex, being one of the most active diamagnetic mediators for isobutene polymerization.
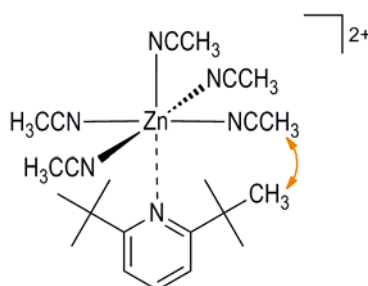
Figure 3.3.2. Proposed interaction between the complex and DTBP: Coordination of the pyridine-nitrogen to the metal center.

In this reaction an excess of DTBP is added to a solution of $[Zn(CH_3CN)_{4/6}][B(C_6F_5)_4]_2$ in dry deuterated methylene chloride. ^{1}H NMR spectroscopy was conducted for a first examination. At room temperature the acetonitrile signals were broadened and not resolved (see Figure 3.3.3, section) temperature was stepwise lowered to 188 K to achieve complete separation (see Figure 3.3.3) without clouding of the clear solution. The spectrum shows the existence of two different pyridine species ($*_1$, $*_2$) with the respective signals from the *tert*-butyl groups ($\delta(ppm) = 1.48$ and 1.26), accompanied by four signals for the corresponding aromatic protons ($\delta(ppm) = 8.40, 7.52; 7.81, 7.07$). The acetonitrile shows only a single peak at $\delta(ppm) = 2.02$ ppm (+). Unexpectedly, a broad peak of a newly formed proton can be observed at 10.99 ppm. Additional attempts to do ^{67}Zn- and ^{15}N-NMR spectroscopy were unsuccessful as the sample was not isotopically enriched.
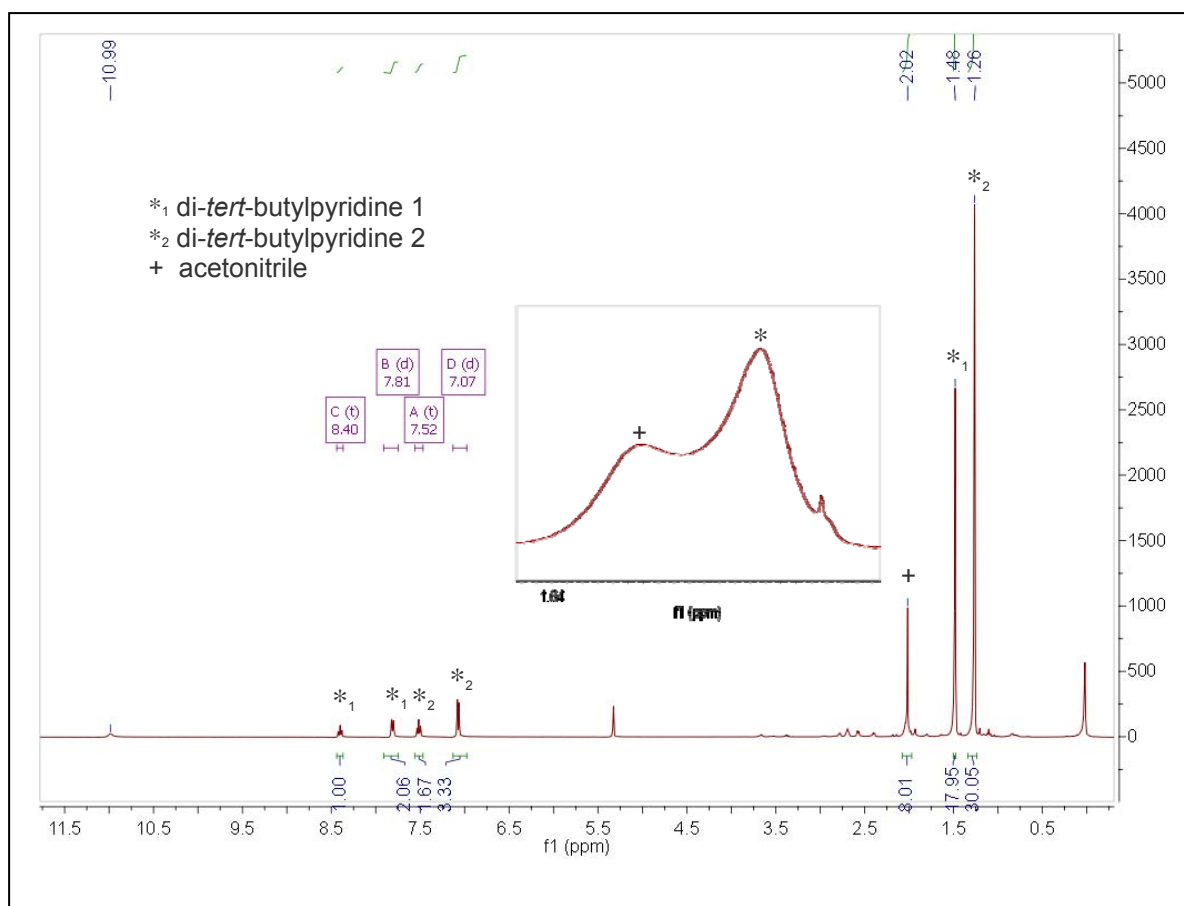
Figure 3.3.3. ^{1}H NMR spectrum of $[Zn(CH_3CN)_{4/6}][B(C_6F_5)_4]_2$ and 2,6-di-*tert*-butylpyridine (excess) in CD_2Cl_2, 188 K (spectrum), 298 K (section).

The NOESY-spectrum (see Figure 3.3.4) at 188 K shows coupling between protons of the two DTBP species (methyl groups and aromatic respectively) but no interaction between the methyl groups and acetonitrile.
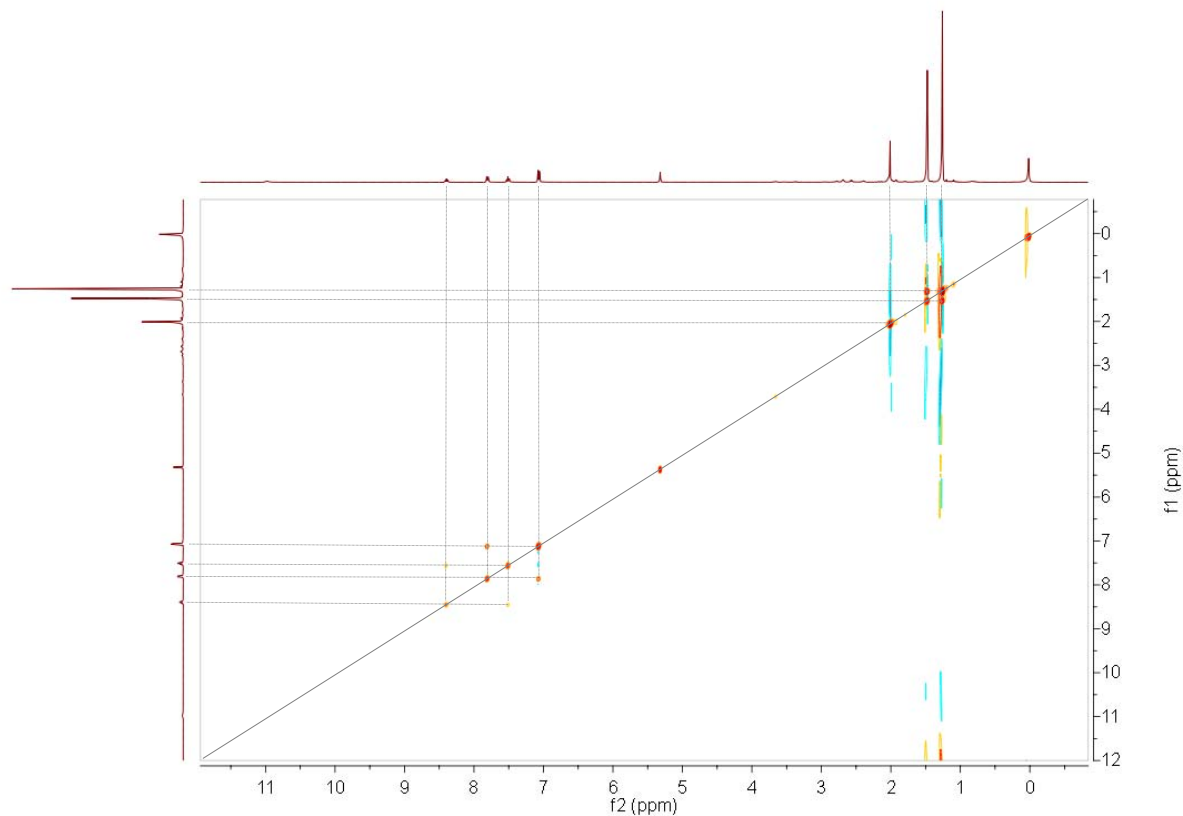
Figure 3.3.4. NOESY spectrum of [Zn(CH$_3$CN)$_{4/6}$][B(C$_6$F$_5$)$_4$]$_2$ and 2,6-di-*tert*-butylpyridine (excess) in CD$_2$Cl$_2$, 188 K.

3.4.2 X-ray single crystal diffraction

Crystals suitable for X-ray crystallography were grown from this reaction by overlaying with pentane for both [Zn(CH$_3$CN)$_{4/6}$][B(C$_6$F$_5$)$_4$]$_2$ as well as [Cu(C$_6$H$_5$CN)$_5$][B(C$_6$F$_5$)$_4$]$_2$ (see Chapter III 4.2). Addition of DTBP to the bright green Cu^{2+} solution resulted in the formation of a dark brown precipitate and colorless crystals. Colorless crystals were also obtained from the analogous Zn(II) reaction.

The structures, which were obtained by X-ray crystallography of these colorless crystals, show in all cases distorted DTBP coordinated with one of the weakly coordinating anions of the former complex (see Figure 3.3.5).
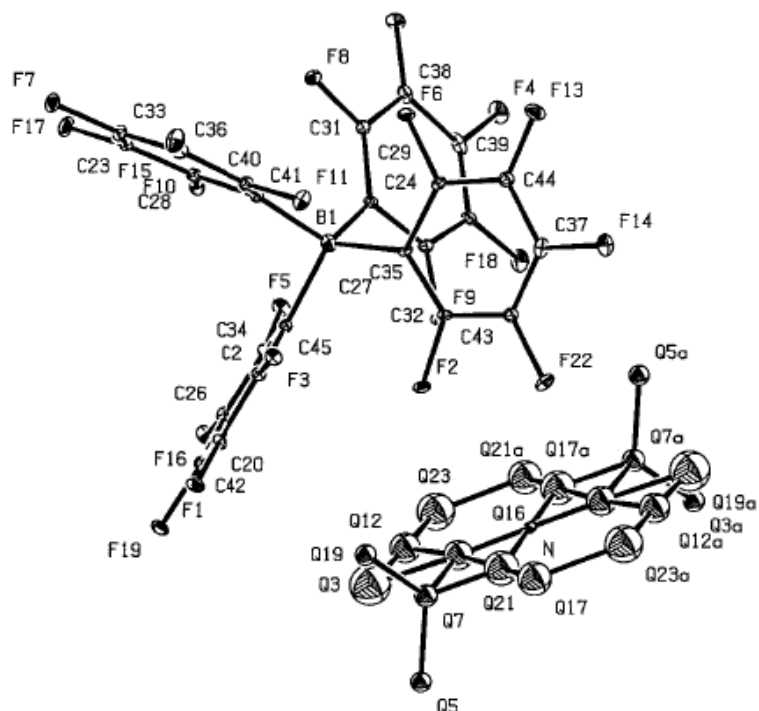
Figure 3.3.5. Preliminary ORTEP drawing of distorted [(CH₃)₃C-(C₅H₄N)-C(CH₃)₃][B(C₆F₅)₄] at 173 K with thermal ellipsoids set at the 50 % probability level.

3.5 Conclusion

Combination of the results from NMR spectroscopy with the crystallographic data shows the protonation of the DTBP. This can be deducted from the newly created proton signal in the ^{1}H NMR spectrum with a chemical shift which is typical for protons coordinated to the nitrogen atom of aromatic *N*-heterocycles together with the presence of the counterion in the crystal structure.[25]

Thus, inhibition of the isobutene polymerization when adding stoichiometric amounts of DTBP related to the amount of mediator is most likely not caused by coordination of the pyridine-nitrogen to the metal core but by decomposition of the complex (as can be seen in case of the copper complex). In both cases, when using the Zn(II) complex as well as when using its Cu(II) congener, redox reactions are involved. Either reduction of the metal center occurs or a reaction with the nitrile ligands or the solvent, causing the formation of a new anion for the metal to maintain its oxidation state (see Scheme 3.3.5).
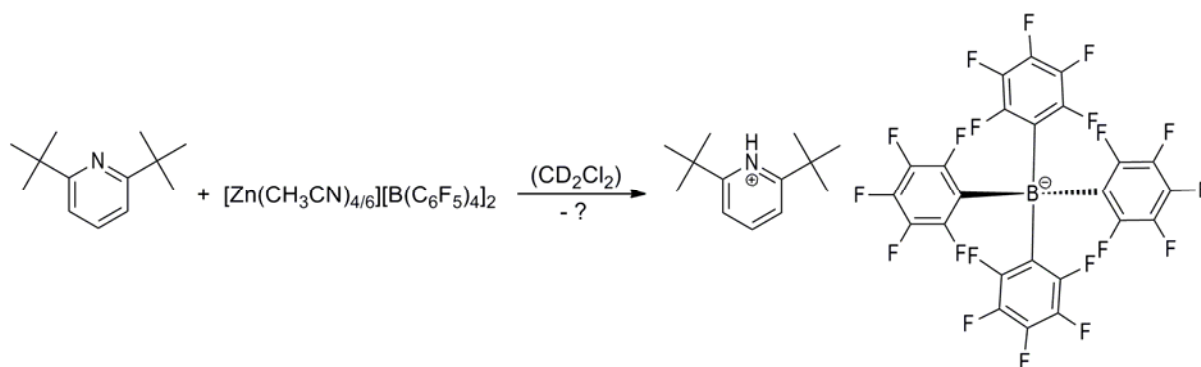
Scheme 3.3.5. Reaction of $[Zn(CH_3CN)_{4/6}][B(C_6F_5)_4]_2$ with DTBP.

Hence, as 2,6-di-*tert*-butylpyridine reacts with the mediators in focus, it is not suitable for proving whether protons are involved in the mechanism or not. With respect to the observed redox reaction and the results of the following chapter it should be mentioned that DTBP can react with radical cations leading to protonation of the pyridine nitrogen.[26]

4. Initiation of isobutene polymerization by radicals or radical cations – an alternative not to be neglected?

4.1 Background

Nitrile ligated transition metal complexes with WCAs can successfully be applied as mediators for isobutene polymerization.[3] Knowledge of the mechanism of this reaction under the applied conditions is essential for further improvement of these mediators. Several possibilities focusing on a cationic mechanism were published.[6] However, as discussed above (see Chapter III. 1.3) several observations are in contrast to the proposed cationic mechanism. Eventually, the question of an alternative mechanism arose, either a different way or a combination of miscellaneous processes.

A suggestion which appears to be exotic at first glance is radical polymerization, since it is often believed that isobutene can not be polymerized radically. However, it is nowadays rarely known that the radical-cationic polymerization of isobutene was reported long ago. First proposed in 1966, using $VOCl_3$ and different activators,[27] followed by radiation- and heat-induced processes only one year later.[28] Subsequent articles with methods leading to radical(-cationic) polymerization of isobutene were published in the following years.[29] Two publications in the *Journal of the American Chemical Society* in 2006 and 2009 brought the possibility of radical isobutene-polymerization back into focus.[30] With this option of potential radical or radical cationic initiation, literature was studied in depth to evaluate the available data. First of all, the classical polymerization types are explained (Figure 3.4.1).
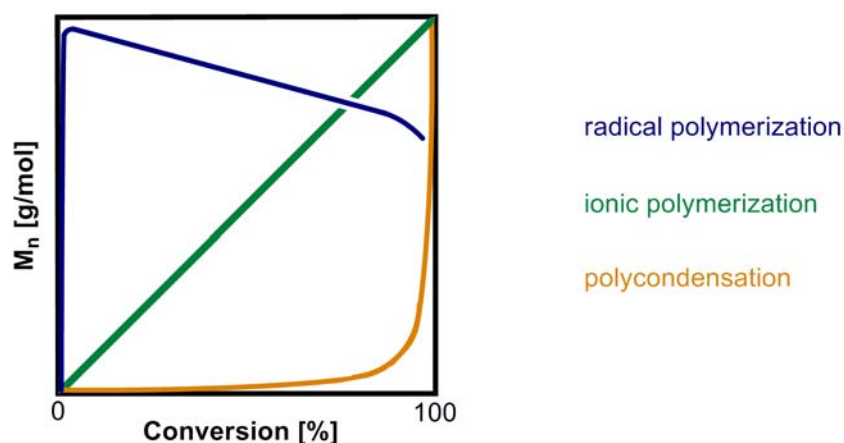
Figure 3.4.1. Dependence of the average molecular weight on conversion (schematized).

Radical polymerization (blue curve): Upon initiation, radicals are created and attach to monomer molecules forming the propagating active species. These active centers migrate due to chain growth and stay at the end of the chains until their deactivation. Propagation is very fast and therefore high molecular weights are obtained directly from the start (order of magnitude: 1 s) of a radical polymerization. When the chain growth has been terminated, the formed polymers do not participate in polymerization reactions anymore (exception: potential chain transfer reactions).

Attenuation of chain growth can take place due to termination of the growing chain by transfer of a radical to another species, such as a polymer, a monomer, a solvent molecule, *etc*. The consequences of chain transfer, like a decrease of the polymer chain length, can be derived from the *Mayo* equation (see Equation 3.4.1), where x_n is the length of the polymer chain, $x_{n,0}$ is the chain length in absence of transfer reactions, k_{tr}^s is the rate constant for chain transfer to the solvent, k_p is the rate constant for propagation, $[S]$ is the solvent concentration and $[M]$ is the monomer concentration.

$$\frac{1}{x_n} = \frac{1}{x_{n,0}} + \frac{k_{tr}^s [S]}{k_p [M]}$$

Equation 3.4.1

As the quantity of solvent is generally huge in comparison to the amount of other present compounds, transfer to the solvent is assumed to predominate all other transfer reactions. Thus, x_n decreases with decreasing monomer concentration, *i.e.* with increasing conversion.

Additionally, diffusion control of the polymerization reaction becomes increasingly important with increasing viscosity of the reaction mixture. As polymerization occurs only at active chain ends, k_{tr}^{s} is much larger than k_{p}, when the mobility of long polymer chains is reduced in comparison with the mobility of newly formed low molecular weight active radicals. Consequently smaller polymers are formed, lowering the average molecular weight with proceeding monomer conversion.[31]

Ionic polymerization (green curve): In case of ionic polymerization, all chains grow at a constant rate from a constant number of the ionic active centers. If no termination reactions occur, it leads to a linear relationship between the average molecular weight and the monomer conversion.[31c]

Polycondensation (orange curve): In a polycondensation reaction the molecular weight is strongly dependent on the conversion. All functional groups have the same reactivity independent of being on a monomer or an oligomeric unit, thus polymerization is not favored over oligomerization. Bi- or multifunctional monomers can react with other monomers possessing the appropriate functional end group. Accordingly, the polymerization starts with dimer formation and successive oligomerization. High molecular weight polymers are only created at higher conversions by the combination of oligomers. This is represented by the exponential increase of the molecular weight at high conversions (approaching 100 %).[31b, 31c]

Indeed, many parallels can be found when comparing the data obtained when using nitrile ligated transition metal complexes with polyfluorinated borate anions (see Figure 3.4.2)[2b] with data obtained under conditions which are known for radical(-cationic) polymerization (VCl$_4$, -20 °C; see Figure 3.4.3)[29d] and the idealized, general curve for radical polymerization (see Figure 3.4.1).
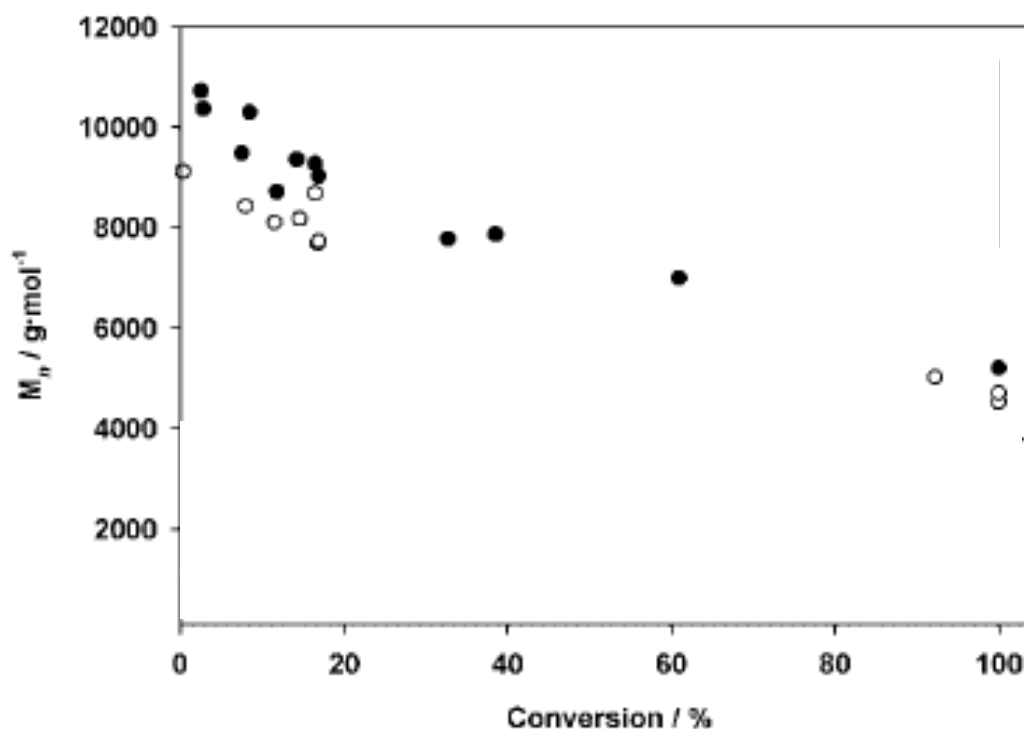
Figure 3.4.2. Dependence of isobutene conversion on the average molecular weight of the polymers (complexes: $[Mn(CH_3CN)_6[A]_2$, $A = B(C_6H_3(CF_3)_2)_4^-$: black dots, $(C_6F_5)_3B-C_3H_3N_2-B(C_6F_5)_3^-$: white dots; $c_{complex} = 2.5 \cdot 10^{-3}$ mol/L, $c_{isobutene} = 1.38$ mol/L, solvent: dichloromethane, T = 30 °C)[2b]
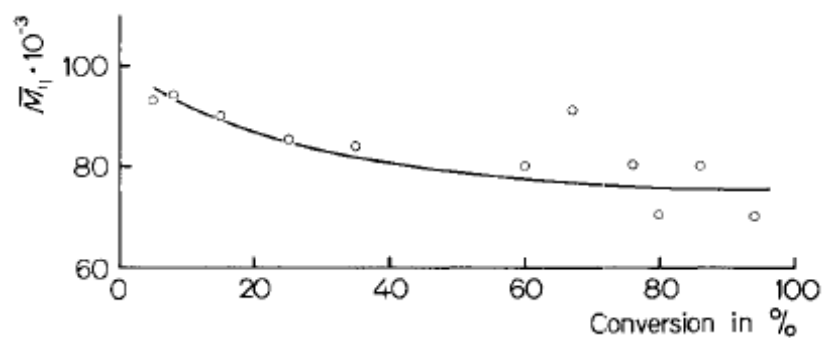
Figure 3.4.3. Dependence of isobutene conversion on the average molecular weight of the polymers ($c_{VCl4} = 3.9 \cdot 10^{-3}$ mol/L, $c_{isobutene} = 1.23$ mol/L, solvent: heptane, T = -20 °C).[29d]

The decrease of the average molecular weight with increasing conversion is a first important hint in direction of radical polymerization. However, the question arises, if it can be proven that the complexes of interest really polymerize via the formation of radical species. Furthermore, if a radical polymerization is occurring the underlying mechanism has to be analyzed. Is this process solely a matter of radical-cations, caused by single electron

transfer, or a combination of concurrent radical-cationic and cationic? A selection of exemplary model compounds was made for simplification of testing and analysis.

Model compounds

2,4,4-trimethylpent-1-ene (diisobutene) was used as model monomer for the conducted measurements. Diisobutene is, in contrast to gaseous isobutene (bp = -6.9 °C), liquid at room temperature and at least copolymerizable via a radical pathway.[32] Moreover, this compound is known to be resistant to extensive propagation (in cationic polymerization) because of steric hindrance.[33] This is in accordance with earlier results which were obtained for the polymerization of isobutene using acetonitrile ligated transition metal complexes with polyfluorinated phenyl borates as mediators where it acts as terminating agent.[34] Additionally, diisobutene was expected to act as a radical scavenger in forming stable (observable) radicals because of steric reasons.

As paramagnetic $[Cu(C_6H_5CN)_5][B(C_6F_5)_4]_2$ showed the best performance in isobutene polymerization in toluene,[3] this compound was used for the majority of further investigations. It turned out that this complex was hardly dissolvable in toluene. Without stirring, green crystals of this compound only partly dissolved in toluene, yielding in a dark brown supernatant after several weeks. Stirred and heated up to 30 °C (the common polymerization temperature) crystals dissolved or decomposed within seconds.

Triphenylmethyl tetrakis(pentafluorophenyl)borate ($[Ph_3C][B(C_6F_5)_4]$) was used as simple reference for mechanistic studies with the analogous transition metal complex. $[Ph_3C][B(C_6F_5)_4]$ is known to be able to initiate isobutene polymerization at temperatures of -20 °C or below.[33] Recent results indicate isobutene polymerization even at room temperature with a mechanism which is believed to be truly cationic and a behavior in isobutene polymerization which is similar to the one observed with nitrile ligated transition metal complexes (see Scheme 3.4.1).[34]

$$Ph_3C^+B(C_6F_5)_4^- \ + \ 2\,H_2O \ \rightleftharpoons \ Ph_3COH \ + \ H_3O^+B(C_6F_5)_4^-$$

$$\xrightarrow{M} HM^+B(C_6F_5)_4^-$$
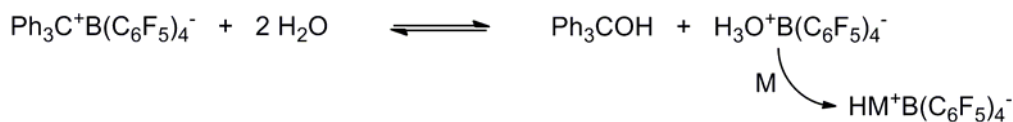
Scheme 3.4.1. Proposed mechanism of the initiation of isobutene polymerization catalyzed by triphenylmetyl tetrakis-(pentafluorophenyl)borate (M = monomer, isobutene) and traces of water.[33]

Buckminsterfullerene (C_{60}) was used in trapping experiments. This substance as well as carbon nanotubes are known to form stable adducts with radicals and have successfully been applied in radical polymerizations as trapping agent.[35]

In the following sections first an improved synthesis of $[Cu(C_6H_5CN)_5][B(C_6F_5)_4]_2$ is described, together with a full characterization. Second, this complex is used in the model system, as aforementioned, to conduct analytical measurements. EPR spectroscopy was employed to detect radical species. This method, in combination with MALDI-TOF spectrometry, was also used for radical trapping experiments. Additionally, possible participation of the polyfluorinated anions was investigated by ESI-MS spectrometry. Qualitative monitoring of the reaction progress could be achieved with UV/Vis spectroscopy. Finally, NMR spectroscopy of the paramagnetic reaction mixture was conducted to gain further insight into the mechanism.

4.2 Synthesis of $[Cu(C_6H_5CN)_5][B(C_6F_5)_4]_2$

As described in Chapter 3, the synthesis of nitrile ligated transition metal complexes with WCAs using silver salts as metathesis reagents has several drawbacks such as bad separability of reaction products and remaining impurities. Thus, a new method was developed for the synthesis of $[Cu(C_6H_5CN)_5][B(C_6F_5)_4]_2$ similar to the one described above for $[Zn(CH_3CN)_{4/6}][B(C_6F_5)_4]_2$. During the design of a new synthesis for the desired benzonitrile ligated Cu(II) complex with the weakly coordinating tetrakis(pentafluorophenyl)borate anion, dependent on the oxidation state of the employed copper precursor, both oxidation and reduction were not negligible side reactions. Details for

the redox behavior of copper salts in solution can be found in the synthesis of Cu(I) and Cu(II) complexes with WCAs in Chapter III. 2.2.

Following a procedure for the synthesis of nitrile ligated dimeric[36] and monomeric[15, 37] transition metal tetrafluoroborates, which is based on the reaction of the respective metal acetates with tetrafluoroboric acide, it was decided to react Cu(II)acetate with the oxonium acid of $[B(C_6F_5)_4]^-$. This reaction was conducted in the dark to avoid undesirable light induced reduction at room temperature in methylene chloride. Direct reaction in benzonitrile gave mixtures of copper(II) and copper(I) species. After completion of the reaction (*i.e.* when all insoluble copper acetate was consumed), an excess of benzonitrile was added. Volatiles were removed in vacuum and subsequent crystallization from methylene chloride and pentane over night gave the desired product selectively in 75 % (see Scheme 3.4.2).

$$\frac{1}{2}\,\{Cu[CH_3COO]_2\}_2 \xrightarrow[\substack{-\,4\,OEt_2 \\ -\,2\,CH_3COOH}]{2\,[H(OEt_2)_2][B(C_6F_5)_4]} $$
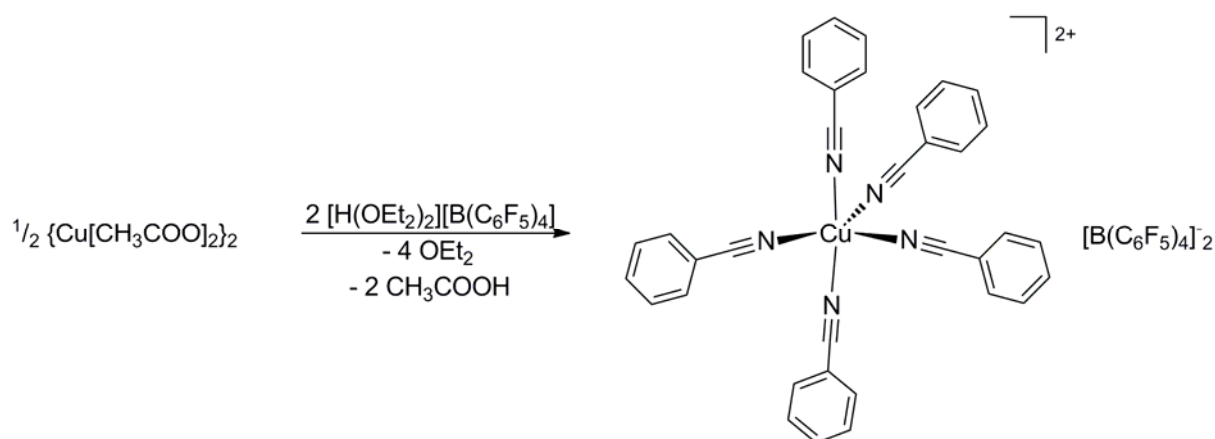
Scheme 3.4.2. Synthesis of $[Cu(C_6H_5CN)_5][B(C_6F_5)_4]_2$ (solvent: methylene chloride, benzonitrile, rt).

4.3 Characterization

Crystallization of the product yielded complexes with five coordinated solvent ligands (see Figure 3.4.4). This is contrary to previously published nitrile ligated copper(II) complexes with weakly coordinating polyfluorinated borate anions, that had six solvent ligands,[3, 8b, 38] and also to complexes with (less weakly) coordinating anions that had four solvent ligands (with two coordinated WCAs),[12, 39] all resulting in an approximately octahedral environment. The reason for coordination with five ligands is still unclear, but might arise from the fact that (a)

the anion of the neighbor occupies part of the coordination sphere of the cation and blocks one position or (b) the five ligand complex is energetically favored.

These complexes are stable for a short periode of time when exposed to argon flow or vacuum unlike acetonitrile coordinated complexes (see Chapter III. 3.3).
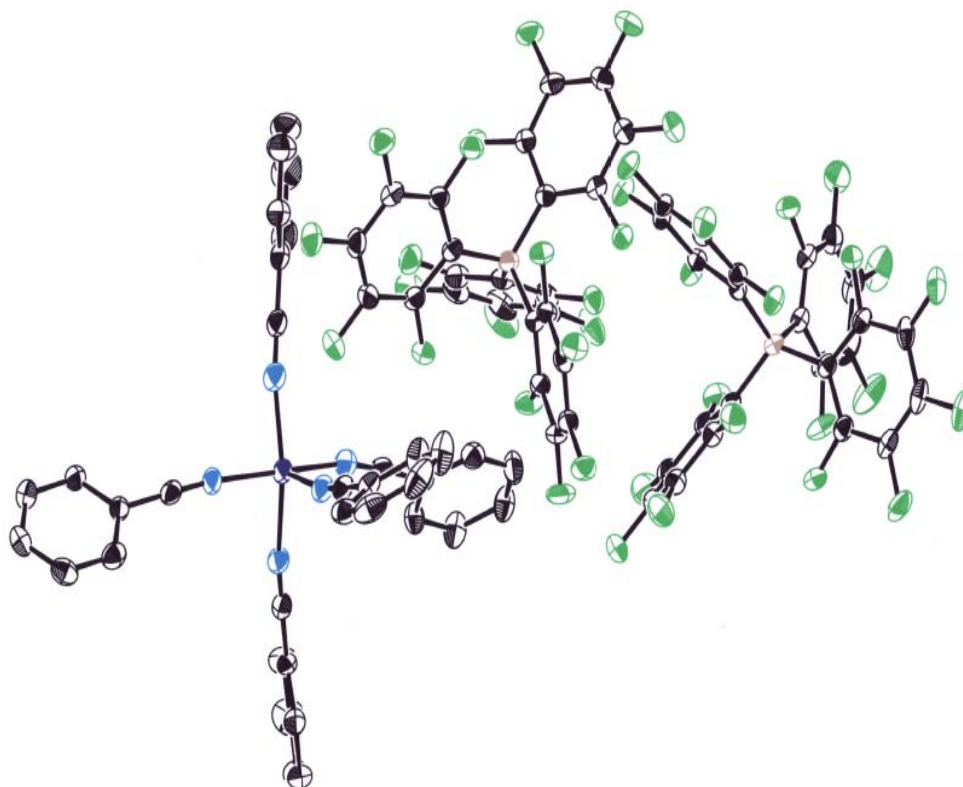
Figure 3.4.4. ORTEP style depiction of $[Cu(C_6H_5CN)_5][B(C_6F_5)_4]_2$ in the solid state. Thermal ellipsoids are drawn at the 50 % probability level.

Table 3.4.1. Selected Bond Lengths and Bond Angles for [Cu(C6H5CN)5][B(C6F5)4]2.

distance [Å]		angle [deg]	
Cu(1)-N(1)	2.0145 (16)	N(1)-Cu(1)-N(2)	152.21 (7)
Cu(1)-N(2)	1.9913 (18)	N(1)-Cu(1)-N(3)	90.06 (7)
Cu(1)-N(3)	1.9686 (18)	N(1)-Cu(1)-N(4)	85.46 (7)
Cu(1)-N(4)	1.9761 (19)	N(1)-Cu(1)-N(5)	100.82 (7)
Cu(1)-N(5)	2.1223 (18)	N(2)-Cu(1)-N(3)	92.08 (7)
		N(2)-Cu(1)-N(4)	87.60 (7)
		N(2)-Cu(1)-N(5)	106.51 (7)
		N(3)-Cu(1)-N(4)	169.65 (8)
		N(3)-Cu(1)-N(5)	95.81 (7)
		N(4)-Cu(1)-N(5)	94.20 (7)

4.4 EPR spectroscopic investigation of the model system

The up to six sharp equidistant lines in each spectrum originate from the Mn^{2+} standard.

4.4.1 EPR measurements with [Cu(C6H5CN)5][B(C6F5)4]2

[Cu(C6H5CN)5][B(C6F5)4]2 in toluene
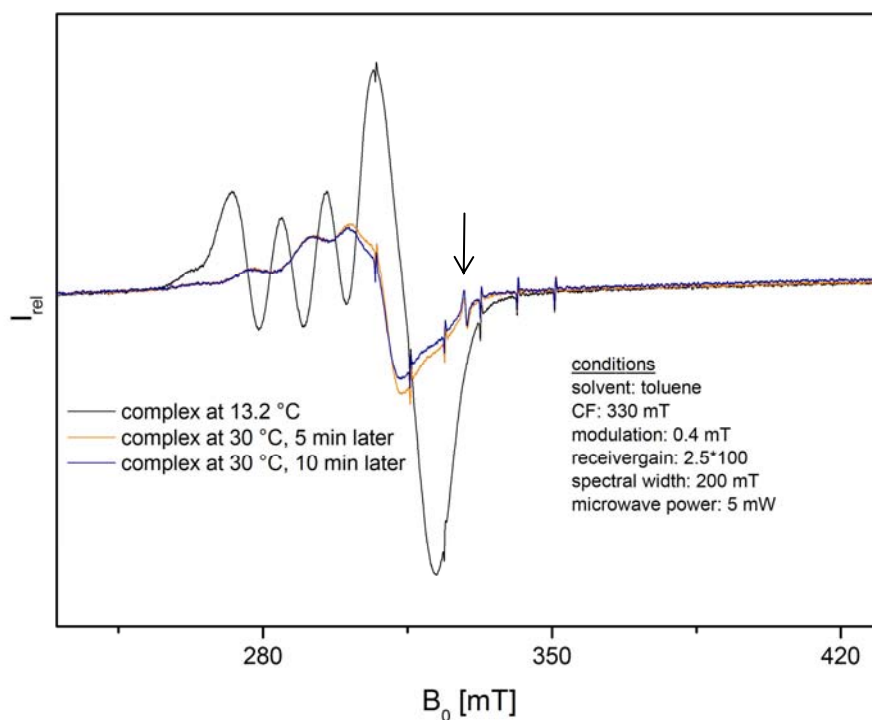
Figure 3.4.5. EPR spectrum of [Cu(C6H5CN)5][B(C6F5)4]2 crystals with toluene supernatant at 13.2 °C (black) and after heating to 30 °C (brown and blue).

At first the complex of $[Cu(C_6H_5CN)_5][B(C_6F_5)_4]_2$ was characterized by EPR spectroscopy. Figure 3.4.5 shows three isotropic EPR spectra of $[Cu(C_6H_5CN)_5][B(C_6F_5)_4]_2$ crystals with a toluene supernatant. The black curve displays the typical pattern of Cu^{2+} complexes.[40] The $^{63+65}Cu$ hyperfine splitting (quartet of lines; I = 3/2; a nucleus with spin I has 2I + 1 allowed orientations with respect to the direction of an applied field so that the hyperfine multiplet consists of 2*I* + 1 equally intense, equally spaced lines) due to interaction of the unpaired electron with the nuclear spins of ^{63}Cu and ^{65}Cu (natural abundance: 69 and 31 % respectively, isotropic splitting not resolved) is only slightly resolved for the parallel part of the EPR spectrum. The irregular broad lines are a consequence of restricted mobility in the crystalline material. The 3 lines on the right side stem from the partly dissolved complex (the fourth of the equidistant lines is underneath the broad line of the crystalline material on the right side; g = 2,2528; A = 11,083 mT = 110,83 G, calculated with experimental data).

Upon heating the sample to 30 °C, the common temperature used for isobutene polymerization with this complex, the color of the supernatant changed from colorless to intensive brown. As can be concluded from the resulting brown and blue curves, temperature has also dramatic effect on the shape of the spectrum. The line of the mother crystals disappears and those of the complex in solution shift, probably because of the appearance of a newly formed powdery material of different nature. Increasing time and temperature lead to the formation of a radical species, visible in an additional line which turns up at approximately 330 mT in the spectrum (marked by an arrow; g = 2,00358, calculated with experimental data).
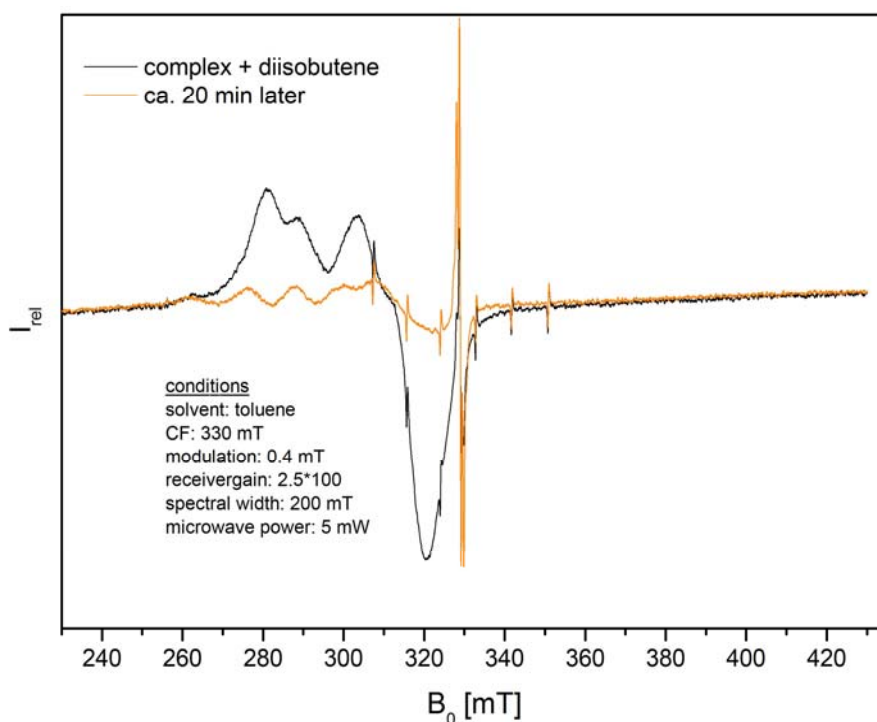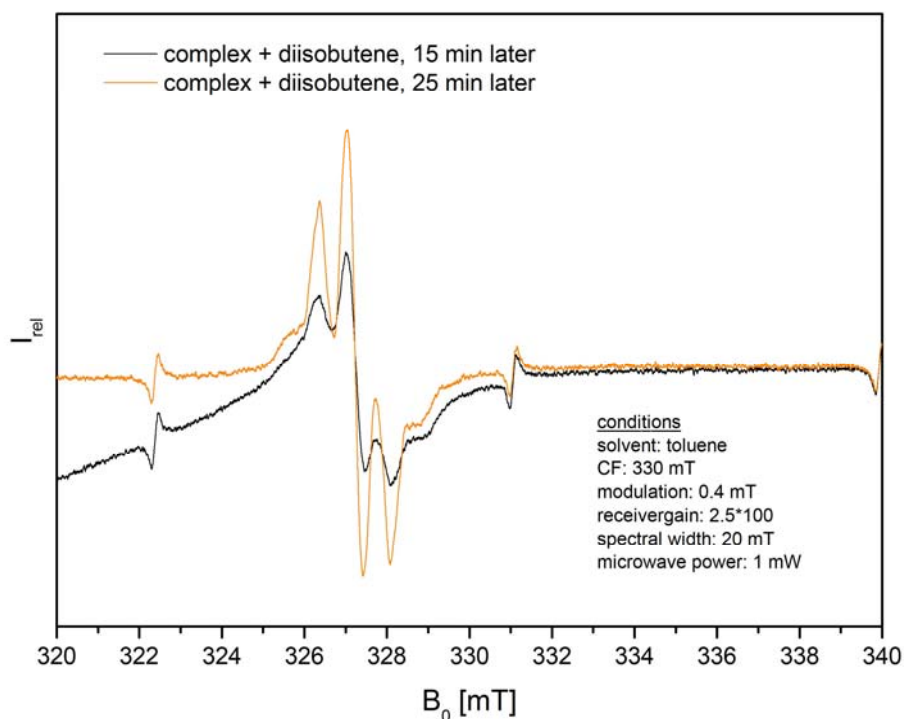
Figure 3.4.6. EPR spectrum of $[Cu(C_6H_5CN)_5][B(C_6F_5)_4]_2$ crystals with toluene supernatant, after addition of diisobutene.

After addition of diisobutene, the solubility and the brown color of the supernatant increase drastically accompanied with a remarkable increase of the intensity of the radical signal (see Figure 3.4.6). In contrast, the lines originated from the Cu(II) species decrease. The latter show an inhomogeneous broadening due to, either a poorly resolved hyperfine structure or anisotropic interactions in randomly oriented systems. Dipolar interactions with other fixed paramagnetic species could be a reason, as well (s.a.).

Figure 3.4.7. Resolved radical signal in the EPR spectrum of $[Cu(C_6H_5CN)_5][B(C_6F_5)_4]_2$ crystals with toluene supernatant, after addition of diisobutene with lowered microwave power.

Closer examination of the radical signal by focusing the spectrum from a spectral width of 200 mT to 20 mT (increased resolution of the radical signal) and reduction of the microwave power from 5 mW to 1 mW reveals a splitting of the radical signal after addition of diisobutene (see Figure 3.4.7). These lines are obviously of organic origin and do not correspond to Cu^{2+} species, as the range of magnetic field is too narrow. Even better resolution could be obtained with the normal microwave power of 5 mW and reduced modulation of 0.02 mT (see Figure 3.4.8; g = 2,00396 , A = 2926 mT = 2,926 G, calculated with experimental data).

This (in first approximation) quintet spectrum indicates four equivalent hydrogen atoms, but simulation of the spectrum could not be carried out in the time frame of this work. Hence the radical signal can not be assigned to proposed radical species.
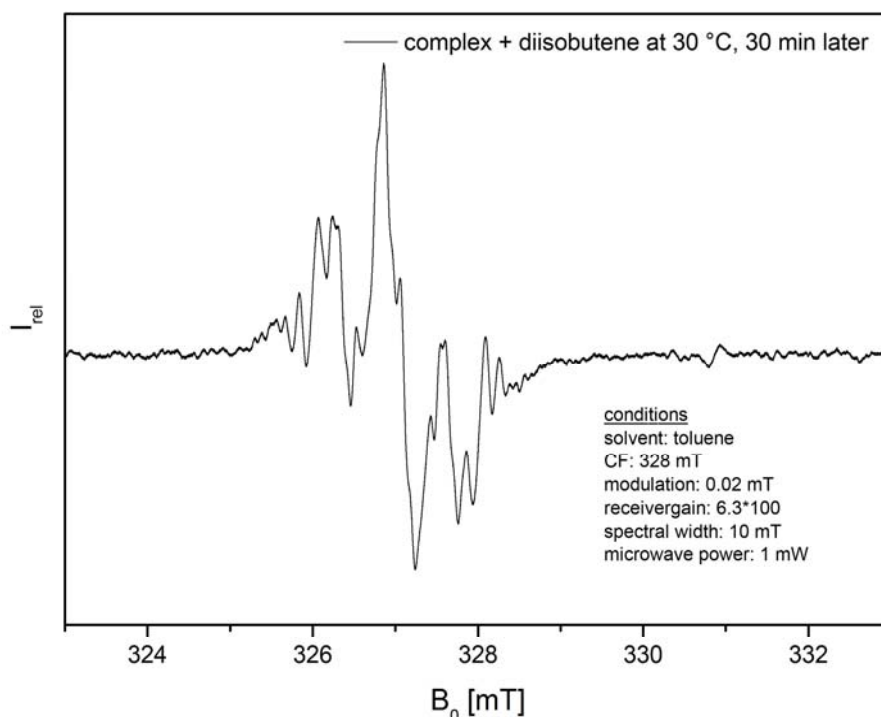
Figure 3.4.8. Expanded EPR spectrum of $[Cu(C_6H_5CN)_5][B(C_6F_5)_4]_2$ crystals with toluene supernatant, after addition of diisobutene, after heating to 30 °C and reducing modulation.

$[Cu(C_6H_5CN)_5][B(C_6F_5)_4]_2$ in dichloromethane

If a radical or radical cationic mechanism is assumed radicals would have to be formed both in toluene and methylene chloride, the common polymerization media. It can be shown that, in contrast to the results obtained in toluene the Cu(II) complex behaves differently in methylene chloride solution. Due to the stability of the complex in methylene chloride (see synthesis, Chapter III. 4.2) no radical formation without diisobutene addition is expected.

Indeed, no splitting of the copper lines can be resolved in the (light green) solution of the complex in dichloromethane. This is a result of the solvent polarity. It could be shown that no radicals are formed even after heating to 40 °C (see Figure 3.4.9). This changes rapidly upon addition of diisobutene. The copper(II) lines start to disappear together with the appearance and growing of a radical line. The intensity of this line is lower, than the one formed in toluene and cannot be obtained in good resolution. Therefore, it could not be concluded whether the formed radical species are identical.
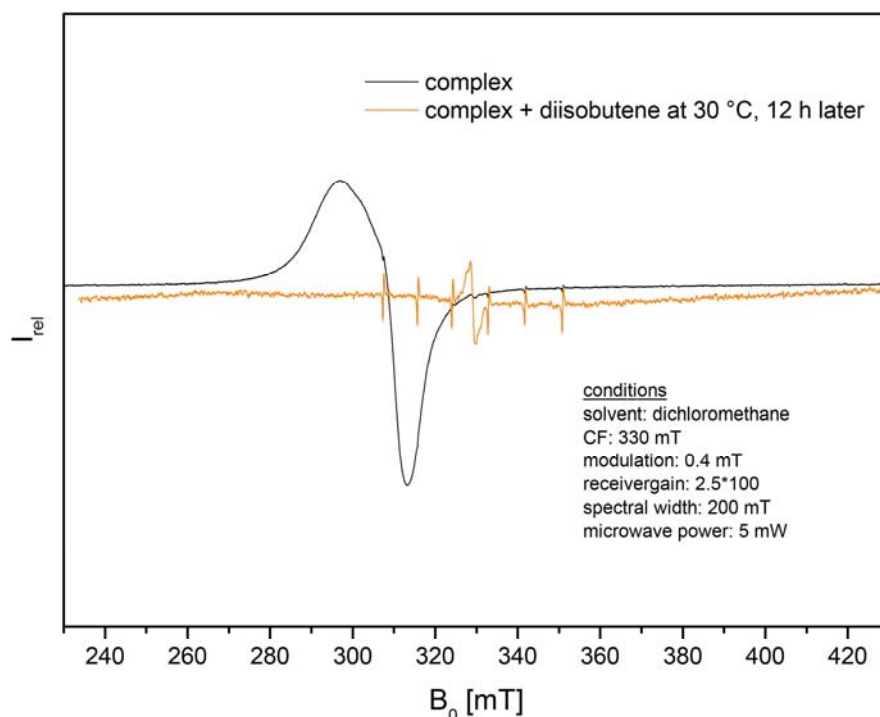
Figure 3.4.9. EPR spectrum of $[Cu(C_6H_5CN)_5][B(C_6F_5)_4]_2$ in dichloromethane solution before and 12 h after addition of diisobutene.

Reference experiments and conclusion:

Pure toluene or diisobutene as well as a mixture of them do not form radicals which are visible in EPR under the same conditions. Neither do $[Zn(C_6H_5CN)_5][B(C_6F_5)_4]_2$ and $[Zn(CH_3CN)_6][B(C_6F_5)_4]_2$. In case of the latter ones this is probably due to instability of the radical species.

Different possibilities for the disappearance of the copper(II) signal when forming the radical species are conceivable. The most probable involves reduction of Cu(II) to Cu(I) when transferring an electron from either toluene or diisobutene to the metal core. However, this is not the only option for EPR-nondetectable copper. In several cases the metal ions are strongly coupled Cu(II)-Cu(II) pairs. The most prominent example is copper acetate, the starting materials for our complexes, where two spins are exchange coupled into a singlet ground state with an excited triplet 300 cm^{-1} above. Responsible for spin-spin coupling in acetate dimers is super exchange via the carboxylate bridges. Accordingly, this compound is basically diamagnetic over a large range of temperatures. Thus, a high concentration of triplet states exists and no hyperfine structure is resolved at room temperature. The triplet

concentration decreases significantly and hyperfine splitting from two equivalent copper atoms appears, when cooled to 77 K. At temperatures of 20 K or below all spins are paired and the lines disappear. Similar behaviour can also be observed in various other copper compounds.[40-41]

4.4.2 EPR measurements with [(C$_6$H$_5$)$_3$C][B(C$_6$F$_5$)$_4$]

As the experiments above show a clear formation of a radical species in the reaction of the employed copper complex with diisobutene and due to the very similar reaction behavior of both, the copper complex and the trityl-salt in isobutene polymerization, EPR spectroscopy was used to investigate formation of radicals as well. Additionally radical formation during isoprene polymerization was reported when using [(C$_6$H$_5$)$_3$C][SbCl$_6$] as initiator.[42]

Thus a solution of triphenylmethyl tetrakis(pentafluorophenyl)borate (tritylborate) in toluene with added diisobutene was heated to 30 °C and tested for EPR activity. The obtained radical signal of relatively low intensity showed almost no dependence on time (see Figure 3.4.10; g = 2,00416) and no change was detected after 12 hours. To exclude radical signals originating from the EPR tube, the emptied vial was controlled in a blank test where no radical signal could be observed.
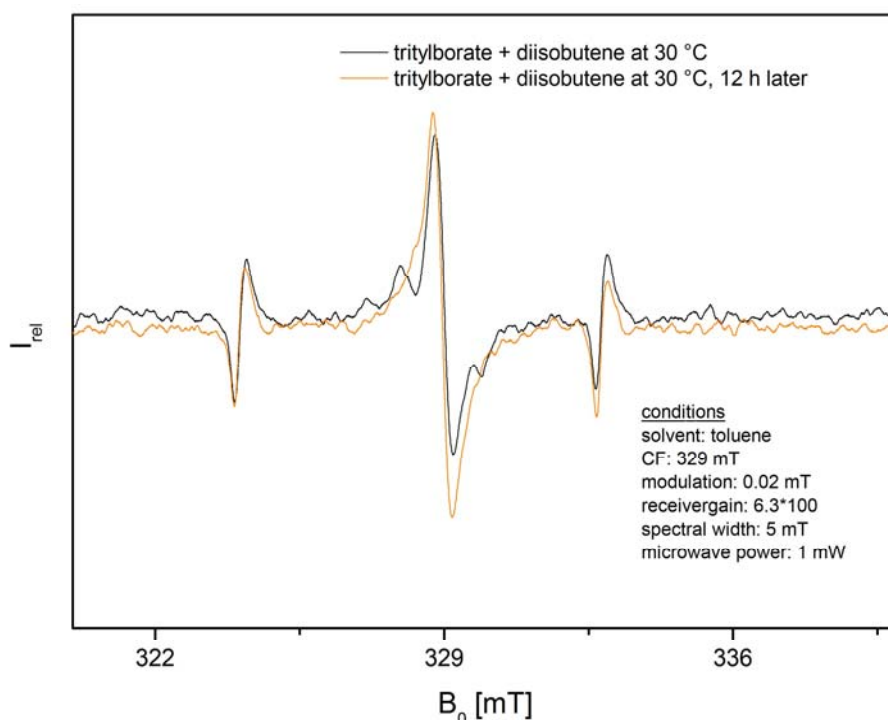
Figure 3.4.10. Expanded EPR spectrum of $[(C_6H_5)_3C][B(C_6F_5)_4]$ in toluene solution after addition of diisobutene and heating to 30 °C.

4.5 Radical trapping experiments with fullerene C_{60}

4.5.1 EPR measurements

Buckminster fullerene is described as a suitable radical trapping agent in polymerization reactions. Especially useful is the absence of strongly coordinating donor functionalities when combined with highly sensitive metal cations. For instance methyl radicals which were formed during the initiation of the propylene polymerization in presence of zirconium or titanium complexes and methylalumoxane (MAO) could be trapped successfully with C_{60}.[35b, 35c]

When using the supernatant of the reaction mixture of $[Cu(C_6H_5CN)_5][B(C_6F_5)_4]_2$, diisobutene and toluene for EPR experiments the observed hyperfine splitting is poorly resolved. The addition of C_{60} to the very same solution leads to highly resolved hyperfine splitting (see Figure 3.4.11). This indicates a reaction between fullerene and a part of the previous reaction mixture. No assignment of formed species could be made.
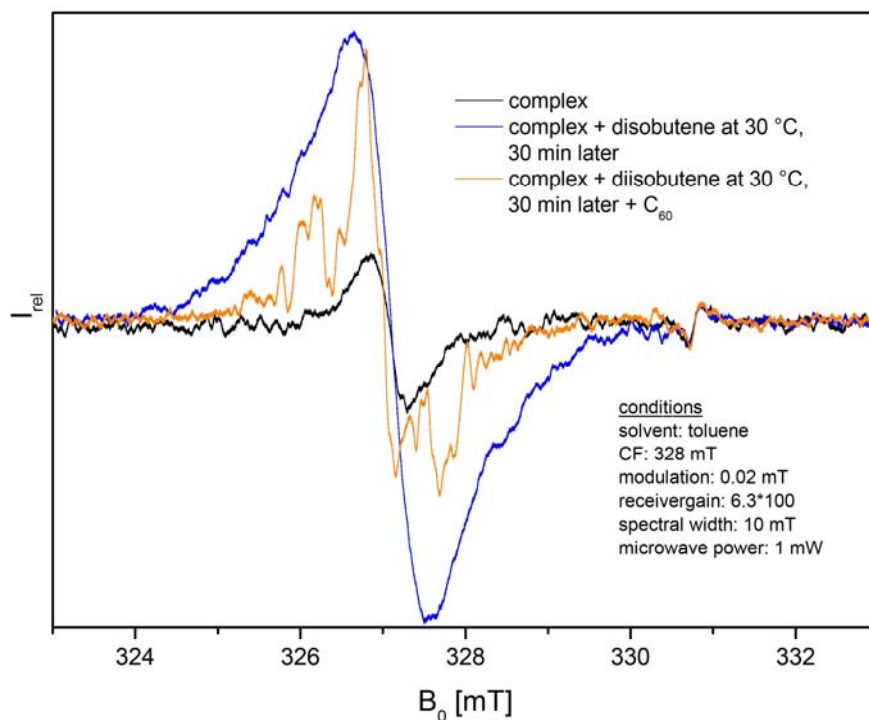
Figure 3.4.11. Expanded EPR spectrum of [Cu(C$_6$H$_5$CN)$_5$][B(C$_6$F$_5$)$_4$]$_2$ in toluene solution after addition of diisobutene and C$_{60}$, heated to 30 °C.

The occurrence of a hyperfine splitting, as in toluene, can not be observed with the copper complex in methylene chloride solution (see Figure 3.4.12).
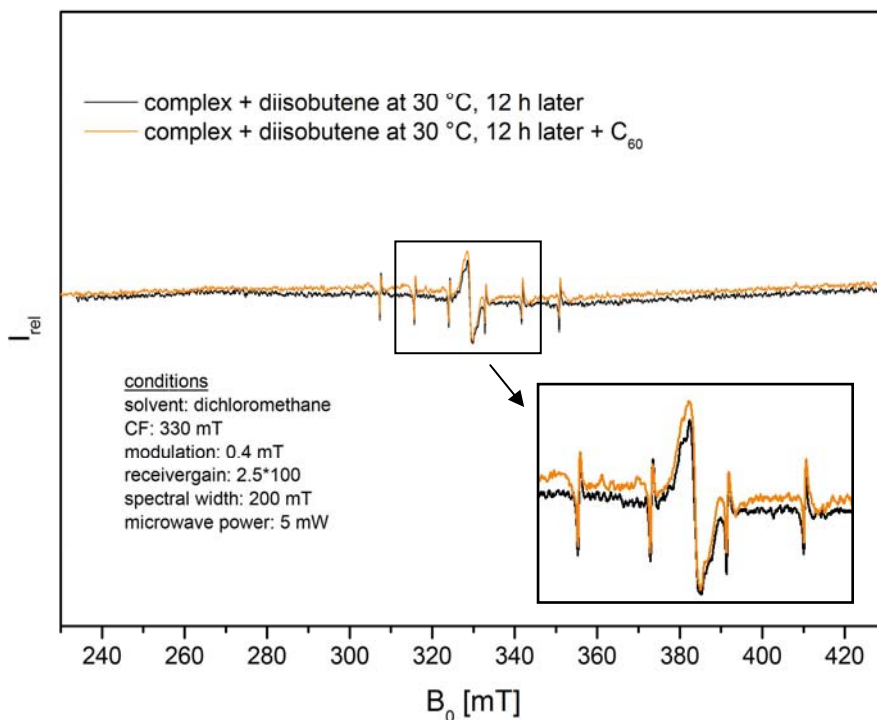
Figure 3.4.12. EPR spectrum of [Cu(C$_6$H$_5$CN)$_5$][B(C$_6$F$_5$)$_4$]$_2$ in methylene chloride solution after addition of diisobutene and C$_{60}$, heated to 30 °C.

4.5.2 MALDI/TOF spectrometry

In the above mentioned literature formation of radical adducts to C_{60} was also monitored via MALDI/TOF spectrometry.

MALDI/TOF analysis shows one Cu(I) ion attached to one fullerene molecule, as well as to aggregates of C_{60} decomposition products (see Figure 3.4.13). Unfortunately no radical coordinated C_{60} species could be observed, presumably due to steric reasons preventing associations.
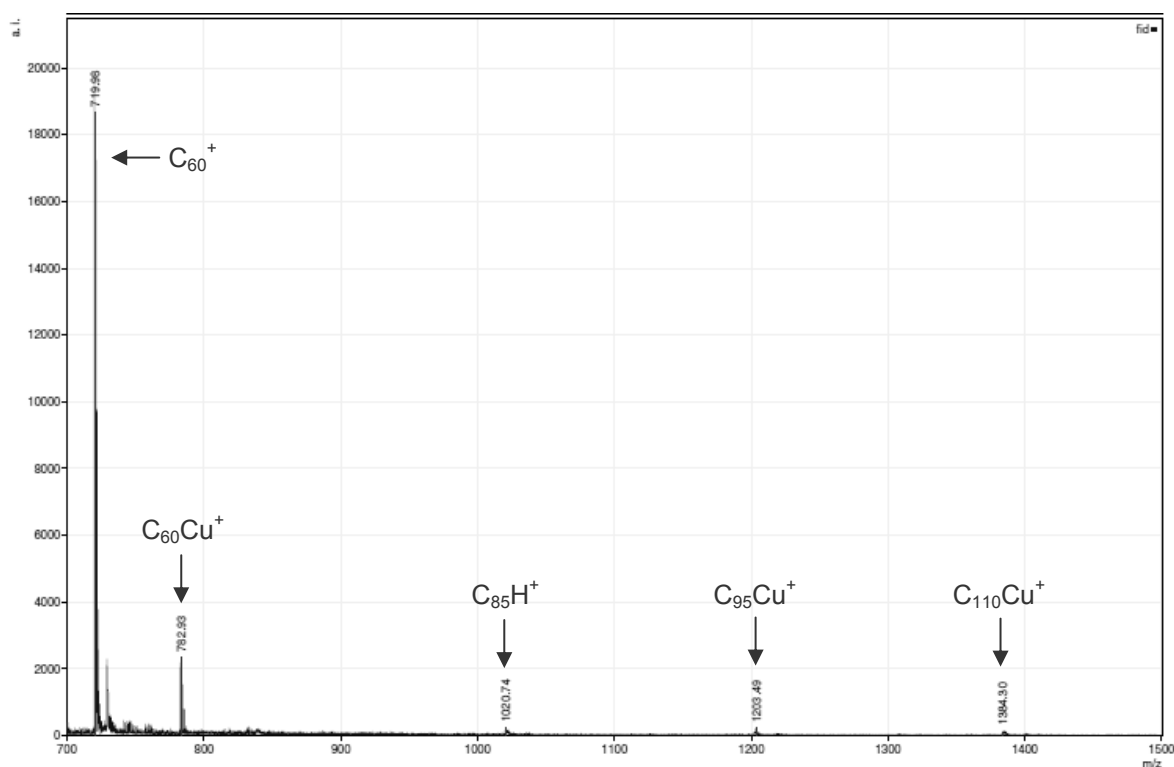
Figure 3.4.13. MALDI/TOF monitoring of the mixture of $[Cu(C_6H_5CN)_5][B(C_6F_5)_4]_2$ with toluene, diisobutene and fullerene C_{60}.

4.6 ESI-MS spectroscopy control experiments

To exclude decomposition products of anion molecules resulting from an involvement during the radical formation, ESI-MS spectra were acquired in the negative ion mode (cone voltage 80 V).

Stoichiometric amounts of $[Cu(C_6H_5CN)_5][B(C_6F_5)_4]_2$ or $[(C_6H_5)_3C][B(C_6F_5)_4]$ were reacted with diisobutene in toluene solution at 30 °C over 20 h and were afterwards tested for the

existence of $[B(C_6F_5)_4]^-$. The obtained spectra are identical (see Figure 3.4.14, 3.4.15) and only the counter ion $[B(C_6F_5)_4]^-$ at M/z 678.6 as well as fragmentation products from ionization can be observed (m/z 166.9, 314.8, 528.7). The fragmentation during ionization was ascertained with a blank test of the parent compounds before reaction with diisobutene. These results, as well as subsequent ^{11}B- and ^{19}F NMR-spectra, which show no evidence for the formation of new species, exclude anion decay during radical formation (see Chapter V. Appendix).
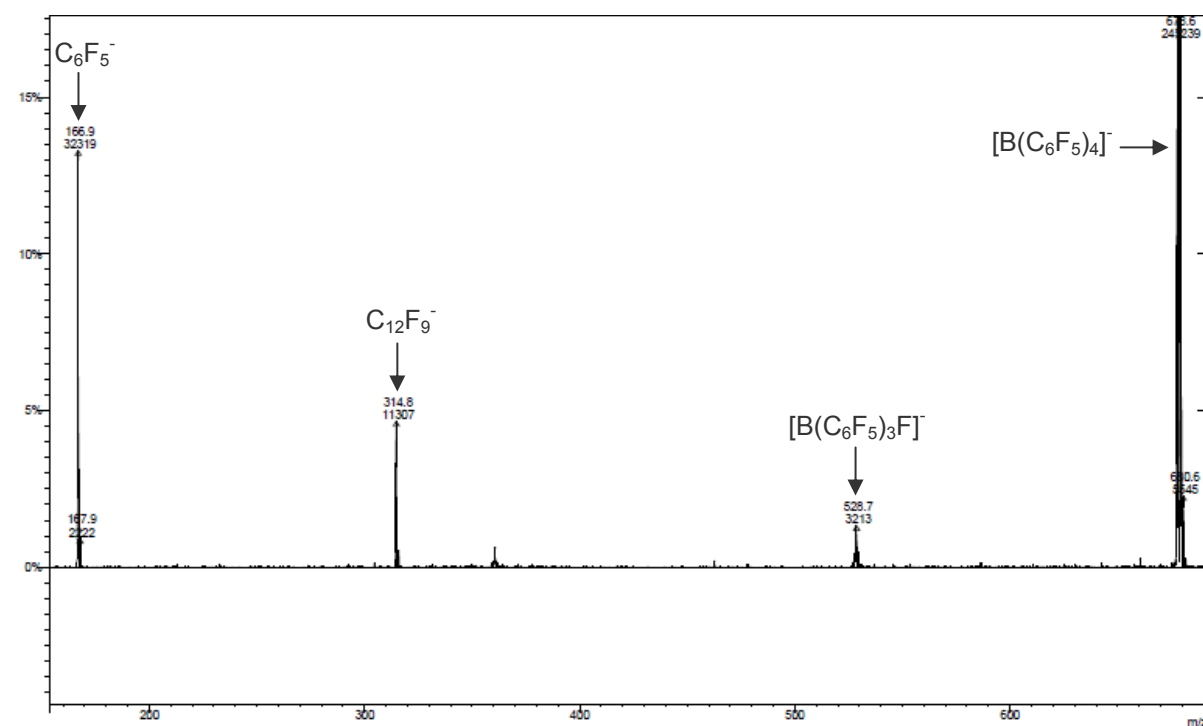
Figure 3.4.14. ESI-MS spectrum of $[Cu(C_6H_5CN)_5][B(C_6F_5)_4]_2$ in toluene solution, after addition of diisobutene and heating to 30 °C.
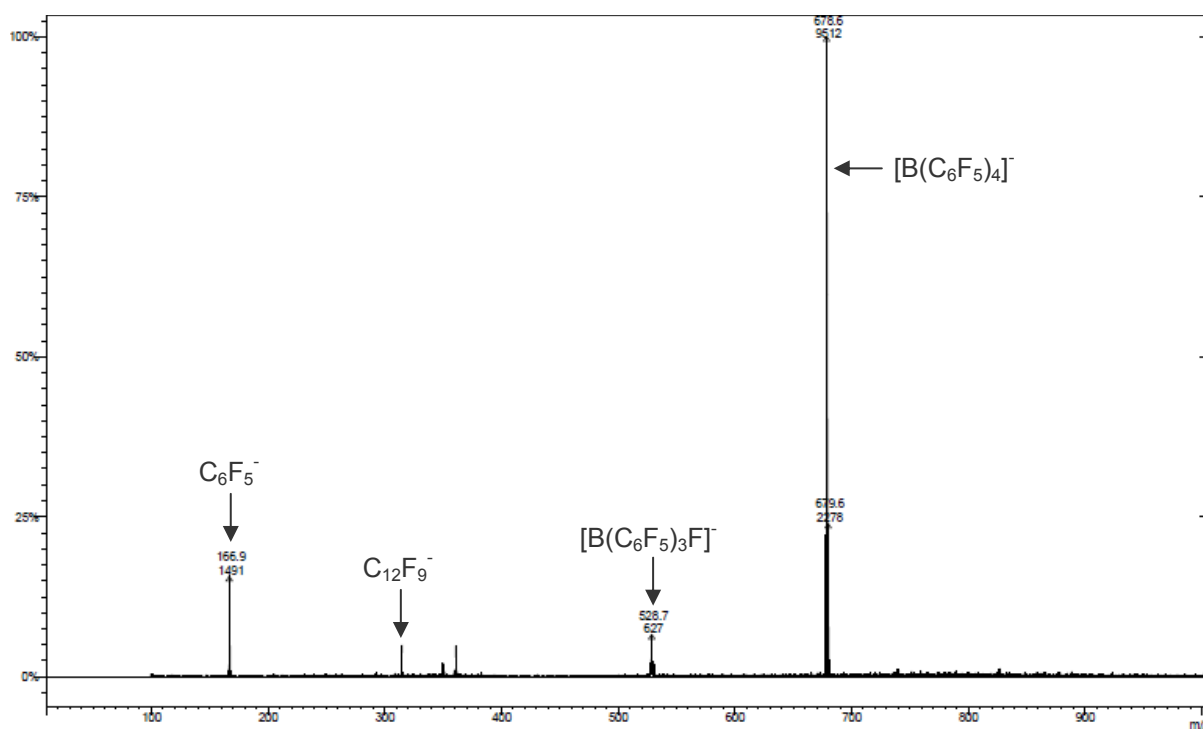
Figure 3.4.15. ESI-MS spectrum of $[(C_6H_5)_3C][B(C_6F_5)_4]$ in toluene solution, after addition of diisobutene and heating to 30 °C.

4.7 UV/Vis investigations for qualitative reaction control

UV/Vis spectroscopy is known to be applicable in the qualitative monitoring of a reaction progress. As a drastic color change occurred during the conducted reactions of $[Cu(C_6H_5CN)_5][B(C_6F_5)_4]_2$ UV/Vis spectroscopy was applied to find out if the reactions occur quantitatively.

It was shown by comparison of the UV/Vis spectrum from the originally green solution of $[Cu(C_6H_5CN)_5][B(C_6F_5)_4]_2$ in dichloromethane (see Figure 3.4.16) with the spectrum obtained after diisobutene addition (see Figure 3.4.17), that the absorption band of blue green $[Cu(C_6H_5CN)_5][B(C_6F_5)_4]_2$ (λ_{max} = 705.0 nm, broad) completely disappeared after diisobutene addition and heating to 30 °C for 30 min. At the same time a broadening of the band below 400 nm to approximately 450 nm occurred together with the appearance of a shoulder at approximately 530 nm.
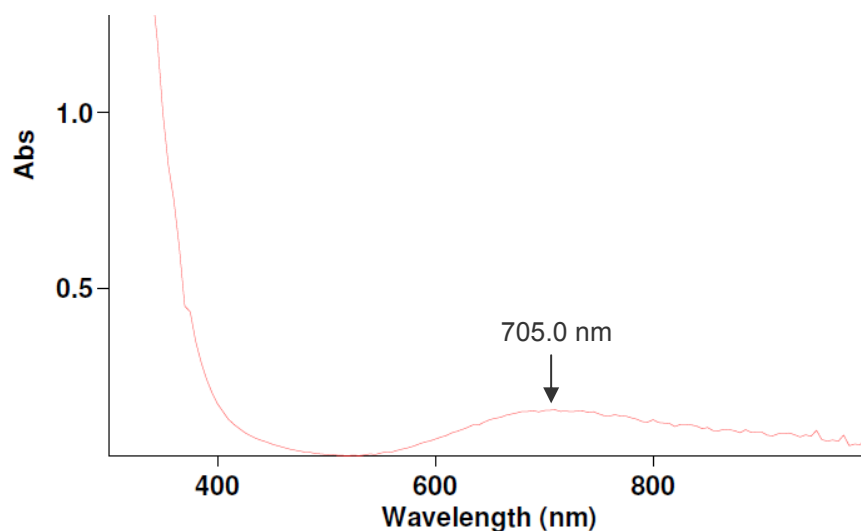
Figure 3.4.16. UV/Vis spectrum of $[Cu(C_6H_5CN)_5][B(C_6F_5)_4]_2$ in dichloromethane.
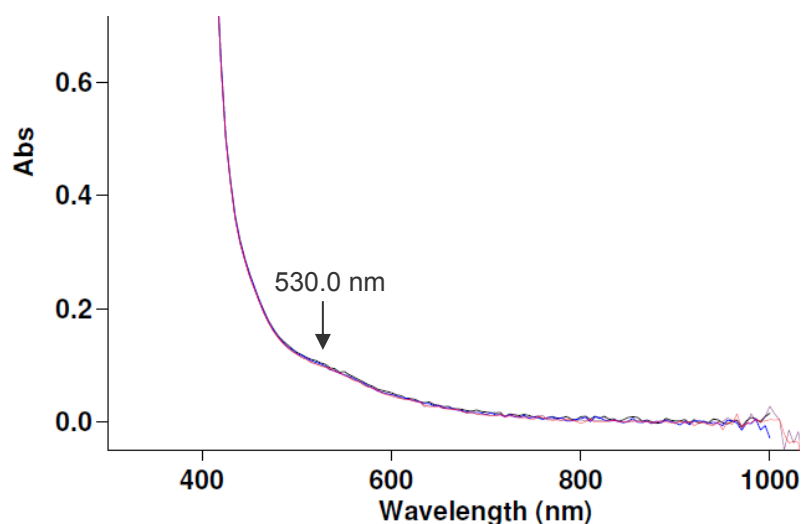
Figure 3.4.17. UV/Vis spectrum of $[Cu(C_6H_5CN)_5][B(C_6F_5)_4]_2$ and diisobutene in dichloromethane after reaction at 30 °C for 30 min.

The band at 705 nm cannot be observed in toluene and toluene/diisobutene solutions of the complex (see Figure 3.4.18, 3.4.19), though a sharp band at λ_{max} = 405.0 nm occurs independently from diisobutene addition.[43] This is in accordance with observed decomposition of the copper complex in toluene, as already indicated from EPR spectroscopy.
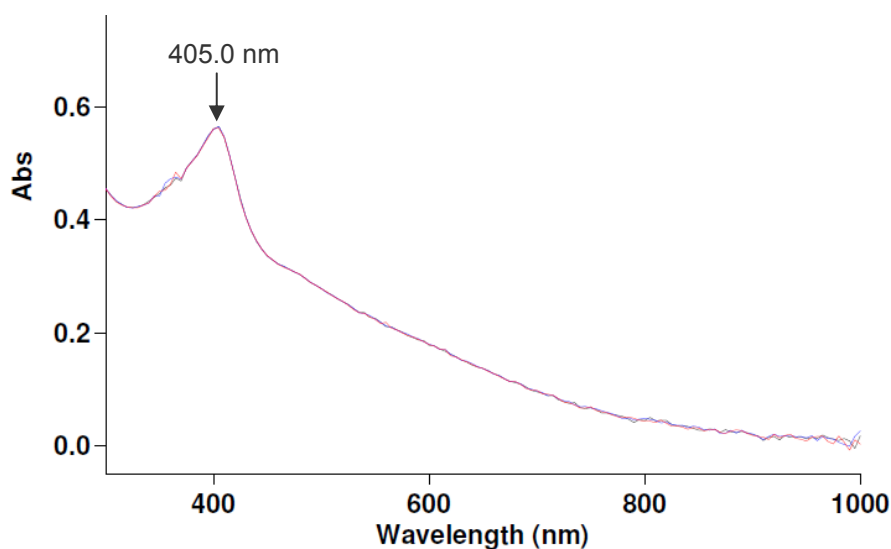
Figure 3.4.18. UV/Vis spectrum of [Cu(C$_6$H$_5$CN)$_5$][B(C$_6$F$_5$)$_4$]$_2$ in toluene.
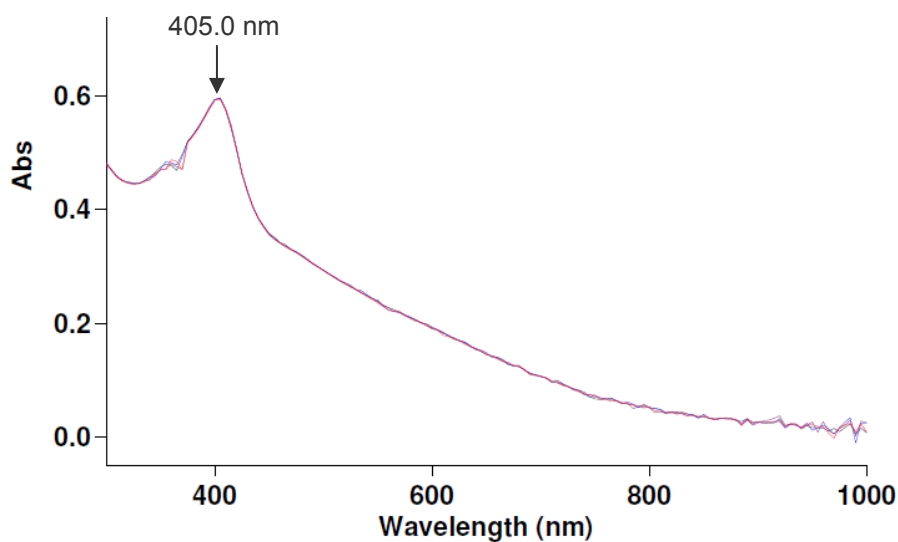
Figure 3.4.19. UV/Vis spectrum of [Cu(C$_6$H$_5$CN)$_5$][B(C$_6$F$_5$)$_4$]$_2$ and diisobutene in toluene.

The reason for the color change when adding toluene or diisobutene (unlike dichloromethane) to [Cu(C$_6$H$_5$CN)$_5$][B(C$_6$F$_5$)$_4$]$_2$ is most likely the formation of charge transfer complexes via the C=C bonds (see Figure 3.4.20) which induces the generation of radicals. This is in accordance with the starting point of literature known radical-cationic polymerizations of isobutene.[27, 29l, 29r]

$$[M(C_6H_5CN)_x][B(C_6F_5)_4]_2$$
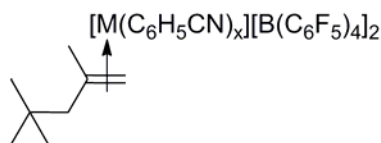
Figure 3.4.20. Potentially formed charge transfer complex.

4.8 NMR spectroscopy of the paramagnetic reaction mixture

NMR spectroscopy was conducted to gain further insight in the reaction of $[Cu(C_6H_5CN)_5][B(C_6F_5)_4]_2$ with toluene and diisobutene.

Figure 3.4.21 shows the ^{1}H NMR spectrum of $[Cu(C_6H_5CN)_5][B(C_6F_5)_4]_2$ and toluene in C_6D_6. The toluene proton peaks (δ (ppm) = 2.11, 7.14, 7.20) show no observable shift in comparison with those of free toluene in C_6D_6 and the signals are split.[44] The peaks of the benzonitrile protons (δ (ppm) = 7.36, 6.69) are paramagnetically broadened as these molecules are directly bond to the Cu^{2+} center. Considerable spin density is induced on the ligands and selective spin transferred to the protons of benzonitrile.[45]
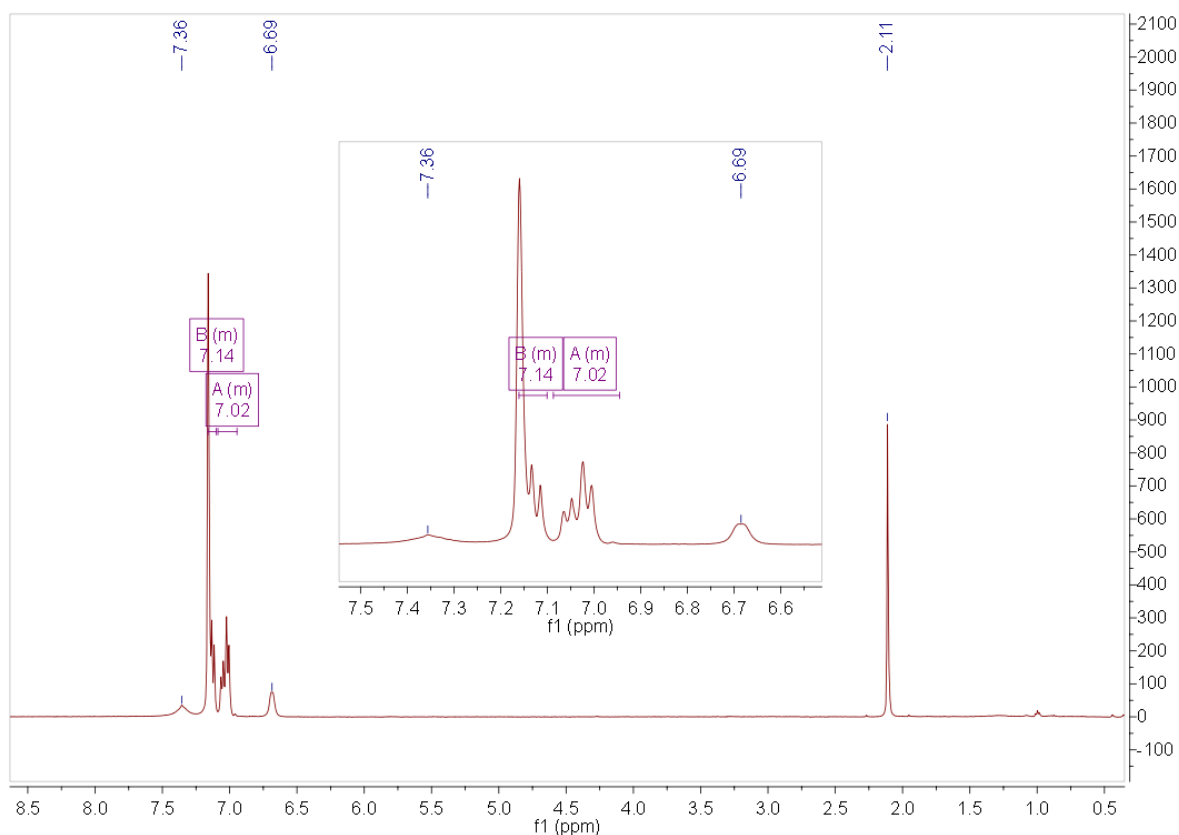
Figure 3.4.21. ^{1}H NMR spectrum of the reaction of $[Cu(C_6H_5CN)_5][B(C_6F_5)_4]_2$ with toluene in C_6D_6.

Only toluene carbons can be identified in the ^{13}C-NMR spectrum of $[Cu(C_6H_5CN)_5][B(C_6F_5)_4]_2$ and toluene in C_6D_6 (see Figure 3.4.22). The reason for the absence of the peaks of the benzonitrile carbon atoms is unknown. All of the peaks originated from the aromatic carbon atoms belonging to toluene are unshifted when compared with literature known values (see Table 3.4.2).[44] Intriguingly, the peak assigned to the methyl carbon is, in contrast, shifted closer to the directly bond aromatic carbon.
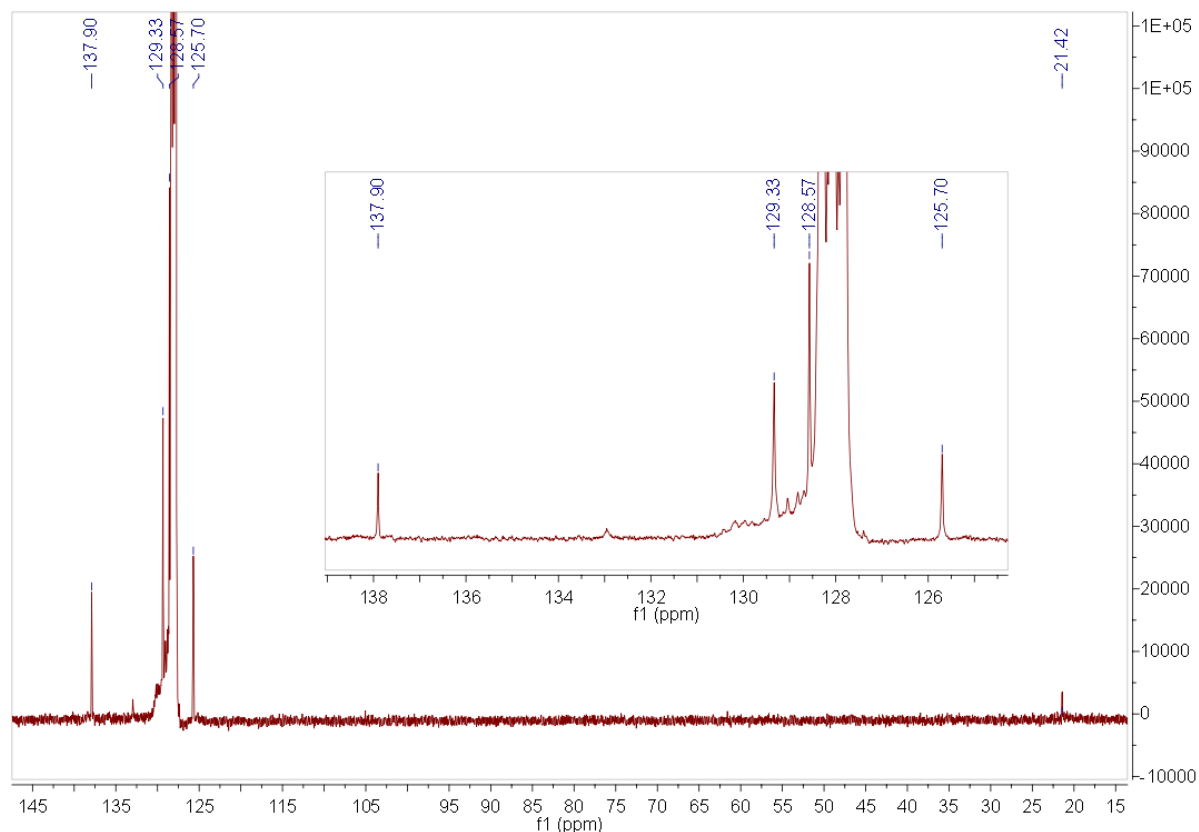
Figure 3.4.22. ^{13}C-NMR spectrum of the reaction of $[Cu(C_6H_5CN)_5][B(C_6F_5)_4]_2$ with toluene in C_6D_6.

Table 3.4.2. ^{13}C-NMR chemical shifts of toluene in C_6D_6 [ppm].

	δ_{CH3}	$\delta_{C(1)}$	$\delta_{C(2,6)}$	$\delta_{C(3,5)}$	$\delta_{C(4)}$
pure[44]	21.1	137.9	129.3	128.6	125.7
with $[Cu(C_6H_5CN)_5][B(C_6F_5)_4]_2$	21.4	137.9	129.3	128.6	125.7

This shift of the methyl carbon may be due to interaction with the paramagnetic metal center and could be an indication for the formation of a charge transfer complex. This would be in accordance with earlier studies of the influence of paramagnetic metallocenes on aromatic

solvents by *Köhler*.[46] Another possibility is the presence of radicals located at the methyl carbons (see EPR spectroscopic measurements of Chapter III. 4.4.1).

Interestingly when measuring ^{1}H NMR spectra of the reaction of $[Cu(C_6H_5CN)_5][B(C_6F_5)_4]_2$, toluene and diisobutene in C_6D_6 under slightly different parameters (see table 3.4.3) the observed peaks and intensities show divergence. Figures 3.4.23 and 3.4.24 display two ^{1}H NMR spectra, taken under different conditions repeatedly with the same sample.

The toluene and benzonitrile signals of spectrum 3.4.24 (even though measured with different parameters, see Table 3.4.3) correspond to those of the sample without isobutene (see Figure 3.4.21), although the two visible benzonitrile signals are each shifted closer to each other when diisobutene is present (δ (ppm): 7.36 → 7.26; 6.69 → 6.75). The broad signal in the middle of the spectrum in Figure 3.4.24 is an artefact due to impurities in the probe head and can be neglected. In contrast the resolution of the spectrum in Figure 3.4.23 is very poor and the benzonitrile signal at δ = 7.26 ppm can not be observed. These differences are even more obvious in a superposition of both spectra (see Figure 3.4.25).

Both spectra show only the *tert*-butyl group protons of diisobutene (δ = 7.26 ppm). No traces of the other expected proton signals can be found. Neither as signals shifted to considerable higher or lower fields (what can be the case for protons of paramagnetic compounds) nor as broad signals. Hence, the signals can either be shifted to low fields and overlapped by the more intensive aromatic protons or broadened beyond the detection limit and not distinguishable form the baseline. The latter would be typical for fast nuclear relaxation of paramagnetic substances. Additional significant signal broadening can occur because of delocalization of spin density with ligands as secondary spin sources.[47] The probability of shifts to very high or low fields (*i.e.* several 100 ppm) is low as the shift of the signal of the protons of the *tert*-butyl group (δ = 1.22 ppm) is small when comparing with the original signal of diisobutene in C_6D_6 (δ = 0.91 ppm).

Table 3.4.3. Selected parameters of the ^{1}H-NMR measurements shown in the spectra in Figure 3.4.21-3.4.24.

parameter	Figure 3.4.21, 3.4.23	Figure 3.4.24
Relaxation delay	1.0000	1.0000
Pulse width	11.7000	7.9000
Acquisition time	0.8159	3.9846

A possible explanation for the differences in the spectra in Figure 3.4.23 and 3.4.24 can be found in the experimental parameters (listed in Table 3.4.3). The resolution of a spectrum is clearly dependent on the time which spins have for relaxation. If this time is too short and the spins do not have enough time to relax into their original state before the start of the next pulse, the signal resolution will be reduced or it might be not observable at all. This could be the reason for the clear differences in the aromatic region of these spectra.
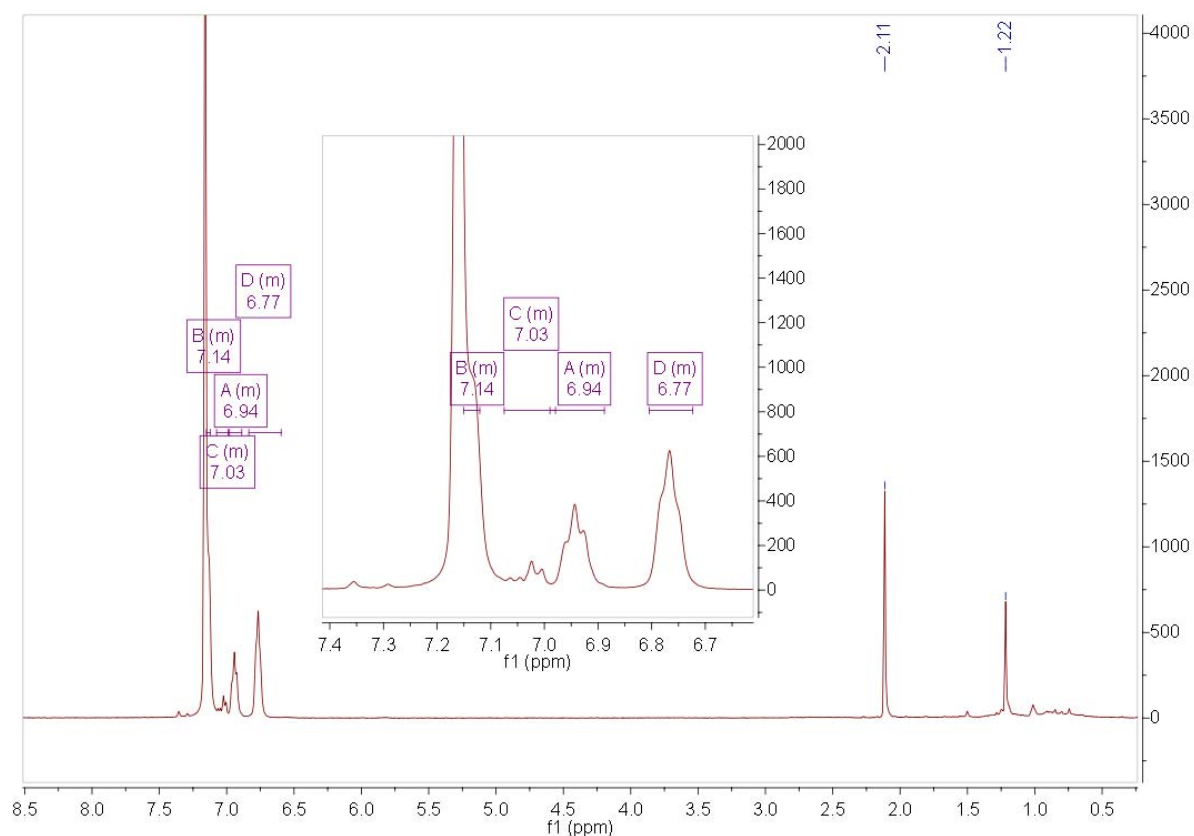
Figure 3.4.23. ^{1}H NMR spectrum of the reaction of $[Cu(C_6H_5CN)_5][B(C_6F_5)_4]_2$ with diisobutene and toluene in C_6D_6.
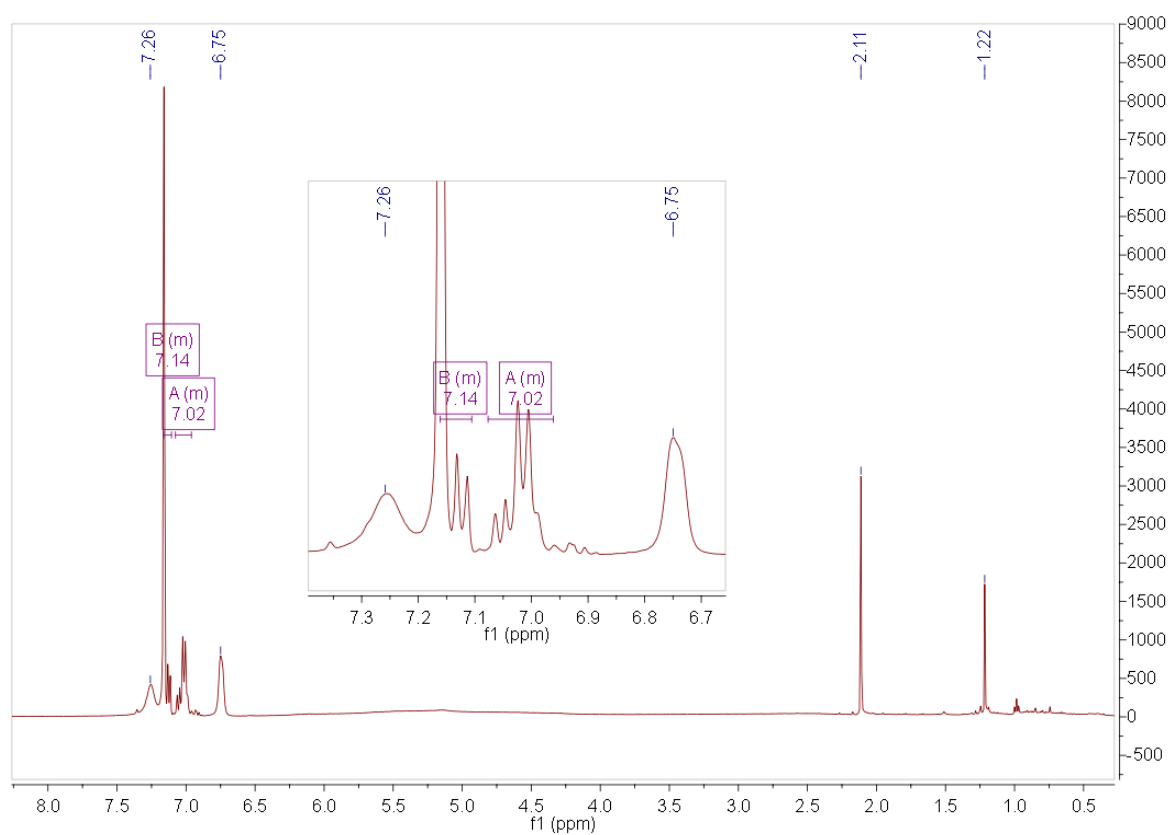
Figure 3.4.24. ^{1}H NMR spectrum of the reaction of [Cu(C$_6$H$_5$CN)$_5$][B(C$_6$F$_5$)$_4$]$_2$ with diisobutene and toluene in C$_6$D$_6$.
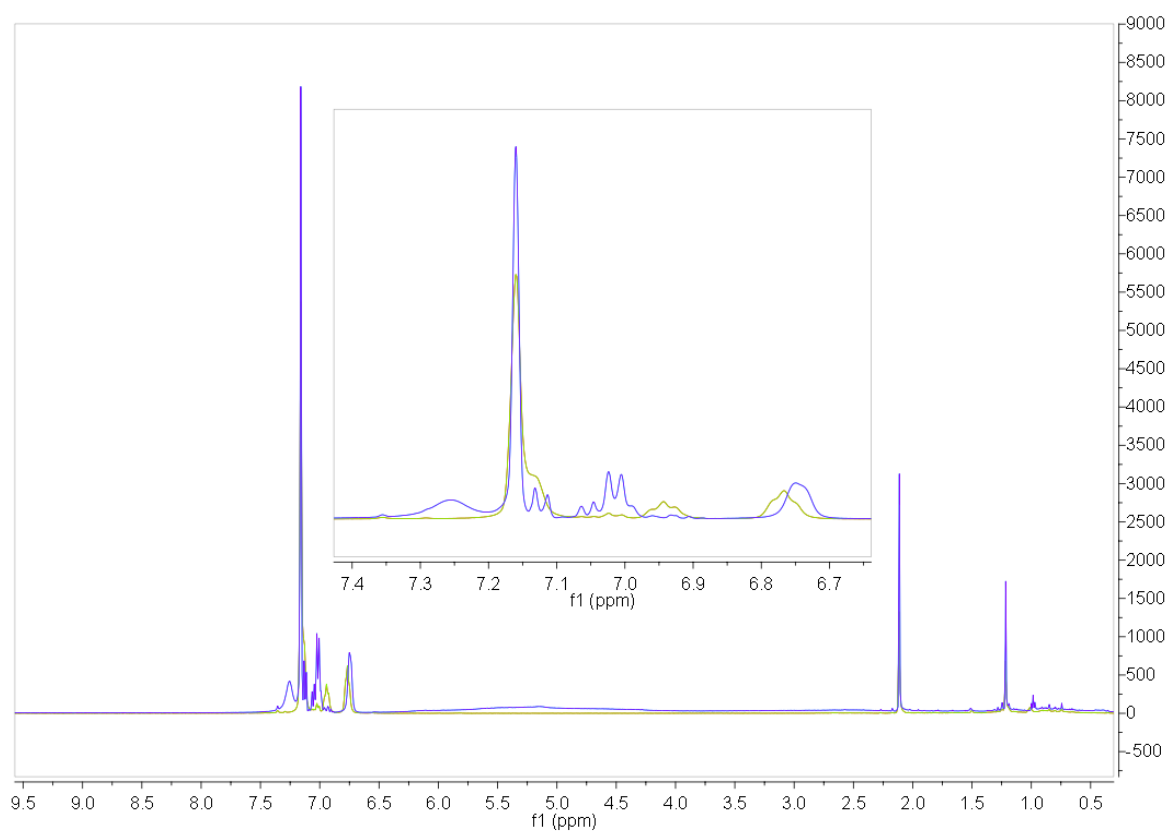
Figure 3.4.25. Superposition of the ^{1}H NMR spectra of Figure 3.4.23 and 3.4.24.

The signal width at half height is proportional to $(1/\pi T_{2N})$, with $(1/T_{2N})$ being the spin-spin relaxation rate. Thus the possibility to detect a signal via NMR spectroscopy is, amongst others, strongly limited by the spin-spin relaxation rate. $(1/T_{2N})$ is highly dependent on the electron relaxation time (T_E). Compounds having long electron relaxation times can only be recorded via NMR measurements with some difficulty and amongst these Cu[II] containing species are generally seen as being hardly detectable. One possibility to accelerate slow electron relaxation is to increase the temperature. However, temperature dependent ^{1}H-NMR measurements (steps of 5 °C from 298 to 353 K) did not lead to the formation of new signals but to shifts of all of the signals relative to C_6H_6 and better resolution at higher temperatures (see Figure 3.4.26, Table 3.4.4).[47b]
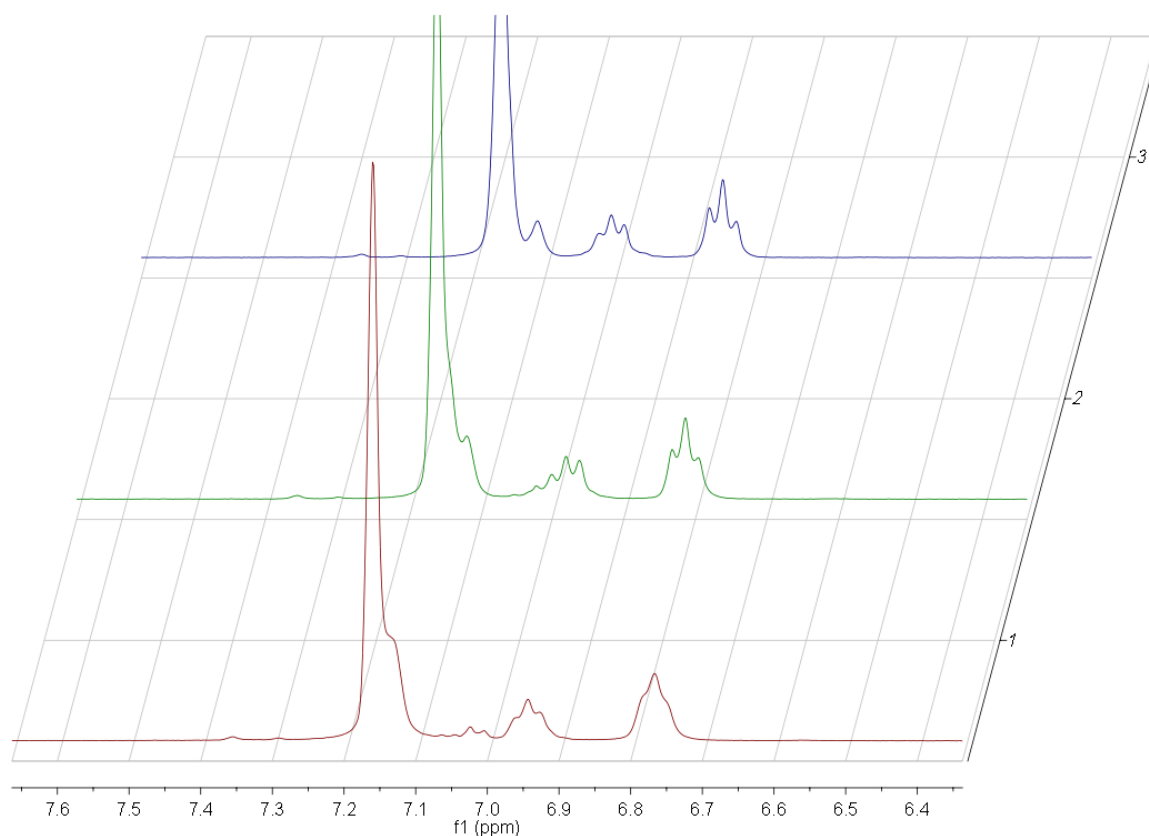
Figure 3.4.26. ^{1}H NMR spectrum of the reaction of $[Cu(C_6H_5CN)_5][B(C_6F_5)_4]_2$ with diisobutene and toluene in C_6D_6 (1: T = 298 K, 2: T = 323 K, 3: T = 348 K).

These temperature dependent shifts of the benzonitrile signals (see Figure 3.4.26, δ [ppm] = 6.94, 6.77) follow the principle: the higher the temperature is, the higher is the absolute value of the signal shift relative to the position of the signal of its isostructural

diamagnetic congener (diamagnetic molecules are usually independent of temperature). The opposite can be observed for toluene and diisobutene signals (In this context has to be mentioned that no direct conclusions can be drawn for the multiplet at δ [ppm] = 7.07-6.98 which is increasingly superimposed by its neighboring benzonitrile signal). A reason for this opposing behavior is probably weaker bonding of benzonitrile ligands to the paramagnetic metal center with increasing temperature, whereas the formation of charge transfer complexes via the unsaturated C-C bonds may be favored. This would also be in accordance with the formation of a higher amount of radicals above room temperature (see Chapter III. 4.4.1). However, the [1]H-signals which can be perceived are in all likelihood not of pure organic origin. The spectral width of purely organic radicals in NMR are extremely concentration dependent and would most likely not be seen at all in the degree of dilution which was used for recording these NMR measurements (c = $1.36 \cdot 10^{-2}$ mol/L).[47b]

Table 3.4.4. Temperature dependence of chemical shifts in ^{1}H-NMR spectra of mixtures of [Cu(C$_6$H$_5$CN)$_5$][B(C$_6$F$_5$)$_4$]$_2$, toluene and diisobutene in C$_6$D$_6$.

T [K]	$\delta_{tol.}$ [ppm]	$\delta_{tol.}$ [ppm]	$\delta_{benzon.}$ [ppm]	$\delta_{benzon.}$ [ppm]	$\delta_{tol.}$ [ppm]	$\delta_{diisob.}$ [ppm]
298		7.03	6.94	6.77	2.11	1.22
303		7.03	6.95	6.78	2.12	1.22
308	7.13	7.03	6.96	6.79	2.12	1.22
313	7.12		6.97	6.79	2.12	1.22
318	7.12		6.98	6.80	2.12	1.22
323	7.12		6.98	6.81	2.13	1.23
328	7.12		6.98	6.82	2.13	1.23
333	7.12		6.98	6.83	2.13	1.23
338	7.11		6.99	6.83	2.13	1.23
343	7.11		7.00	6.84	2.13	1.23
348	7.11		7.01	6.85	2.14	1.23
353	7.11		7.01	6.86	2.14	1.23

The fact that only signals of the protons of the *tert*-butyl (end)group of diisobutene are clearly visible in the NMR spectra (see Table 3.4.4) indicate the others being too close to a paramagnetic metal center. This again would be in favor of the existence of a charge transfer complex with a paramagnetic center and no organic radical stable on the NMR timescale (see Figure 3.4.27).
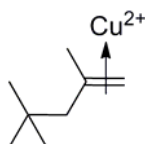
Figure 3.4.27. Presumably formed charge transfer complex of diisobutene with a Cu^{2+} ion.

4.9 Conclusions and an attempt to transfer the obtained results to the polymerization of isobutene

Radicals of pure organic origin were recorded via EPR spectroscopy. NMR spectra in contrast show organic species which are bond to a paramagnetic metal center (Cu^{2+}). UV-Vis spectroscopy additionally points to the formation of a charge transfer complex. These results only contradict each other on the first glance, as the obvious differences in case of NMR- and EPR spectroscopy can be explained by the resolved time scale. EPR spectroscopy enables the detection of fast relaxation processes (*i.e.* relaxation of electrons) whereas NMR measurements provide the possibility to detect comparatively slow relaxation processes (*i.e.* relaxation of nucleons). The existence of a dynamic system (see Scheme 3.4.3) with fast reaction of system b) or c) to a) and slow reaction of the more stable a) to b) or c) could give an explanation for the above mentioned controversial experimental results. Organic radicals are normally highly reactive and have a very short lifetime. This dynamic system could also be the reason why these organic radicals were detectable via EPR spectroscopy and why these radical signals proved to be time stable or even more intensive with increasing time. A conjugated π electron system in case of toluene and hyperconjugation of the *tert*-butyl group in case of diisobutene could probably make an additional contribution to the stability of these radicals.[43, 48] The stability of this formed, sterically hindered species, is most likely the

reason why diisobutene acts as termination reagent in isobutene polymerization when using the tested transition metal complexes as mediator.[34]

Due to the increased stabilization an existence of the radical-cationic species c) could be obtained by isomerization. As the EPR measurements could not be clearly assigned this has to be treated as hypothetic.
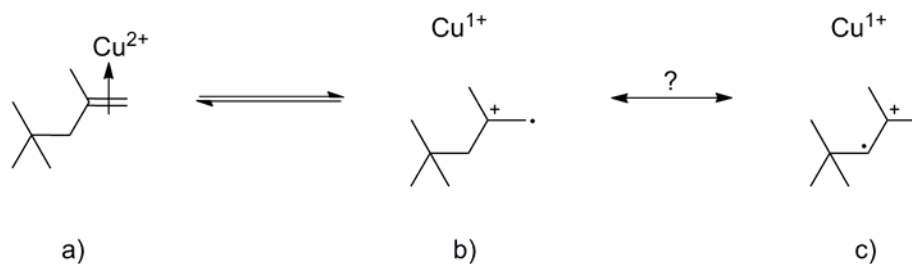
Scheme 3.4.3. Equilibrium between charge transfer complex and radical.

In analogy, the existance of an equilibrium between a (dormant) metal coordinated species and an active radical is also known in the controlled radical polymerization reaction (ATRP; atom transfer radical polymerization). As the reaction equilibrium is mainly on the side of the dormant species, radical concentration is low, preventing side reactions, recombination of radicals and causes a controlled reaction. A similar behavior might be the reason for the low polydispersity in isobutene polymerization with nitrile ligated transition metal complexes bearing weakly coordinating counter anions under certain conditions.

Continual activation and deactivation could also be the reason for the controlled polymerization which is observed when using isobutene instead of the non-polymerizable model if the polymerization is proceeding via a radical mechanism.

Analog conclusions may be drawn for the application of related trityl salts as model initiator instead of the copper complex. *Gaylord* and *Švestka*[42] proposed an initiation mechanism for isoprene polymerization which involved the formation of a charge transfer complex and a subsequent electron transfer from the isoprene monomer to the triphenylmethyl cation to yield an isoprene radical cation (see Scheme 3.4.4). The assumed propagation proceeds via cyclopolymerization by successive radical and cationic additions.
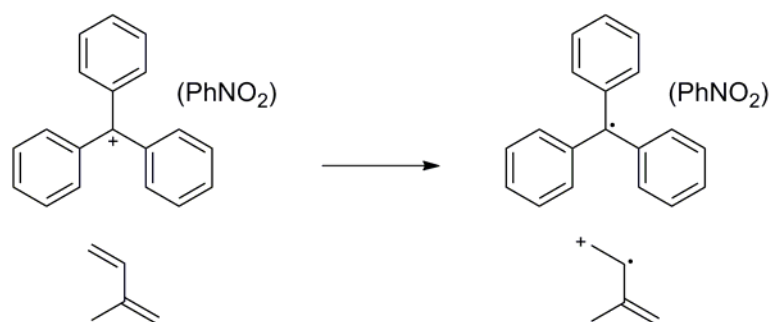
Scheme 3.4.4. Proposed initiation of the isoprene polymerization with $[(C_6H_5)_3C^+][SbCl_6^-]$ in nitrobenzene.[42]

However, the possibility of propagation via a pure cationic mechanism can not be excluded in this stage of our research, even though the slope of the plot: number average molecular weight against conversion is similar to a nonliving radical polymerization.

5. Conclusions

Numerous experiments were performed to gain insight into the polymerization mechanism of isobutene with nitrile ligated transition metal complexes with weakly coordinating anions. The obtained results are compiled in the following section.

Isobutene polymerization with selected monovalent transition- (Cu(I), Ag(I)[2b]) and alkali metal compounds (K(I), Li(I)) with polyfluorinated borates shows no activity. This leads to the assumption that mediators based on metal atoms in oxidation state +1 are unlikely to show activity in isobutene polymerization at room temperature.

Experiments with $[Zn(CH_3CN)_6][BF_4]_2$ and $[Cu(CH_3CN)_4][BF_4]_2$ show, that even in cases where the BF_4^- anion is only weakly coordinated to the central metal atom (*e.g.* $[Zn(CH_3CN)_6][BF_4]_2$) respective complexes have no considerable activity in isobutene polymerization.

Formerly reported tests dealing with the influence of water on the polymerization of isobutene with $[Mn(CH_3CN)_6][B(C_6F_5)_4]_2$ using DTBP as proton trap have to be regarded as problematic. The intended proton trap DTBP could be shown to react with the similar $[Zn(CH_3CN)_{4/6}][B(C_6F_5)_4]_2$ and $[Cu(C_6H_5CN)_5][B(C_6F_5)_4]_2$ complexes, either leading to reduction of these or to the formation of a different coordination environment on the metal.[2b]

Additionally, several preliminary experiments relating the possibility of radical cationic polymerization of isobutene were conducted. Obtained EPR spectra depict the formation of organic radicals and NMR spectra indicate coordination of diisobutene to the metal center. From these and other tests (UV-Vis, MALDI-TOF, ESI-MS) no defined structure can be proven. Clear indication for the formation of a charge transfer complex involving radical cations could be obtained.

Because of the structural similarity of diisobutene and isobutene the described results on the model system diisobutene show the necessity for mechanistic studies involving formation of radicals in the polymerization of isobutene.

6. Experimental

6.1 Materials and methods

All preparations and manipulations were carried out under argon atmosphere using standard Schlenk techniques and all solvents were dried by standard procedures. Removal of volatiles was preformed under oil pump vacuum ($1 \cdot 10^{-3}$ mbar).

NMR measurements were performed on a Bruker AVANCE-DPX-400 MHz or a JEOL-JNM-GX-400 MHz spectrometer. Chemical shifts were reported in ppm and are referenced to the solvent as internal standard. Complex concentrations were between 15.0–25.0 mM in $CDCl_3$, CD_2Cl_2 or C_6D_6.

IR spectra were recorded on a Super FT-IR MIR System FTS-7000 spectrometer ($4000\text{-}400$ cm^{-1}), a Perkin Elmer FT spectrometer ($4000\text{-}400$ cm^{-1}) and an FT-Raman spectrometer ($3500\text{-}200$ cm^{-1}) using a diamond mirco ATR accessory or Nujol mulls.

ESI-MS spectra were recorded on a Varian 500-MS IT Mass Spectrometer. All solvents used for the ESI-MS studies were LC-MS grade, purchased from Sigma Aldrich, and used as received.

UV/Vis spectra were recorded with a Varian Cary 50 Scan UV-Visible Spectrometer with a Varian Cary single cell Peltier Acessory. Solution spectra were measured in a quartz cell with a 1-cm pathlength; background: solvent *vs.* solvent. Complex concentrations were between 10.0–15.0 mM in methylene chloride or toluene.

MALDI-TOF were performed on a Bruker Biflex III or a Bruker-Daltonic, Ultraflex TOF/TOF without matrix. The samples were prepared by diluting C_{60}, $[Cu(C_6H_5CN)_5][B(C_6F_5)_4]_2$ and diisobutene in a ratio of 1:1:1 in toluene. Elemental analyses were carried out at the Mikroanalytisches Labor of the Anorganisch-chemisches Institut at the Technische Universität München.

X-ray crystal analysis were carried out on an area detecting system (APEX II, κ-CCD) at the window of a rotating anode (Bruker AXS, FR591) and graphite-monochromated Mo-$K\alpha$ radiation ($\lambda = 0.71073$ Å). Data collection was performed at 293 K.

Whenever possible, complexes which were prepared via literature known methods were rapidly identified via X-ray crystal analysis by comparison of the obtained data of the particular unit cells with the previously published ones.

EPR spectra were recorded by means of a JEOL JESRE2X at X-band frequency. Reference was a Mn(II)salt in a MgO-matrix (experimental errors: $\Delta g = \pm 0.003$, $\Delta A = \pm 5 \times 10^{-4}$ cm^{-1}). Complex concentrations were between 20.0–30.0 mM in methylene chloride or toluene.

6.2 Synthesis of the complexes

[Cu(CH$_3$CN)$_4$][BF$_4$]$_2$: Tetrafluoroboricacid-diethylether (0.70 mL, 5.10 mmol) was added to a suspension of copper(II)acetate (0.43 g, 2.37 mmol) in methylene chloride (20 ml) in the dark. A light blue supernatant was formed immediately. After stirring for 1 h, the solution was filtered off some traces off insoluble material. Acetonitrile (15 mL) was added to the filtrate. The dark blue solution was concentrated in vacuum to 5 mL and overlaid with pentane (1 mL) and diethyl ether (15 mL). The supernatant was filtered off the formed crystals, which then were dissolved in acetonitrile. Pentane (30 mL) was added to the vigorously stirred solution, forming blue powder. This powder was again dissolved in acetonitrile (10 mL), some traces of insoluble material were filtered off, the solution was concentrated in vacuum to 5 mL and overlaid with pentane (2 mL) and diethyl ether (15 mL), giving the desired product as dark blue crystals: 0.84 g (89 %). Anal. calcd. for C$_8$H$_{12}$B$_2$CuF$_8$N$_4$: C, 23.94; H, 3.01; N, 13.96. Found: C, 23.67; H, 3.50; N, 14.00. See appendix for x-ray crystal data.

[Cu(CH$_3$CN)$_4$][BF$_4$]:[11b] Nitrosoniumtetrafluoroborate (1.85 g, 15.84 mmol) was washed with ethyl acetate (10 mL), dried in vacuum and added to copper powder (1.51 g, 23.76 mmol). Acetonitrile (40 mL) was poured on the mixture at 45 °C. Brown gas is formed immediately. The flask is slightly evacuated (3 x) and refilled with argon (3 x) and again evacuated until boiling of the solvent. After stirring for 2.5 h, the supernatant is filtered through a heated frit. Colorless crystals formed when the solution was allowed to cool down to ambient

temperature. The supernatant was filtered off and the desired product was received as colorless crystals after re-crystallization from hot acetonitrile (20 mL): 3.24 g (65 %). Anal. calcd. for $C_8H_{12}BCuF_4N_4$: C, 30.55; H, 3.85; N, 17.81. Found: C, 30.48; H, 3.98; N, 18.23. Elementary cell: a = 23.882 Å, b = 8.3285 Å, c = 20.338 Å, β = 107.548 °, V = 4045.2 Å.

[Cu(CH$_3$CN)$_4$][B(C$_6$F$_5$)$_4$]:[11a] A suspension of [Li(H$_2$O)][B(C$_6$F$_5$)$_4$] (1.30 g, 1.85 mmol) in acetonitrile (16 mL) is added to a suspension of tetrakis(acetonitrile)hexafluorophosphate (0.63 g, 1.69 mmol) in acetonitrile (6 mL). After stirring for 1 h, deionized, degassed water (200 mL) is added to the solution, forming a white precipitate. The supernatant is removed via filtration. The powder is dried in vacuum for 12 h and washed with hexane (20 mL). The solid is dissolved in acetonitrile (20 mL) filtered to remove un-dissolved impurities, concentrated to 2 mL and stored at -30 °C, yielding the desired product as colorless crystals: 0.51 g (33 %). Elementary cell: a = 11.4125 Å, b = 16.2928 Å, c = 19.1983 Å, β = 106.4778 °, V = 3423.15 Å.

[Zn(CH$_3$CN)$_6$][BF$_4$]$_2$:

Method A:[12] Nitrosonium tetrafluoroborate (2.78 g, 23.82 mmol) was added to a suspension of zinc powder (0.78 g, 11.91 mmol) in acetonitrile (20 mL). Intense gas formation and heating can be observed immediately. A colorless solution was formed within 5 min. Crystals were obtained by concentrating to 10 mL and overlaying with hexane (2 mL) and diethyl ether (20 mL) at -30 °C. After filtration and re-crystallization from acetonitrile/hexane/diethyl ether (5 mL/1 mL/30 mL) the desired product was received as colorless crystals: 5.32 g (92 %).

Method B: Tetrafluoroboricacid-diethylether (1.11 mL, 8.06 mmol) was added to a suspension of zinc acetate (0.74 g, 4.03 mmol) in acetonitrile (20 mL). After stirring for 10 min, the solution was concentrated to 9 mL via vacuum and overlaid with hexane (2 mL) and diethyl ether (11 mL). The supernatant of the crystals which were obtained at -30 °C was

removed via filtration. The solid was dissolved in acetonitrile (10 mL) and a trace of insoluble material was removed via filtration. Concentration to 5 mL, overlaying with hexane (1 mL) and diethyl ether (30 mL) lead to the formation of the desired product as colorless crystals: 1.70 g (87 %). Selected Raman (ATR, cm^{-1}): ν_{BF4-} = 518; ν_{CCN} = 404; ν_{BF4-} = 355; ν_{ZnN} = 208; ν_{N-Zn-N} = 132. Anal. calcd. for $C_{9.4}H_{14.1}B_2F_8N_{4.7}Zn$ ([$Zn(CH_3CN)_{4.7}$][BF_4]$_2$): C, 26.14; H, 3.29; N, 15.24. Found: C, 25.94; H, 3.36; N, 15.31. See appendix for x-ray crystal data.

[H(Et$_2$O)$_2$][B(C$_6$F$_5$)$_4$]. A 2.5 M solution of *n*-butyllithium in *n*-hexane (17.82 mL, 40.50 mmol) was added drop wise, within 10 min, to a stirred solution of (5.88 mL, 40.50 mmol) iodopentafluorobenzene in diethyl ether (30 mL) at -78 °C. After the solution was stirred for an additional 20 min, a 1 M solution of boron trichloride in *n*-hexane (10.16 mL, 10.16 mmol) was added dropwise, over a 10 minute periode. The reaction mixture was kept stirring for 10 min and warmed up to 0 °C, at which point LiCl precipitated immediately. After the addition of a 2 M solution of hydrogen chloride in diethyl ether (10.0 mL, 20.0 mmol), the mixture was stirred overnight at ambient temperature. The solution was separated from the solid by filtration and concentrated under vacuum (oil pump) to 10 mL. The fast addition of pentane (60 mL) to the stirred solution afforded the product as a white solid, which was re-dissolved in diethyl ether (10 mL) and filtered to remove a small amount of a white insoluble impurity (presumably LiCl). After the fast addition of pentane (60 mL), the resulting white solid was isolated by filtration and dried under vacuum: yield 3.22 g (38 %). ^{1}H NMR (400 MHz, CDCl$_3$, T = 298 K, δ(ppm)): 3.95 (q, ^3J = 7.1 Hz, 8 H, CH$_2$), 1.36 (t, ^3J = 7.1 Hz, 12 H, CH$_3$). ^{19}F NMR (376 MHz, CDCl$_3$, T = 298 K, δ(ppm)): -133.0 (d, J_{F-F} = 10.1 Hz, *o*-F), -166.9 (t, J_{F-F} = 20.4 Hz, *p*-F), -162.7 (virt. t, J_{F-F} ≈ 18.1 Hz, *m*-F). ^{11}B NMR (128 MHz, CDCl$_3$, T = 298 K, δ(ppm)): -13.62. Anal. Calcd for $C_{32}H_{21}BF_{20}O_2$: C, 46.40; H, 2.56. Found: C, 45.52; H, 2.44.

[Cu(C$_6$H$_5$CN)$_5$][B(C$_6$F$_5$)$_4$]$_2$. A solution of [H(Et$_2$O)$_2$][B(C$_6$F$_5$)$_4$] (2.20 g, 2.66 mmol) in dichloromethane (15 mL) was added dropwise to a stirred suspension of copper(II)acetate

(0.23 g, 1.27 mmol) in dichloromethane (5 mL), in the dark. Immediately, a dark green solution formed. After stirring for 30 min, the solution was concentrated under vacuum to 5 mL. By the addition of benzonitrile (1.2 mL) the color changes to a light green. The volatiles were removed under vacuum ($1 \cdot 10^{-3}$ mbar, 2 h), affording a honey-like liquid. The desired product was obtained by crystallization from dichloromethane/pentane (1:2) as light green crystals: yield 1.85 g (75 %). Selected IR (Nujol, cm^{-1}): ν_{CN} = 2273 (sh). Anal. Calcd for $C_{83}H_{25}B_2CuF_{40}N_5$: C, 51.46; H, 1.30; N, 3.62. Found: C, 51.50; H, 1.19; N, 3.64.

$[Zn(CH_3CN)_{4/6}][B(C_6F_5)_4]_2$:

Method A: A solution of $[H(Et_2O)_2][B(C_6F_5)_4]$ (0.83 g, 1.00 mmol) in methylene chloride (15 mL) was added dropwise to a stirred solution of zinc acetate (0.09 g, 0.49 mmol) in methylene chloride (10 mL). After 12 h, acetonitrile (1.5 mL) was added and the volatiles were removed in vacuum. The remaining highly viscous liquid was dissolved in methylene chloride (4 mL) and precipitated by the addition of pentane (40 mL) to the vigorously stirring solution. The solvent was removed via filtration and the creamy solid was washed two times with vigorously stirring pentane (20 mL). The desired product was obtained by repeated crystallization (2 x) from methylene chloride/pentane (1/2). Yield: 0.43 g (0.26 mmol, 54 %).

Method B: A 1.0 M solution of diethylzinc in hexane (0.62 mL, 0.62 mmol) was added dropwise to a stirred solution of $[H(Et_2O)_2][B(C_6F_5)_4]$ (1.03 g, 1.24 mmol) in diethylether (15 mL). Instantaneous gas formation was observed. The flask was slightly evacuated. After stirring for 2 h, the solution was concentrated to 2 mL. By fast addition of pentane (10 mL), a white-yellow resin-like precipitate was formed. The supernatant was removed and the residue dissolved in 2 mL diethylether. By repeated addition of pentane (10 mL) to the stirred solution, an off-white solid was formed. This was dissolved in acetonitrile (1 mL). The volatiles were removed under vacuum (2 h), affording a yellow, honey-like liquid. The desired product was obtained by crystallization from dichloromethane/pentane (1:3) as colorless crystals: yield 0.82 g (81 %).^{1}H NMR (400 MHz, CD$_2$Cl$_2$, T = 298 K, δ(ppm)): 2.29 (s, 3 H,

CH_3). Selected ^{13}C NMR (75.5 MHz, CD_2Cl_2, T = 298 K, δ(ppm)): 118.3 (s, NC), 2.1 (s, H_3C),Selected IR (Nujol, cm^{-1}): ν_{CN} = 2324, 2297, 2285. Anal. calcd. for $C_{58}H_{15}B_2F_{40}N_5Zn$ (%): C, 42.77; H, 0.93; N, 4.30. Found (%): C, 42.52; H, 1.29; N, 4.31. See appendix for x-ray crystal data.

[Zn(C_6H_5CN)$_5$][B(C_6F_5)$_4$]$_2$: Benzonitrile (0.10 mL, 0.10 g, 0.98 mmol) was added to a solution of [Zn(CH_3CN)$_5$][B(C_6F_5)$_4$]$_2$ (0,27 g, 0.16 mmol) in methylene chloride (2 mL). All volatiles were removed under vacuum (2 h) and the remaining oil was re-dissolved in methylene chloride (2 mL) and benzonitrile (0.05 mL, 0.05 g, 0.49 mmol). The volatiles were again removed under vacuum (2 h), affording a honey-like liquid. The desired product was obtained by crystallization from dichloromethane/pentane (1:2) as colorless crystals: 0.26 g (85 %). ^{1}H NMR (400 MHz, CD_2Cl_2, T = 298 K, δ(ppm)): 7.9 (t, ^3J = 7.7 Hz, 1 H, p-H), 7.8 (d, ^3J = 7.9 Hz, 2 H, o -H), 7.7 (virt. t, ^3J ≈ 7.9 Hz, 2 H, m-H). Selected ^{13}C NMR (75.5 MHz, CD_2Cl_2, T = 298 K, δ(ppm)): 136.8 (s, p-C), 133.8 (s, o-C), 130.4 (s, m-C), 107.2 (s, i-C). Anal. calcd. for $C_{83}H_{25}B_2F_{40}N_5Zn$ (%): C, 51.41; H, 1.30; N, 3.61. Found (%): C, 50.98; H, 1.26; N, 3.61.

6.3 Polymerization of isobutene

For higher screening efficiency, isobutene was homopolymerized in pressure tubes, using a dry box. A maximum of 12 tubes were prepared at the same time.

Each tube was filled with dichloromethane (20 mL) at -40 °C and the complex was added. Isobutene, which had been condensed into a separate tube previously, was added. The pressure tubes were sealed and removed quickly from the dry box. The polymerization was performed in a water bath mounted on a magnetic stirring plate; a temperature accuracy of ±0.1 °C could be obtained. The polymerization was stopped with methanol (5 mL) and 2,2'-methylenebis(4-methyl-6-di-tert-butyl)phenol (0.2 g) was added to prevent oxidation. The solvents were removed in an oil-pump vacuum and the remaining polymer was dried to

constant weight in high vacuum at 30 °C. The polymeric products were stored under an inert gas atmosphere. All polymerization experiments were performed with a control experiment.

6.4 Test reactions

[H{(CH$_3$)$_3$C}$_2$C$_5$H$_3$N][B(C$_6$F$_5$)$_4$]:

Method A: Several crystals of [Zn(CH$_3$CN)$_5$][B(C$_6$F$_5$)$_4$]$_2$ were dissolved in methylene chloride. By addition of a drop of 2,6-di-*tert*-butylpyridine white clouding can be observed. The desired product can be obtained as colorless crystals via overlaying with pentane (1:2).

Method B: Several crystals of [Cu(C$_6$H$_5$CN)$_5$][B(C$_6$F$_5$)$_4$]$_2$ were dissolved in methylene chloride. By addition of a drop of 2,6-di-*tert*-butylpyridine black precipitate is formed. The desired product can be obtained as colorless crystals via overlaying with pentane (1:2). See appendix for x-ray crystal data.

References

[1] a) H. Auer, U. Kanne, A. De Vos, Keil & Weinkauf, **2004**, *US2040039141A1*; b) P. Hanefeld, V. Böhm, M. Sigl, N. Challand, M. Röper, H.-M. Walter, B. Voigt, F. E. Kühn, A. K. Hijazi, R. K. Narayanan, Germany, **2007**, *DE200510055817 20051121*; c) H. P. Rath, BASF AG., **1995**, *US00548018A*; d) H. P. Rath, T. Perner, E. Schauß, BASF AG (DE), **2005**, *DE10361633A1*.

[2] a) M. Vierle, Y. Zhang, E. Herdtweck, M. Bohnenpoll, O. Nuyken, F. E. Kühn, *Angew. Chem. Int. Ed.* **2003**, *42*, 1307; b) M. Vierle, Y. Zhang, A. M. Santos, K. Köhler, C. Haeßner, E. Herdtweck, M. Bohnenpoll, O. Nuyken, F. E. Kühn, *Chem. Eur. J.* **2004**, *10*, 6323.

[3] Y. Li, L. T. Voon, H. Y. Yeong, A. K. Hijazi, N. Radhakrishnan, K. Köhler, B. Voit, O. Nuyken, F. E. Kühn, *Chem. Eur. J.* **2008**, *14*, 7997.

[4] A. K. Hijazi, N. Radhakrishnan, K. R. Jain, E. Herdtweck, O. Nuyken, H.-M. Walter, P. Hanefeld, B. Voit, F. E. Kühn, *Angew. Chem. Int. Ed.* **2007**, *46*, 7290.

[5] A. Sakthivel, A. K. Hijazi, H. Y. Yeong, K. Köhler, O. Nuyken, F. E. Kühn, *J. Mater. Chem.* **2005**, *15*, 4441.

[6] O. Nuyken, M. Vierle, F. E. Kühn, Y. Zhang, *Macromol. Symp.* **2006**, *236*, 69.

[7] H. Chaffey-Millar, F. E. Kühn, *Appl. Catal. A-Gen.* **2010**, *384*, 154.

[8] a) N. Radhakrishnan, A. K. Hijazi, H. Komber, B. Voit, S. Zschoche, F. E. Kühn, O. Nuyken, M. Walter, P. Hanefeld, *J. Polym. Sci., Part A: Polym. Chem.* **2007**, *45*, 5636; b) A. K. Hijazi, A. Al Hmaideen, S. Syukri, N. Radhakrishnan, E. Herdtweck, B. Voit, F. E. Kühn, *Eur. J. Inorg. Chem.* **2008**, *2008*, 2892.

[9] D. Alberti, K.-R. Pörschke, *Organometallics* **2004**, *23*, 1459.

[10] A. F. Holleman, E. Wiberg, N. Wiberg, in *Lehrbuch der Anorganischen Chemie, Vol. 102*, de Gruyter, Berlin, **2007**, pp. 1439.

[11]   a) H.-C. Liang, E. Kim, C. D. Incarvito, A. L. Rheingold, K. D. Karlin, *Inorg. Chem.* **2002**, *41*, 2209; b) B. J. Hathaway, D. G. Holah, J. D. Postlethwaite, *J. Chem. Soc.* **1961**, 3215.

[12]   B. J. Hathaway, D. G. Holah, A. E. Underhill, *J. Chem. Soc.* **1962**, 2444.

[13]   R. A. Heintz, J. A. Smith, P. S. Szalay, A. Weisgerber, K. R. Dunbar, *Inorg. Synth.* **2002**, *33*, 75.

[14]   a) P. Bergamini, A. Maldotti, S. Sostero, O. Traverso, J. Sýkora, *Inorganica Chimica Acta* **1984**, *85*, L15; b) E. Cervone, F. Diomedi Camassei, I. Giannini, J. Sýkora, *Journal of Photochemistry* **1979**, *11*, 321; c) O. Horváth, *J. Photoch. Photobio. A* **1989**, *48*, 243; d) J. Sýkora, I. Giannini, F. D. Camassei, *J. Chem. Soc., Chem. Commun.* **1978**, 207; e) J. Kochi, *J. Am. Chem. Soc.* **1962**, *84*, 2121.

[15]   R. F. De Souza, A. L. Monteriro, M. Seferin, M. O. De Souza, F. C. Stedile, C. N. Wyrvalski, I. J. R. Baumvol, *J. Coord. Chem. A* **1996**, *40*, 311

[16]   a) Y. C. Bae, R. Faust, *Macromolecules* **1997**, *30*, 7341; b) L. Balogh, R. Faust, *Polym. Bull.* **1992**, *28*, 367.

[17]   N. Radhakrishnan, Dissertation thesis, Technische Universität Dresden (Dresden), **2007**.

[18]   P. Jutzi, C. Müller, A. Stammler, H. G. Stammler, *Organometallics* **2000**, *19*, 1442.

[19]   a) E. Y. X. Chen, T. J. Marks, *Chem. Rev.* **2000**, *100*, 1391; b) I. Krossing, I. Raabe, *Angew. Chem. Int. Ed.* **2004**, *43*, 2066; c) B. J. Hathaway, A. E. Underhill, *J. Chem. Soc.* **1960**, 3705; d) G. J. Kubas, *Inorg. Synth.* **1979**, *19*, 90; e) S. H. Strauss, *Chem. Rev.* **1993**, *93*, 927; f) S. V. Ivanov, S. M. Miller, O. P. Anderson, K. A. Solntsev, S. H. Strauss, *J. Am. Chem. Soc.* **2003**, *125*, 4694; g) W. Beck, K. Sünkel, *Chem. Rev.* **1988**, *88*, 1405.

[20]   a) W. E. Buschmann, J. S. Miller, *Inorg. Synth.* **2002**, *33*, 83; b) W. E. Buschmann, J. S. Miller, *Chem. Eur. J.* **1998**, *4*, 1731.

[21]   A. N. Chernega, A. J. Graham, M. L. H. Green, J. Haggitt, J. Lloyd, C. P. Mehnert, N. Metzler, J. Souter, *J. Chem. Soc., Dalton Trans.* **1997**, 2293.

[22]   Y. Sarazin, M. Schormann, M. Bochmann, *Organometallics* **2004**, *23*, 3296.

[23]   D. A. Walker, T. J. Woodman, D. L. Hughes, M. Bochmann, *Organometallics* **2001**, *20*, 3772.

[24]   H. Wasada, Y. Wasada-Tsutsui, T. Hashimoto, S. Funahashi, *Int. J. Quantum Chem.* **2009**, *109*, 2208.

[25]   M. Hesse, H. Meier, B. Zeeh, *Spektroskopische Methoden in der organischen Chemie*, 7 ed., Thieme Verlag, Stuttgart, **2005**.

[26]   a) V. D. Parker, Y. Chao, B. Reitstöen, *J. Am. Chem. Soc.* **1991**, *113*, 2336; b) J. Xue, V. D. Parker, *J. Org. Chem.* **1994**, *59*, 6564.

[27]   N. Yamada, K. Shimada, T. Hayashi, *J. Polym. Sci. B: Polym. Lett.* **1966**, *4*, 477.

[28]   K. Tsuji, H. Yoshida, K. Hayashi, S. Okamura, *J. Polym. Sci. B: Polyme. Lett.* **1967**, *5*, 313.

[29]   a) L. Toman, M. Marek, J. Jokl, *J. Polym. Sci. A: Polym. Chem.* **1974**, *12*, 1897; b) L. Toman, J. Pilař, J. Spěváček, M. Marek, *J. Polym. Sci. A: Polym. Chem.* **1978**, *16*, 2759; c) M. Marek, L. Toman, *J. Polym. Sci. C: Polym. Symp.* **1973**, *42*, 339; d) L. Toman, M. Marek, *Makromol. Chem.* **1976**, *177*, 3325; e) T. Diem, J. P. Kennedy, *J. Macromol. Sci., Part A: Pure Appl. Chem.* **1978**, *12*, 1359 ; f) X.-C. Dong, N. Salhi-Benachenhou, S. Lunell, *J. Mol. Struct.* **1997**, *392*, 111; g) O. Edlund, P.-O. Kinell, A. Lund, A. Shimizu, *J. Polym. Sci. B: Polym. Lett.* **1968**, *6*, 133; h) M. S. El-Shall, *Acc. Chem. Res.* **2008**, *41*, 783; i) M. S. El-Shall, G. M. Daly, Z. Yu, M. Meot-Ner, *J. Am. Chem. Soc.* **1995**, *117*, 7744; j) M. S. El-Shall, Z. Yu, *J. Am. Chem. Soc.* **1996**, *118*, 13058; k) F. R. Khalafov, F. M. Nasirov, N. E. Melnikova, B. A. Krentsel, T. N. Shakhatakhtinsky, *Makromol. Chem., Rapid Commun.* **1985**, *6*, 29; l) M. Marek, L. Toman, J. Pilař, *J. Polym. Sci. A: Polym. Chem.* **1975**, *13*, 1565; m) M. Meot-Ner, L. W. Sieck, M. S. El-Shall, G. M. Daly, *J. Am. Chem. Soc.* **1995**, *117*, 7737; n) J. Michl, *Chem. Listy* **2008**, *102*, 873; o) E. Oberrauch, T. Salvatori, S. Cesca, *J. Polym. Sci. B: Polym. Lett.* **1978**, *16*, 345; p) M. Taha, G. Rigal, Y. Piétrasanta, N. Platzer, P. Sudres, S. Raynal, *Makromol. Chem.* **1981**, *182*, 2545; q) L. Toman, J. Pilař, M.

Marek, *J. Polym. Sci. A: Polym. Chem.* **1978**, *16*, 371; r) L. Toman, J. Spěváček, P. Vlček, P. Holler, *J. Am. Chem. Soc.* **2000**, *38*, 1568; s) L. Toman, M. Marek, *J. Macromol. Sci., Part A: Pure Appl. Chem.* **1981**, *15*, 1533.

[30]   a) K. Vyakaranam, J. B. Barbour, J. Michl, *J. Am. Chem. Soc.* **2006**, *128*, 5610; b) V. Volkis, H. Mei, R. K. Shoemaker, J. Michl, *J. Am. Chem. Soc.* **2009**, *131*, 3132.

[31]   a) J. M. Cowie, *Polymers: Chemistry & Physics of modern Materials*, 2 ed., CRC Press, Boca Raton, **2000**; b) M. D. Lechner, K. Gehrke, E. H. Nordmeier, *Makromolekulare Chemie*, Birkhäuser Verlag, Basel, **1993**; c) B. Vollmert, *Polymer Chemistry*, Springer-Verlag, New York, **1973**.

[32]   a) M. Rätzsch, M. Arnold, V. Steinert, *Acta Polym.* **1985**, *36*, 8; b) M. Rätzsch, H. Friedrich, W. Haubold, *Acta Polym.* **1982**, *33*, 327.

[33]   T. D. Shaffer, J. R. Ashbaugh, *J. Polym. Sci. A: Polym. Chem.* **1997**, *35*, 329.

[34]   *unpublished results*.

[35]   a) P. C. P. Watts, P. K. Fearon, W. K. Hsu, N. C. Billingham, H. W. Kroto, D. R. M. Walton, *J. Mater. Chem.* **2003**, *13*, 491; b) V. Volkis, A. Lisovskii, B. Tumanskii, M. Shuster, M. S. Eisen, *Organometallics* **2006**, *25*, 2656; c) V. Volkis, B. Tumanskii, M. S. Eisen, *Organometallics* **2006**, *25*, 2722; d) C. Corvaja, in *Fullerenes: from synthesis to optoelectronic properties* (Eds.: D. M. Guldi, N. Martin), Kluwer Academic Publishers, New York, **2002**, pp. 213; e) B. L. Tumanskii, M. V. Tsikalova, R. Gasanov, A. V. Usatov, E. V. Martynova, A. R. Sabirov, I. V. Stankevich, Y. N. Novikov, in *Fullerene Research Advances* (Ed.: C. N. Kramer), Nova Science Publishers, Inc., New York, **2007**, pp. 117.

[36]   a) F. E. Kühn, J. R. Ismeier, D. Schön, W.-M. Xue, G. Zhang, O. Nuyken, *Macromol. Rapid. Commun.* **1999**, *20*, 555; b) F. A. Cotton, K. J. Wiesinger, *Inorg. Chem.* **1991**, *30*, 871; c) F. A. Cotton, J. L. Eglin, K. J. Wiesinger, *Inorg. Chim. Acta* **1992**, *195*, 11; d) M. E. Prater, L. E. Pence, R. Clérac, G. M. Finniss, C. Campana, P. Auban-Senzier, D. Jérome, E. Canadell, K. R. Dunbar, *J. Am. Chem. Soc.* **1999**, *121*, 8005.

[37]   R. T. Henriques, E. Herdtweck, F. E. Kühn, A. D. Lopes, J. Mink, C. C. Romão, *J. Chem. Soc., Dalton Trans.* **1998**, 1293.

[38]   A. K. Hijazi, H. Y. Yeong, Y. Zhang, E. Herdtweck, O. Nuyken, F. E. Kühn, *Macromol. Rapid Commun.* **2007**, *28*, 670.

[39]   a) X. Liu, A. Qiu, D. T. Sawyer, *J. Am. Chem. Soc.* **1993**, *115*, 3239; b) J. Irangu, M. J. Ferguson, R. B. Jordan, *Inorg. Chem.* **2005**, *44*, 1619.

[40]   A. Carrington, A. D. McLachlan, in *Introduction to Magnetic Resonance*, Chapman and Hall Ltd., London, **1979**, pp. 146.

[41]   A. S. Brill, in *Molecular Biology, Biochemistry and Biophysics Vol. 26* (Eds.: A. Kleinzeller, G. F. Springer, H. G. Wittmann), Springer, Berlin, **1977**, pp. 40.

[42]   N. G. Gaylord, M. Švestka, *J. Macromol. Sci., Part A: Pure Appl. Chem.* **1969**, *3*, 897.

[43]   E. Breitmaier, G. Jung, *Organische Chemie: Grundlagen, Stoffklassen, Reaktionen, Konzepte*, 5 ed., Thieme, Stuttgart, **2005**.

[44]   G. R. Fulmer, A. J. M. Miller, N. H. Sherden, H. E. Gottlieb, A. Nudelman, B. M. Stoltz, J. E. Bercaw, K. I. Goldberg, *Organometallics* **2010**, *29*, 2176.

[45]   B. Bräunlein, F. H. Köhler, W. Strauß, H. Zeh, *Z. Naturforsch.* **1995**, *50b*, 1739.

[46]   F. H. Köhler, *Z. Naturforsch.* **1980**, *35 b*, 187.

[47]   a) S. F. Rach, F. E. Kühn, *Chem. Rev.* **2009**, *109*, 2061; b) F. H. Köhler, in *Magnetism: Molecules to Materials I: Models and Experiments* (Eds.: J. S. Miller, M. Drillon), Wiley-VCH, Weinheim, **2001**, pp. 379.

[48]   F. Gerson, W. Huber, *Electron Spin Resonance Spectroscopy of Organic Radicals*, 1 ed., Wiley-VCH, Weinheim, **2003**.

IV. Synthesis of divalent WCAs as model compounds for WCA-based support materials

1. Introduction

Nitrile ligated transition metal complexes bearing weakly coordinating counter anions are effective mediators for the polymerization of isobutene in homogeneous phase.[1] In particular benzonitrile stabilized Cu(II) cations with tetrakis-(pentafluorophenyl)borate as counter anions, which are active even in non-chlorinated solvents like toluene, show excellent performance in the fabrication of highly reactive polyisobutenes.[2]

Although homogeneous catalysis has many advantages to its heterogeneous analogue (see Table 4.1) with high selectivity as most prominent feature, the latter outshine their homogeneous congeners with facile separability.[3] Hence, heterogeneous catalysis is favoured for industrial application. To combine the positive features of both systems the so called "heterogenized homogeneous catalysts" were developed.[4]

Table 4.1. Comparison between homogeneous and heterogeneous catalysis.[3]

	Homogeneous	Heterogeneous
Effectivity		
Active centers	all metal atoms	only surface atoms
Concentration	low	high
Selectivity	high	lower
Diffusion problems	practically absent	present (mass-transfer controlled reaction)
Reaction conditions	mild (50 – 200 °C)	severe (often > 250 °C)
Applicability	limited	wide
Activity loss	irreversible reaction with	sintering of the metal

	products (cluster formation, poisoning)	crystallites, poisoning
Catalyst properties		
Structure/stoichiometry	defined	undefined
Modification possibilities	high	low
Thermal stability	low	high
Catalyst separation	sometimes laborious (chemical decomposition, distillation, extraction)	fixed bed: unnecessary suspension: filtration
Catalyst recycling	possible	unnecessary (fixed bed) or easy (suspension)
Cost of catalyst losses	high	low

In the last several years many attempts have been made to immobilize nitrile ligated transition metal complexes with weakly coordinating counter anions (WCAs). However, until now, it is not possible to keep them active for isobutene polymerization when grafted to an inorganic or polymeric support - neither by immobilizing the cation[5] nor by anchoring the anion[6] (*via* surface hydroxyl- or pyridine-groups of the supports). Reasons for the occurring hindrance can be unreacted functional (donor) groups that bind protons, which are possibly formed during the polymerization process and are part of many mechanistic proposals. The functional groups can also interfere by a too strong coordination of the metal as it is known that complexes with less weakly coordinating anions are not reactive, as well as complexes with stronger coordinating solvent ligands.[7] Usage of the WCA as supporting material itself could prevent all of these factors - as well as leaching problems and limitation of diffusion by mass transport (*e.g.* in porous materials).

In this chapter the preparation of diborates that possess polyfluorinated aryl linkers is described. The obtained low molecular weight compounds can serve as models for di- and polyanionic WCAs with polymeric connective units. The latter ones could be applied as non-soluble support materials for nitrile ligated transition metal cations, applicable *e.g.* in the polymerization of isobutene.

2. Background

2.1 General concept

Based on tetrakis(pentafluorophenyl)borate ($[B(C_6F_5)_4]^-$), the anion which was found to be most suitable for the homopolymerization of isobutene[2, 8] and the analogous divalent anion $[(C_6F_5)_3B\text{-}C_6F_4\text{-}B(C_6F_5)_3]^{2-}$ (see Figure 4.1, left) used by Marks *et al.*[9] for the polymerization of olefins, the idea to create di- or multianionic polymeric weakly coordinating anions in expanding the distance between the borate units was developed (see Figure 4.1, right).

Figure 4.1. Structure of the trityl bisborate dianion (left),[9] potential polymeric bisborate dianion salts (right).

Decrease of nucleophilicity and hence more weakly coordination of the anion to the cation can be achieved by increased delocalization of the negative charge over additional atoms. This can take place upon connection of two borates via a linker (*e.g.* imidazole) generating a new monoanion such as $[N_2C_3H_3\{B(C_6F_5)_3\}_2]_2^-$ (see Figure 4.2). This weakly coordinating anion (WCA) is already under investigation for polymerization of isobutene.[1a, 1c, 8] Alternatively perfluorinated arenes can be applied as linkers, generating dianions such as the aforementioned $[(C_6F_5)_3B\text{-}C_6F_4\text{-}B(C_6F_5)_3]^{2-}$ (see Figure 4.1 left).[10]
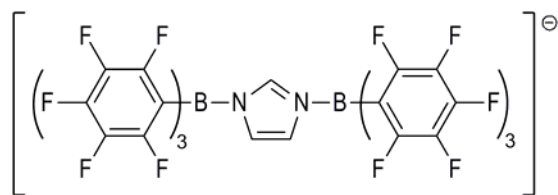
Figure 4. 2. Imidazole linked monoanionic diborate $[N_2C_3H_3\{B(C_6F_5)_2\}_2]^-$.

To ensure charge delocalization also in polyfluorinated borates as support with WCA properties the linking or polymeric bridging unit has to be electro conductive.

## 2.2 Properties of conductive polymers

The majority of synthetic polymers are electric insulators. Nevertheless, a number of unsaturated polymers with (located) conjugated π-molecular orbitals exist which possess latent electric conductivity. Introduction of electrons to or removal of electrons from these originally semi- or non-conducting polymers by doping leads to negatively or positively charged conductive polymers. The charge is delocalized over the entire conjugated polymer chain (see Scheme 4.1). Typical examples for such polymers are poly(aniline), poly(pyrrole), poly(thiophene) and their derivatives.[11] Due to their unique properties, these materials have found various practical applications in batteries, sensors, electrochemical displays, magnetic recorders, etc.[11a, 12] The importance of this discovery was highlighted with the Nobel Prize in Chemistry, 2000, which was awarded to A. J. Heeger, A. G. McDiarmid and H. Shirakawa "for the discovery and development of electrically conductive polymers".[13]
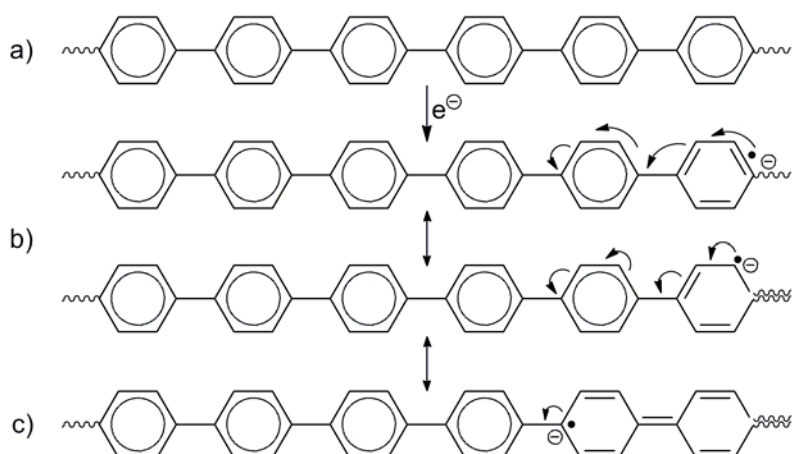
Scheme 4.1. a) uncharged polymer, b) negatively charged polymer, c) electron "wandering" along a polymer chain.

This proves the interest in conducting polymers hence these synthetic materials are the focus of numerous review papers.[12, 14] Likewise, since the discovery that these compounds can be applied for light emitting diodes by *Friend et al.* 20 years ago,[15] much time and effort has been put in the design of even superior conductive polymers by OLED (organic light emitting diode) reliant industries.[13] Nevertheless, as to avoid creation of any (potentially intervening) functional groups, particular attention was paid to the simplest representatives of this class, namely poly(acetylene), poly(*para*-phenylene) (PPP) and poly(*para*-phenylenevinylene) (see Figure 4.3).
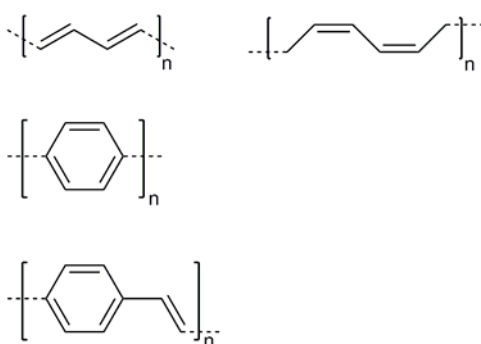
Figure 4.3. Poly(acetylene), poly(*para*-phenylene), poly(*para*-phenylenevinylene) (from above to below).

2.3 Synthetic Concept

As poly(*para*-phenylene) is quite similar to the organic part of our favoured counter anion, tetrakis(pentafluorophenyl)borate, as well as to the connecting group of *Marks*' bisborate dianion,[9] this polymer was chosen as basis for our low molecular weight model support materials.

During the years, several methods have been developed and improved to produce poly(*para*-phenylene) in high yield and with numerous different end groups.[11b, 11c, 16] The most important representatives can be divided in four major groups:

- Oxidative polymerization of benzene (Kovacic method, see Scheme 4.2):[16a, 17]
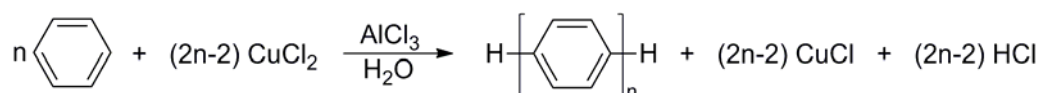
Scheme 4.2. Oxidation of benzene with $CuCl_2$ via the Kovacic method.

- Reductive coupling of 1,4-dihalobenzenes (or their substituted dimmers) with, for example, alkali metals (*Wurtz-Fittig* reaction),[17] copper powder (Ullmann reaction)[18] and $NiCl_2$(bpy)/Mg or Ni(cod)$_2$ (*Yamamoto*; bpy = 2,2'-bipyridine, cod = 1,5-cyclooctadiene)[19] respectively, as well as coupling of 1,4-dihaloarenes with aryl diboronic acids or of monomers containing both functional groups (Suzuki reaction, see Scheme 4.3).[20]
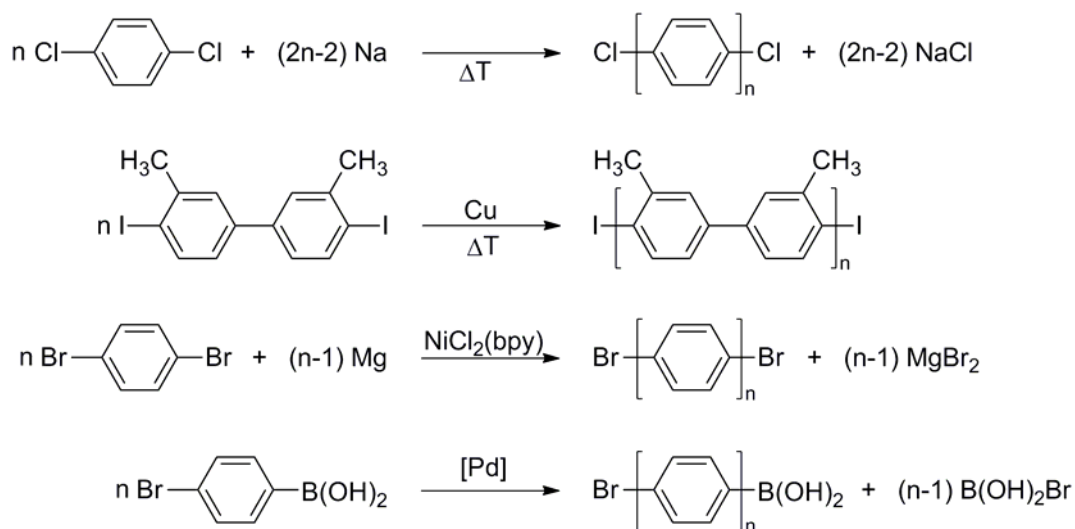
Scheme 4.3. Reductive coupling reactions for the generation of poly(*para*-phenylene).

- Electrochemical polymerization of benzene[21] or 1,4-dibromobenzene by the Fauvarque method (see Scheme 4.4).[22]
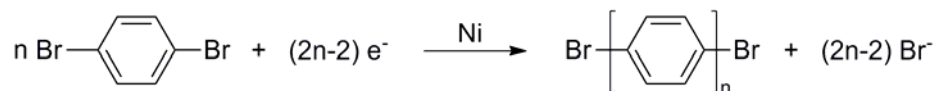
Scheme 4.4. Electro reductive polymerization of 1,4-dibromobenzene.

- Thermal treatment of polymers obtained from a derivatized *cis*-dihydrocatechol in the Ballard method (see Scheme 4.5).[23]

$$R = CH_3CO, CH_3OCO, \text{ etc.}$$
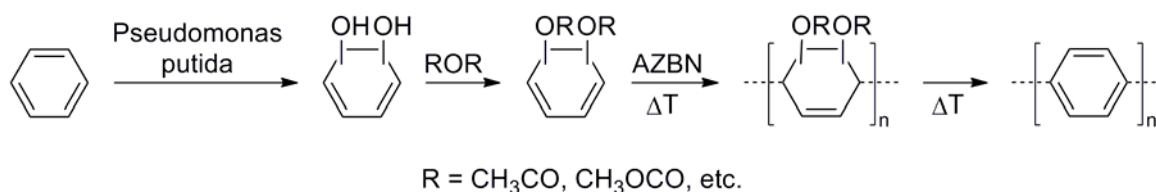
Scheme 4.5. Synthesis of poly(*para*-phenylene) via derivatized 5,6-*cis*-dihydroxycyclohexa-1,3-diene, derived from fermented benzene.

Among the aforementioned polymerization methods, coupling reactions leading to oligomers/polymers containing iodide or bromide as functional end groups seem to be ideally suitable for the creation of polymeric precursors.

The solubility of poly(*para*-phenylene) in organic solvents (such as toluene) decreases with increasing molecular weight. Consequently the analyzability of the obtained polymers and resulting target complexes will be complicated. Thus previous to the synthesis of polymeric support materials, the viability of this concept has to be tested on low molecular weight oligomeric materials. The formation of borates with different length of the connective phenyl chain can be achieved *via* different polymerization techniques. The polymerization of 1,4-dibromobenzene with magnesium in a Grignard reaction results in low molecular weight oligomers. In contrast $Ni(cod)_2$, in the presence of bpy and cod, generates oligomers with higher degree of polymerization. By both methods oligomers with bromide end groups are obtained.[24]

Provided that the low molecular weight models are active for the polymerization of isobutene, the subsequent synthesis of polymeric linkers or networks and dendritic anions are

theoretically possible as support materials (see Figure 4.4). Especially interesting would be a replacement of poly(*para*-phenylene) by its fluorine substituted congener to design potentially more weakly coordinating anionic polymers.
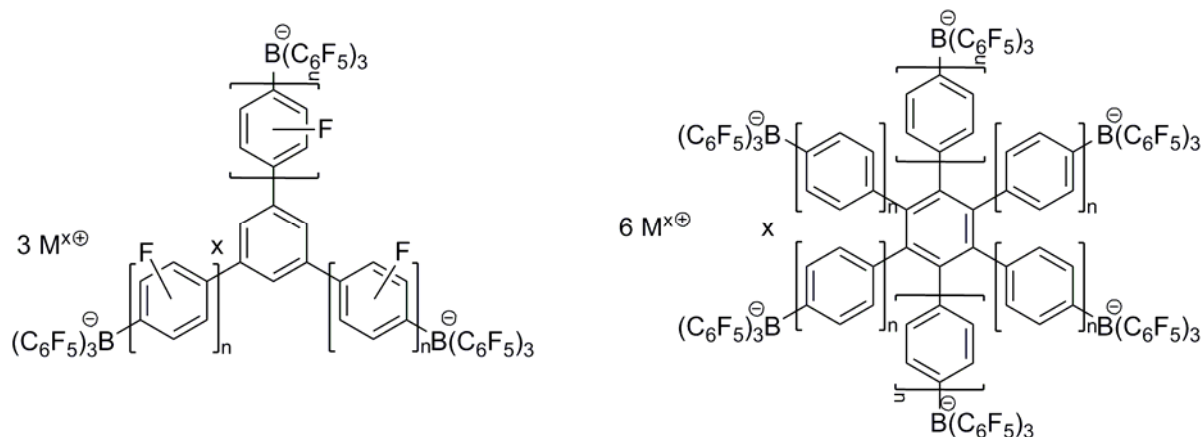

Figure 4.4. Theoretically possible polyfluorinated dendritic polyaryl borate salts.

3. Results and discussion

3.1 Synthesis

As polyfluorinated borates show lower coordination than their non-fluorinated congeners (s.a.), the commercially available 1,4-dibromotetrafluorobenzene and 4,4'-dibromooctafluorobiphenyl were chosen as starting materials for two simple model borates. These compounds were synthesized analogue to the commonly used precursor Li[B(C$_6$F$_5$)$_4$] and slightly modified procedures of *Neckers* and *Marks* and co-workers (see Scheme 4.6).[10, 25]
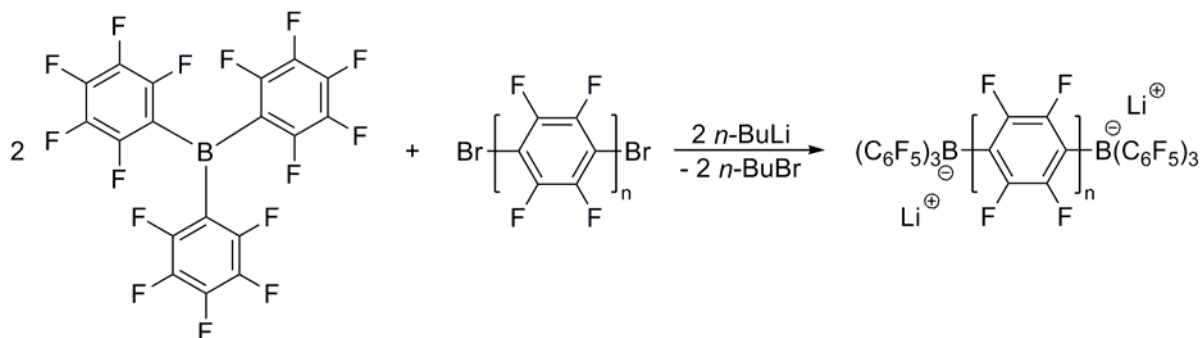
Scheme 4.6. Synthesis of lithium mono- or diaryl bisborates, solvent: diethyl ether ((n = 1), toluene (n = 2), T = - 78 °C.

The reaction of one equivalent 1,4-dibromotetrafluorobenzene or 4,4'-dibromooctafluorobiphenyl with two equivalent *n*-BuLi and tris-(pentafluorophenyl)borate gave the corresponding lithium bisborates. The synthesis of the lithium diaryl monoborate was conducted in diethyl ether. For lithium diaryl bisborate the solvent had to be changed to toluene as the product is insoluble in diethyl ether.

In a next step, Li$^+$ was exchanged by H$^+$ to provide facile access to desired transition metal complexes (for example to the Cu^{2+} salt, using Cu(OAc)$_2$ as starting material (see Scheme 4.7, procedure analogue chapter III. 4.2).
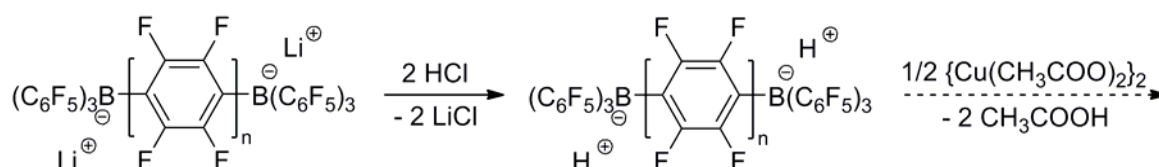
Scheme 4.7. Reaction of lithium mono- or diaryl bisborates with HCl in diethylether, solvent: diethyl ether (n = 1), toluene (n = 2) and proposed following reaction with a metal precursor.

3.2 Characterization

Both diaryl bisborates are soluble in dichloromethane and insoluble in nonpolar solvents such as pentane. They are stable at room temperature but air- and moisture sensitive.

^{1}H NMR spectroscopy as well as elementary analysis indicate that both compounds are etherates. H$_2$[(C$_6$F$_5$)$_3$B-C$_6$F$_4$-B(C$_6$F$_5$)$_3$] coordinates four ether molecules, H$_2$[(C$_6$F$_5$)$_3$B-(C$_6$F$_4$)$_2$-B(C$_6$F$_5$)$_3$] three. This is analog the related H[B(C$_6$F$_5$)$_4$] which is a dietherate.[25c]

Both oxonium salts crystallize from diethyl ether (monoborate) or toluene (bisborate) solutions and overlaied pentane (1:2) in colorless needles.

4 Conclusions

[H$_2$(Et$_2$O)$_4$][(C$_6$F$_5$)$_3$B-C$_6$F$_4$-B(C$_6$F$_5$)$_3$] and [H$_2$(Et$_2$O)$_3$][(C$_6$F$_5$)$_3$B-(C$_6$F$_4$)$_2$-B(C$_6$F$_5$)$_3$] were synthesized via a simple procedure and were obtained analytically pure by facile crystallization. Both oxonium salts of them are soluble in common solvents such as

dichloromethane. Thus, their application as precursors for nitrile ligated transition metal complexes in heterogenization studies seems to be promising.

5. Experimental

General: All preparations and manipulations were carried out under argon atmosphere using standard Schlenk techniques and all solvents were dried using standard procedures. $B(C_6F_5)_3$ was prepared as described in literature.[25d] NMR measurements were performed on a Bruker AVANCE-DPX-400 MHz spectrometer. Chemical shifts are reported in ppm and are referenced to the solvent as internal standard. Elemental analyses were carried out at the Mikroanalytisches Labor of the TU München.

[$H_2(Et_2O)_4$][($C_6F_5)_3B-C_6F_4-B(C_6F_5)_3$]. A 2.5 M solution of *n*-butyllithium in *n*-hexane (0.78 mL, 1.94 mmol) was added drop wise, within 10 min, to a stirred solution of (0.30 g, 0.97 mmol) 1,4-dibromotetrafluorobenzene in diethyl ether (20 mL) at -78 °C. After the solution was stirred for an additional 30 min, a cooled solution of tris(pentafluorophenyl)borane (0.99 g, 1.94 mmol) in diethyl ether (20 mL) was added dropwise, over a 10 minute periode. The reaction mixture was kept stirring for 2 h and allowed to gradually warm up to RT. The formed white precipitate was filtered of after stirring for 12 h. The solvent was removed and the remaining white solid was washed twice with pentane (2x 40 mL). The solid was dissolved in diethyl ether (20 mL) susequently. After the addition of a 2 M solution of hydrogen chloride in diethyl ether (1.94 mL, 3.88 mmol), the mixture was stirred overnight at rt. The supernatant was separated from the precipitate by filtration and dried via oil pump vacuum. The resulting off-white solid was washed three times with pentane (3x 60 mL) and freeze dried: yield 0.81 g (57 %). ^{1}H NMR (400 MHz, CD_2Cl_2, T = 298 K, δ(ppm)): 8.42 (v. br. 1 H, Et_2OH), 3.93 (q, ^3J = 7.1 Hz, 8 H, CH_2), 1.35 (t, ^3J = 7.1 Hz, 12 H, CH_3). ^{19}F NMR (376 MHz, CD_2Cl_2, T = 298 K, δ(ppm)): -167.6 (m, 16 F, *m*-F, C_6F_4), -163.6 (m, 6 F, *p*-F), -

133.3 (m, 12 F, *o*-F). ^{11}B NMR (128 MHz, CD_2Cl_2, T = 298 K, δ(ppm)): -13.62. Anal. Calcd for

$C_{58}H_{42}B_2F_{34}O_4$: C, 47.37; H, 2.88; F: 43.93. Found: C, 46.92; H, 2.56; F: 43.9.

[$H_2(Et_2O)_3$][(C_6F_5)$_3$B-(C_6F_4)$_2$-B(C_6F_5)$_3$]. A 2.5 M solution of *n*-butyllithium in *n*-hexane

(1.02 mL, 2.54 mmol) was added drop wise, within 10 min, to a stirred solution of (0.58 g,

1.27 mmol) 4,4'-dibromooctafluorobiphenyl in toluene (40 mL) at -78 °C. After the solution

was stirred for an additional 2 h, a cooled solution of tris(pentafluorophenyl)borane (1.30 g,

2.54 mmol) in toluene (20 mL) was added dropwise, over a 10 minute periode. The reaction

mixture was allowed to gradually warm up to RT. The solvent was removed after stirring for

12 h and the remaining white solid was washed twice with pentane (2x 25 mL). The solid was

dissolved in toluene (20 mL) susequently. After the addition of a 2 M solution of hydrogen

chloride in diethyl ether (10.19 mL, 20.38 mmol), the mixture was stirred overnight at rt. The

supernatant was separated from the precipitate by filtration and dried via oil pump vacuum.

The resulting off-white solid was washed three times with pentane (3x 25 mL) and freeze

dried: yield 0.73 g (37 %). ^{1}H NMR (400 MHz, CD_2Cl_2, T = 298 K, δ(ppm)): 8.40 (v. br. 1 H,

Et_2OH), 3.93 (q, [3]*J* = 7.1 Hz, 8 H, CH_2), 1.35 (t, [3]*J* = 7.1 Hz, 12 H, CH_3). ^{11}B NMR (128 MHz,

CD_2Cl_2, T = 298 K, δ(ppm)): -11.44. Anal. Calcd for $C_{60}H_{32}B_2F_{38}O_3$: C, 46.66; H, 2.09; F:

46.74. Found: C, 46.43; H, 1.92; F: 47.0.

References

[1]   a) M. Vierle, Y. Zhang, A. M. Santos, K. Köhler, C. Haeßner, E. Herdtweck, M. Bohnenpoll, O. Nuyken, F. E. Kühn, *Chem. Eur. J.* **2004**, *10*, 6323; b) A. K. Hijazi, A. Al Hmaideen, S. Syukri, N. Radhakrishnan, E. Herdtweck, B. Voit, F. E. Kühn, *Eur. J. Inorg. Chem.* **2008**, *2008*, 2892; c) M. Vierle, Y. Zhang, E. Herdtweck, M. Bohnenpoll, O. Nuyken, F. E. Kühn, *Angew. Chem. Int. Ed.* **2003**, *42*, 1307; d) N. Radhakrishnan, A. K. Hijazi, H. Komber, B. Voit, S. Zschoche, F. E. Kühn, O. Nuyken, M. Walter, P. Hanefeld, *J. Polym. Sci., Part A: Polym. Chem.* **2007**, *45*, 5636.

[2]   Y. Li, L. T. Voon, H. Y. Yeong, A. K. Hijazi, N. Radhakrishnan, K. Köhler, B. Voit, O. Nuyken, F. E. Kühn, *Chem. Eur. J.* **2008**, *14*, 7997.

[3]   J. Hagen, *Industrial Catalysis: A Practical Approach*, Second ed., Wiley-VCH, Weinheim, **2006**.

[4]   a) N. End, K.-U. Schöning, *Top. Curr. Chem.* **2004**, *242*, 241; b) D. J. Cole-Hamilton, *Science* **2003**, *299*, 1702.

[5]   a) A. Sakthivel, A. K. Hijazi, H. Y. Yeong, K. Köhler, O. Nuyken, F. E. Kühn, *J. Mater. Chem.* **2005**, *15*, 4441; b) S. Gago, Y. Zhang, A. M. Santos, K. Köhler, F. E. Kühn, J. A. Fernandes, M. Pillinger, A. A. Valente, T. M. Santos, P. J. A. Ribeiro-Claro, I. S. Gonçalves, *Micropor. Mesopor. Mater.* **2004**, *76*, 131; c) A. Sakthivel, A. K. Hijazi, A. I. A. Hmaideen, F. E. Kühn, *Micropor. Mesopor. Mater.* **2006**, *96*, 293; d)S. Syukri, A. K. Hijazi, A. Sakthivel, A. I. Al-Hmaideen, F. E. Kühn, *Inorg. Chim. Acta* **2007**, *360*, 197.

[6]   S. Syukri, C. E. Fischer, A. Al Hmaideen, Y. Li, Y. Zheng, F. E. Kühn, *Micropor. Mesopor. Mater.* **2008**, *113*, 171.

[7]   *unpublished results.*

[8]   A. K. Hijazi, H. Y. Yeong, Y. Zhang, E. Herdtweck, O. Nuyken, F. E. Kühn, *Macromol. Rapid Commun.* **2007**, *28*, 670.

[9]   a) H. Li, C. L. Stern, T. J. Marks, *Macromolecules* **2005**, *38*, 9015; b) N. Guo, L. Li, T. J. Marks, *J. Am. Chem. Soc.* **2004**, *126*, 6542; c) G. P. Abramo, L. Li, T. J. Marks, *J. Am. Chem. Soc.* **2002**, *124*, 13966; d) H. Li, L. Li, T. J. Marks, *Angew. Chem. Int. Ed.* **2004**, *43*, 4937; e) L. Li, M. V. Metz, H. Li, M.-C. Chen, T. J. Marks, L. Liable-Sands, A. L. Rheingold, *J. Am. Chem. Soc.* **2002**, *124*, 12725; f) H. Li, L. Li, T. J. Marks, L. Liable-Sands, A. L. Rheingold, *J. Am. Chem. Soc.* **2003**, *125*, 10788.

[10]   K. Ren, J. H. Malpert, H. Li, H. Gu, D. C. Neckers, *Macromolecules* **2002**, *35*, 1632.

[11]   a) B. Scrosati, *Mat. Sci. Forum* **1989**, *42*, 207; b) A. Pron, *Mat. Sci. Forum* **1987**, *21*, 13; c) N. Toshima, S. Hara, *Prog. Polym. Sci.* **1995**, *20*, 155.

[12]   D. Kumar, R. C. Sharma, *Eur. Polym. J.* **1998**, *34*, 1053.

[13]   R. Menon, *Curr. Sci.* **2000**, *79*, 1632.

[14]   a) J. Mort, *Science* **1980**, *208*, 819; b) S. Roth, *Physica* **1984**, *127B*, 151; c) J. E. Frommer, *Acc. Chem. Res.* **1986**, *19*, 2.

[15]   J. H. Burroughes, D. D. C. Bradley, A. R. Brown, R. N. Marks, K. Mackay, R. H. Friend, P. L. Burns, A. B. Holmes, *Nature* **1990**, *347*, 539.

[16]   a) P. Kovacic, M. B. Jones, *Chem. Rev.* **1987**, *87*, 357; b) J. G. Speight, P. Kovacic, F. W. Koch, *J. Macromol. Sci., Part C: Revs. Macromol. Chem.* **1971**, *5*, 295

[17]   G. Goldfinger, *J. Polym. Sci. A: Polym. Chem.* **1949**, *4*, 93.

[18]   a) W. Kern, R. Gehm, *Angew. Chem.* **1950**, *62*, 337; b) H. O. Wirth, R. Müller, W. Kern, *Makromol. Chem.* **1964**, *77*, 90.

[19]   a) T. Yamamoto, Y. Hayashi, A. Yamamoto, *Bull. Chem. Soc. Jpn.* **1978**, *51*, 2091; b) T. Yamamoto, A. Morita, Y. Miyazaki, T. Maruyama, H. Wakayama, Z. H. Zhou, Y. Nakamura, T. Kanbara, S. Sasaki, K. Kubota, *Macromolecules* **1992**, *25*, 1214.

[20]   a) M. Rehahn, A.-D. Schlüter, G. Wegner, *Makromol. Chem.* **1990**, *191*, 1991; b) A. R. Martin, Y. Yang, *Acta Chem. Scand.* **1993**, *47*, 221; c) J. Huber, K. Müllen, J. Salbeck, H. Schenk, U. Scherf, T. Stehlin, R. Stern, *Acta Polym.* **1994**, *45*, 244.

[21]   J. H. Golden, P. F. Mutolo, E. B. Lobkovsky, F. J. DiSalvo, *Inorg. Chem.* **1994**, *33*, 5374.

[22]   J.-F. Fauvarque, M.-A. Petit, F. Pfluger, A. Jutand, C. Chevrot, M. Troupel, *Makromol. Chem., Rapid Commun.* **1983**, *4*, 455.

[23]   D. G. H. Ballard, A. Courtis, I. M. Shirley, S. C. Taylor, *Macromolecules* **1988**, *21*, 294.

[24]   C. Ego, A. C. Grimsdale, F. Uckert, G. Yu, G. Srdanov, K. Müllen, *Adv. Mater.* **2002**, *14*, 809.

[25]   a) M. Kuprat, M. Lehmann, A. Schulz, A. Villinger, *Organometallics* **2010**, *29*, 1421; b) D. Alberti, K.-R. Pörschke, *Organometallics* **2004**, *23*, 1459; c) P. Jutzi, C. Müller, A. Stammler, H. G. Stammler, *Organometallics* **2000**, *19*, 1442; d) A. G. Massey, A. J. Park, *J. Organomet. Chem.* **1964**, *2*, 245; e) L. Li, M. V. Metz, H. Li, M.-C. Chen, T. J. Marks, *J. Am. Chem. Soc.* **2002**, *124*, 12725.

V. Synthesis and characterization of the complex [Ag(C$_6$H$_5$CN)$_2$][B(C$_6$F$_5$)$_4$]

1. Introduction

As a result of their ability to enhance the reactivity of metal complexes, the use of weakly or non-coordinating anions as counteranions (WCAs) is of significant interest in both synthesis and catalysis.[1] Of these WCAs, the tetrakis(pentafluorophenyl)borate B(C$_6$F$_5$)$_4$$^-$, discovered by *Massey* and *Park*,[2] is of particular interest in current researches, due to their structural simplicity, high symmetry and well-established availability. Silver(I) and thallium(I)[3] salts of B(C$_6$F$_5$)$_4$$^-$ are useful reagents for metathesis reactions via halide abstraction.[4,5] The Tl[B(C$_6$F$_5$)$_4$][3] has been reported as a stable salt, while the Ag$^+$[B(C$_6$F$_5$)$_4$] is light sensitive and therefore more difficult to handle. The stabilization of this compound via solvent ligation of the silver ion, forming [Ag(benzene)$_3$]$^+$,[6] [Ag(toluene)$_3$]$^+$,[7] [Ag(Et$_2$O)$_3$]$^+$,[7] and [Ag(CH$_3$CN)$_4$]$^+$,[8] is an accurate way to decrease its light sensitivity.

The preparation and characterization of the bis-(benzonitrile) silver(I) complex [Ag(C$_6$H$_5$CN)$_2$][B(C$_6$F$_5$)$_4$] is examined in this study.

2. Results and Discussion

2.1 Synthesis

The silver(I) complex [Ag(C$_6$H$_5$CN)$_2$][B(C$_6$F$_5$)$_4$] was synthesized by ligand exchange of [Ag(CH$_3$CN)$_4$][B(C$_6$F$_5$)$_4$][8] in benzonitrile. The solvent including the released non-ligated ("free") actonitrile was removed *in vacuo*. The complex was crystallized from dichloromethane/pentane (1/2).

2.2 Vibrational Spectroscopy

The vacuum distillation removing non ligated ("free") benzonitrile from [Ag(C$_6$H$_5$CN)$_2$][B(C$_6$F$_5$)$_4$] was attended by liquid IR spectroscopy and compared with its solid IR spectra (Figure 5.1). The ν_{CN} stretching frequency of the compound dissolved in benzonitrile is lower shifted (2250 cm^{-1}) than in solid state (2275 cm^{-1}), caused by a significantly stronger benzonitrile-silver ion interaction in solid state than in solution. This indicates a higher coordination environment of benzonitirile ligands around the silver ion in solution than in solid state. *Liang et al.* described a similar phenomenon for the vibrational spectra of [Cu(CH$_3$CN)$_n$][B(C$_6$F$_5$)$_4$] in dependence of the coordination numbers n = 2, 4.[9]
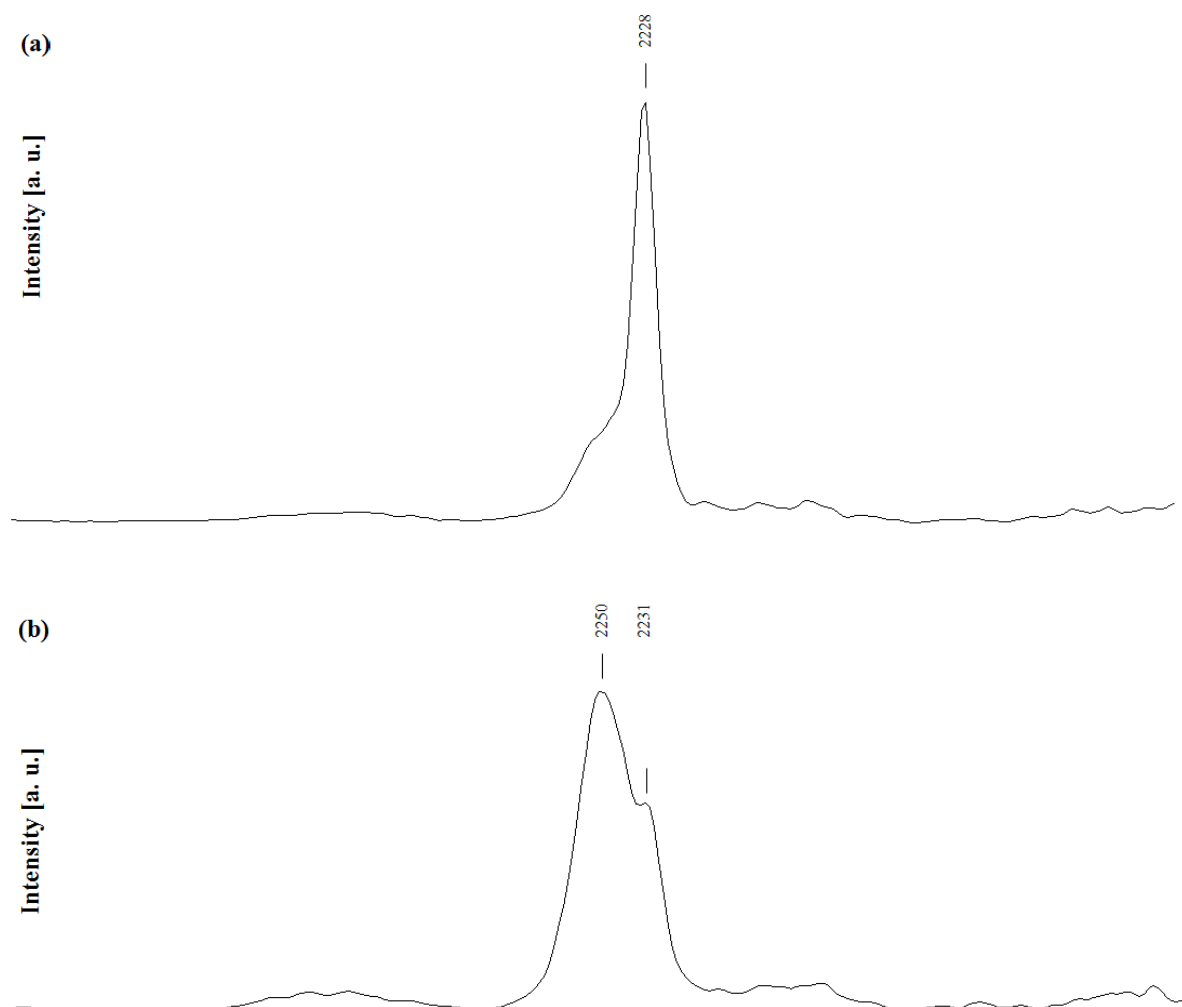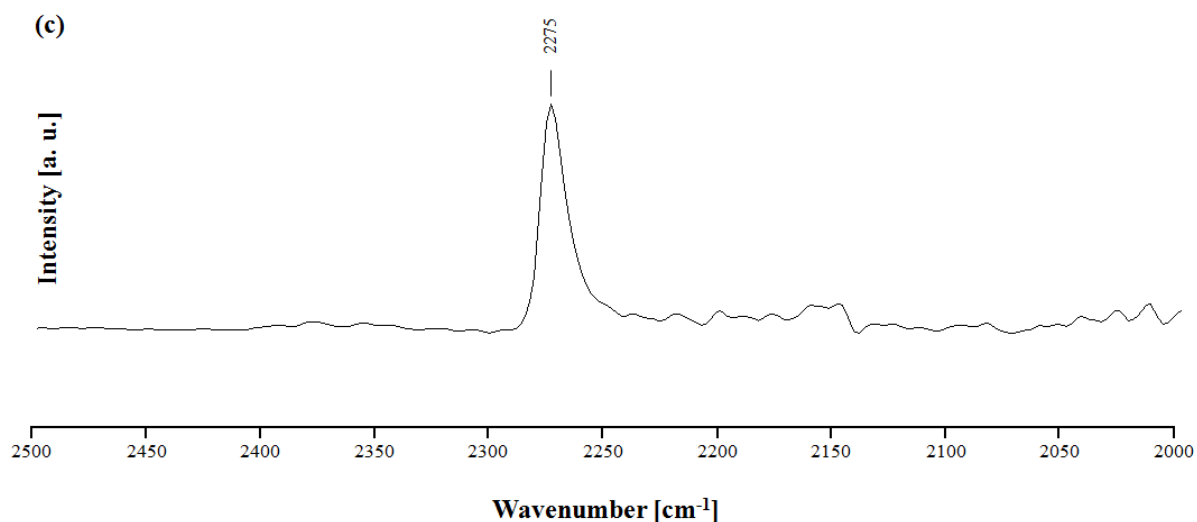
Figure 5.1. Comparison of the IR spectrum of [Ag(C$_6$H$_5$CN)$_2$][B(C$_6$F$_5$)$_4$] (c) with the liquid-IR spectra of [Ag(C$_6$H$_5$CN)$_2$][B(C$_6$F$_5$)$_4$] in benzonitrile in liquid (after 2 h vacuum distillation; c ~ 0.05 molL^{-1}) (a) and in viscous state (after 8 h vacuum distillation; c ~ 0.4 molL^{-1}) (b).

2.3 X-ray single crystal diffraction

Crystals of Ag(C$_6$H$_5$CN)$_2$][B(C$_6$F$_5$)$_4$] suitable for X-ray single-crystal diffraction were grown in dichloromethane/pentane (Figure 5.2). The bis-benzonitrile silver(I) complex contains a centrosymmetric C$_6$H$_5$CN-Ag(I)-NCC$_6$H$_5$ cation ($\forall$(N1-Ag1-N1) = 180.0°), with a similar cationic structure to complexes, such as [Cu(CH$_3$CN)$_2$][B(C$_6$F$_5$)$_4$],[9] [Ag(CH$_3$CN)$_2$][B{C$_6$H$_3$(*m*-CF$_3$)$_2$}$_4$][8] and [Au(CH$_3$CN)$_2$][SbF$_6$].[10] In contrast to the X-ray structure of [Cu(CH$_3$CN)$_2$][B(C$_6$F$_5$)$_4$], no silver-fluorine interactions with the B(C$_6$F$_5$)$_4^-$ anion can be observed.
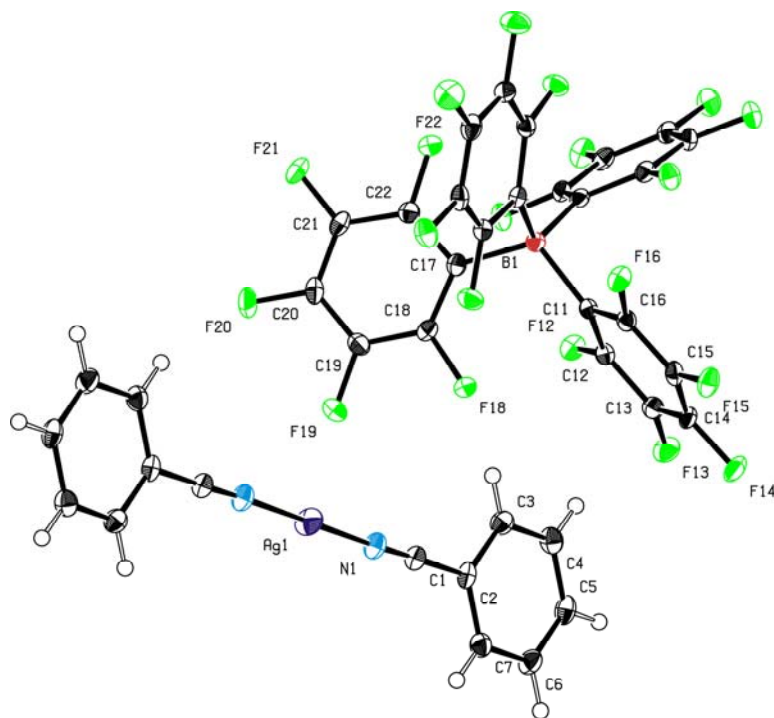
Figure 5.2. ORTEP style depiction of [Ag(C$_6$H$_5$CN)$_2$][B(C$_6$F$_5$)$_4$] in the solid state. Thermal ellipsoids are drawn at the 50 % probability level.

The Ag-N bond length of [Ag(C$_6$H$_5$CN)$_2$][B(C$_6$F$_5$)$_4$] of 2.098(2) Å is typical for bis-(nitrile) silver(I) complexes like [Ag(CH$_3$CN)$_2$][B{C$_6$H$_3$(*m*-CF$_3$)$_2$}$_4$] (2.066(4) and 2.097(2) Å)[8] and significantly shorter than the characteristic Ag-N bond lengths of tetrahedral silver complexes, *e.g.* [Ag(RCN)$_4$][WCA] (WCA = BF$_4^-$, CF$_3$SO$_3^-$)[11,12] and [Ag(C$_2$H$_5$CN)$_4$][B(C$_6$F$_5$)$_4$][13] (Table 5.1).

Table 5.1. Selected bond lengths and bond angles of nitrile ligated silver complexes [Ag(RCN)$_n$][WCA] (R = CH$_3$, C$_2$H$_5$, C$_6$H$_5$) in dependence of the coordination number n = 2, 4.

complex	Distance [Å]		Angle [°]
	M-N	N-C	N-M-N
[Ag(C$_6$H$_5$CN)$_2$][B(C$_6$F$_5$)$_4$]*	2.098(2)	1.142(2)	180.0
[Ag(CH$_3$CN)$_2$][B(C$_6$H$_3$(CF$_3$)$_2$)$_4$][8]	2.097(2)		180
	2.066(4)		
[Ag(CH$_3$CN)$_4$][BF$_4$][11]	2.229(3) -		104.2(1) -
	2.316		115.8(1)

[Ag(CH_3CN)$_4$][CF_3SO_3][12]	2.26(1)	
[Ag(C_2H_5CN)$_4$][B(C_6F_5)$_4$][13]	2.281(3)	103.4(12)
	2.265(3)	125.5(12)
	2.279(3)	98.8(12)
	2.298(3)	107.3(12)
		124.9(12)
		99.0(12)

*: this work

3. Conclusions

[Ag(C_6H_5CN)$_2$][B(C_6F_5)$_4$] was synthesized via ligand exchange of [Ag(CH_3CN)$_4$][B(C_6F_5)$_4$]. IR spectroscopic measurements were conducted, showing differences in the bond strength of Ag(I) and the benzonitrile ligands in the solid state (strong interaction) and in benzonitrile solution (weaker interaction). Single crystal structure analysis indicates a linear Ag(I) compound ligated by two benzonitrile molecules. Bond lengths are similar to those of the analog acetonitrile complex [Ag(CH_3CN)$_2$][B{C_6H_3(m-CF_3)$_2$}$_4$]. No interaction between the Ag(I) core and the anion can be observed.

4. Experimental

General. All preparations and manipulations were carried out under argon atmosphere using standard Schlenk techniques and all solvents were dried using standard procedures. [Ag(CH_3CN)$_4$][B(C_6F_5)$_4$] was synthesized as described in literature.[8] IR measurements were recorded on a Varian C670-IR spectrometer using a Gladiator ATR unit. ^{1}H-NMR and ^{13}C-NMR measurments were performed on a Bruker AVANCE-DPX-400 spectrometer. Chemical shifts are reported in ppm and are referenced to the solvent as internal standard.

IR spectra were recorded on a Perkin Elmer FT-IR spectrometer using a Nujol matrix. Elemental analyses were carried out at the Mikroanalytisches Labor of the TU München.

[Ag(C$_6$H$_5$CN)$_2$][B(C$_6$F$_5$)$_4$]. [Ag(CH$_3$CN)$_4$][B(C$_6$F$_5$)$_4$] (0.32 g, 0.34 mmol) was suspended in methylene chloride (4 mL) in the darkness. By addition of benzonitrile (0.07 mL, 0.07 g, 0.68 mmol) all solid was dissolved immediately. All volatiles were removed under vacuum (2 h) and the remaining solid was re-dissolved in methylene chloride (4 mL) and benzonitrile (0.07 mL). The volatiles were again removed under vacuum (2 h), affording a honey-like liquid. The desired product was obtained by crystallization from dichloromethane/pentane (1:2) as colourless crystals: 0.30 g (90 %). ^{1}H NMR (400 MHz, CD$_2$Cl$_2$, T = 298 K, δ(ppm)): 7.97-7.72 (m, 3 H, *o,p*-H), 7.72-7.55 (m, 2 H, *m*-H). ^{13}C NMR (75.5 MHz, CD$_2$Cl$_2$, T = 298 K, δ(ppm)): 148.5 (d, $^1J_{C-F}$ = 241.8 Hz), 138.6 (d, $^1J_{C-F}$ = 237.0 Hz), 136.7 (d, $^1J_{C-F}$ = 246.3 Hz), 134.8 (s, C$_{para}$), 133.5 (s, C$_{ortho}$), 130.2 (s, C$_{meta}$), 124.5 (br.), 121.0 (s, NC), 108.5 (s, *i*-C). Selected MIR (ATR, cm^{-1}): ν$_{CN}$, 2275. Elemental analysis calcd (%) for C$_{38}$H$_{10}$AgBF$_{20}$N$_2$: C 45.96, H 1.01, N 2.82; Found: C 45.74, H 0.99, N 2.83.

References

[1] a) S. H. Strauss, *Chem. Rev.* **1993**, *93*, 927; b) I. Krossing, I. Raabe, *Angew. Chem. Int. Ed.* **2004**, *43*, 2066.

[2] a) A. G. Massey, A. J. Park, F. G. A. Stone, *Proc. Chem. Soc.* **1963**, 212; b) A. G. Massey, A. J. Park, *J. Organomet. Chem.* **1964**, *2*, 245; c) A. G. Massey, A. J. Park, *J. Organomet. Chem.* **1966**, *5*, 218.

[3] D. Alberti, K.-R. Pörschke, *Organometallics* **2004**, *23*, 1459.

[4] S. F. Rach, F. E. Kühn, *Chem. Rev.* **2009**, *109*, 2061.

[5] M. Bochmann, *Coord. Chem. Rev.* **2009**, *253*, 2000.

[6] K. Ogawa, T. Kitagawa, S. Ishida, K. Komatsu, *Organometallics* **2005**, *24*, 4842.

[7] M. Kuprat, M. Lehmann, A. Schulz, A. Villinger, *Organometallics* **2010**, *29*, 1421.

[8] Y. Zhang, A. M. Santos, E. Herdtweck, J. Mink, F. E. Kühn, *New J. Chem.* **2005**, *29*, 366.

[9] H.-C. Liang, E. Kim, C. D. Incarvito, A. L. Rheingold, K. D. Karlin, *Inorg. Chem.* **2002**, *41*, 2209.

[10] a) B. v. Ahsen, B. Bley, S. Proemmel, R. Wartchow, H. Willner, *Z. anorg. allg. Chem.* **1998**, *624*, 1125; b) H. Willner, J. Schaebs, G. Hwang, F. Mistry, R. Jones, J. Trotter, F. Aubke, *J. Am. Chem. Soc.* **1992**, *114*, 8972.

[11] A. A. M. Aly, B. Walfort, H. Lang, *Z. Kristallogr.- New Cryst. Struct.* **2004**, *219*, 489.

[12] K. Ozutsumi, A. Kitakaze, M. Iinomi, H. Ohtaki, *J. Mol. Liq.* **1997**, *73-74*, 385.

[13] M. Vierle, Y. Zhang, A. M. Santos, K. Köhler, C. Haeßner, E. Herdtweck, M. Bohnenpoll, O. Nuyken, F. E. Kühn, *Chem. Eur. J.* **2004**, *10*, 6323.

VI. Synthesis and characterization of the molybdenum(IV) complexes [MoO(CH$_3$CN)$_4$(*ax*-CH$_3$CN)][B(C$_6$F$_5$)$_4$]$_2$ and [MoO(C$_6$H$_5$CN)$_4$][B(C$_6$F$_5$)$_4$]$_2$

This chapter originated from the following publication:

Bernd E. Diebl, Silvana F. Rach, Christian E. Fischer, Hui Yee Yeong, Mirza Cokoja,

Eberhardt Herdtweck, Brigitte Voit and Fritz E. Kühn, *Appl. Catal. A-Gen.* **2010**, *submitted*.

1. Introduction

Industry increasingly focuses on the finding and application of environmentally benign, energy-saving processes. During the last years, energy-conserving alternatives to conventional cationic polymerization processes have been successfully developed for isobutene polymerization, which is traditionally executed at low temperatures (< - 30 °C) on large scale. When using acetonitrile ligated transition metal cations of general formula [M(CH$_3$CN)$_6$]$^{2+}$ (M= Cr,[1] Mn,[2,] Fe,[1] Co,[1] Ni,[1] Cu[3] and Zn[1]) or M(III) complexes of composition [MoCl(MeCN)$_5$]$^{2+}$ [4] bearing non coordinating anions (WCAs), e. g. B(C$_6$F$_5$)$_4^-$, B{C$_6$H$_3$(*m*-CF$_3$)$_2$}$_4^-$ or C$_3$N$_2$H$_3${B(C$_6$F$_5$)$_3$}$_2^-$ in catalytic amounts, the polymerization of isobutene takes place at moderate temperatures (between 20 °C and 40 °C) in solvents such as dichloromethane or, even more interesting, toluene.[5] A particular advantage of this process is the possibility to access polyisobutenes (PIB) with up to 90 % of *exo* double bonds (HR-PIB) and polydispersities below 1.9.[2b, 2c, 3b],

However, the intricate and comparatively expensive synthesis of both the cations and the WCA, e. g. of the molybdenum(III) complexes [MoCl(CH$_3$CN)$_5$]$^{2+}$[WCA]$_2$, prevented so far any industrial application. Therefore, a focus of the currently ongoing work is set on the investigation of alternative Mo(III) complexes of comparable activities for isobutene polymerization, using inexpensive synthesis strategies. Additionally, the synthesis of

[H(Et$_2$O)$_2$][B(C$_6$F$_5$)$_4$], a precursor of the counter anion, originally published by *Jutzi et al.* has been enhanced.[6]

2. Results and Discussion

2.1 Synthesis of [MoO(CH$_3$CN)$_{4/5}$][B(C$_6$F$_5$)$_4$]$_2$ and [MoO(C$_6$H$_5$CN)$_4$][B(C$_6$F$_5$)$_4$]$_2$

The oxo-bridged Mo(III) dimer [Mo$_2$(μ-O)(CH$_3$CN)$_{10}$]$^{4+}$ first reported by *Wilkinson et al.*[7] seemed to be a possible candidate for a more easily available isobutene polymerization mediator. [Mo$_2$(μ-O)(CH$_3$CN)$_{10}$][BF$_4$]$_4$ is synthesized *via* oxidation of [Mo(CO)$_3$(CH$_3$CN)$_3$] in the presence of HBF$_4$·OEt$_2$ in air.[7] Hence, this synthetic route should be easy to modify by using [H(OEt$_2$)$_2$][B(C$_6$F$_5$)$_4$].[6] However, it was found that a monomeric Mo(IV) complex of the structure [MoO(CH$_3$CN)$_{4/5}$][B(C$_6$F$_5$)$_4$]$_2$ is formed instead of the expected formation of an oxo-bridged Mo(III) dimer of the structure [Mo$_2$(μ-O)(CH$_3$CN)$_{10}$][B(C$_6$F$_5$)$_4$]$_4$ (see Scheme 6.1). *Dunbar et al.* describe the reaction of MoCl$_3$(THF)$_3$ with AgBF$_4$ in refluxing acetonitrile forming [Mo$_2$(μ-F)(CH$_3$CN)$_8$O$_2$][BF$_4$]$_3$.[8] Therefore, the formation of a [Mo(IV)O(CH$_3$CN)$_5$]$^{2+}$ species is assumed to be an intermediate.[8]
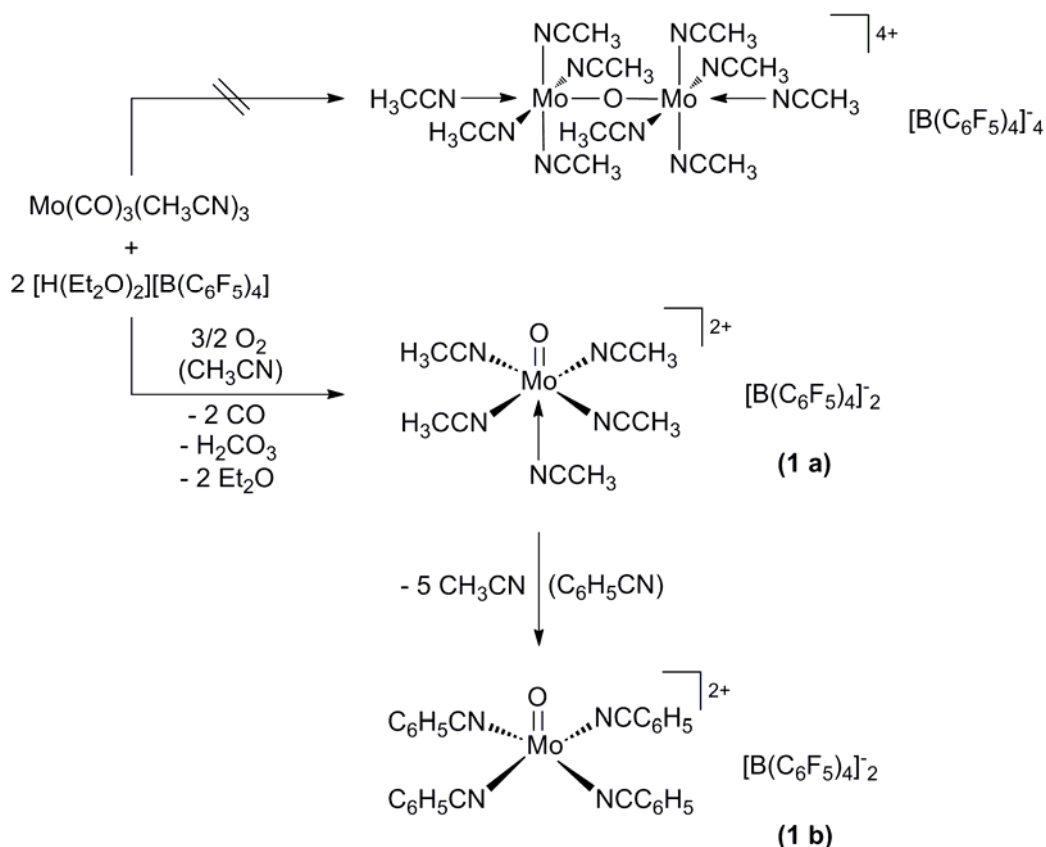
Scheme 6.1. Synthetic route for the synthesis of [MoO(CH₃CN)₅][B(C₆F₅)₄]₂ **(1)** and [MoO(C₆H₅CN)₄][B(C₆F₅)₄]₂ **(1 b).**

The oxonium acid [H(OEt₂)₂][B(C₆F₅)₄] can be prepared either from Li[B(C₆F₅)₄] and gaseous HCl as reported by *Jutzi et al.*,[6] or by adding a solution of HCl in diethyl ether to an *in situ* reaction of C₆F₅I with stoichiometric amounts of *n*-BuLi and BCl₃ at 0 °C (see Chapter III. 3.2.1.).

The protonation of Mo(CO)₃(CH₃CN)₃ in CH₃CN with 2.4 equiv. [H(OEt₂)₂][B(C₆F₅)₄] in air and at RT (25 °C) occurs with a color change from orange to green to form [MoO(CH₃CN)₄/₅][B(C₆F₅)₄]₂ after 10-15 min. The synthesis of this compound is only achieved in presence of oxygen. When the synthesis is carried out under argon atmosphere and distilled water, no formation of it can be observed within a time period of 3 h. Unreacted [H(OEt₂)₂][B(C₆F₅)₄] is removed from the complex by extraction with toluene. [MoO(CH₃CN)₄/₅][B(C₆F₅)₄]₂ is well soluble in polar solvents such as CH₂Cl₂, diethyl ether and CHCl₃, but not in aliphatic hydrocarbons. It is slightly soluble in aromatic hydrocarbons e.g. toluene. Elemental analysis suggests the presence of a [MoO(CH₃CN)₄]²⁺ cation containing

only four actonitrile ligands. The loss of one acetonitrile ligand is most presumably caused by the drying process of a sample of the complex *in vacuo* (10^{-2} mbar) for several hours. This effect is known and is described in literature for a large number of metal-acetonitrile complexes, *e.g.* $Mo_2(CH_3CN)_8(ax-CH_3CN)_2]^{2+}$.[9] In order to increase the solubility in non polar solvents such as toluene, the acetonitrile ligands were exchanged by benzonitrile forming $[MoO(C_6H_5CN)_4][B(C_6F_5)_4]_2$. The complex $[MoO(C_6H_5CN)_4][B(C_6F_5)_4]_2$ is formed by exchanging the acetonitrile ligands of $[MoO(CH_3CN)_{4/5}][B(C_6F_5)_4]_2$ with benzonitrile ligands by dissolving in dry benzonitrile. Acetonitrile is removed from the reaction mixture by vacuum distillation. Traces of uncoordinated benzonitrile were extracted by a solvent mixture of CCl_4 and cyclohexane.

2.2 Vibrational Spectroscopy

The infrared (IR) spectra of compounds $[MoO(CH_3CN)_{4/5}][B(C_6F_5)_4]_2$ and $[MoO(C_6H_5CN)_4][B(C_6F_5)_4]_2$ were recorded in Nujol. The shift of the ν_{CN} stretching frequencies of non ligated ("free") or ligated acetonitrile are splitted due to Fermi resonance interactions between the combination mode $\nu_3 + \nu_4$ and the ν_{CN} stretching mode.[5, 10] The ν_{CN} stretching frequencies of weak intensities at 2328 and 2297 cm^{-1} and of middle intensities at 2314 and 2287 cm^{-1} show two types of acetonitrile ligation in $[MoO(CH_3CN)_{4/5}][B(C_6F_5)_4]_2$ (see Figure 6.1 a). Due to the comparably weak intensities of the ν_{CN} stretching frequencies at 2328 and 2297 cm^{-1} these vibrations are assigned to the acetonitrile ligand in axial position. The absorptions at 2314 and 2287 cm^{-1} represent the ν_{CN} stretching frequencies of the acetonitrile ligands in equatorial position quite similar to the situation observed for acetonitrile ligated Mo(III) complexes $[MoCl(CH_3CN)_5][B(C_6F_5)_4]_2$ (2321 and 229 cm^{-1})[4], $[Mo(NO)(CH_3CN)_5][PF_6]_2$ (2320 and 2292 cm^{-1})[11] as well as the oxo-bridged Mo(III) dimer $[Mo_2(\mu-O)(CH_3CN)_{10}][BF_4]_4$ (2319 and 2285 cm^{-1}).[7] A similar phenomenon has also been described by *Cotton et al.* for different acetonitrile ligations in the dimeric Mo(II) complex $[Mo_2(CH_3CN)_8(ax-CH_3CN)_2][BF_4]_4$ (2325, 2293 and 2247 cm^{-1})[9a] The ν_{CN} stretching

frequency at 2248 cm^{-1} of ligated benzonitrile in [MoO(C_6H_5CN)$_4$][B(C_6F_5)$_4$]$_2$ is shifted to a higher frequency compared to the corresponding mode in non ligated ("free") benzonitrile (2230 cm^{-1}) (see Figure 6.1b).
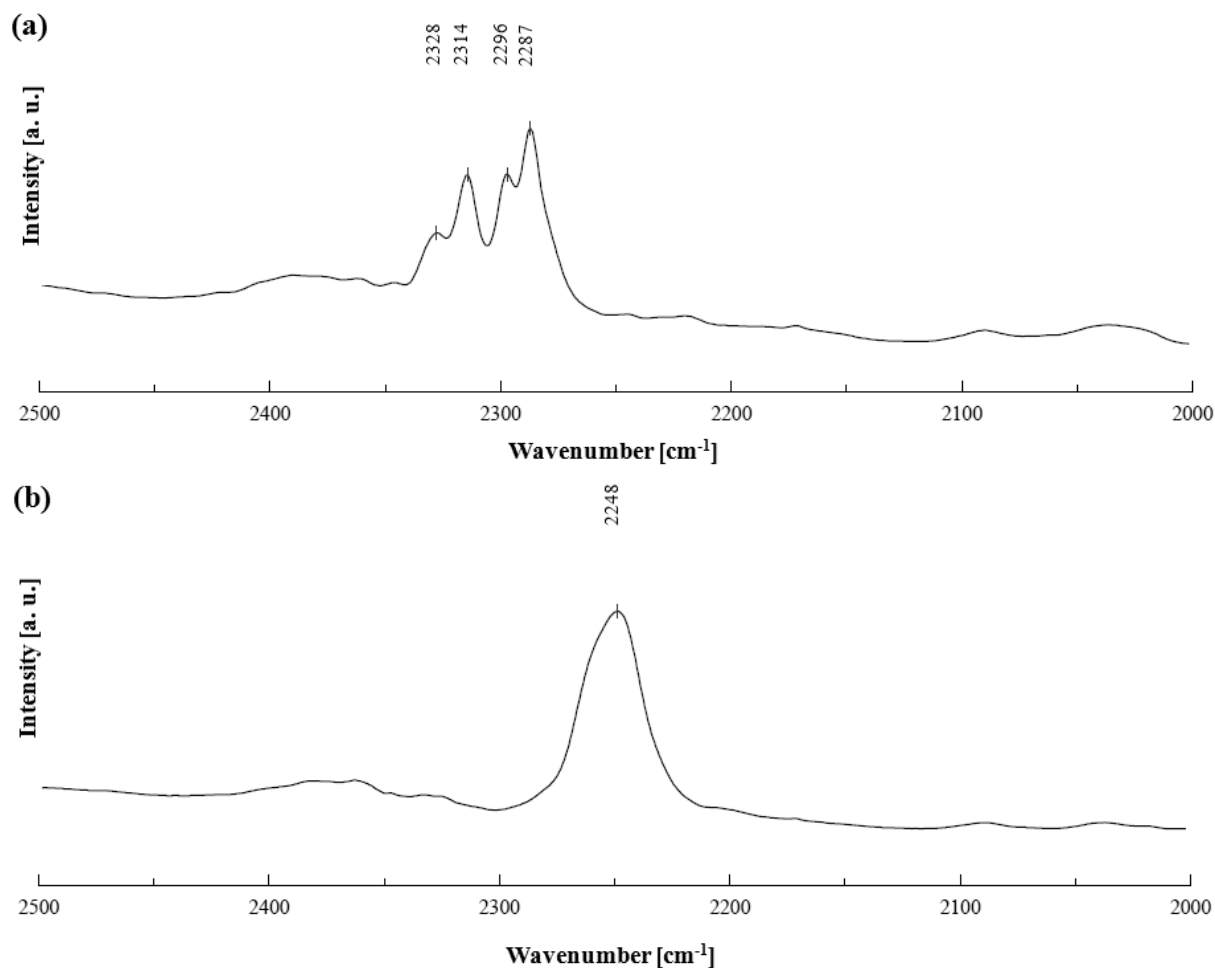
Figure 6.1. Infrared spectra of compound [MoO(CH$_3$CN)$_{4/5}$][B(C_6F_5)$_4$]$_2$ in **(a)** and [MoO(C_6H_5CN)$_4$][B(C_6F_5)$_4$]$_2$ in **(b)** in the ν_{CN} stretching region.

2.3 ^{95}Mo-NMR spectroscopy

Examination of [MoO(CH$_3$CN)$_{4/5}$][B(C_6F_5)$_4$]$_2$ by ^{95}Mo-NMR spectroscopy, the spectrum being recorded in dry CH$_3$CN with Na$_2$MoO$_4$·2 H$_2$O as an external reference revealed the Mo signal at -116 ppm (see Figure 6.2). The signal of the Mo(III) center in [Mo$_2$(μ-O)(CH$_3$CN)$_{10}$][BF$_4$] is observed at -2816 ppm.

122
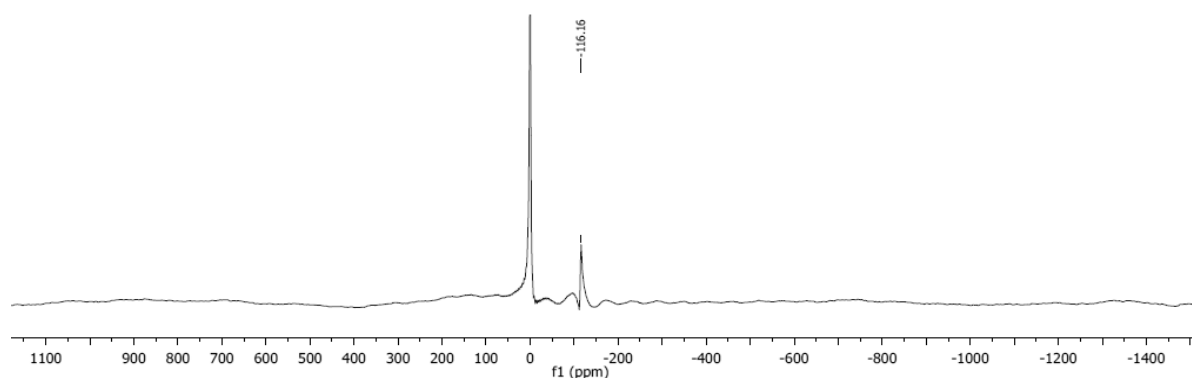
Figure 6.2. ^{95}Mo-NMR spectra of [MoO(CH$_3$CN)$_{4/5}$][B(C$_6$F$_5$)$_4$]$_2$. The larger signal stems from the external standard.

2.4 Thermogravimetric analysis

Samples of [MoO(CH$_3$CN)$_{4/5}$][B(C$_6$F$_5$)$_4$]$_2$ and [MoO(C$_6$H$_5$CN)$_4$][B(C$_6$F$_5$)$_4$]$_2$ were examined by thermogravimetric analysis in combination with an online fragment detection *via* coupled mass spectroscopy (TG-MS), applying a temperature program with a heating rate of 5 °C min^{-1} between 25 and 900 °C. The first onset of decomposition of [MoO(CH$_3$CN)$_{4/5}$][B(C$_6$F$_5$)$_4$]$_2$ occurs at 121 °C and is associated with a total weight loss of about 92 % of the original mass. For compound [MoO(C$_6$H$_5$CN)$_4$][B(C$_6$F$_5$)$_4$]$_2$ a total weight loss of about 83 % of the original mass was detected (see Figure 6.3). The first onset of decomposition of this complex occurs at 155 °C and is associated with a weight loss of ca. 11.5 %. The second and final decomposition step starts at 195 °C and corresponds to a weight loss of 56.7 % at 275 °C. The first step originates from the anion decomposition, as indicated by detection of F$^-$ and CF$^+$ fragments, resulting from the decomposition of B(C$_6$F$_5$)$_4^-$ anion with a local minimum at about 195 °C. However, a second maximum in the MS curves of F$^-$ and CF$^+$ fragments is observed at about 240 °C. This may hint that the decomposition of the [MoO(C$_6$H$_5$CN)$_4$]$^{2+}$ cation *via* loss of benzonitrile ligands is simultaneously in progress with the stepwise decomposition of the B(C$_6$F$_5$)$_4^-$ anions. For comparison, in K[B(C$_6$F$_5$)$_4$] the anion degradation is not observed below 240 °C.[1] The higher temperature sensitivity of the B(C$_6$F$_5$)$_4^-$ anion in [MoO(C$_6$H$_5$CN)$_4$][B(C$_6$F$_5$)$_4$]$_2$ in comparison to K[B(C$_6$F$_5$)$_4$] indicates that the decomposition of the counter anions in [MoO(C$_6$H$_5$CN)$_4$][B(C$_6$F$_5$)$_4$]$_2$ is accelerated by the

molybdenum cation. This behavior is in agreement with observations of *Buschmann et al.* for the decomposition process of $[M(CH_3CN)_6][B(C_6H_3\{m\text{-}CF_3\}_2)_4]_2$ (M = V - Zn).[12]
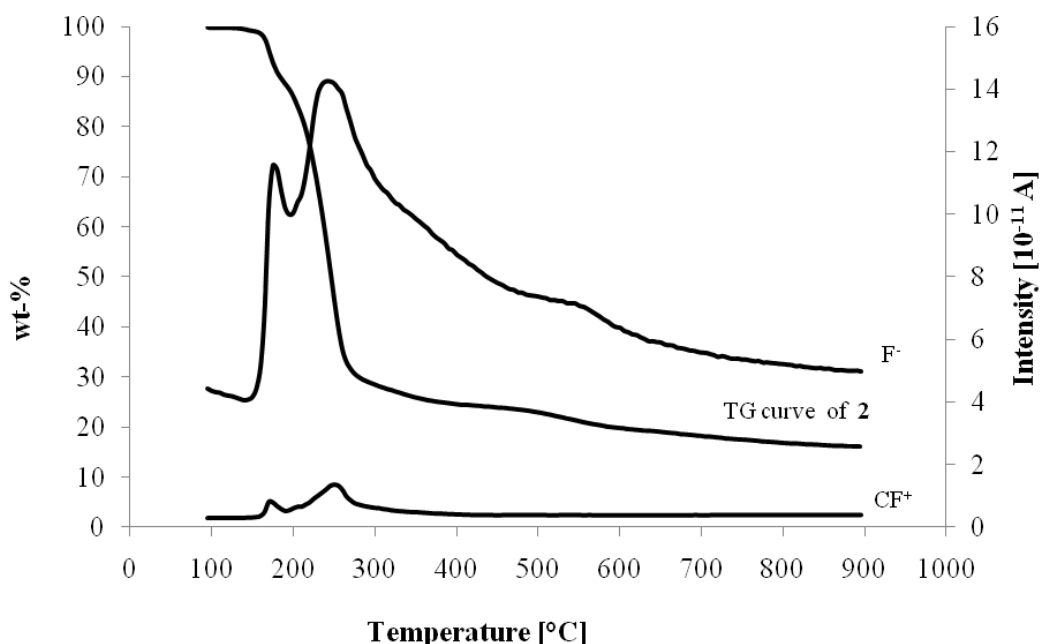
Figure 6.3. TG plot of $[MoO(C_6H_5CN)_4][B(C_6F_5)_4]_2$ and the MS intensity of fragments of the mass 19.00 (F$^-$) and 31.00 (CF$^+$).

2.5 X-ray single crystal diffraction

Crystals of $[MoO(CH_3CN)_{4/5}][B(C_6F_5)_4]_2$ suitable for X-ray single-crystal diffraction were grown by overlaying a solution of dry methylene chloride with dry pentane and a few drops of dry CH_3CN at room temperature. An ORTEP-style plot of the $[MoO(CH_3CN)_5]^{2+}$ dication is shown in Figure 6.4. The divalent molybdenum dication adopts a distorted octahedral coordination environment of five acetonitrile ligands and one oxo ligand around the molybdenum center similar to the observed geometry in $[MoCl(CH_3CN)_5][B(C_6F_5)_4]_2$.[4a] The Mo-N$_{cis}$ bond length of axially ligated acetonitrile to the metal center is clearly elongated (2.301(4) Å) in comparison to the Mo-N bond lengths in equatorial position (2.103(4) to 2.136(5) Å). The stretching of the Mo-N$_{trans}$ bond length of axial acetonitrile is caused by a *trans* effect influenced by the oxo ligand. In agreement with the observed v_{CN} stretching frequencies of $[MoO(CH_3CN)_{4/5}][B(C_6F_5)_4]_2$ the N1-C1 bond length (1.133(6) Å) of axially ligated acetonitrile

124

is slightly shorter than the N-C bond lengths (1.137(6) to 1.147(7) Å) of equtorially ligated acetonitriles. Furthermore, the *cis* influence of the oxo-ligand also explains the enlargement of the O-Mo-N$_{eq}$ angles (95.5(2) to 101.1(2)°) > 90°. The Mo1-O1 bond length of 1.686(3) Å is typical for Mo=O double bonds, *e.g.* obtained for [MoO$_2$X$_2$(bipy)] (X = Cl at 1.697(3)-1.699(2) Å, X = Br at 1.711(4)-1.728(3) Å and X = Me at 1.707(2)-1.708(2) Å).[13]

The weaker ligation of axially ligated acetonitrile is supported by the results obtained by elemental analysis, which show that a dication of composition [MoO(CH$_3$CN)$_4$]$^{2+}$ is obtained after drying the sample several hours under high vacuum (10^{-2} mbar).
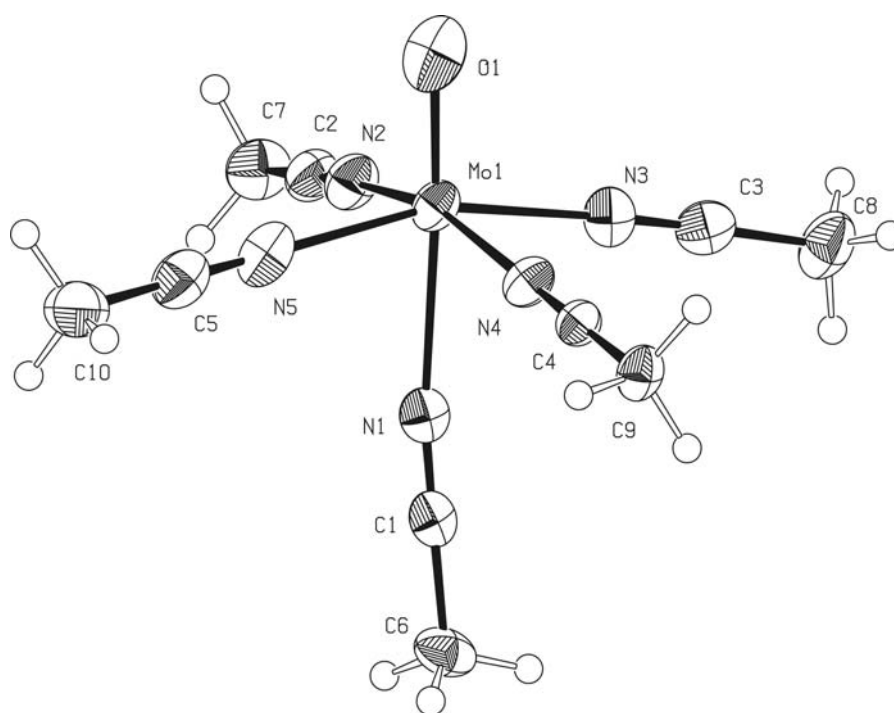
Figure 6.4. ORTEP style plot of the [MoO(CH$_3$CN)$_5$]$^{2+}$ dicationic part of [MoO(CH$_3$CN)$_{4/5}$][B(C$_6$F$_5$)$_4$]$_2$. Thermal ellipsoids are drawn at the 50 % probability level. Selected bond lengths [Å] and bond angles [°]: Mo1-O1 1.686(3), Mo1-N1 2.310(4), Mo1-N2 2.119(4), Mo1-N3 2.126(3), Mo1-N4 2.103(4), Mo1-N5 2.136(5); O1-Mo1-N1 176.3(2), O1-Mo1-N2 98.0(2), O1-Mo1-N3 101.1(2), O1-Mo1-N4 98.2(2), O1-Mo1-N5 95.5(2).

2.6 Application of [MoO(CH$_3$CN)$_{4/5}$][B(C$_6$F$_5$)$_4$]$_2$ and [MoO(C$_6$H$_5$CN)$_4$][B(C$_6$F$_5$)$_4$]$_2$ for the polymerization of isobutene

Isobutene has been polymerized at 30 °C in dichloromethane for 20 h using [MoO(CH$_3$CN)$_{4/5}$][B(C$_6$F$_5$)$_4$]$_2$ and [MoO(C$_6$H$_5$CN)$_4$][B(C$_6$F$_5$)$_4$]$_2$ as mediators (see Table 6.1).

Both complexes exhibit a significant catalytic activity, yielding high amounts of low to medium molar mass polyisobutene similar to the previously published results obtained with [MoCl(CH$_3$CN)$_5$][B(C$_6$F$_5$)$_4$]$_2$ (**3**).[4a] When applying [MoO(C$_6$H$_5$CN)$_4$][B(C$_6$F$_5$)$_4$]$_2$ as mediator, no significant change of the activity was observed at the applied polymerization conditions. The molecular weight (M$_n$) obtained for both compounds is approximately 1600 with a polydispersity (PDI) of 2.9 for [MoO(CH$_3$CN)$_{4/5}$][B(C$_6$F$_5$)$_4$]$_2$ and 2.8 for [MoO(C$_6$H$_5$CN)$_4$][B(C$_6$F$_5$)$_4$]$_2$.

Table 6.1. Homopolymerization of isobutylene using the complexes [MoO(CH$_3$CN)$_{4/5}$][B(C$_6$F$_5$)$_4$]$_2$ (**1**) and [MoO(C$_6$H$_5$CN)$_4$][B(C$_6$F$_5$)$_4$]$_2$ (**2**) in comparison to [MoCl(CH$_3$CN)$_5$][B(C$_6$F$_5$)$_4$]$_2$ (**3**).[4b] [IB]$_0$ = 1.78 mol/L, solvent = dichloromethane, reaction temperature = 30 °C, time = 20 h.

Complex	Complex Concentration [10^{-4} mol/L]	Conversion [%]	Molar Masses M$_n$ [g/mol] / PDI
1	0.39	80	1600 / 2.9
2	0.69	88	1600 / 2.8
3[a)	0.5	89	1300 / 3.2
3[a)	1.25	86	1400 / 3.0

a) data for compound **3** from ref.[4a]

3. Conclusion

The compounds [MoO(CH$_3$CN)$_4$(*ax*-CH$_3$CN)][B(C$_6$F$_5$)$_4$]$_2$ and [MoO(C$_6$H$_5$CN)$_4$][B(C$_6$F$_5$)$_4$]$_2$ can be easily synthesized. *Wilkinson et al.*[5] describe the formation of the oxo-bridged molybdenum(+III) dimer [Mo$_2$(μ-O)(CH$_3$CN)$_{10}$][BF$_4$]$_4$ by using HBF$_4$·OEt$_2$ instead of [H(OEt$_2$)$_2$][B(C$_6$F$_5$)$_4$] under the same reaction conditions whereas only a mononuclear compound was observed in our case. As shown by single crystal structure analysis, the [MoO(CH$_3$CN)$_4$(*ax*-CH$_3$CN)]$^{2+}$ cation displays a distorted octahedral. The Mo-N$_{trans}$ bond length (2.30-2.33 Å) of *trans* ligated acetonitrile in [MoO(CH$_3$CN)$_5$]$^{2+}$ is elongated in

comparison to the Mo-N$_{cis}$ bond lengths of *cis* ligated acetonitrile, indicating a trans effect of the oxo-ligand.

Polymerization experiments demonstrate that compound [MoO(CH$_3$CN)$_{4/5}$][B(C$_6$F$_5$)$_4$]$_2$ and [MoO(C$_6$H$_5$CN)$_4$][B(C$_6$F$_5$)$_4$]$_2$ show a similar activity for isobutene polymerization at room temperature, being also comparable to the previously reported [MoCl(CH$_3$CN)$_5$][B(C$_6$F$_5$)$_4$]$_2$.[4b] Since the new complexes are prepared by straight forward oxidation of the readily available [Mo(CO)$_3$(CH$_3$CN)$_3$] with [H(OEt$_2$)$_2$][B(C$_6$F$_5$)$_4$] and oxygen (from air) as co-oxidizer, a more facile and cost-efficient alternative to [MoCl(CH$_3$CN)$_5$][B(C$_6$F$_5$)$_4$]$_2$ as mediator for the room temperature isobutene polymerization process is now available.

4. Experimental

4.1 Measurements and Preparations

All preparations and manipulations were carried out under argon atmosphere using standard Schlenk techniques. All solvents were dried by standard procedures (carbon tetrachloride and dichloromethane under sodium, acetonitrile, benzonitrile, cyclohexane and *n*-hexane under CaH$_2$), distilled under argon and kept over molecular sieves (benzonitirile, carbon tetrachloride, cyclohexane dichloromethane and *n*-pentan over 4 Å molecular sieves, acetonitrile under 3 Å molecular sieves). Mo(CO)$_3$(CH$_3$CN)$_3$ was synthesized as described in literature.[14] IR measurements were recorded on a Varian C670-IR spectrometer using Nujol mulls. ^{1}H-NMR, ^{13}C-NMR and ^{95}Mo-NMR measurements were performed on a Bruker AVANCE-DPX-400 spectrometer. Elemental analyses were carried out at Mikroanalytisches Labor of TU München. Thermogravimetric analysis (TGA) studies were performed using a Mettler TA 3000 system at a heating rate of 5 °C min^{-1} under a static air atmosphere.

4.2 Preparation of the complexes

[H(Et$_2$O)$_2$][B(C$_6$F$_5$)$_4$]. A 2.5 M solution of *n*-butyllithium in *n*-hexane (17.82 mL, 40.50 mmol) was added drop-wise, within 10 min, to a stirred solution of (5.88 mL, 40.50 mmol) iodopentafluorobenzene in diethyl ether (30 mL) at -78 °C. After the solution was stirred for an additional 20 min, a 1 M solution of boron trichloride in *n*-hexane (10.16 mL, 10.16 mmol) was added drop-wise, over a period of 10 min. The reaction mixture was kept stirring for 10 min and warmed up to 0 °C, at which point LiCl precipitated immediately. After the addition of a 2 M solution of hydrogen chloride in diethyl ether (10.0 mL, 20.0 mmol), the mixture was stirred overnight at ambient temperature. The solution was separated from the solid by filtration and concentrated under vacuum (oil pump) to 10 mL. The fast addition of pentane (60 mL) to the stirred solution afforded the product as a white solid, which was re-dissolved in diethyl ether (10 mL) and filtered to remove a small amount of a white insoluble impurity (presumably LiCl). After the fast addition of pentane (60 mL), the resulting white solid was isolated by filtration and dried under vacuum: yield 3.22 g (38 %). ^{1}H NMR (400 MHz, CDCl$_3$, T = 298 K, δ(ppm)): 3.95 (q, ^3J = 7.1 Hz, 8 H, CH$_2$), 1.36 (t, ^3J = 7.1 Hz, 12 H, CH$_3$). ^{19}F NMR (376 MHz, CDCl$_3$, T = 298 K, δ(ppm)): -133.0 (d, $J_{F\text{-}F}$ = 10.1 Hz, *o*-F), -166.9 (t, $J_{F\text{-}F}$ = 20.4 Hz, *p*-F), -162.7 (virt. t, $J_{F\text{-}F}$ ≈ 18.1 Hz, *m*-F). ^{11}B NMR (128 MHz, CDCl$_3$, T = 298 K, δ(ppm)): -13.62. Anal. Calcd for C$_{32}$H$_{21}$BF$_{20}$O$_2$: C, 46.40; H, 2.56. Found: C, 45.52; H, 2.44.

[MoO(CH$_3$CN)$_4$(*ax*-CH$_3$CN)][B(C$_6$F$_5$)$_4$]$_2$. To [Mo(CO)$_3$(CH$_3$CN)$_3$] (69 mg, 0.23 mmol), dissolved in acetonitrile (10 mL) a solution of 2.4 equiv. [H(OEt$_2$)$_2$][B(C$_6$F$_5$)$_4$] (450 mg, 0.54 mmol) in acetonitrile (5 mL) was added drop-wise. The orange solution was stirred over night in air. During this time the solution changes color to dark green. After filtration, the solvent was removed *in vacuo*. The crude product was washed several times with dry toluene to remove residues of un-reacted [H(OEt$_2$)$_2$][B(C$_6$F$_5$)$_4$]. After removing the solvent *in vacuo*, the product was dissolved in ca. 2 mL dry dichloromethane, overlaid with dry *n*-

pentane and kept in the dark at -35 °C for re-crystallization. $[MoO(CH_3CN)_{4/5}][B(C_6F_5)_4]_2$ was isolated as a light green solid. Yield: 0.27 g (71 %). ^{1}H-NMR (400 MHz, CD_3CN, 298 K, δ(ppm)): 2.79 (s, 1H), 2.65 (s, 4H); ^{13}C-NMR (100 MHz, CD_3CN, 298 K, δ(ppm)): 148.9 (d, J(CF) = 238 Hz, C_{ortho}), 139.2 (d, J(CF) = 243 Hz, C_{para}), 137,2 (d, J(CF) = 241 Hz, C_{meta}), ~124 (br, C_{ipso}), 117 (s, CN), 1.4 (s, CH_3); ^{95}Mo-NMR (26 MHz, CD_3CN, 298 K, δ(ppm)): -116.2 (s). TGA: 91.8 % weight loss between 121 °C (T_{onset}) and 900 °C leaving a black residue. Selected MIR (Nujol, cm^{-1}): v_{CN} 2328 (w), 2314 (m), 2297 (w), 2287 (m). Elemental analysis calcd (%) for $C_{56}H_{12}B_2F_{40}MoN_4O$: C 41.16, H 0.74, N 3.43; found: C 41.30, H 1.33, N 3.15.

$[MoO(C_6H_5CN)_4][B(C_6F_5)_4]_2$. $[MoO(CH_3CN)_{4/5}][B(C_6F_5)_4]_2$ (50 mg, 0.03 mmol) was dissolved in 3 mL benzonitrile. The solution was concentrated to about 0.5 mL *in vacuo* and the procedure was repeated several times to ensure complete removal of acetonitrile. The remaining solution was diluted in carbon tetrachloride (30 mL) forming a suspension. Cyclohexane (10 mL) was added to complete precipitation. After filtration, the crude product was washed two times with cyclohexane (10 mL), dissolved in dichloromethane (2 mL) and re-crystallized by overlaying with *n*-hexane at -35 °C. The desired product was obtained as a light green solid. The yield was quantitative (55 mg). ^{1}H-NMR (400 MHz, CD_2Cl_2, 298 K, δ(ppm)): 7.77 (2H, d, $^3J_{HH}$= 4.9 Hz, ortho-H); 7.61-7.59 (3H , m, meta-H, para-H). TGA: 82.7 % weight loss between 155 °C (T_{onset}) and 900 °C leaving a black residue. Selected MIR (Nujol, cm^{-1}): v_{CN} 2248 (m). Elemental analysis calcd (%) for $C_{76}H_{20}B_2F_{40}MoN_4O$: C 48.49, H 1.07, N 2.98; found: C 49.02, H 1.50, N 2.90.

4.3 Single-crystal X-ray structure determination of [MoO(CH₃CN)₄/₅][B(C₆F₅)₄]₂

Crystal data and details of the structure determination: formula: $[(C_{10}H_{15}MoN_5O)^{2+}]$, $2[(C_{24}BF_{20})^-]$, $3(CH_2Cl_2)$; M_r=1930.09; crystal color and shape: colorless fragment, crystal dimensions=0.30×0.41×0.56 mm; crystal system: monoclinic; space group $P2_1/c$ (no. 14); a=13.235(1), b=35.281(4), c=16.673(2) Å; β=109.861(2)°; V=7322.3(13) Å³; Z=4; μ (Mo$_{K\alpha}$)=0.546 mm⁻¹; ρ_{calcd}=1.751 gcm⁻³; Θ range=6.93–25.38; data collected: 30215; independent data $[I_o>2\sigma(I_o)/\text{all data}/R_{int}]$: 9473/10526/0.031; data/restraints/parameters: 10526/0/1073; $R1$ $[I_o>2\sigma(I_o)/\text{all data}]$: 0.0515/0.0564; $wR2$ $[I_o>2\sigma(I_o)/\text{all data}]$: 0.1246/0.1270; GOF=1.068; $\Delta\rho_{max/min}$: 0.73/-0.77 e Å⁻³. For more details see the X. Appendix.

4. 4 Polymerization Reactions

The polymerization reactions were carried out in pressure tubes in a glove box. Each tube was filled with dried (over molecular sieves) dichloromethane (20 mL), the pre-calculated amounts of complex and a magnetic stirring bar. The temperature of the tubes was kept constantly at -25 °C before the addition of the monomer. A pre-condensed amount of isobutene was then added and the pressure tube was sealed and removed from the glove box. The polymerization was preformed in a water bath, the temperature maintained at 30 °C. The polymerization reaction was quenched by addition of methanol (5 mL). The product obtained was passed through alumina to remove traces of the complexes. The solvent was removed *in vacuo* to afford the purified product.

References

[1]   A. K. Hijazi, A. A. Hmaideen, S. Syukri, N. Radhakrishnan, E. Herdtweck, B. Voit, F. E. Kühn, *Eur. J. Inorg. Chem.* **2008**, *18*, 2892.

[2]   a) O. Nuyken, M. Vierle, F. E. Kühn, Y. Zhang, *Macromol. Symp.* **2006**, *236*, 69; b) M. Vierle, Y. Zhang, E. Herdtweck, M. Bohnenpoll, O. Nuyken, F. E. Kühn, *Angew. Chem. Int. Ed.* **2003**, *42*, 1307; c) M. Vierle, Y. Zhang, A. M. Santos, K. Köhler, C. Haeßner, E. Herdtweck, M. Bohnenpoll, O. Nuyken, F. E. Kühn, *Chem. Eur. J.* **2004**, *10*, 6323.

[3]   a) Y. Li, L. T. Voon, H. Y. Yeong, A. K. Hijazi, N. Radhakrishnan, K. Köhler, B. Voit, O. Nuyken, F. E. Kühn, *Chem. Eur. J.* **2008**, *14*, 7997; b) A. K. Hijazi, H. Y. Yeong, Y. Zhang, E. Herdtweck, O. Nuyken, F. E. Kühn, *Macromol. Rapid Commun.* **2007**, *28*, 670.

[4]   a) A. K. Hijazi, N. Radhakrishnan, K. R. Jain, E. Herdtweck, O. Nuyken, H.-M. Walter, P. Hanefeld, B. Voit, F. E. Kühn, *Angew. Chem. Int. Ed.* **2007**, *46*, 7290; b) B. E. Diebl, Y. Li, M. Cokoja, F. E. Kühn, N. Radhakrishnan, S. Zschoche, H. Komber, H. Y. Yeong, B. Voit, O. Nuyken, P. Hanefeld, H.-M. Walter, *J. Polym. Sci. A: Polym. Chem.* **2010**, *in press.*

[5]   S. F. Rach, F. E. Kühn, *Chem. Rev.* **2009**, *109*, 2061.

[6]   P. Jutzi, C. Müller, A. Stammler, H.-G. Stammler, *Organometallics* **2000**, *19*, 1442.

[7]   B. S. McGilligan, T. C. Wright, G. Wilkinson, *J. Chem. Soc. Dalton Trans.* **1988**, 1737.

[8]   J. H. Matonic, S.-J. Chen, L. E. Pence, K. R. Dunbar, *Polyhedron* **1992**, *11*, 541.

[9]   a) F. A. Cotton, K. J. Wiesinger, *Inorg. Chem.* **1991**, *30*, 871; b) J. M. Mayer, E. H. Abbott, *Inorg. Chem.* **1983**, *22*, 2774.

[10]   a) R. A. Walton, *Rev. Chem. Soc* **1965**, *19*, 126; b) G. Socrates, *Infrared and Raman Characteristic Group Frequencies: Tables and Charts*, 3 ed., John Wiley & Sons Inc.,

2004; c) K. Nakamoto, *Infrared and Raman Spectra of Inorganic and Coordination Compounds Part A*, Wiley, **2009**.

[11]   S. Clamp, N. G. Connelly, G. E. Taylor, T. S. Louttit, *J. Chem. Soc. Dalton Trans.* **1980**, 2162.

[12]   W. E. Buschmann, J. S. Miller, *Chem. Eur. J.* **1998**, *4*, 1731.

[13]   a) F. E. Kühn, M. Groarke, E. Bencze, E. Herdtweck, A. Prazeres, A. M. Santos, M. J. Calhorda, C. C. Romao, I. S. Goncalves, A. D. Lopes, M. Pillinger, *Chem.-Eur. J.* **2002**, *8*, 2370; b) F. E. Kühn, A. M. Santos, M. Abrantes, *Chem. Rev.* **2006**, *106*, 2455.

[14]   D. P. Tate, W. R. Knipple, J. M. Augl, *Inorg. Chem.* **1962**, *1*, 433.

VII. Summary

Nitrile ligated transition metal complexes bearing polyfluorinated tetra(aryl)borates as counter anions are highly active mediators for isobutene polymerization.[1] Nevertheless, the methods by which these compounds are synthesized are too inefficient for widespread use in applied research and industry. Additionally, the exact reaction mechanism, in particular the initiating step, is not proven beyond doubt.

Accordingly, the focus of this thesis was set on three different domains: a) the development of improved synthetic pathways for known and novel nitrile ligated transition metal complexes with weakly coordinating anions (WCAs), b) the generation of a concept for the immobilization of these complexes which keeps them active for isobutene polymerization and c) shedding light on the mechanism of the polymerization of isobutene for the design of potentially more active mediators.

Improved synthesis of known transition metal complexes

Easy synthetic routes for the preparation of several test compounds were designed, with the main focus being on Zn(II)- and Cu(I)- or Cu(II) complexes.

For instance, procedures for the preparation of $[Cu(C_6H_5CN)_5][B(C_6F_5)_4]_2$ and $[Zn(CH_3CN)_{4/6}][B(C_6F_5)_4]_2$ have been developed, achieving significant improvements with respect to synthetic efficiency and costs compared to the established procedures. Additionally, the synthesis of the oxonium salt $[H(Et_2O)_2][B(C_6F_5)_4]$, which was used as starting material, was enhanced. The characterization includes X-ray crystal structures of both complexes.
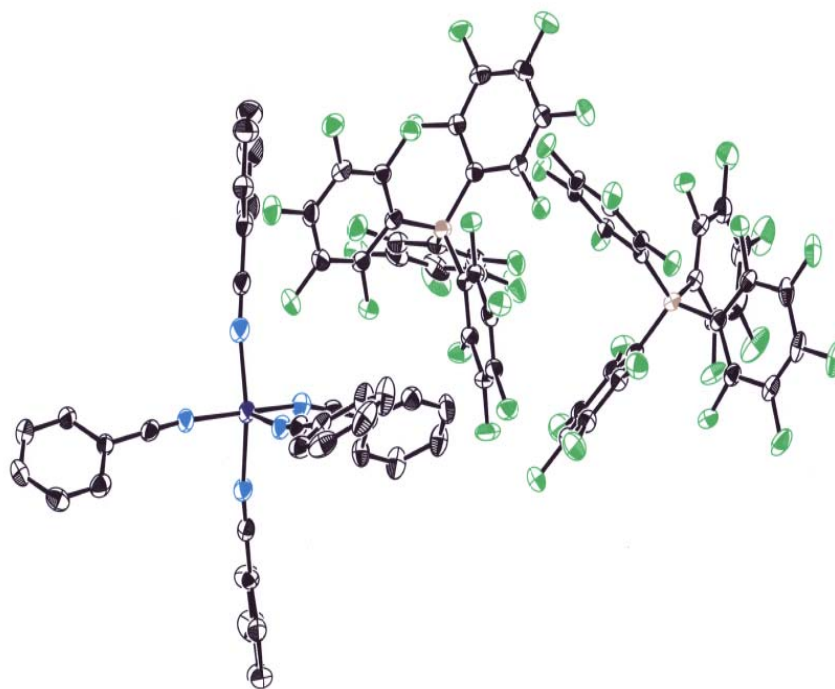
Figure 7.1. ORTEP style depiction of $[Cu(C_6H_5CN)_5][B(C_6F_5)_4]_2$ in the solid state. Thermal ellipsoids are drawn at the 50 % probability level.

Synthesis of new Mo(IV) complexes

The two novel complexes $[MoO(CH_3CN)_5][B(C_6F_5)_4]_2$ and $[MoO(C_6H_5CN)_4][B(C_6F_5)_4]_2$ were prepared more conveniently and cost efficiently, compared to the analogous $[MoCl(CH_3CN)_5][B(C_6F_5)_4]_2$ (see Scheme 7.1).[1b] Furthermore, they were successfully tested as mediators for isobutene polymerization. The full characterization comprises X-ray structure analysis, [95]Mo-NMR- and IR spectroscopy, as well as TG MS spectrometry.
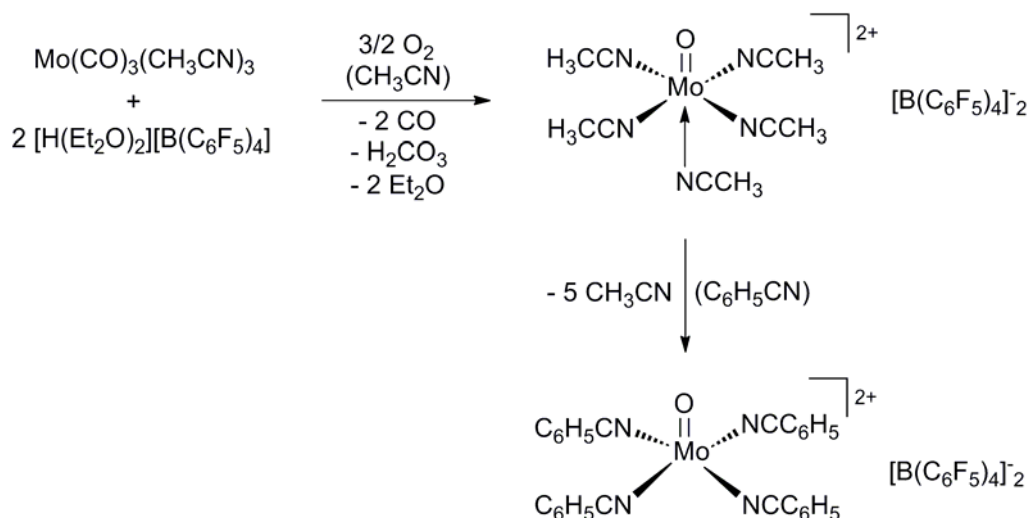
Scheme 7.1. Schematic representation of the route for the synthesis of $[MoO(CH_3CN)_5][B(C_6F_5)_4]_2$ (above) and $[MoO(C_6H_5CN)_4][B(C_6F_5)_4]_2$ (below).

134

Concept for the immobilization of mediators for isobutene polymerization

$[H_2(Et_2O)_4][(C_6F_5)_3B-C_6F_4-B(C_6F_5)_3]$ and $[H_2(Et_2O)_3][(C_6F_5)_3B-(C_6F_4)_2-B(C_6F_5)_3]$ (see Figure 7.2) were synthesized as low molecular weight WCA based model precursors. After a subsequent reaction with appropriate metal salts, the two polyfluorinated oxonium bisborates could be used as easy analyzable test systems for the heterogenization of nitrile ligated transition metal complexes.
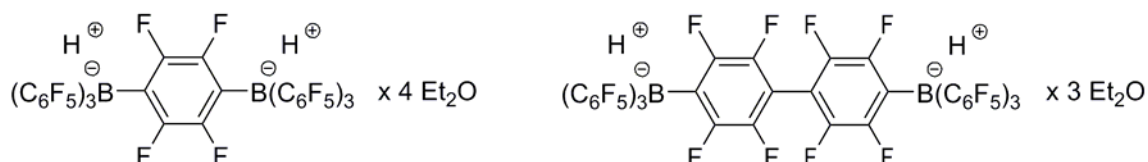

Figure 7.2. Schematic structures of the two polyfluorinated oxonium bisborates.

Mechanistic studies

Alkali salts with $[B(C_6F_5)_4]^-$ as counter anion, as well as acetonitrile ligated Cu(I)-complexes with $[B(C_6F_5)_4]^-$ and $[BF_4]^-$ were shown to be inactive in isobutene polymerization. $[Cu(II)(CH_3CN)_4][BF_4]_2$ and $[Zn(II)(CH_3CN)_6][BF_4]_2$, however, possess at least some activity, with slight differences regarding the reaction product. The influence of the oxidation state, the nature of the metal ion and the coordination ability of the anion on the polymerization reaction could be deduced from the obtained results.

X-ray crystallography of the reaction products, as well as ^{1}H-NMR spectroscopic examinations of (deutero)methylene chloride solutions of $[Zn(CH_3CN)_5][B(C_6F_5)_4]_2$ or $[Cu(C_6H_5CN)_5][B(C_6F_5)_4]_2$ respectively with 2,6-di-*tert*-butylpyridine (DTBP), a supposed proton trap for isobutene polymerization, indicate a reaction between these complexes and DTBP, leading to the formation of 2,6-di-*tert*-butylpyridinium tetrakis(pentafluorophenyl)borate (see Figure 7.3).
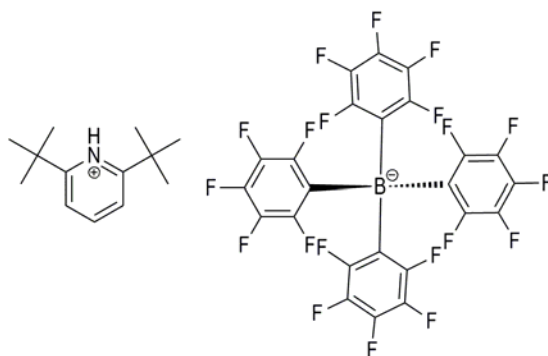
Figure 7.3. Schematic structure of the protonated DTBP with the $[B(C_6F_5)_4]^-$ anion.

Close examination of literature data for radical or radical cationic polymerization of isobutene and comparison with information obtained for this polymerization, employing nitrile ligated transition metal complexes bearing polyfluorinated phenyl borate anions showed interesting parallels.

Thus, test experiments including EPR-, NMR- and UV/Vis spectroscopy as well as MALDI-TOF- and ESI-MS spectrometry using 2,4,4-trimethyl-pent-1-ene (diisobutene) as non-polymerizable model monomer with the mediators $[Cu(C_6H_5CN)_5][B(C_6F_5)_4]_2$ and $[(C_6H_5)_3C][B(C_6F_5)_4]$ were designed and conducted.

EPR spectra of organic radicals were obtained when reacting $[Cu(C_6H_5CN)_5][B(C_6F_5)_4]_2$ with toluene or the toluene (alternatively methylene chloride) solution of the complex with diisobutene (see Figure 7.4). Addition of diisobutene to a solution of $[(C_6H_5)_3C][B(C_6F_5)_4]$ in toluene leads to radical formation, as well.
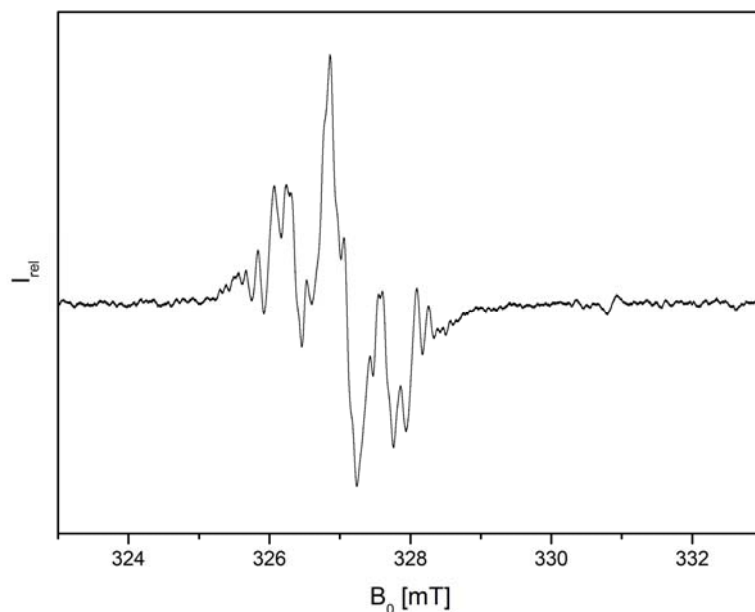
Figure 7.4. EPR spectrum of the reaction of $[Cu(C_6H_5CN)_5][B(C_6F_5)_4]_2$ with toluene and diisobutene, heated to 30 °C.

Due to information derived from ^{11}B- and ^{19}F-NMR as well as ESI-MS spectra, anion decay is excluded during radical formation.

Evidence for quantitative involvement of the Cu(II) complex can be obtained from EPR- and UV-Vis spectroscopy. In all cases the bands originating from the original complex disappear after toluene or diisobutene addition (see Figure 7.5)
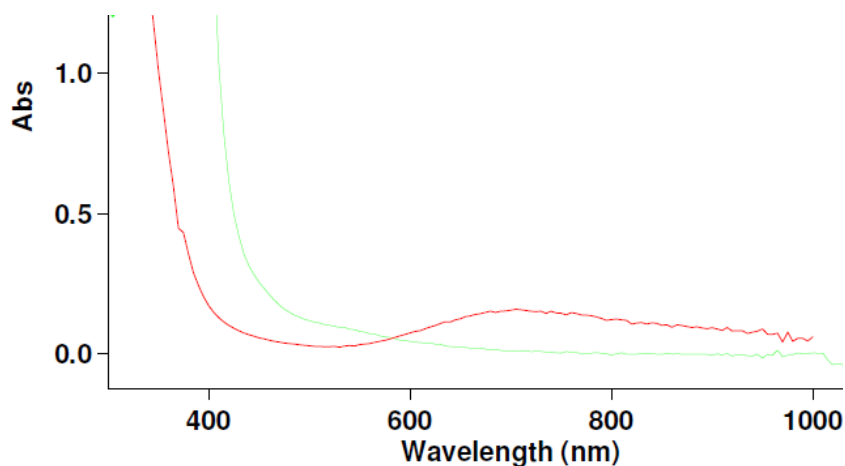
Figure 7.5. Superimposed UV/Vis spectra of the solution of $[Cu(C_6H_5CN)_5][B(C_6F_5)_4]_2$ in methylene chloride before (red) and after addition of diisobutene (green).

Additionally, UV/Vis- and ^{1}H-/^{13}C-NMR spectra point to the formation of charge transfer complexes (see Scheme 7.2), with toluene or diisobutene coordinating to the Cu(II) ion.
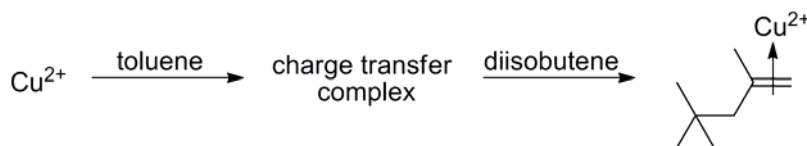
Scheme 7.2. Proposed formation of charge transfer complexes of $[Cu(C_6H_5CN)_5][B(C_6F_5)_4]_2$ with toluene and diisobutene; the anions are omitted.

Combination of the obtained results indicates an equilibrium between charge transfer complexes and a radical species (see Scheme 7.3).

In analogy, this equilibrium between a (dormant) metal coordinated species and an active radical could be the reason for the observed controlled polymerization of isobutene under certain conditions (low PDIs). However, mechanistic studies with isobutene instead of diisobutene would be necessary to prove this theory.
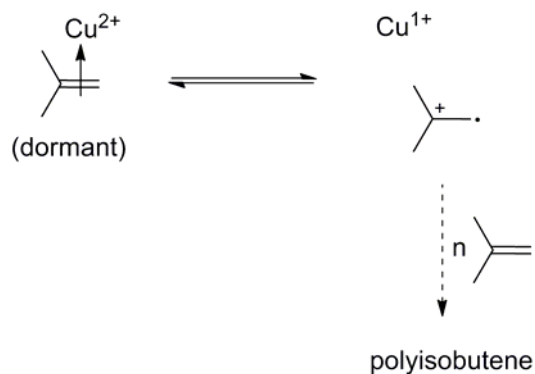
Scheme 7.3. Possible initiation of isobutene polymerization using $[Cu(C_6H_5CN)_5][B(C_6F_5)_4]_2$ as mediator.

References

[1]   a) Y. Li, L. T. Voon, H. Y. Yeong, A. K. Hijazi, N. Radhakrishnan, K. Köhler, B. Voit, O. Nuyken, F. E. Kühn, *Chem. Eur. J.* 2008, *14*, 7997; b) A. K. Hijazi, N. Radhakrishnan, K. R. Jain, E. Herdtweck, O. Nuyken, H.-M. Walter, P. Hanefeld, B. Voit, F. E. Kühn, *Angew. Chem. Int. Ed.* 2007, *46*, 7290.

VIII. Zusammenfassung

Nitril koordinierte Übergangsmetallkomplexe mit polyfluorierten Tetra(aryl)boraten als Gegenionen, sind hochreaktive Mediatoren für die Isobutenpolymerisation.[1] Leider sind die Methoden zur Herstellung dieser Verbindungen für eine breite Verwendung in angewandter Forschung oder Industrie bislang zu ineffizient. Zudem ist der genaue Reaktionsmechanismus, und hier insbesondere der Initiierungsschritt, bislang noch nicht zweifelsfrei belegt.

Daher wurde der Schwerpunkt dieser Doktorarbeit auf drei verschiedene Bereiche gelegt:

a) Das Entwickeln von verbesserten Syntheserouten für bekannte und neuartige Nitril stabilisierte Übergangsmetallkomplexe mit schwach koordinierenden Anionen (WCAs).

b) Das Erstellen eines Konzepts zur Immobilisierung dieser Komplexe, welche deren Aktivität in der Isobutenpolymerisation erhält.

c) Das Untersuchen des Mechanismus der Polymerisation von Isobuten um das effektive Design von neuen Mediatoren zu ermöglichen.

Verbesserte Synthese von bekannten Übergangsmetallkomplexen

Für die Herstellung von verschiedenen Test-Verbindungen wurden einfache Syntheserouten entwickelt, wobei das Hauptaugenmerk auf Zn(II)- und Cu(I)- oder Cu(II)-Komplexen lag.

So wurden Verfahren für die Darstellung von $[Cu(C_6H_5CN)_5][B(C_6F_5)_4]_2$ und $[Zn(CH_3CN)_5][B(C_6F_5)_4]_2$ erarbeitet, durch welche im Vergleich zu den bestehenden Methoden signifikante Verbesserungen bezüglich synthetischer Effizienz und Kosten erzielt werden konnten. Zusätzlich wurde die Synthese von dem als Ausgangsmaterial verwendeten Oxoniumsalz $[H(Et_2O)_2][B(C_6F_5)_4]$ optimiert. Die Charakterisierung beinhaltet Röntgenkristallstrukturen beider Komplexe.
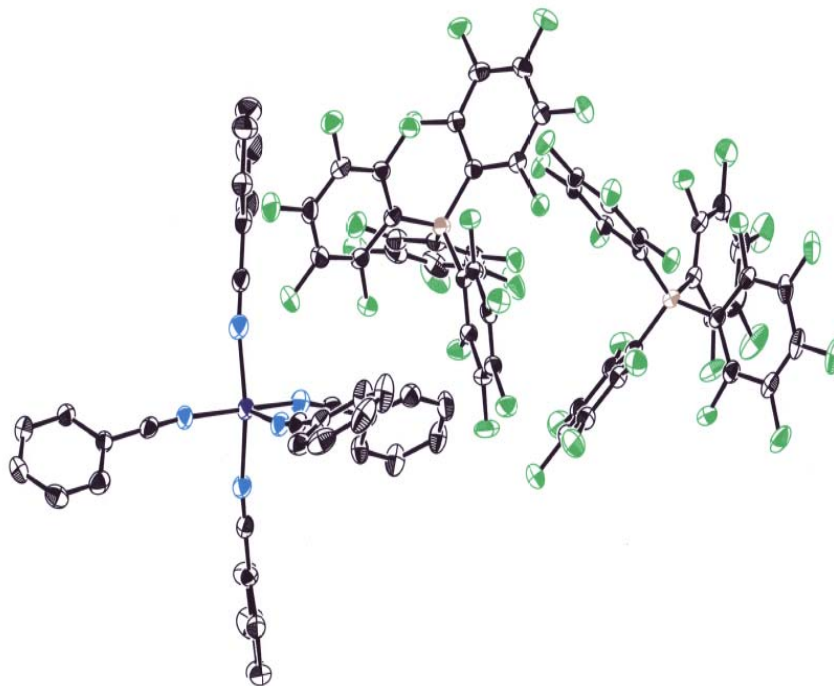
Abbildung 8.1. ORTEP-Darstellung der Molekülstruktur von $[Cu(C_6H_5CN)_5][B(C_6F_5)_4]_2$ im Festkörper. Die thermischen Schwingungsellipsoide entsprechen einer Aufenthaltswahrscheinlichkeit von 50 %.

Synthese neuer Mo(IV) Komplexe

Die zwei neuen Komplexe $[MoO(CH_3CN)_5][B(C_6F_5)_4]_2$ und $[MoO(C_6H_5CN)_4][B(C_6F_5)_4]_2$ wurden im Vergleich zu dem analogen $[MoCl(CH_3CN)_5][B(C_6F_5)_4]_2$ auf einfachere und kostengünstigere Art und Weise hergestellt (siehe Schema 8.1).[1b] Des weiteren wurden sie erfolgreich als Mediatoren für die Isobutenpolymerisation getestet. Die vollständige Charakterisierung beinhaltet Röntgenstrukturanalyse, [95]Mo-NMR- und IR spektroskopische, sowie TG MS spektrometrische Untersuchungen.
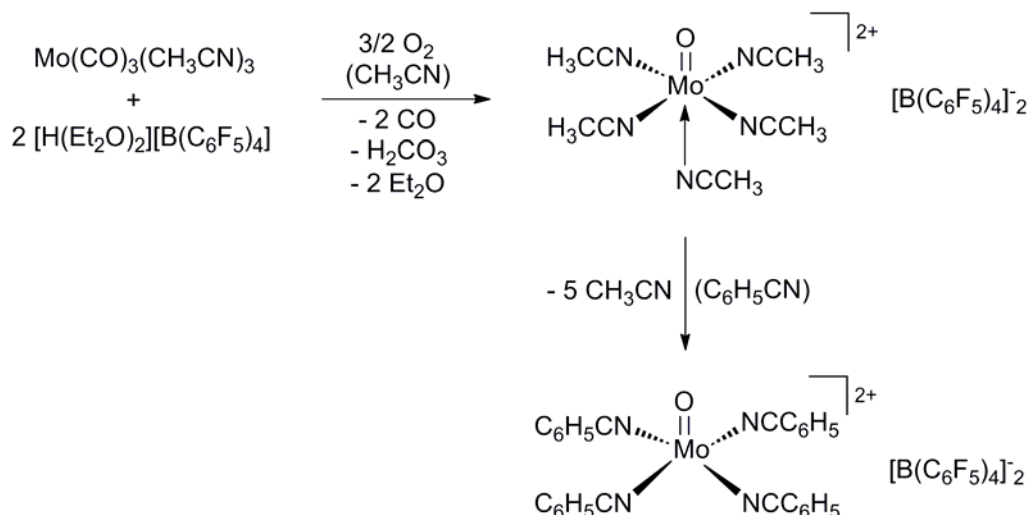
Schema 8.1. Schematische Darstellung der Syntheseroute für [MoO(CH$_3$CN)$_5$][B(C$_6$F$_5$)$_4$]$_2$ (oben) und [MoO(C$_6$H$_5$CN)$_4$][B(C$_6$F$_5$)$_4$]$_2$ (unten).

Konzept zur Immobilisierung von Mediatoren für die Isobutenpolymerisation

Die Oxoniumsalze [H$_2$(Et$_2$O)$_4$][(C$_6$F$_5$)$_3$B-C$_6$F$_4$-B(C$_6$F$_5$)$_3$] und [H$_2$(Et$_2$O)$_3$][(C$_6$F$_5$)$_3$B-(C$_6$F$_4$)$_2$-B(C$_6$F$_5$)$_3$] (siehe Abbildung 8.2) wurden als niedermolekulare WCA basierte Modell-Vorstufen hergestellt, welche nach der Umsetzung mit geeigneten Metallsalzen als einfach analysierbare Test-Systeme für die Heterogenisierung von Nitril koordinierten Übergangsmetallkomplexen eingesetzt werden könnten.
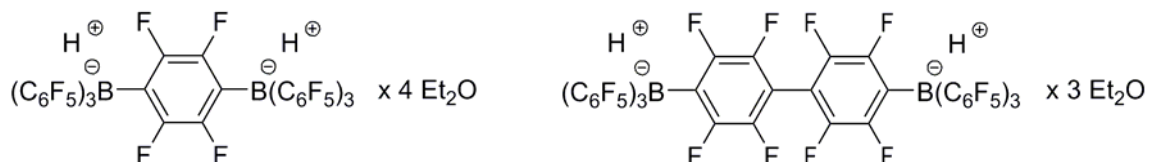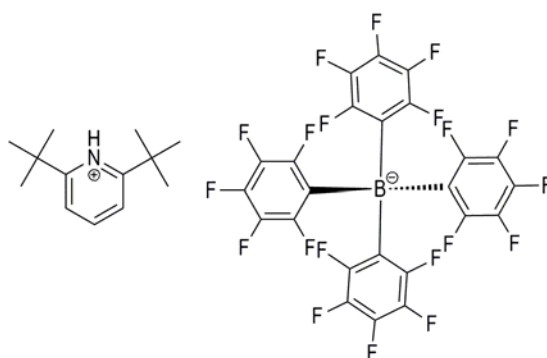

Abbildung 8.2. Schematische Strukturen der beiden polyfluorierten Oxoniumbisborate.

Mechanismusstudien

Es zeigte sich, dass Alkaliboratsalze mit [B(C$_6$F$_5$)$_4$]$^-$ als Gegenion, sowie Acetonitril koordinierte Cu(I)-Komplexe mit [B(C$_6$F$_5$)$_4$]$^-$ und [BF$_4$]$^-$ keine Aktivität als Mediatoren in der Polymerisation von Isobuten haben. [Cu(II)(CH$_3$CN)$_4$][BF$_4$]$_2$ und [Zn(II)(CH$_3$CN)$_6$][BF$_4$]$_2$, hingegen waren zumindest schwach aktiv, wobei die Reaktionsprodukte Unterschiede im Polymerisationsgrad aufwiesen. An Hand der erhaltenen Ergebnisse konnte der Einfluss der formalen Oxidationsstufe, der Art des Metallions wie

auch der Koordinationsfähigkeit des Anions auf die Polymerisationsreaktion abgeleitet werden.

Röntgenkristallografische und ^{1}H-NMR spektroskopische Untersuchungen von [Zn(CH$_3$CN)$_5$][B(C$_6$F$_5$)$_4$]$_2$ oder [Cu(C$_6$H$_5$CN)$_5$][B(C$_6$F$_5$)$_4$]$_2$, welche jeweils in (Deutero)methylenchlorid gelöst und mit 2,6-Di-*tert*-butylpyridin (DTBP), einer vermeintlichen Protonenfalle für die Isobutenpolymerisation, versetzt wurden, weisen auf eine Reaktion zwischen den Komplexen und DTBP hin, welche zur Bildung von 2,6-Di-*tert*-butylpyridinium tetrakis(pentafluorophenyl)borat führt (siehe Abbildung 8.3).


Abbildung 8.3. Schematische Struktur des protonierten DTBP mit [B(C$_6$F$_5$)$_4$]$^-$ als Anion.

Eine eingehende Prüfung der Literatur bekannten Daten für die radikalische oder Radikal-kationische Polymerisation von Isobuten und das Vergleichen mit Informationen, welche für diese Polymerisation unter Verwendung von Nitril koordinierten Übergangsmetallkomplexen mit polyfluorierten Phenylborat-Anionen erhalten wurden zeigen interessante Parallelen.

Deshalb wurden Testexperimente, darunter EPR-, UV/Vis- und NMR-Spektroskopie, sowie MALDI-TOF- und ESI-MS-Spektrometrie unter Verwendung von 2,4,4-Trimethyl-pent-1-en (Diisobuten) als nicht-polymerisierbares Modell-Monomer mit den Mediatoren [Cu(C$_6$H$_5$CN)$_5$][B(C$_6$F$_5$)$_4$]$_2$ und [(C$_6$H$_5$)$_3$C][B(C$_6$F$_5$)$_4$] entwickelt und durchgeführt.

Bei der Reaktion von [Cu(C$_6$H$_5$CN)$_5$][B(C$_6$F$_5$)$_4$]$_2$ mit Toluol oder dem Versetzen von Toluol- bzw. Methylenchlorid Lösungen mit Diisobuten wurden EPR Spektren von organischen Radikalen erhalten (siehe Abbildung 8.4). Analog zeigte sich, dass die Zugabe von Diisobuten zu einer Toluol-Lösung von [(C$_6$H$_5$)$_3$C][B(C$_6$F$_5$)$_4$] ebenfalls zu einer Radikalbildung führt.
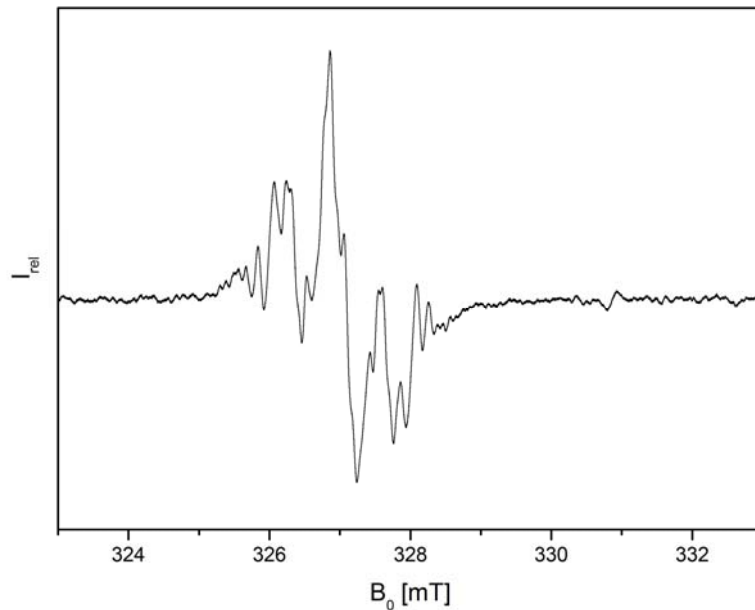
Abbildung 8.4. EPR Spektrum der Reaktion von $[Cu(C_6H_5CN)_5][B(C_6F_5)_4]_2$ mit Toluol und Diisobuten, erhitzt auf 30 °C.

Auf Grund der Informationen, welche aus ^{11}B- und ^{19}F-NMR sowie ESI-MS Spektren erhalten wurden, kann ein Zerfall der Anionen im Laufe der Radikalbildung ausgeschlossen werden. Der Beleg für eine quantitative Beteiligung des Cu(II) an der Reaktion kann durch EPR- und UV-Vis Spektroskopie erhalten werden. In allen Fällen verschwinden die Banden, welche von dem ursprünglichen Komplex stammen, nach Zugabe von Toluol oder Diisobuten (siehe Abbildung 8.5).
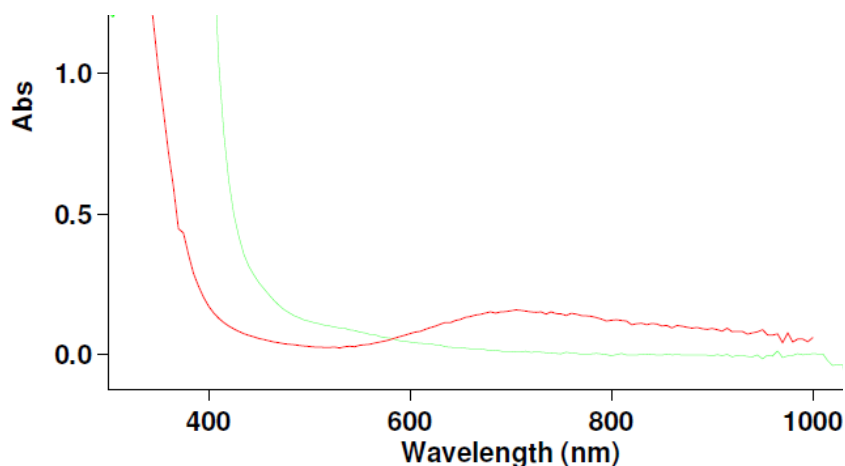
Abbildung 8.5. Übereinander gelagerte UV/Vis Spektren der Lösung von $[Cu(C_6H_5CN)_5][B(C_6F_5)_4]_2$ in Methylenchlorid vor (rot) und nach dem Versetzen mit Diisobuten (grün).

Zudem weisen UV/Vis- und ^{1}H-/^{13}C-NMR Spektren auf die Bildung eines Charge Transfer Komplexes hin (siehe Abbildung 8.2) in welchem das Cu(II) ion an Toluol oder Diisobuten koordiniert ist.
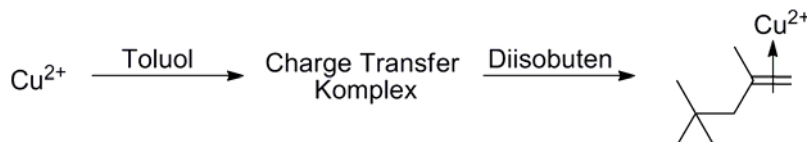
Schema 8.2. Vorgeschlagene Bildung eines Charge Transfer Komplexes von [Cu(C$_6$H$_5$CN)$_5$][B(C$_6$F$_5$)$_4$]$_2$ mit Toluol und Diisobuten; Anionen wurden weggelassen.

Die Kombination der erhaltenen Resultate weist auf ein Gleichgewicht zwischen dem zuvor beschriebenen Charge Transfer Komplex und einer radikalischen Spezies hin (siehe Schema 8.3).

In Analogie könnte dieses Gleichgewicht zwischen einer (schlafenden) Metall koordinierten Spezies und eines aktiven Radikals der Grund für die, unter bestimmten Umständen beobachtete, kontrollierte Polymerisationsreaktion von Isobuten sein (ersichtlich an teilweise niedrigen Polydispersitätsindices). Allerdings sind zur Überprüfung dieser Annahme detaillierte Mechanismusstudien mit Isobuten an Stelle des Modellsystems Diisobuten nötig.
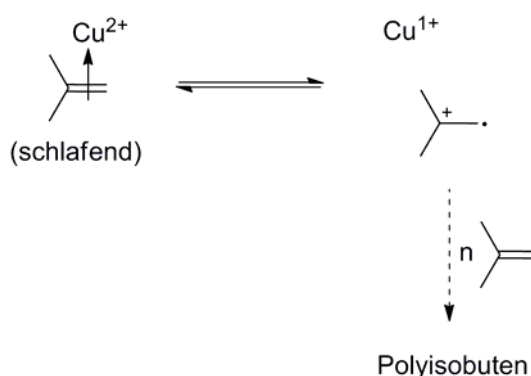
Schema 8.3. Mögliche Initiierung der Isobutenpolymerisation unter Verwendung von [Cu(C$_6$H$_5$CN)$_5$][B(C$_6$F$_5$)$_4$]$_2$ als Mediator.

Literatur

[1]   a) Y. Li, L. T. Voon, H. Y. Yeong, A. K. Hijazi, N. Radhakrishnan, K. Köhler, B. Voit, O. Nuyken, F. E. Kühn, *Chem. Eur. J.* 2008, *14*, 7997.

b) A. K. Hijazi, N. Radhakrishnan, K. R. Jain, E. Herdtweck, O. Nuyken, H.-M. Walter, P. Hanefeld, B. Voit, F. E. Kühn, *Angew. Chem. Int. Ed.* 2007, *46*, 7290.

IX. Outlook

Industrial application of nitrile ligated transition metal complexes with weakly coordinating anions (WCAs) would be an interesting prospect for the polymerization of isobutene. Ideally, mediators used therefore should be able to be recycled, what could be realized through immobilization. However, it has to be ascertained if the complexes in regard can be regenerated at all after isobutene polymerization, as decomposition could make further efforts towards the immobilization of these compounds futile. Thus the obtained experimental data suggest additional mechanistic studies to get insights into the limitations and possibilities of this reaction system.

A search for evidence of complex decomposition in form of radical reactions was undertaken during the course of this thesis. Indeed, the formation of radical species when adding toluene or toluene and diisobutene respectively to $[Cu(C_6H_5CN)_4][B(C_6F_5)_4]_2$ or $[(C_6H_5)_3C][B(C_6F_5)_4]$ was tested and could be ascertained. However, due to the complexity of the system it is still unknown what kind of radicals are formed, and in what regard they influence the isobutene polymerization. The implementation of the following experiments may lead to new insights on these open questions.

1. NMR studies of paramagnetic substances

One handicap of herein reported ^{1}H-NMR spectra, which were recorded in the presence of paramagnetic substances (see Chapter III. 4.8) is overlapping of broad and narrow signals. These are hardly separable and thus can not clearly be correlated to their corresponding protons. Several things could be done in future experiments in order to obtain NMR spectra with better resolution. For example, the appearance of broad lines might be avoided by special pulse sequences.[1]

Another move towards the correct identification of signals in ^{1}H-NMR spectra could be made using deuterated benzonitrile or toluene instead of their protonated congeners. Thus, similar

observations concerning the formation of radical species could most likely be made, while the signals of the deuterated reagents should not appear in the spectra.

In addition, ^{2}H-NMR spectroscopy is a very useful alternative for measurements in presence of paramagnetic compounds. Signal shifts of deuterated molecules are virtually unchanged while the signal half width is decreased by a factor up to $[\gamma(^1H)/\gamma(^2H)]^2 = 42.6$ (γ = nuclear gyromagnetic ratio) when compared with their protonated congeners. Therefore, ^{2}H-NMR spectroscopy can be conducted for precise measurements of hyperfine coupling constants of signals that may not even be detected in ^{1}H-NMR spectra at all. [1]

2. Trapping of radical species

A further approach to identify the formed radical species would be their trapping *via* radical coupling[2] (with *e.g.* Bu$_3$SnH) or isolation of specific recombination products (see Scheme 9.1).[3] Analysis of these could be conducted with, for example, simple NMR spectroscopic measurements. However, the interference of the metal complex could be problematic.
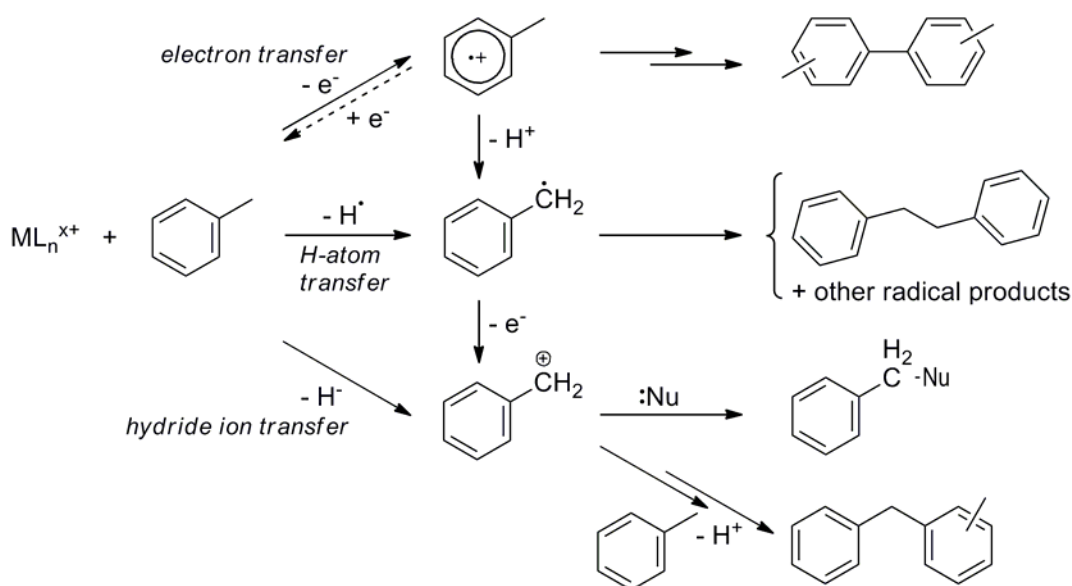
Scheme 9.1. Different pathways in metal-mediated oxidations of toluene (M = metal, L = ligand) and formation of their specific products.[3]

3. Transfer of the model system to isobutene polymerization

Differences between the model and the real system can affect the experimental results adversely and lead to misdirection. Therefore, the parent system containing isobutene instead of diisobutene should be tested for the formation of radicals during the polymerization reaction. However, experiments with, at room temperature gaseous, isobutene are much more difficult to handle. Consecutive *in situ* tests, based on the addition of radical scavengers or proton traps to the reaction mixture could contribute to the clarification of the mechanism.[4] Fullerene C_{60}, a radical scavenger which is known to retard free radical polymerization of methyl methacrylate and styrene could be used in this respect.[5] In both reported cases, the addition of C_{60} to the polymerization mixture led to the formation of polymers containing stable free radicals with molecular weights far lower than those of control samples without C_{60}. The achievement of similar or contrary results with isobutene and the complexes in regard could lead to new answers concerning the reaction mechanism. Another option for a common radical scavenger is oxygen. However, the application of the latter is risky, as it can not only act as radical scavenger in isobutene polymerization[6] but also as co-initiator.[7]

References

[1]   F. H. Köhler, in *Magnetism: Molecules to Materials I: Models and Experiments* (Eds.: J. S. Miller, M. Drillon), Wiley-VCH, Weinheim, **2001**, pp. 379.

[2]   D. G. H. Hetterscheid, J. Kaiser, E. Reijerse, T. P. J. Peters, S. Thewissen, A. N. J. Blok, J. M. M. Smits, R. d. Gelder, B. d. Bruin, *J. Am. Chem. Soc.* **2005**, *127*, 1895.

[3]   J. M. Mayer, A. S. Larsen, J. R. Bryant, K. Wang, M. Lockwood, G. Rice, T.-J. Won, in *Activation and Functionalization of C-H Bonds* (Eds.: K. I. Goldberg, A. S. Goldman), American Chemical Society, Washington, DC, **2004**.

[4]   L. Toman, J. Spěváček, P. Vlček, P. Holler, *J. Am. Chem. Soc.* **2000**, *38*, 1568.

[5]   a) K. Kirkwood, D. Stewart, C. T. Imrie, *J. Polym. Sci. A: Polym. Chem.* **1997**, *35*, 3323; b) D. Stewart, C. T. Imrie, *Chem. Commun.* **1996**, 1383.

[6]   L. Toman, M. Marek, *J. Macromol. Sci., Part A: Pure Appl. Chem.* **1981**, *15*, 1533.

[7]   V. Volkis, H. Mei, R. K. Shoemaker, J. Michl, *J. Am. Chem. Soc.* **2009**, *131*, 3132.

X. Appendix

1. Supplementary data for chapter III

1.1. X-ray crystal data
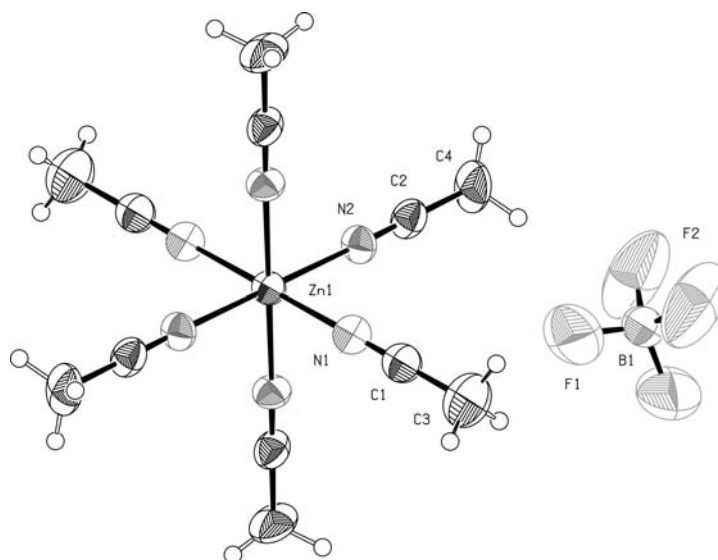
Figure 10.1. ORTEP style depiction of one of the weakly coordinating anions and the dicationic part of [Zn(CH$_3$CN)$_6$][BF$_4$]$_2$ in the solid state. Thermal ellipsoids are drawn at the 50 % probability level.
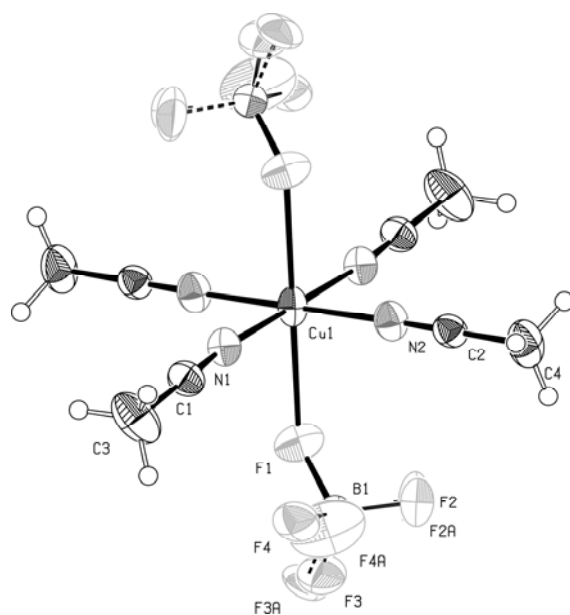
Table 10.1. Crystallographic data, collection parameters and refinement parameters of [Zn(CH$_3$CN)$_6$][BF$_4$]$_2$.

Formula	C$_{12}$H$_{18}$N$_6$Zn, 2(BF$_4$)
Formula weight	485.33
Crystal System	Monoclinic
Space group	C2/m (No. 12)
a, b, c [Å]	12.2358(10) 16.9719(12) 5.7341(5)
α, β, γ [deg]	90 106.071 (3) 90
V [Å^3]	1144.24(16)
Z	2
D (calc) [g/cm^3]	1.409
Mu (MoKa)	1.145
F (000)	488
Crystal Size [mm]	0.51 x 0.56 x 0.58

Temperature [K]	153
Radiation [Å]	MoKa 0.71073
Theta-Min-Max [Deg]	2.1, 25.4
Dataset	-14 : 14; -17 : 20; -6 : 6
Tot., Uniq. Data, R (int)	6493, 1090, 0.047
Observed Data [I > 0.0 σ(I)]	1063
Nref, Npar	1090, 74
R, wR2, S	0.0509, 0.1429, 1.14
w = 1/[\s^2^(Fo^2^)+(0.0905P)^2^+1.7044P]	where P=(Fo^2^+2Fc^2^)/3
Max. and Av. Shift/Error	0.00, 0.00
Flack x	0.002 (5)
Min. and Max. Resd Dens. [e/Ang^3]	-0.55, 0.92

Table 10.2. Selected Bond Lengths and Bond Angles for [Zn(CH$_3$CN)$_6$][BF$_4$]$_2$.

distance [Å]		angle [deg]	
Zn1-N1	2.146 (4)	N1-Zn1-N2	88.03 (11)
Zn1-N2	2.117 (3)	N1-Zn1-N1_b	180.00
Zn1-N1_b	2.146 (4)	N1-Zn1-N2_b	91.97 (11)
Zn1-N2_b	2.117 (3)	N1-Zn1-N2_c	91.97 (11)
Zn1-N2_c	2.117 (3)	N1-Zn1-N2_d	88.03 (11)
Zn1-N2_d	2.117 (3)	N1_b-Zn1-N2	91.97 (11)
		N2-Zn1-N2_b	89.25 (11)
		N2-Zn1-N2_c	180.00
		N2-Zn1-N2_d	90.75 (11)
		N1_b-Zn1-N2_b	88.03 (11)
		N1_b-Zn1-N2_c	88.03 (11)
		N1_b-Zn1-N2_d	91.97 (11)
		N2_b-Zn1-N2_c	90.75 (11)
		N2_b-Zn1-N2_d	180.00
		N2_c-Zn1-N2_d	89.25 (11)

Figure 10.2. ORTEP style depiction of [Cu(CH$_3$CN)$_4$][BF$_4$]$_2$ in the solid state. Thermal ellipsoids are drawn at the 50 % probability level.

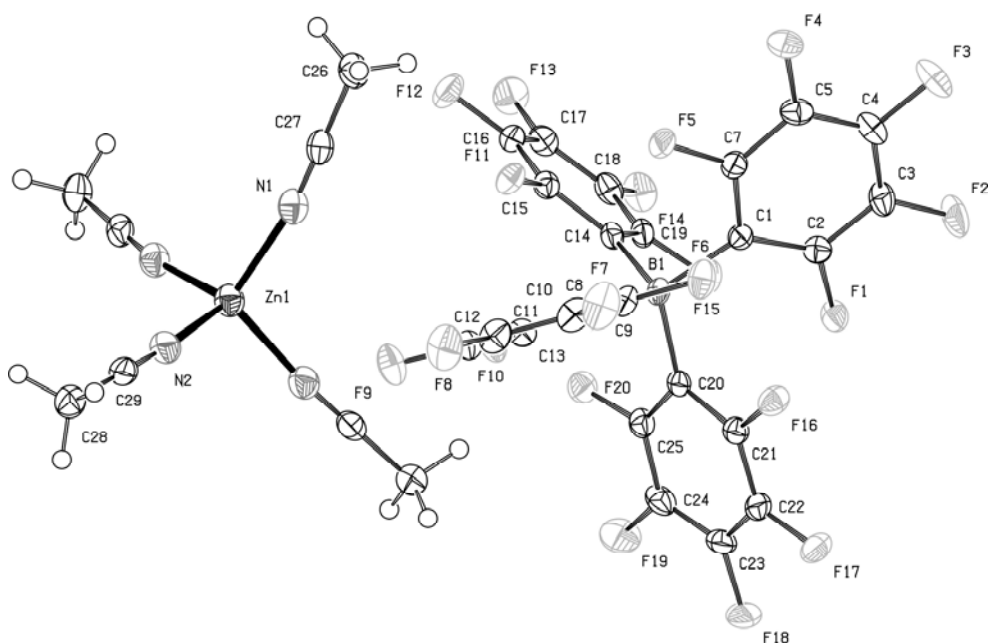**Table 10.3.** Crystallographic data, collection parameters and refinement parameters of [Cu(CH$_3$CN)$_4$][BF$_4$]$_2$.

Formula	C$_8$H$_{12}$B$_2$CuF$_8$N$_4$
Formula weight	401.39
Crystal System	Orthorhombic
Space group	Pbca (No. 61)
a, b, c [Å]	12.7161(5) 10.1577(4) 12.8543(5)
α, β, γ [deg]	1660.34(11)
V [Å^3]	1144.24(16)
Z	4
D (calc) [g/cm^3]	1.606
Mu (MoKa)	1.393
F (000)	796
Temperature [K]	153
Radiation [Å]	MoKa 0.71073
Theta-Min-Max [Deg]	2.1, 25.4
Dataset	-15: 15 ; -12: 12 ; -15: 15
Tot., Uniq. Data, R (int)	59392, 1513, 0.028
Observed Data [I > 0.0 σ(I)]	1365

Nref, Npar	1513, 136
R, wR2, S	0.0238, 0.0692, 1.12
w = 1/[\s^2^(Fo^2^)+(0.304P)^2^+0.676P]	where P=(Fo^2^+2Fc^2^)/3
Max. and Av. Shift/Error	0.00, 0.00
R	0.02
Min. and Max. Resd Dens. [e/Ang^3]	-0.28, 0.23

Table 10.4. Selected Bond Lengths and Bond Angles for [Cu(CH$_3$CN)$_4$][BF$_4$]$_2$.

distance [Å]		angle [deg]	
Cu1-N1	1.9751(16)	F1-Cu1-N1	86.94(5)
Cu1-N2	1.9685(16)	F1-Cu1-N2	91.67(5)
Cu1-N1_a	1.9751(16)	F1-Cu1-F1_a	180.00
Cu1-N2_a	1.9685(16)	F1-Cu1-N1_a	93.06(5)
Cu1-F1	2.3871(12)	F1-Cu1-N2_a	88.33(5)
Cu1-F1_a	2.3871(12)	N1-Cu1-N2	90.70(6)
		F1_a-Cu1-N1	93.06(5)
		N1-Cu1-N1_a	180.00
		N1-Cu1-N2_a	89.30(6)
		F1_a-Cu1-N2	88.33(5)
		N1_a-Cu1-N2	89.30(6)
		N2-Cu1-N2_a	180.00
		F1_a-Cu1-N1_a	86.94(5)
		F1_a-Cu1-N2_a	91.67(5)
		N1_a-Cu1-N2_a	90.70(6)

Figure 10.3. ORTEP style depiction of one of the weakly coordinating anions and the dicationic part of [Zn(CH$_3$CN)$_4$][B(C$_6$F$_5$)$_4$]$_2$ in the solid state. Thermal ellipsoids are drawn at the 50 % probability level.

Table 10.5. Crystallographic data, collection parameters and refinement parameters of [Zn(CH$_3$CN)$_4$][B(C$_6$F$_5$)$_4$]$_2$.

Formula	2(C$_{24}$BF$_{20}$), C$_8$H$_{12}$N$_4$Zn
Formula weight	1587.71
Crystal System	Monoclinic
Space group	C2/c (No. 15)
a, b, c [Å]	29.271(2) 13.8866(10) 20.531(2)
α, β, γ [deg]	90 134.5400 90
V [Å^3]	5948.2(8)
Z	4
D (calc) [g/cm^3]	1.773
Mu (MoKa)	0.583
F (000)	3104
Temperature [K]	123
Radiation [Å]	MoKa 0.71073
Theta-Min-Max [Deg]	1.8, 25.5
Dataset	-35: 25 ; 0: 16 ; 0: 24
Tot., Uniq. Data, R (int)	5462, 5462, 0.000
Observed Data [I > 0.0 σ(I)]	4694

Nref, Npar	5462, 467
R, wR2, S	0.0382, 0.1350, 1.12
w = 1/[\s^2^(Fo^2^)+(0.0900P)^2^+2.5000P]	where P=(Fo^2^+2Fc^2^)/3
Max. and Av. Shift/Error	0.00, 0.00
Flack x	0.002 (5)
Min. and Max. Resd Dens. [e/Ang^3^]	-0.46, 0.65

Table 10.6. Selected Bond Lengths and Bond Angles for $[Zn(CH_3CN)_4][B(C_6F_5)_4]_2$.

	distance [Å]		angle [deg]
Zn1-N1	1.980(3)	N1-Zn1-N2	111.94(11)
Zn1-N2	1.974(3)	N1-Zn1-N1_a	105.86(12)
Zn1-N1_a	1.980(3)	N1-Zn1-N2_a	108.81(14)
Zn1-N2_a	1.974(3)	N1_a-Zn1-N2	108.81(14)
		N2-Zn1-N2_a	109.48(10)
		N1_a-Zn1-N2_a	111.94(11)
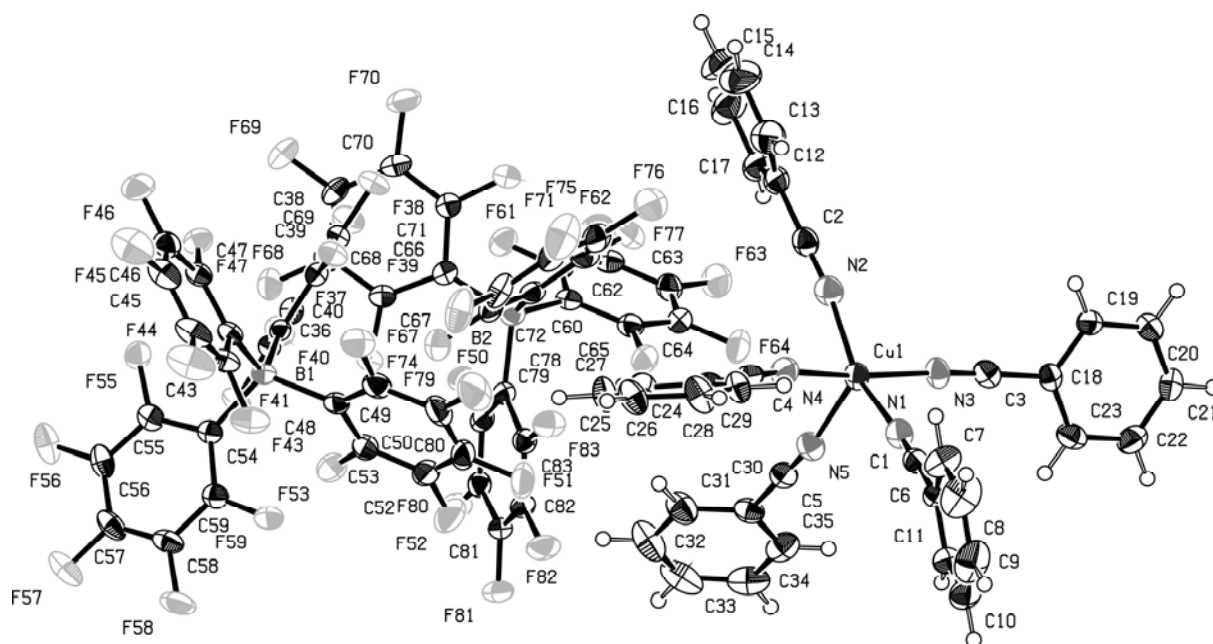
Figure 10.4. ORTEP style depiction of $[Cu(C_6H_5CN)_5][B(C_6F_5)_4]_2$ in the solid state. Thermal ellipsoids are drawn at the 50 % probability level.

Table 10.7. Crystallographic data, data collection parameters and refinement parameters of [Cu(C$_6$H$_5$CN)$_5$][B(C$_6$F$_5$)$_4$]$_2$.

Formula	C$_{35}$H$_{25}$CuN$_5$, 2(C$_{24}$BF$_{20}$)
Formula weight	1937.25
Crystal System	Monoclinic
Space group	P2$_1$ (No. 4)
a, b, c [Å]	12.5883 (5) 23.4992 (10) 13.1799 (6)
α, β, γ [deg]	90 4.3442 (2) 90
V [Å^3]	3887.6 (3)
Z	2
D (calc) [g/cm^3]	1.655
Mu (MoKa)	0.428
F (000)	1914
Crystal Size [mm]	0.20 x 0.30 x 0.38
Temperature [K]	123
Radiation [Å]	MoKa 0.71073
Theta-Min-Max [Deg]	1.5, 25.5
Dataset	-15 : 15; -28 : 28; -15 : 15
Tot., Uniq. Data, R (int)	120692, 14296, 0.035
Observed Data [I > 0.0 σ(I)]	13521
Nref, Npar	14296, 1180
R, wR2, S	0.0240, 0.0580, 1.04
w = 1/[\s^2^(Fo^2^)+(0.0243P)^2^+1.1101P] where P=(Fo^2^+2Fc^2^)/3	
Max. and Av. Shift/Error	0.00, 0.00
Flack x	0.002 (5)
Min. and Max. Resd Dens. [e/Ang^3]	-0.34, 0.30

1.2. NMR spectra
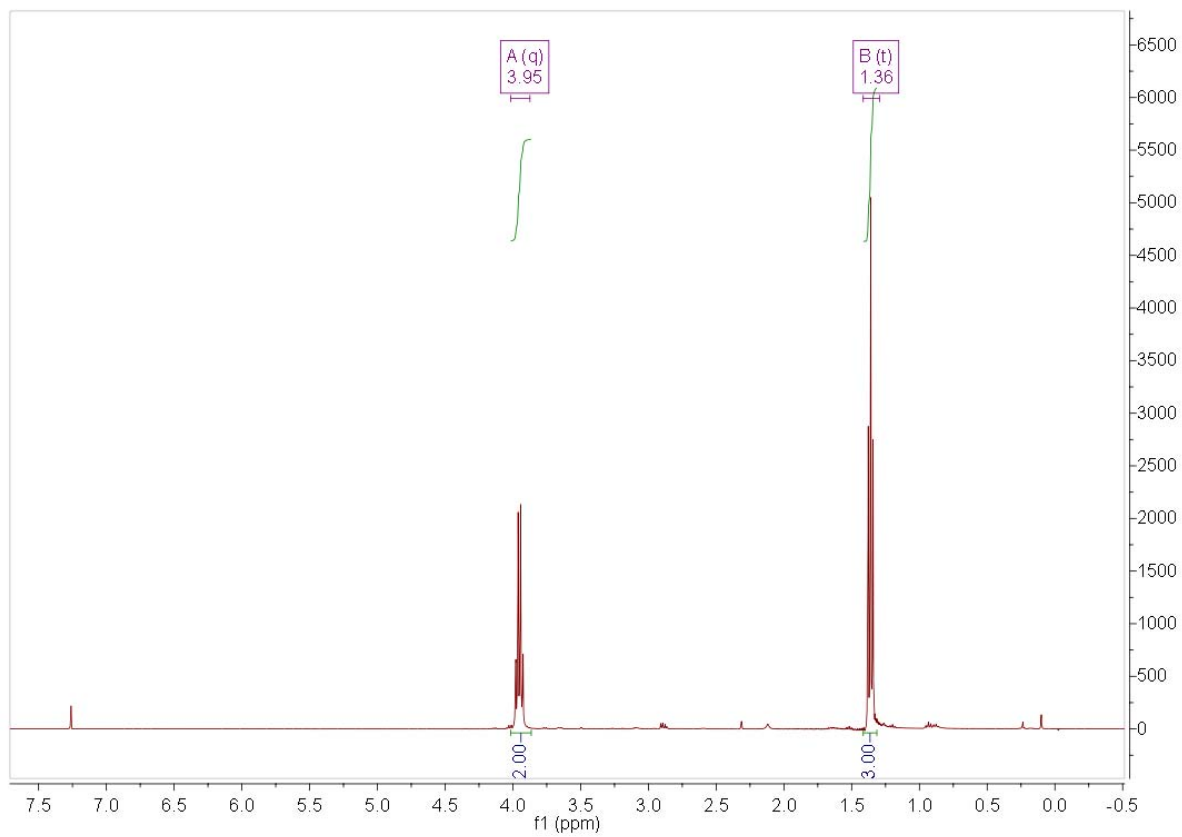
Figure 10.5. ^{1}H NMR spectrum of [H(Et$_2$O)$_2$][B(C$_6$F$_5$)$_4$] in CDCl$_3$.
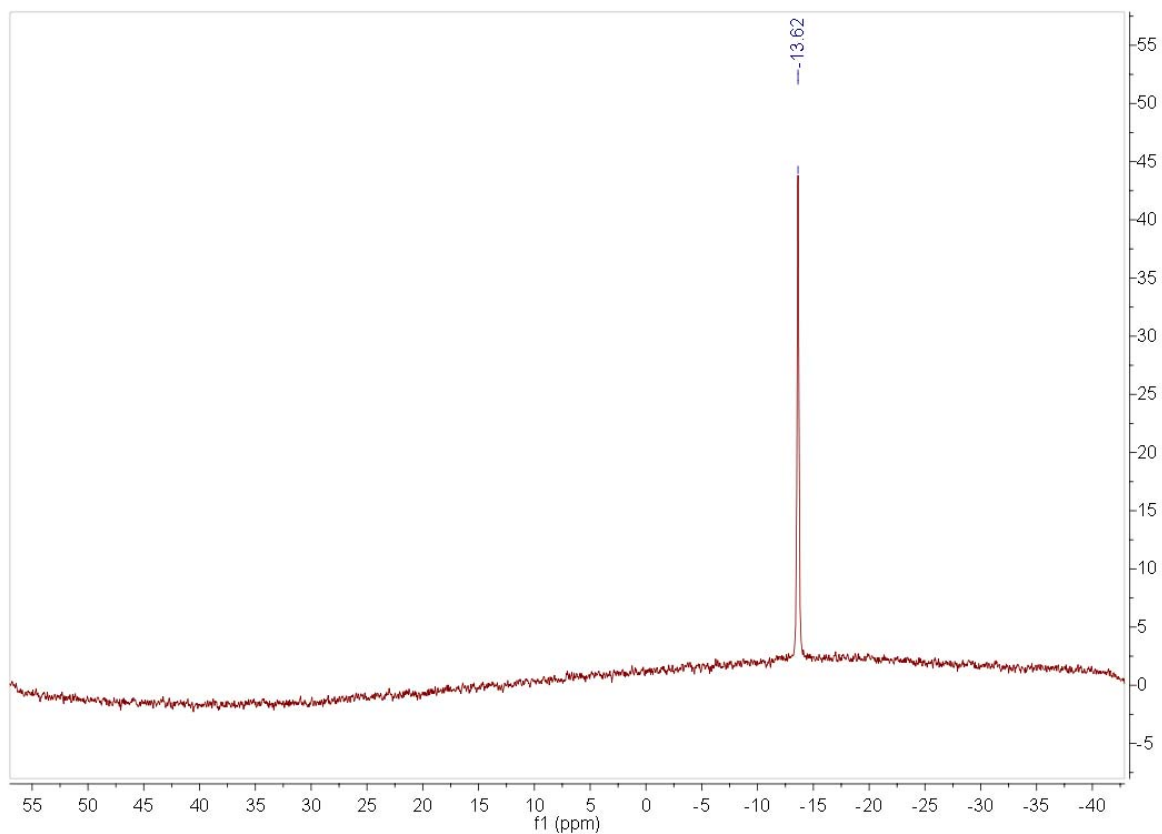
Figure 10.6. ^{11}B NMR spectrum of $[H(Et_2O)_2][B(C_6F_5)_4]$ in $CDCl_3$.
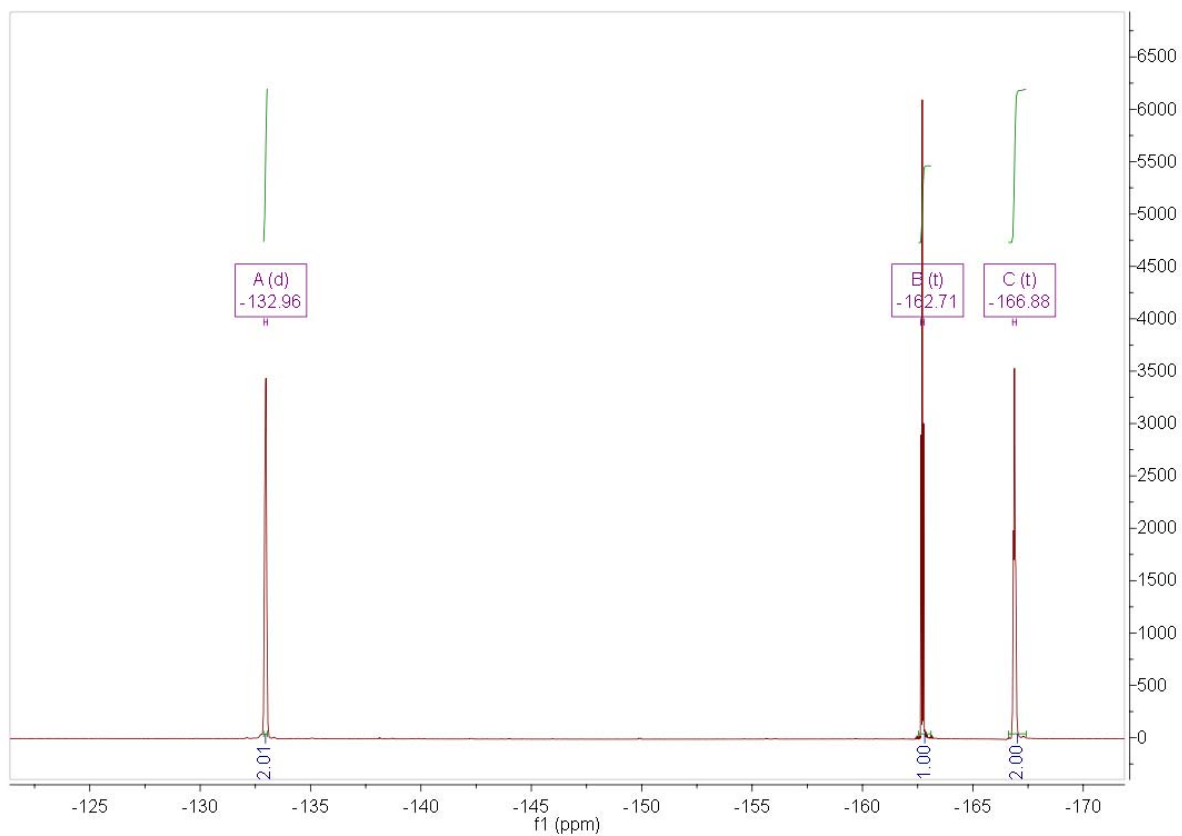
Figure 10.7. ^{19}F NMR spectrum of $[H(Et_2O)_2][B(C_6F_5)_4]$ in $CDCl_3$.
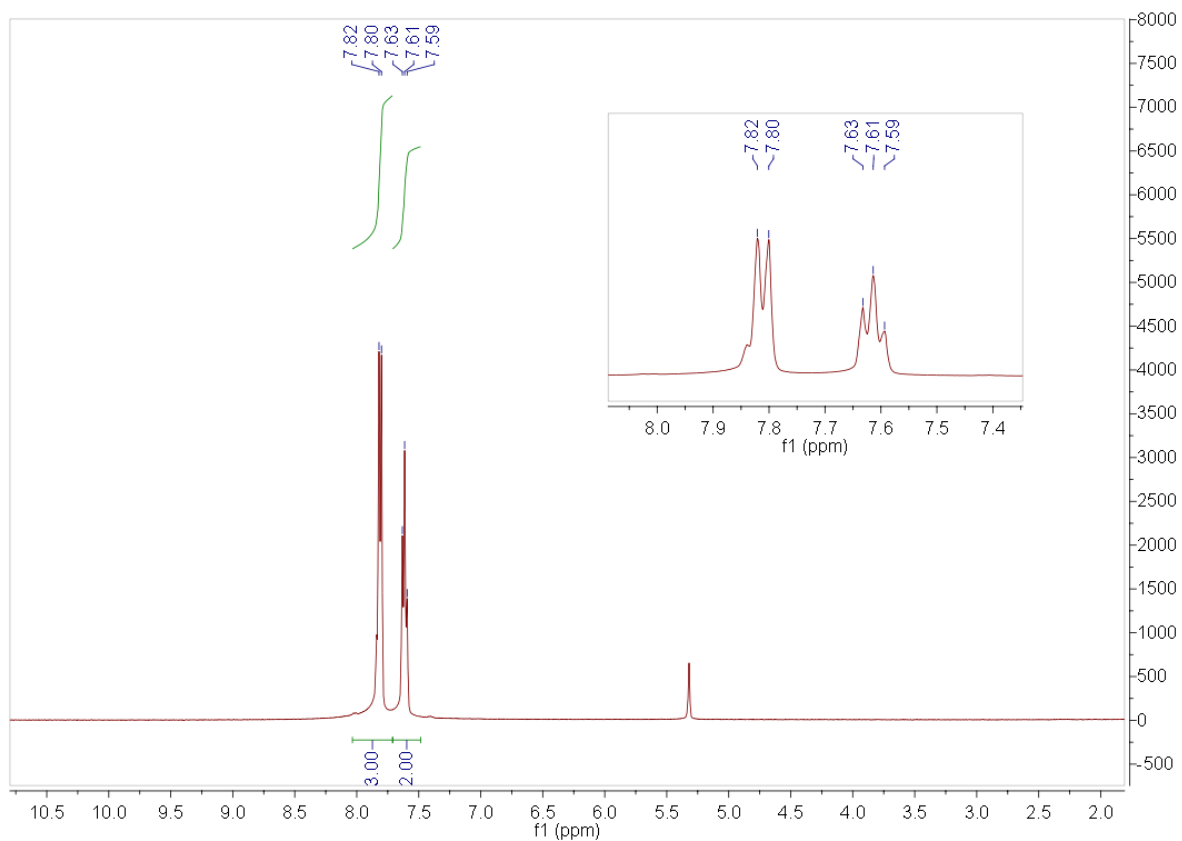
Figure 10.8. ^{1}H NMR spectrum of $[Zn(C_6H_5CN)_5][B(C_6F_5)_4]_2$ in CD_2Cl_2.
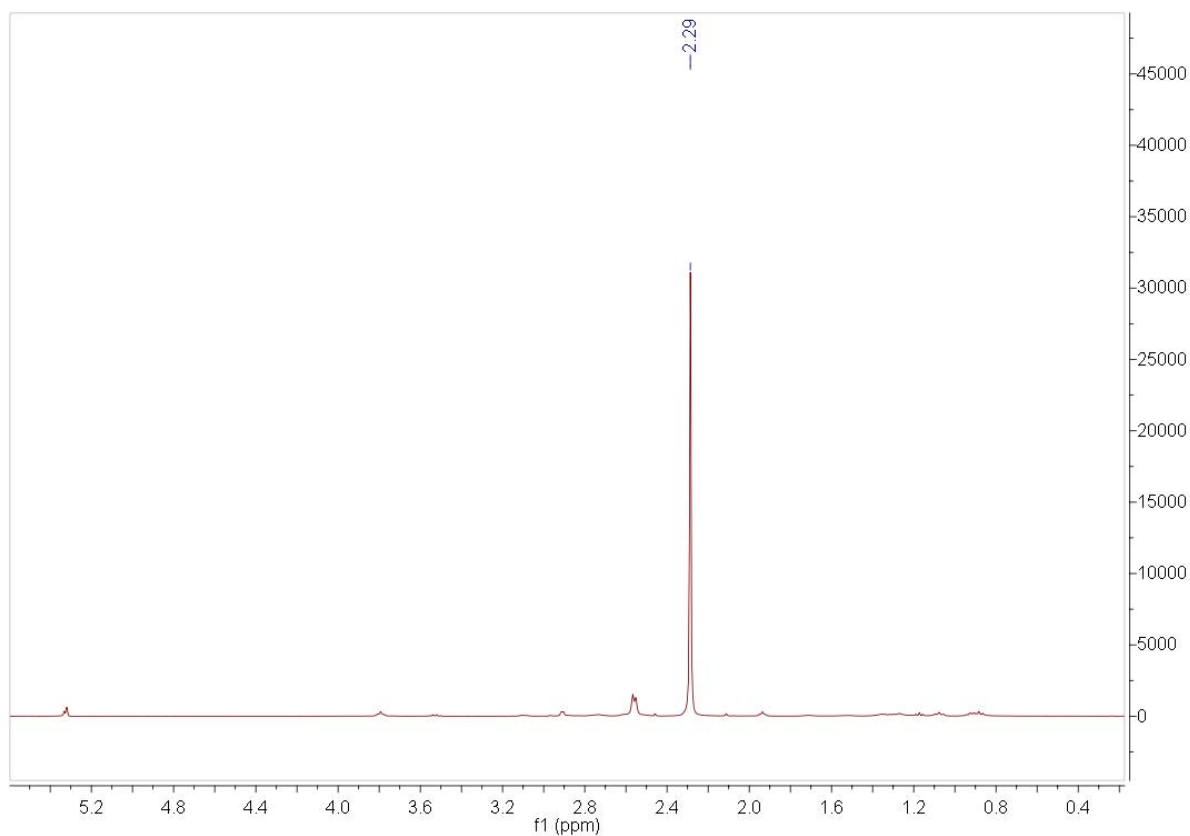
Figure 10.9. ^{1}H NMR spectrum of $[Zn(CH_3CN)_{4/6}][B(C_6F_5)_4]_2$ in CD_2Cl_2.
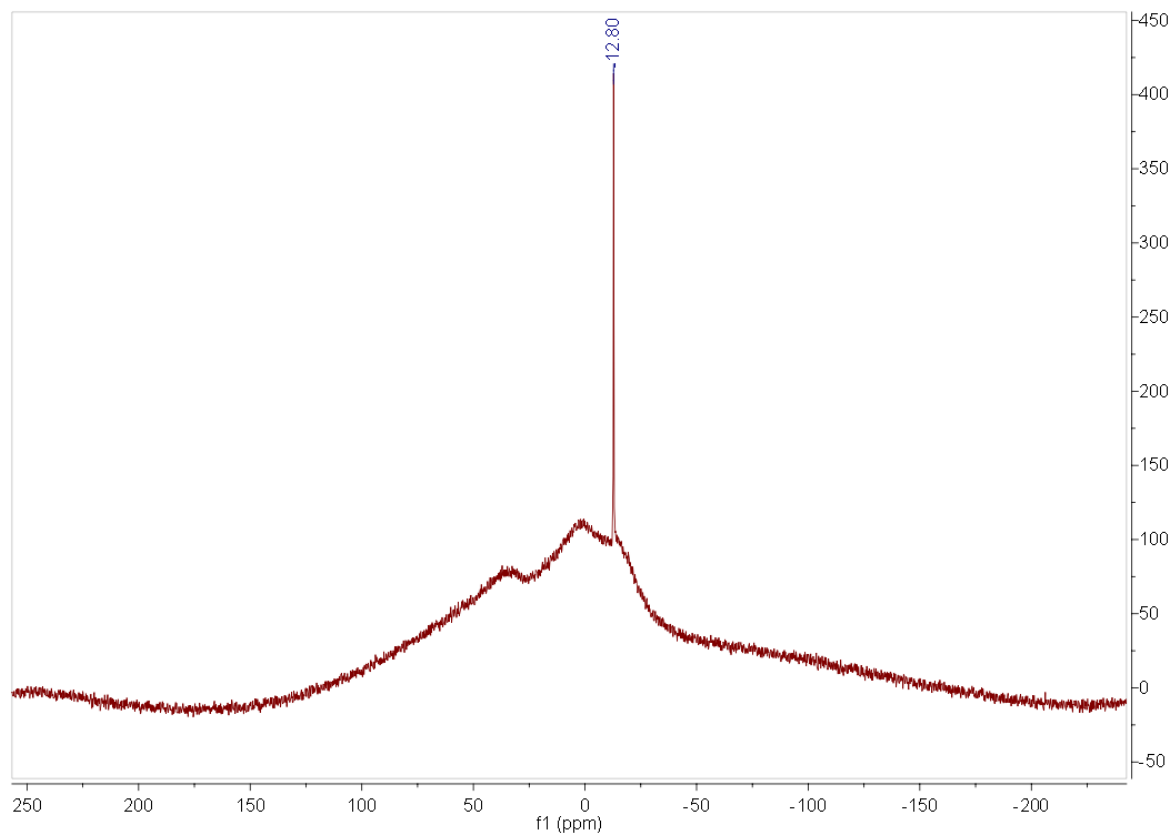
Figure 10.10. ^{11}B NMR spectrum of the reaction of $[Cu(CH_3CN)_5][B(C_6F_5)_4]_2$ with toluene and diisobutene in C_6D_6.
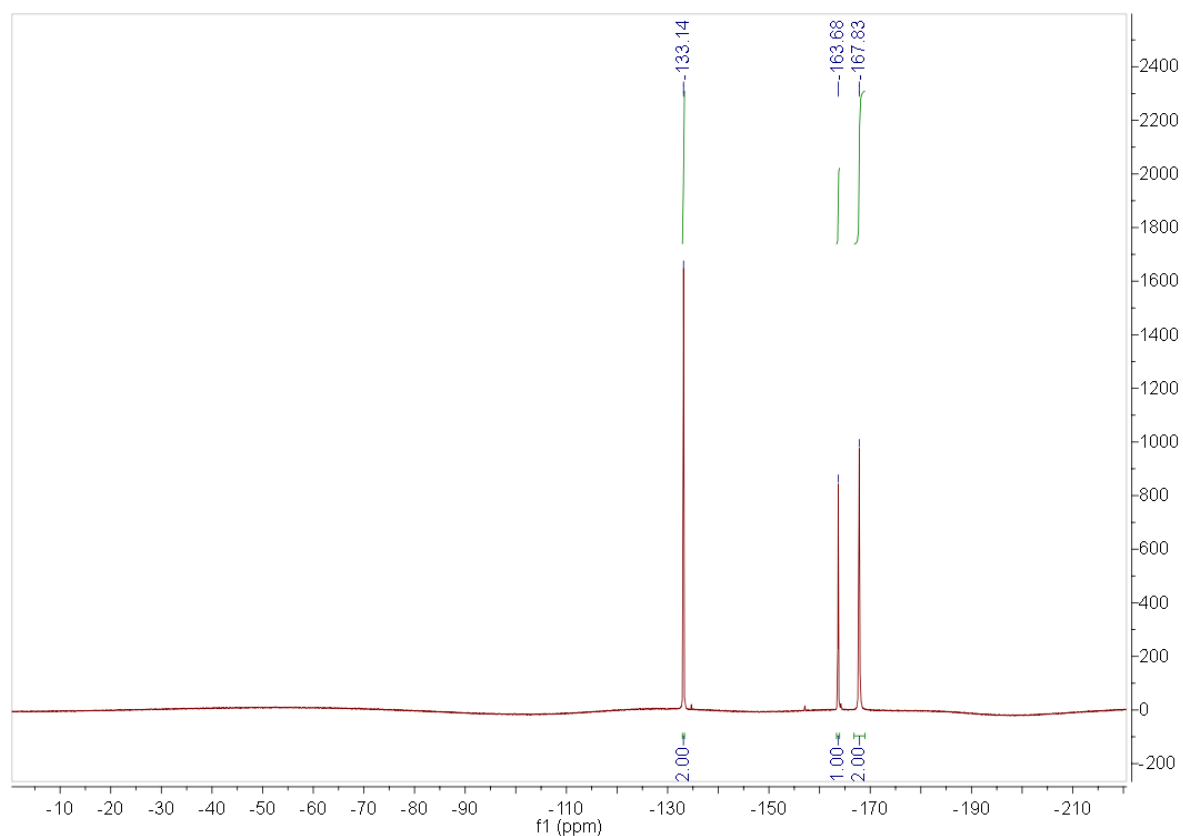
Figure 10.11. ^{19}F NMR spectrum of the reaction of $[Cu(CH_3CN)_5][B(C_6F_5)_4]_2$ with toluene in CD_2Cl_2.
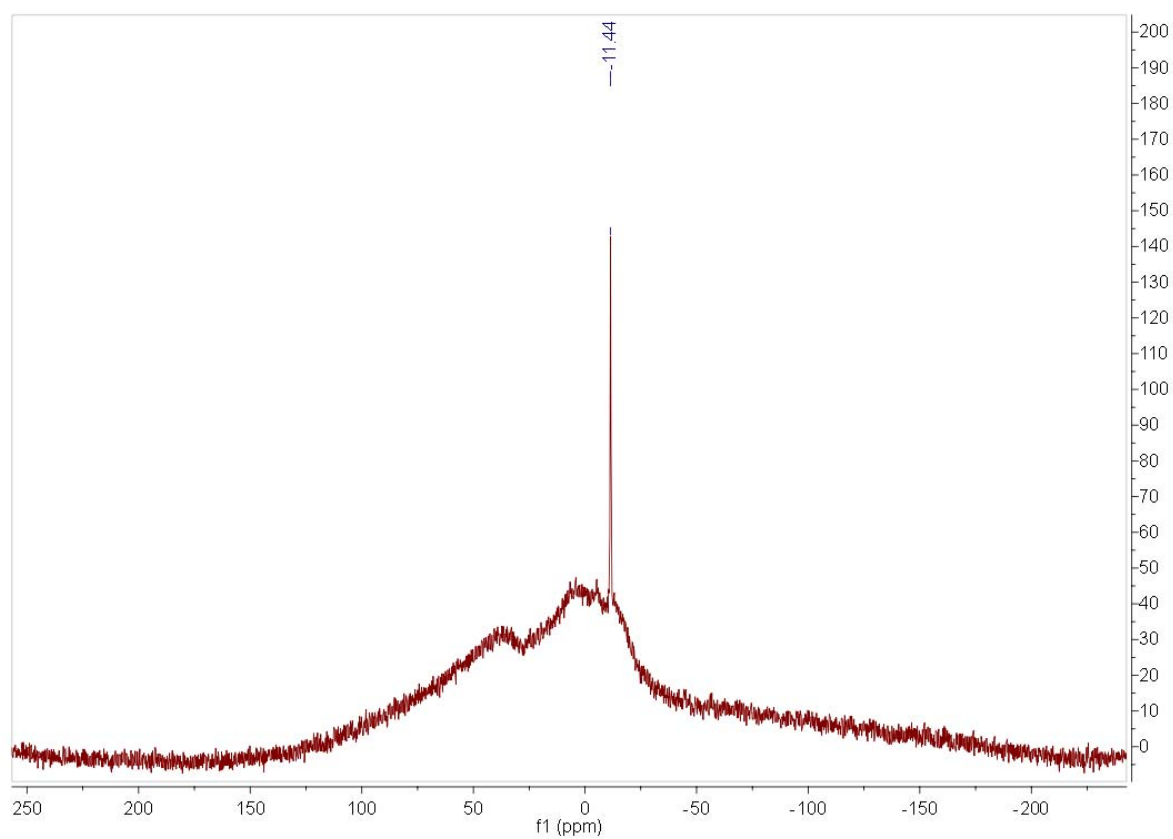
1.3 Raman spectra
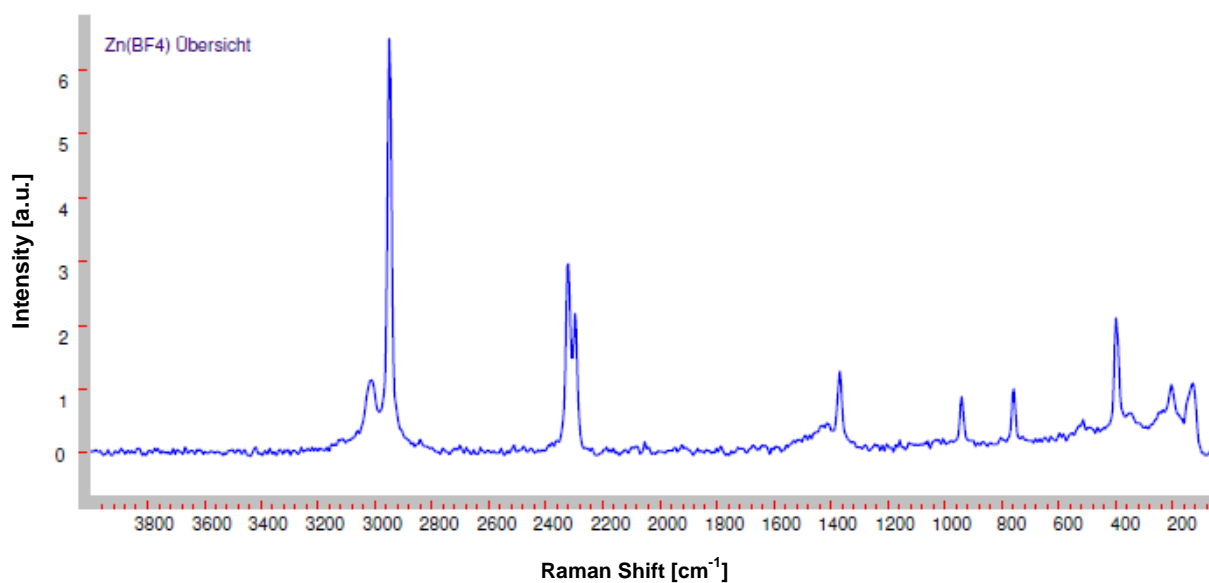
Figure 10.12. Raman spectrum of $[Zn(CH_3CN)_6][BF_4]_2$.
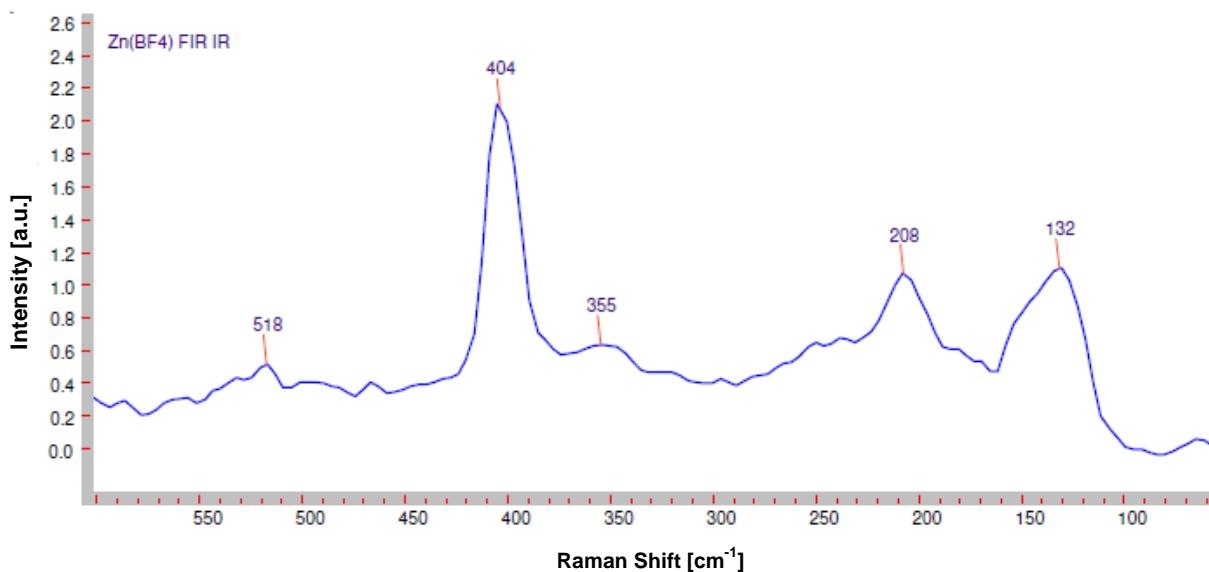
Figure 10.13. Raman spectrum of $[Zn(CH_3CN)_6][BF_4]_2$ (Far-IR).

2. Supplementary data for chapter IV
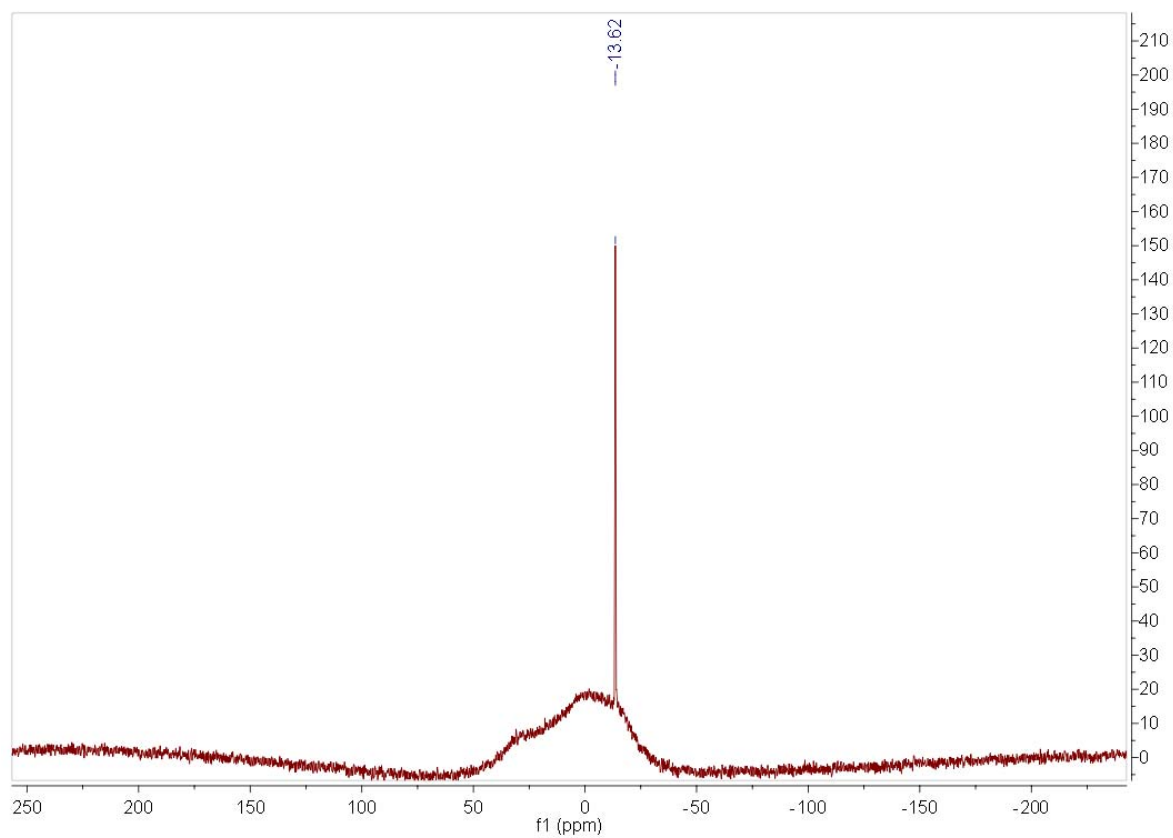
Figure 10.14. ^{11}B NMR spectrum of $[H_2(Et_2O)_4][(C_6F_5)_3B-C_6F_4-B(C_6F_5)_3]$ in CD_2Cl_2.

Figure 10.15. ^{11}B NMR spectrum of [H$_2$(Et$_2$O)$_3$][(C$_6$F$_5$)$_3$B-(C$_6$F$_4$)$_2$-B(C$_6$F$_5$)$_3$] in CD$_2$Cl$_2$.

3. Supplementary data for chapter V

3.1 X-ray crystal data
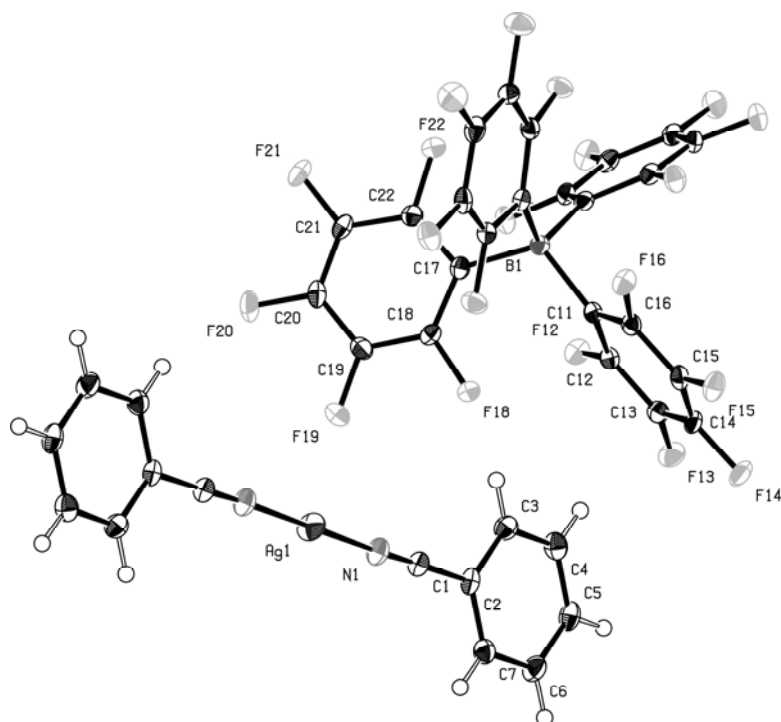
**Figure 10.16.** ORTEP style depiction of one of the weakly coordinating anions and the dicationic part of $[Ag(C_6H_5CN)_2][B(C_6F_5)_4]$ in the solid state. Thermal ellipsoids are drawn at the 50 % probability level.

Table 10.8. Crystallographic data, collection parameters and refinement parameters of $[Ag(C_6H_5CN)_2][B(C_6F_5)_4]$.

Formula	$C_{24}BF_{20}$, $C_{14}H_{10}AgN_2$
Formula weight	993.16
Crystal System	Monoclinic
Space group	C2/c (No. 15)
a, b, c [Å]	18.2915(5) 8.3397(2) 23.2485(7)
α, β, γ [deg]	90 106.9507(13) 90
V [Å^3]	3392.39(16)
Z	4
D (calc) [g/cm^3]	1.945
Mu (MoKa)	0.740
F (000)	1936
Crystal Size [mm]	0.10 x 0.20 x 0.56

Temperature [K]	123
Radiation [Å]	MoKa 0.71073
Theta-Min-Max [Deg]	1.8, 25.4
Dataset	-22: 22 ; -10: 10 ; -28: 28
Tot., Uniq. Data, R (int)	50492, 3134, 0.044
Observed Data [I > 0.0 σ(I)]	3016
Nref, Npar	3134, 282
R, wR2, S	0.0239, 0.0678, 1.06
w = 1/[\s^2^(Fo^2^)+(0.0389P)^2^+5.1497P]	where P=(Fo^2^+2Fc^2^)/3
Max. and Av. Shift/Error	0.00, 0.00
Min. and Max. Resd Dens. [e/Ang^3]	-0.55, 0.58

3.2 NMR spectra
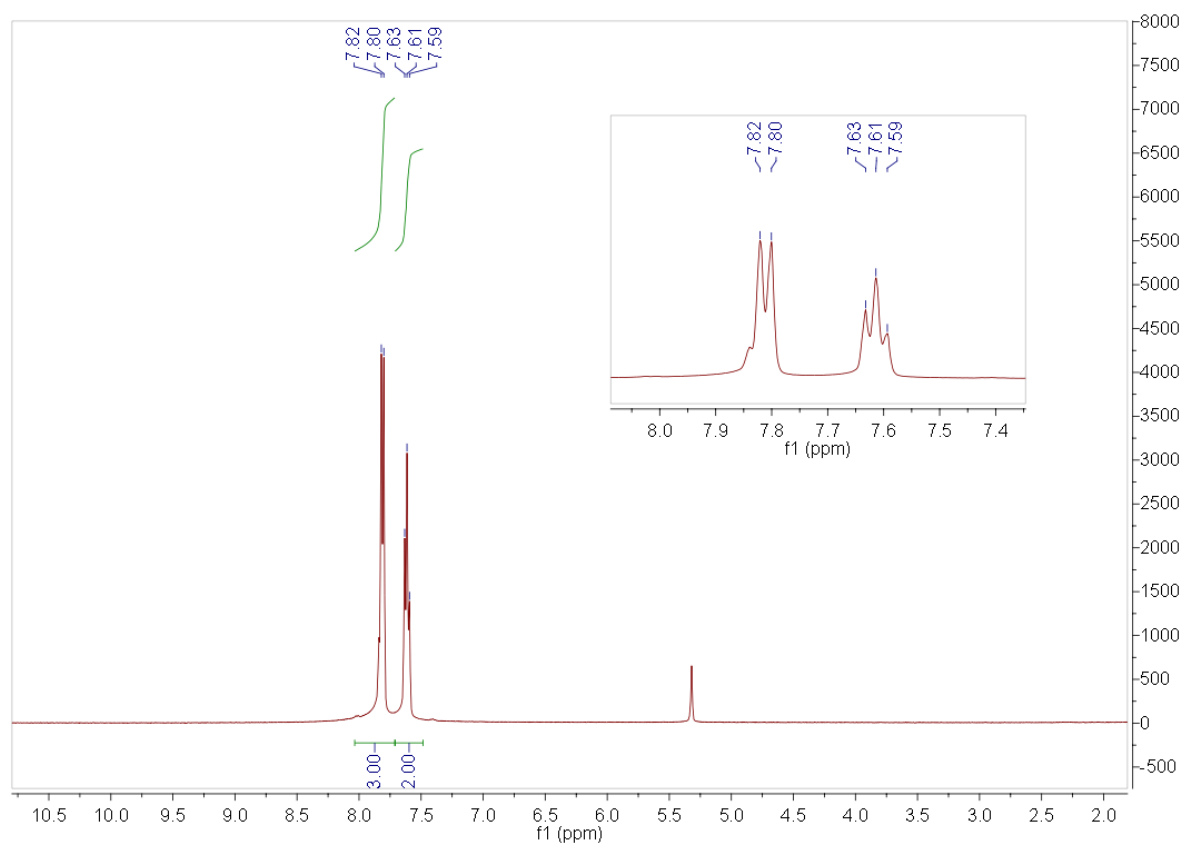
Figure 10.17. ^{1}H NMR spectrum of [Ag(C$_6$H$_5$CN)$_2$][B(C$_6$F$_5$)$_4$] in CD$_2$Cl$_2$.
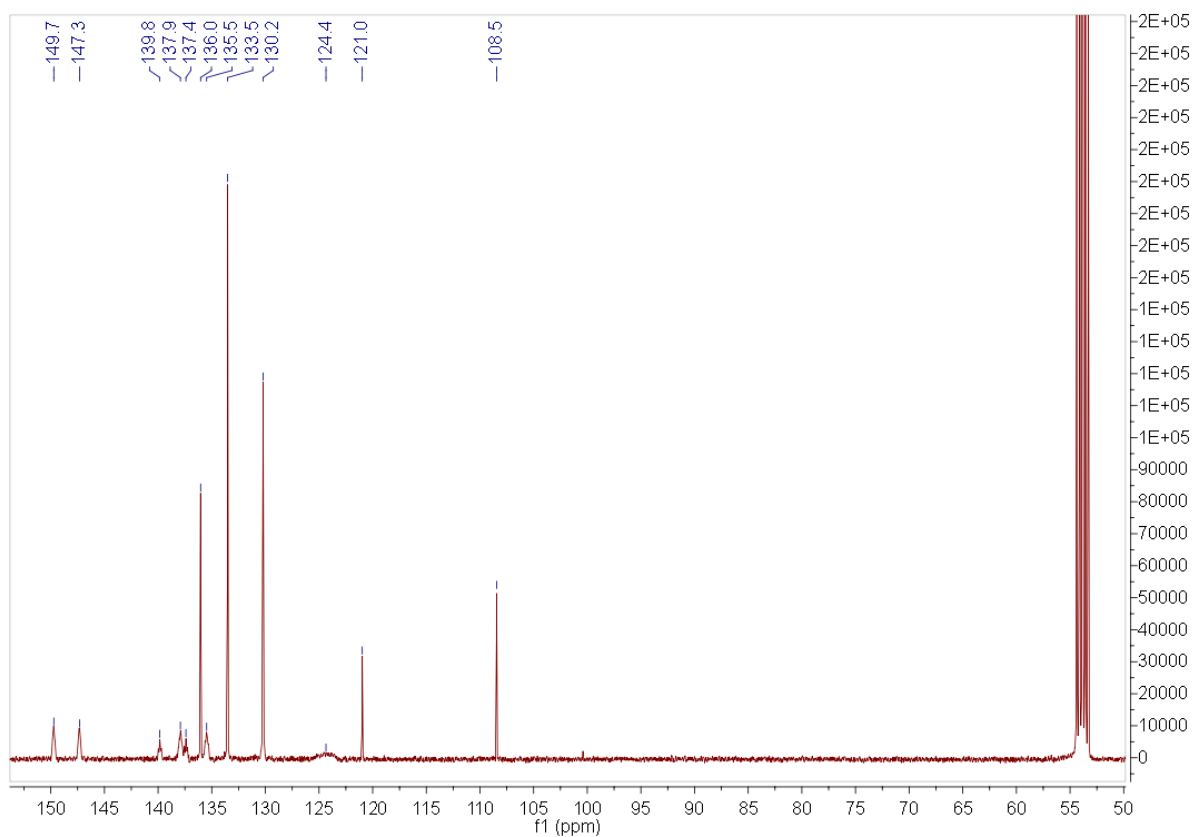
Figure 10.18. ^{13}C NMR spectrum of [Ag(C$_6$H$_5$CN)$_2$][B(C$_6$F$_5$)$_4$] in CD$_2$Cl$_2$.

4. Supplementary data for chapter VI
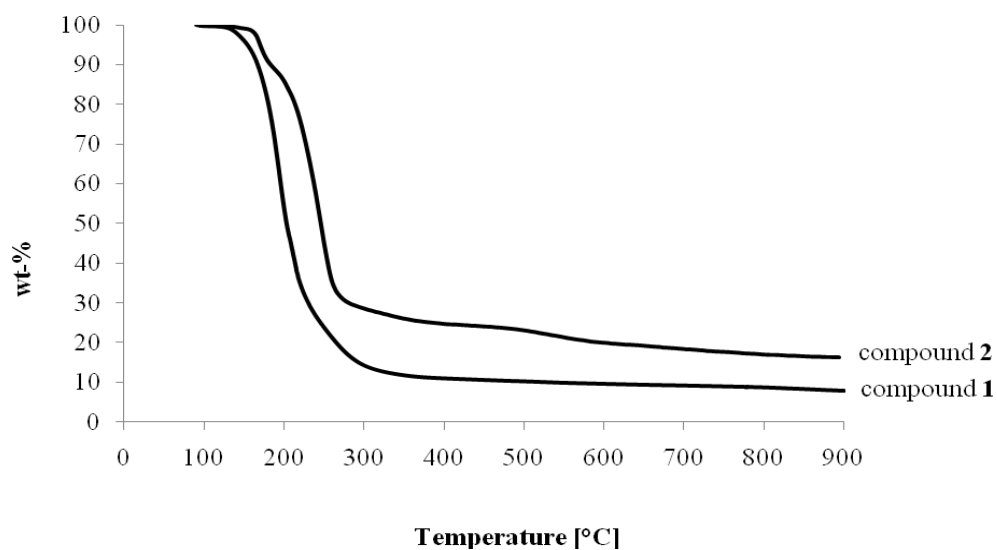
Figure 10.19. TG plot of [MoO(CH$_3$CN)$_5$][B(C$_6$F$_5$)$_4$]$_2$ (**1**) and [MoO(C$_6$H$_5$CN)$_4$][B(C$_6$F$_5$)$_4$]$_2$ (**2**).
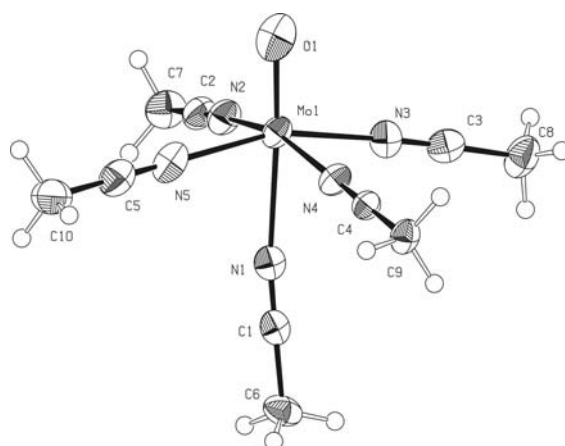
Figure 10.20. ORTEP style plot of the $[MoO(CH_3CN)_5]^{2+}$ dicationic part of $[MoO(CH_3CN)_{4/5}][B(C_6F_5)_4]_2$.

Table 10.9. Crystal structure determination of compound $[MoO(CH_3CN)_5][B(C_6F_5)_4]_2$.

Formula	$[(C_{10}H_{15}MoN_5O)^{2+}]$, $2[(C_{24}BF_{20})^-]$, $3(CH_2Cl_2)$
Formula weight	1930.09
Crystal System	Monoclinic
Space group	P 2_1/c (No. 14)
[1,2] theta range 6.93° < θ < 25.38°	
a, b, c [pm]	1323.5(1) 3528.1(4) 1667.3(2)
β [deg]	109.861(2)
V [pm³]	$7322.3(13) \cdot 10^6$
Z	4
D (calc) [g/cm³]	1.751
Mu (MoKa)	0.71
F(000)	3776
Crystal Size [mm]	$0.30 \times 0.41 \times 0.56$
Temperature [K]	123
Radiation [Å]	MoKa 0.71073
Min. and Max. Resd Dens. [e/Ang³]	-0.77, 0.73

Measurement Range:	6.93° < θ < 25.38°; h: -13/15, k: -42/42, l: -18/15
Measurement Time:	2×5 s per film
Measurement Mode:	measured: 1 run; 738 films / scaled: 1 run; 738 films
	φ movement; Increment: $\Delta\varphi$ = 0.50°; dx = 65.0 mm
LP - Correction:	Yes[2]
Intensity Correction	No/Yes; during scaling[2]

Absorption Correction:	Multi-scan; during scaling; μ = 0.546 mm$^{-1[2]}$
	Correction Factors: T_{min} = 0.6892 T_{max} = 0.7452

Reflection Data:
30417   reflections were integrated and scaled
202   reflections systematic absent and rejected
30215   reflections to be merged
10526   independent reflections
0.031 R_{int}: (basis $F_o{}^2$)
10526   independent reflections (all) were used in refinements
9473   independent reflections with $I_o > 2\sigma(I_o)$
78.4 %   completeness of the data set
1073   parameter full-matrix refinement
9.8   reflections per parameter

Solution: Direct Methods;[3] Difference Fourier syntheses

Refinement Parameters: In the asymmetric unit:
118 Non-hydrogen atoms with anisotropic displacement parameters
1 Non-hydrogen atoms with isotropic displacement parameter

Hydrogen Atoms: In the difference map(s) calculated from the model containing all non-hydrogen atoms, not all of the hydrogen positions could be determined from the highest peaks. For this reason, the hydrogen atoms were placed in calculated positions (d_{C-H} = 98, 99, pm). Isotropic displacement parameters were calculated from the parent carbon atom (U_H = 1.2/1.5 U_C). The hydrogen atoms were included in the structure factor calculations but not refined.

Atomic Form Factors: For neutral atoms and anomalous dispersion[4]

Extinction Correction: no

Weighting Scheme: $w^{-1} = \sigma^2(F_o{}^2)+(a*P)^2+b*P$
with a: 0.0423; b: 21.0147; P: [Maximum(0 or $F_o{}^2$)+2*$F_c{}^2$]/3

Shift/Err: Less than 0.001 in the last cycle of refinement:

Resid. Electron Density: +0.73 e$_0^-$/Å^3; -0.77 e$_0^-$/Å^3

R1: $\Sigma(||F_o|-|F_c||)/\Sigma|F_o|$
$[F_o > 4\sigma(F_o);$ N=9473]: = 0.0515
[all reflctns; N=10526]: = 0.0564

wR2: $[\Sigma w(F_o{}^2-F_c{}^2)^2/\Sigma w(F_o{}^2)^2]^{1/2}$
$[F_o > 4\sigma(F_o);$ N=9473]: = 0.1246
[all reflctns; N=10526]: = 0.1270

Goodness of fit: $[\Sigma w(F_o{}^2-F_c{}^2)^2/(NO-NV)]^{1/2}$ = 1.068

Remarks: Refinement expression $\Sigma w(F_o{}^2-F_c{}^2)^2$

Programs: The program system "WinGX32"[7] with the programs: "PLATON",[6] "SHELXL-97",[5] "SIR92"[3]

References

[1] APEX suite of crystallographic software. APEX 2 Version 2008.4. Bruker AXS Inc., Madison, Wisconsin, USA (2008).

[2] SAINT, Version 7.56a and SADABS Version 2008/1. Bruker AXS Inc., Madison, Wisconsin, USA (2008).

[3] Altomare, A.; Cascarano, G.; Giacovazzo, C.; Guagliardi, A.; Burla, M. C.; Polidori, G.; Camalli M. "**SIR92**", *J. Appl. Cryst.* **1994**, *27*, 435-436.

[4] International Tables for Crystallography, Vol. C, Tables 6.1.1.4 (pp. 500-502), 4.2.6.8 (pp. 219-222), and 4.2.4.2 (pp. 193-199), Wilson, A. J. C., Ed., Kluwer Academic Publishers, Dordrecht, The Netherlands, 1992.

[5] Sheldrick, G. M. "**SHELXL-97**", University of Göttingen, Göttingen, Germany, (1998).

[6] Spek, A. L. "**PLATON**", A Multipurpose Crystallographic Tool, Utrecht University, Utrecht, The Netherlands, (2010).

[7] L. J. Farrugia, "**WinGX** (Version 1.70.01 January 2005) ", *J. Appl. Cryst.* **1999**, *32*, 837-838.

Publication list

Publications as first author

Rach, S. F.; Kühn, F. E. Nitrile Ligated Transition Metal Complexes with Weakly coordinating Counteranions and Their Catalytic Applications. *Chem. Rev.* **2009**, *109*, 2061.

Rach, S. F.; Kühn, F. E. On the Way to Improve the Environmental Benignity of Chemical Processes: Novel Catalysts for a Polymerization Process. *Sustainability* **2009**, *1*, 35.

Rach, S. F.; Herdtweck, E; Kühn, F. E. Molecular Structure and Solution Behavior of a Benzonitrile Ligated Silver(I) Complex [Ag(PhCN)$_2$][B(C$_6$F$_5$)$_4$]. *Z. anorg. allg. Chem.* **2011**, *submitted.*

Rach, S. F.; Herdtweck, E; Kühn, F. E. A straightforward synthesis of cationic nitrile ligated transition metal complexes with the [B(C$_6$F$_5$)$_4$]$^-$ anion. *J. Organomet. Chem.* **2011**, *submitted.*

Curriculum Vitae

Personal Information

Name:	Silvana Rach
Date of Birth:	26.05.1983
Place of Birth:	Bobingen
Civil Status:	Single

Education

09/1989 – 07/1993:	Volksschule Bobingen Siedlung
09/1993 – 06/2002:	Gymnasium Maria Stern Augsburg
10/2002 – 08/2007:	Diploma study of Chemistry at the Technische Universität München
	Diploma thesis at the Wacker-Lehrstuhl für Makromolekulare Chemie: "Hyperbranched Polysiloxanes"
10/2007 – 12/2010:	Ph.D. thesis in the field of Molecular Catalysis at the Technische Universität München under the supervision of Prof. F. E. Kühn
	Scholarship of the International Graduate School of Science and Engineering (IGSSE)
	Scholarship of the MAN-Studienstiftung

Languages

German	Native language
English	Fluent
French	Basic knowledge